Bacterial Peptidoglycan Stem Peptide Probes for Interrogation of Transpeptidase Substrate Preferences

Alexis Jade Apostolos

B.S. Biochemistry, Lehigh University, 2017
M.S. Chemistry, Lehigh University, 2018

A Dissertation
Presented to the Graduate Faculty of the University of Virginia in Candidacy for the Degree of Doctor of Philosophy

Department of Chemistry

University of Virginia
May 2022

Abstract

Bacterial resistance to antibiotics poses an immense threat to the public's health and well-being. Nearly every new antibiotic discovered has been met with resistance, and alternative strategies to combat bacterial infections are necessary. Newly resistant bacterial strains spread when some of the cells survive antibiotic treatment, due to a mutation in their genetic makeup or acceptance of new genetic material. General resistance mechanisms involve decreased permeability into the cell or increased pumping of the antibiotic out of the cell, modification of the antibiotic target, or degradation of the antibiotic, rendering it ineffective. The Centers for Disease Control and Prevention has called for action to attempt to prevent the spread of infection and to improve the collection and distribution of information regarding antibiotic resistance. With the need for a better understanding of bacterial cell processes to implement more creative therapeutic approaches to circumvent resistance, the focus of this thesis is on the development of chemical reporters to study the substrate preferences of bacterial cell wall enzymes that are often the target of antibiotics due to their essentiality for cell survival.

Distinct classes of antibiotics and their targets will be discussed more deeply in Chapter 1, as well as specific methods of resistance that are developed by bacterial cells in the presence of β-lactam antibiotics. The details of the bacterial cell envelope (particularly the peptidoglycan) in Gram-negative, Gram-positive, and mycobacterial classes will be described, as this region is a large antibiotic target since it provides the cells with rigidity and prevents lysis due to external turgor pressure. Specifically, transpeptidase enzymes that crosslink the strands of the peptidoglycan layer in bacterial cells will be described, as well as β-lactam antibiotics, which target these enzymes to prevent cell wall crosslinking and thus result in cell death. To glean insight on the many cell wall processes that occur, significant efforts have been made in the field that rely on chemical reporters for metabolic labeling. Chapter 2 will describe the many recently discovered tools from the field to study metabolic processes of cell wall machinery (including those that label the peptidoglycan, glycans, LPS, teichoic acids, and glycoproteins).

Chapter 3 focuses on novel probes that are used by bacterial cells, exclusively as acyl-acceptor strands in peptidoglycan crosslinking, a process that is necessary for cell wall assembly. The critical nature of the cross-bridge on the PG peptide was demonstrated in live bacterial cells using fluorescently modified stem peptide mimics. The acyl-acceptor probes described provided insight on how chemical remodeling of the stem peptide cross-bridge could modulate cross-linking levels. These specifically acyl-acceptor probes supplemented the acyl-donor probes reported by our group previously, and we envisioned that together, they would provide a versatile platform to interrogate crosslinking in physiologically relevant settings.

Chapters 4 and 5 describe stem peptide probes that use facile chemistry and commercially available reagents to synthesize isosteres for *meso*-diaminopimelic acid (*m*-DAP). *m*-DAP synthesis is challenging due to the presence of internal symmetry and therefore requires the need for orthogonal protecting groups to retain that symmetry. *m*-DAP is not commercially available, thus limiting the probes available to study bacterial cells that contain *m*-DAP in their peptidoglycan. To meet this limitation, we developed *meso*-cystine (m-CYT), a cystine-based *m*-DAP mimetic that retains the structural features of *m*-DAP but is one atom longer and is formed by disulfide exchange chemistry, and *meso*-selenolanthionine (SeLAN), a lanthionine analogue that uses selenoether rather than thioether connectivity. These *m*-DAP mimetics were incorporated into tripeptides mimicking the natural stem peptide found in bacterial peptidoglycan and modified with fluorescent handles to show their incorporation in live bacterial cells via transpeptidase processing.

In Chapter 6, a novel assay platform (“SaccuFlow”) is discussed that preserves the native structure of bacterial peptidoglycan and is compatible with high-throughput flow cytometry analysis. We show the feasibility of isolating sacculi from Gram-positive, Gram-negative, and mycobacterial organisms and subsequently analyzing it using flow cytometry. This platform is intended to serve to access information about how molecules or proteins interact with peptidoglycan, as typical methods that interrogate these interactions are complicated and qualitative, rather than quantitative. Additionally, we show how this

assay can be used in a high-throughput example to identify potential inhibitors of sortase A from *Staphylococcus aureus*, an enzyme of interest as it relates to covalently attaching virulent proteins on the bacterial cell surface.

Lastly, Chapter 7 covers the use of stem peptide mimetic probes modified with a near-infrared (NIR) fluorophore to visualize gut bacteria in a living organism. We sought to image bacterial cells in an *in vivo* murine model, as the development of methods to monitor gut microbiota can lead to improved foundational understanding of the biological events, underpinning the interactions between gut commensals and the host. We envisioned that this strategy of labeling bacterial cells may enable the analysis of cell wall turnover, which has implications for bacterial cellular growth and division, in a live animal.

Table of Contents

Chapter 1 Introduction

1.1 *Antibiotic Resistance*

The discovery of the first antibiotic, penicillin in 1928, was followed by the Golden Age of antibiotic discovery (1940-1960s), a period where 50% of the drugs we use today were discovered.[1] These years were marked by the ability to treat bacterial infections that had previously been life-threatening, an exciting time in which there were a diminishing number of mortalities worldwide as a result of bacterial infections. During these years, most antimicrobials in use originated from naturally occurring microorganisms. However, the early 1940s quickly brought resistance to the antibiotics that were available, which led to a spur of investigation to make the current antimicrobials effective again.[2, 3] Presently, nearly every new antibiotic discovered and approved for use has been met with resistance.[4] As such, it is apparent that bacteria have continuously evolved to withstand drugs that were designed with the intent of lethality ever since the initial discovery of antibiotics. While this process of becoming resistant is natural, it becomes exacerbated when bacteria are continuously exposed to antibiotics. Most of the bacterial population cannot resist the antibiotic presented, but if any of the microorganisms survive due to a mutation in their genetic makeup or acceptance of new genetic material, they can then multiply or transfer their resistance to other cells.[5] This allows the newly resistant group to spread into new environments.

Antimicrobial resistance poses an immense threat to the public's health and well-being. In fact, the Centers for Disease Control and Prevention (CDC) estimates that antibiotic-resistant pathogens are responsible for more than 2.8 million illnesses and at least 35,000 deaths each year in the United States alone, numbers that are nearly two times higher since the prior report published in 2013.[6, 7] Additionally, much of modern medicine (e.g., surgeries, organ transplants, dialysis, cancer treatment) relies on antibiotics to be successful, and resistance threatens the ability for these procedures to continue.[7] The overall development of resistance is rooted in many causes, including overuse of antibiotics and inappropriate prescribing, use in agriculture, availability of a

small number of novel antimicrobials, and strict federal regulation combined with slim economic incentives for the development of new anitbiotics.[8] As antimicrobial resistance continues to develop, we face the potential of reaching a point where productive antibiotics are not available to treat simple infections.[3]

To prevent the nation from reaching the severe point where bacterial infections cannot be combatted by the antibiotics currently available, the CDC has implemented the following actions: prevent infections and reduce the spread of germs, share data and improve its collection, practice appropriate use of antibiotics, invest in the development of vaccines, therapeutics, and diagnostics, and lastly, improve sanitation of the environment to keep threats from entering it.[7] In an effort to address the call for action, our lab has set out to better understand and study the critical processes that bacterial cells employ to build their cell walls, the targets of a large number of antibiotics. We envisioned that this would provide a more encompassing understanding of potential bacterial targets of interest.

1.2 *Antibiotic Categories and their Targets*

The classification of antibiotic groups depends largely on the cellular component that they target but can be further classified into whether they have the intent to kill cells (bactericidal) or inhibit cellular growth (bacteriostatic). Bactericidal antibiotics are categorized into three main groups: quinolones, β-lactams, and aminoglycosides.[9] Quinolone antibiotics cause bacterial cell death by binding to topoisomerases which affects DNA supercoiling. The first generation of this class (nalidixic acid) was a narrow-spectrum drug used largely in the 1960s to treat urinary tract infections. It is rarely prescribed today as it is highly toxic. Shortly after the discovery and administration of nalidixic acid, the fluoroquinolone class was established (including ciprofloxacin and ofloxacin), which had a broader target range and could kill cells from multiple bacterial classes. The ability of quinolones to treat differentiated types of infections led to excessive prescriptions which has since been met with high levels of resistance.[10]

β-lactams prevent bacterial cell wall synthesis from ensuing which leads to cellular lysis and death. This class includes penicillins, cephalosporins, and carbapenems and is currently the most prescribed class for infectious diseases. Penicillin G was the first clinically used β-lactam, followed by the discovery and use of penicillins with improved efficacy against certain pathogens. To evade β-lactam toxicity, bacterial cells developed β-lactamases as a means of resistance and, as such, penicillins are rarely individually used today for treatment. The discovery of cephalosporin C, a naturally occurring penicillinase, provided the means for the development of many novel cephalosporins, some of which are still widely used today. Carbapenems are recognized for being resistant to most β-lactamases and can target a broad-spectrum of bacterial species.[11] Section **1.6** β-lactams for PG Crosslinking and Resistance discusses β-lactams in more detail.

Aminoglycosides inhibit or alter protein synthesis by causing misincorporation of amino acids into the growing peptide chain from the ribosome. These antibiotics are broken up further into categories based on the subunit of the ribosome that they inhibit. In general, access of transfer RNA (tRNA) to the ribosome is blocked by these antibiotics.[9] Resistance to aminoglycosides is often associated with an impairment of the compound being brought into the cell (e.g., change of uptake and/or efflux pumps), enzymes that modify the aminoglycosides, or mutation of the intended binding site. The main drawbacks of this class of antibiotics are related to nephrotoxicity and ototoxicity.[12, 13]

It is becoming increasingly important to understand the mechanisms by which current antibiotics target bacteria as the number of antibiotic resistant bacteria increases. This thesis will focus largely on substrates for enzymes involved in bacterial cell wall synthesis, one of the major targets of antibiotics.

1.3 *Bacterial Cell Wall*

Bacteria are classified into three groups based on the composition of their cell envelope (**Figure 1.1**), which is the main structural component responsible for providing protection

against, and interfacing between, the external milieu. Gram-negative bacteria are characterized by a cell envelope that contains the outer membrane (OM), the peptidoglycan (PG), and the inner membrane. The OM, a lipid bilayer, contains phospholipids on the inner leaflet and glycolipids, primarily lipopolysaccharides (LPS), on the outer leaflet which are critical for providing a barrier for the OM. The OM is decorated with several different proteins, which can be generally characterized as transmembrane proteins or lipoproteins. Transmembrane proteins are often β-barrels that cross the OM entirely and are also referred to as outer membrane proteins (OMPs). These proteins are responsible for allowing the passage of small molecules across the OM. Lipoproteins are typically displayed on the inner leaflet and contain lipids. In addition to OMPs and lipoproteins, LPS also contributes to passage of molecules through the OM. LPS is comprised of acyl chains, a polysaccharide core and extended chain, known as the O-antigen. Typically, the LPS is compact due to the saturated acyl chains, preventing hydrophobic molecules from passing through. The OM is anchored to the next layer of the Gram-negative cell envelope, a thin layer of PG (only a few nanometers (nm) thick), by a lipoprotein (Lpp) called Braun's lipoprotein.[14]

As the name implies, PG is a polymer of linear glycans that becomes crosslinked at short peptides that stem from the glycan strands (termed "stem peptides") by cell wall biosynthesis enzymes. PG is present in nearly all types of bacteria, as it provides structural support and prevents lysis due to osmotic pressure. Due to the fact that PG is critical for providing cellular rigidity, its biosynthesis is often the target of antibiotics. Structurally, the glycan strands contain repeating *N*-acetylglucosamine (GlcNAc) and *N*-acetylmuramic acid (MurNAc) residues in an alternating pattern (i.e., GlcNAc – MurNAc – GlcNAc – MurNAc…) with the stem peptide, typically displaying the sequence L-alanine-D-iso glutamic acid-L-lysine **or** *meso*-diaminopimelic acid-D-alanine-D-alanine, branching from the D-lactoyl group of each MurNAc (**Figure 1.2**). The PG structure is conserved across several different bacterial species with slight variations at specific residues, observed considerably at the third position of the stem peptide sequence. The variation at this position is referred to as an interpeptide bridge and can be anywhere from one to seven amino acids in length, typically Gly, L-Ala, L- or D-Ser, D-Asx, L- or D-Glu residues.

In fact, after the stem peptide is made, it can be further modified by enzymes that ligate different functional groups or amidate particular residues. Aside from the variation at the third position of the stem peptide, the amount of crosslinking from one species to another is inconsistent. For instance, *Staphylococcus aureus* (*S. aureus*) is highly crosslinked to the point that less than 10% of muropeptides exist as monomers, but *Escherichia coli* (*E. coli*) is only 20% crosslinked.[15]

The main distinction of Gram-positive organisms in comparison to Gram-negatives is the lack of an OM, but presence of a thick (30-100 nm) and many-layered PG. In Gram-positive species, the PG is interwoven with teichoic acids (large anionic polymers) that make up more than 60% of the cell wall mass, as well as several proteins. Without an OM, the proteins in Gram-positive organisms are located near the membrane, spanning the membrane, or attached to the PG or teichoic acids. The proteins can be crucial for colonization, virulence, and adhesion of the cell. Of the teichoic acids, there are wall teichoic acids (WTAs) and lipoteichoic acids (LTAs) that are associated with the PG and cell membrane, respectively. WTAs are perpendicular to the PG and extend beyond the PG surface, whereas LTAs are within the PG layer. The teichoic acids are known to play a role in the passage of molecules through the Gram-positive cell envelope. Although Gram-positive organisms do not need teichoic acids of either classification to survive, the absence of their synthesis results in growth defects in the cells.[14]

Mycobacterial cell envelopes contain features of both Gram-negative and Gram-positive organisms. For instance, mycobacteria lack an OM. Rather, the outermost layer contains mycolic acids which are linked to arabinogalactan, followed by a thin PG layer and inner membrane. Mycolic acids are fatty acids that play a role in cell envelope permeability and are covalently attached to the arabinogalactan, a large polysaccharide of galactose and arabinose sugars.[16] In terms of the outer leaflet, the external lipids in mycobacteria are not well characterized due to differences from species to species. In general, the composition of the mycomembrane is largely mixed, comprised of lipids, proteins, and lipoglycans. The mycolic acids trehalose monomycolate (TMM) and dimycolate (TDM), found on the external layer, are shown to be implicated in the

relationship with the host. In general, the mycomembrane is the main gate-keeper for permeation inside of the cell, and it is thought to be anywhere from 100 to 1,000 times less permeable than the Gram-negative cell envelope.[17]

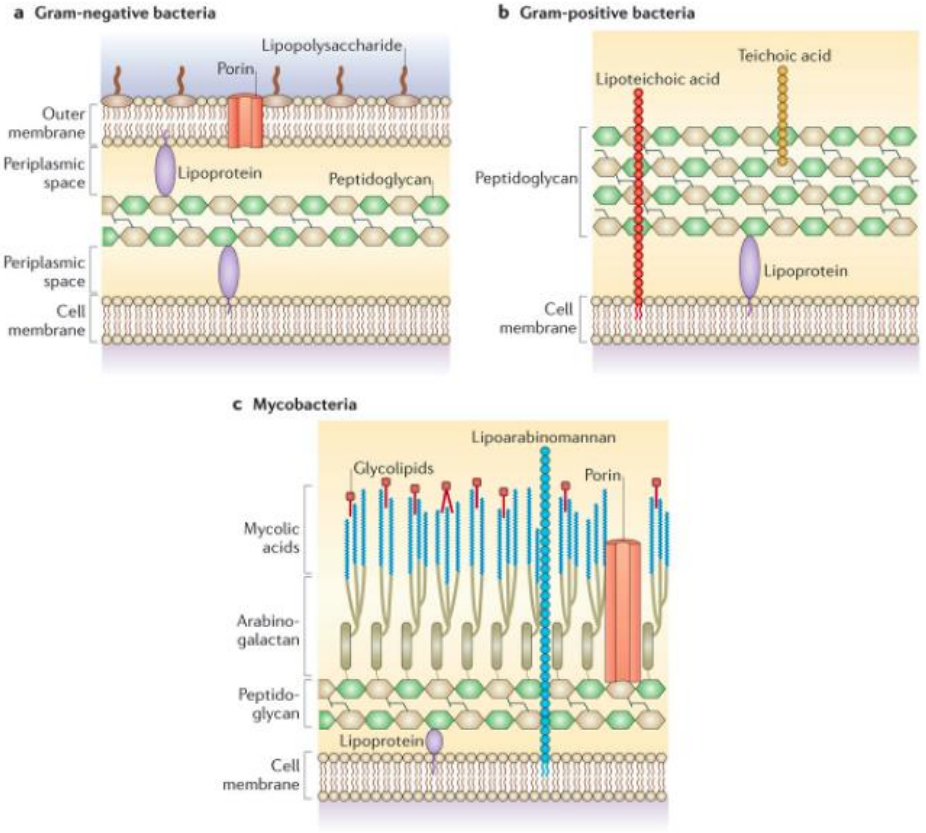

Figure 1.1 *Cellular envelope of Gram-negative, Gram-positive, and Mycobacteria. Reproduced with permission from[18].*

(a) Gram-negative bacteria contain an OM, thin PG layer, and inner membrane. (b) Gram-positive organisms are characterized by a thick PG layer containing teichoic acids and an inner membrane. (c) Mycobacteria have mycolic acids linked to arabinogalactan, a PG layer, and inner membrane.

1.4 *PG Biosynthesis*

The biosynthesis of PG is complex, involving over 20 steps that occur in the cytoplasm as well as on the inner and outer sides of the cytoplasmic membrane. Generally, the synthesis can be split up in to three overarching reactions: (1) synthesis of Park's nucleotide in the cytoplasm, (2) synthesis of lipid I and lipid II on the inner side of the membrane, and (3) transportation to the outer side for polymerization and crosslinking. To begin, fructose-6-phosphate is used as the precursor to generate uridine diphosphate (UDP)-GlcNAc over four enzymatic steps, carried out by the Glm enzymes. The first step designated towards PG synthesis is the generation of UDP-MurNAc from UDP-GlcNAc, performed by MurA and B enzymes. From there, MurC, D, E and F stitch L-Ala, D-Glu, *m*-DAP or L-Lys, and the dipeptide D-Ala-D-Ala to the D-lactoyl group of UDP-MurNAc, respectively, generating Park's nucleotide.[19] MraY covalently attaches Park's nucleotide to undecaprenyl phosphate on the inner side of the cytoplasmic membrane, generating Lipid I.[20] Lipid I becomes Lipid II by MurG, which attaches GlcNAc to MurNAc.[21] A flippase protein (FtsW, RodA, MurJ) flips Lipid II across the cytoplasmic membrane to the outer side (facing the periplasmic space) where polymerization and crosslinking can occur.[22] The enzymes in these processes are suitable antibiotic targets, as the synthesis and presence of PG is critical for bacterial cell survival. Yet, the number of antibiotics that currently exist to target these enzymes is slim, a reminder of why it is becoming increasingly important to search for therapies and drugs to target resistant bacteria as the number of antibiotic resistant bacteria increases.[19]

1.5 *PG Crosslinking*

PG gets processed by transglycosylases, which link GlcNAc-MurNAc disaccharides, and transpeptidases (TPs), which crosslink stem peptides.[23] Penicillin binding proteins (PBPs), also referred to as D,D-transpeptidases (Ddts), are TPs that catalyze the crosslinking reaction between two adjacent stem peptides. In this process, the donor strand (also called the "acyl donor") must be a pentapeptide that sacrifices a terminal D-ala and results in an acyl bond between the active site serine of the PBP and the *C*-terminus of the stem peptide. This acyl-enzyme intermediate is then displaced by the L-Lys or *m*-DAP (depending on the bacterial strain) side chain amine on a nearby PG strand (this "acyl

acceptor" can be any length stem peptide) to create a covalent crosslink between the fourth position D-ala of the donor strand and third position of the acceptor strand (to generate 4-3 crosslinks) (**Figure 1.3**).[24]

Both high- and low- molecular weight (HMW, LMW) PBPs exist. Class A HMW PBPs can perform both transglycosylation and transpeptidation to supplement the growing polysaccharide chain. Class B HMW PBPs perform only transpeptidation. The LMW PBPs typically have solely carboxypeptidase activity, where they hydrolyze the terminal D-Ala of the stem peptide chain. Generally, HMW PBPs are the target of β-lactam antibiotics.[25]

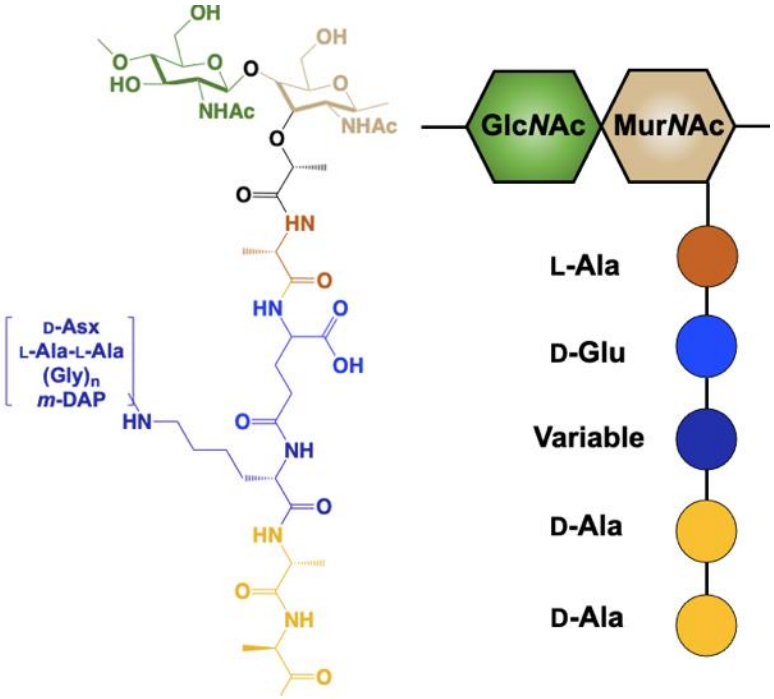

Figure 1.2 *Chemical structure (left) and cartoon structure (right) of a monomer of PG.*

The basic sequence of the stem peptide is shown, with variability typically observed at the third position. The repeating sugar units are GlcNAc and MurNAc.

In addition to PBPs, a newer class of TPs was discovered that are referred to as Ldts and contain an active site cysteine.[26] The main difference in the TP crosslinking process is that Ldts use a tetrapeptide as the donor strand and therefore produce 3-3

crosslinks between the third position of the acyl donor and third position amine of the acyl acceptor.[27] Since the covalent bonds formed as a product of transpeptidation are critical to maintain cell wall strength, these enzymes are often the target of antibiotics.

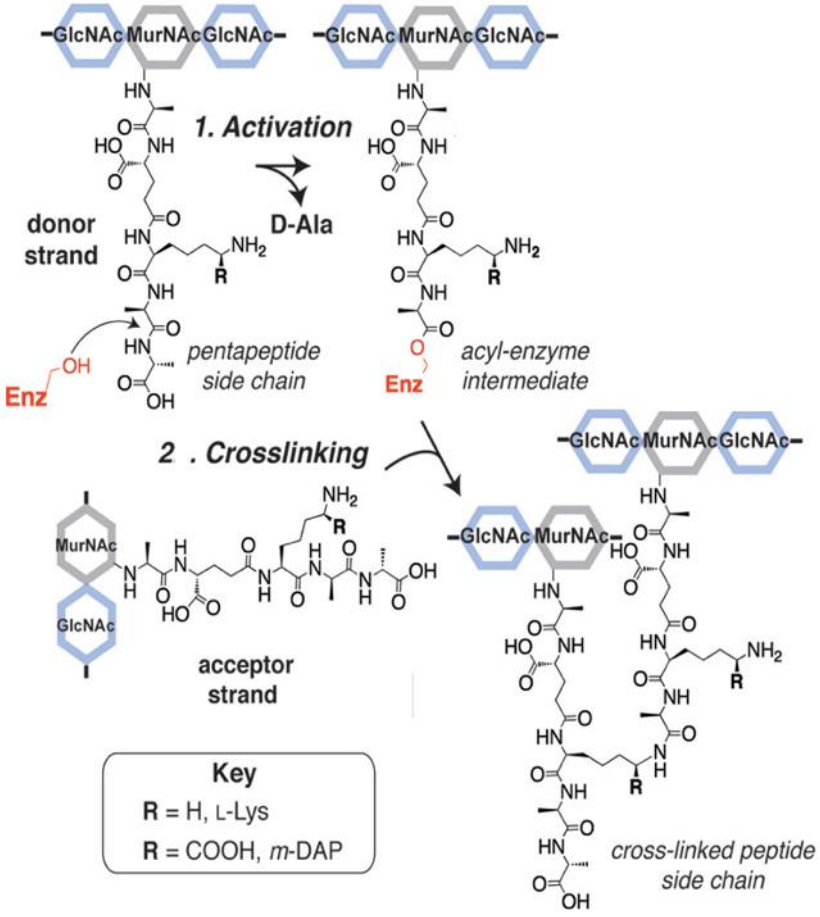

Figure 1.3 *Schematic of cross-linking of stem peptide strands carried out by PBPs. Reproduced with permission from[24].*

The serine active site of a PBP activates the pentapeptide donor strand and cleaves the terminal D-ala to generate an acyl-enzyme intermediate. Crosslinking ensues by the amine on the side chain of the third position in the acceptor strand acting as the nucleophile towards the acyl-enzyme intermediate. If this figure were to depict a reaction catalyzed by Ldts, the active site would be cysteine and the acyl donor strand would start as a tetrapeptide.

***1.6** β-lactams for PG Crosslinking and Resistance*

β-lactam antibiotics (penicillins, carbapenems, and cephalosporins) target TP enzymes by mimicking the D-ala-D-ala substrate that is found within the stem peptide (**Figure 1.4**).[28] These antibiotics form an irreversible bond with the enzyme active site which inhibits transpeptidation, weakens the PG scaffold, and can potentially lead to cell death. Most bacterial cells have more than one TP enzyme, so β-lactam resistance that occurs typically has more than one resistance mechanism. These mechanisms include (1) a decrease in membrane permeability or an increase of efflux out of the cell, (2) expression of PBPs with reduced β-lactam affinity, (3) use of Ldts to bypass crosslinking with PBPs, and/or (4) β-lactam degradation by β-lactamases.[29]

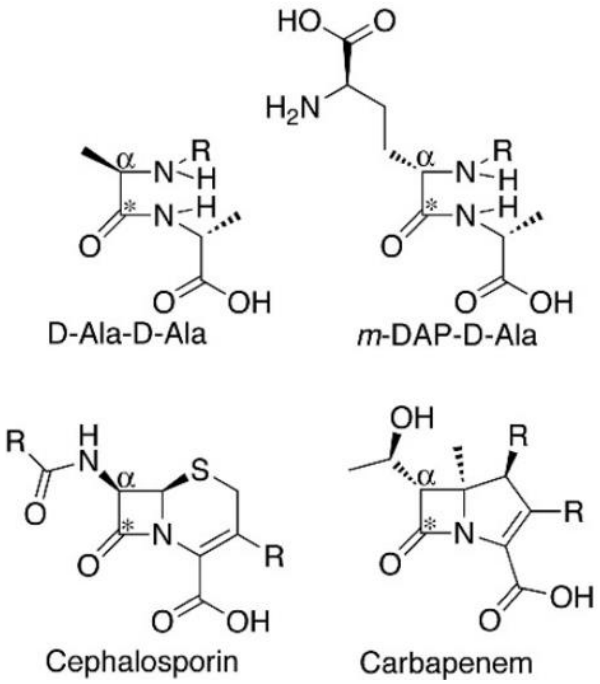

***Figure 1.4** Structures of natural PG TP recognition sequences (D-Ala-D-Ala and m-DAP-D-Ala) and cephalosporin and carbapenem β-lactams. The chirality of the α-carbon in each structure is indicated. Reproduced with permission from[30].*

Cephalosporins have the same chirality of D-Ala-D-Ala and can inhibit PBPs, whereas carbapenems have the same chirality of *m*-DAP-D-Ala and can inhibit PBPs and Ldts.

While bacteria of all classes contain a formidable cell envelope that toll-keeps on substances being brought into or out of the cell, Gram-negative organisms contain an additional OM that adds to decreased permeability into the cell (as mentioned in Section **1.3** Bacterial Cell Wall). Aside from this barrier, some bacteria contain efflux pump proteins that are responsible for recognizing antibiotics and other antimicrobial agents and subsequently pumping them out of the cell into the external environment. These pumps make it possible for bacteria to manage the intracellular concentration of the antibiotic with or without modifying the permeability of the OM (e.g., presence of LPS or porins). The presence of efflux pumps as a means of antimicrobial resistance has been suggested to become more present amongst bacterial species over time.[31]

In an effort to avoid inhibition by β-lactams, bacterial species have been shown to mutate their PBP protein sequence to reduce the affinity by the antibiotic for the enzyme. These mutations have been observed in the entire sequence but are usually concentrated at the enzyme active site.[29] For instance, *Staphylococcus aureus* (*S. aureus*) cells express a transpeptidation enzyme (PBP2a) in an antibiotic challenge that has low affinity for β-lactams. This enzyme has a modification in one of the subunits and can allow the transpeptidation reaction to progress when the primary PBP, PBP2, is shut down by a β-lactam.[32]

In addition to efflux pumps and mutations in PBP sequences, bacterial cells have also developed Ldts to catalyze the transpeptidation reaction to bypass the need for PBPs. The presence of Ldts is often coupled with a high expression of D,D-carboxypeptidases, which clip the terminal D-alanine residue in the stem peptide to generate tetrapeptides, the acyl donor substrate for Ldts. As previously mentioned (in Section **1.5** PG Crosslinking), Ldts have an active site cysteine (rather than serine found in PBPs) and recognize L,D-stereocenters rather than D,D-stereocenters. This allows Ldts to escape inactivation by β-lactams.[29] One class of β-lactams, the carbapenems, can inactivate Ldts by forming a thioester bond with the active site cysteine. Ldts have been recognized in *Mycobacterium tuberculosis*, *Mycobacterium abscessus*, *Clostridium difficile*, and *Enterococci faecium*.[26, 33]

The last mechanism by which bacterial cells counteract β-lactams is by employing a means to degrade the presented antibiotic. β-lactamases are expressed by bacterial cells to degrade the β-lactam ring of antibiotics, rendering them ineffective and unable to covalently bond to the active site of the TP enzyme. β-lactamases are the main mechanism of resistance in Gram-negative bacteria. To overcome this resistance mechanism, combination therapies of different types of antibiotics are typically used.[29]

1.7 *References*

1. Davies, J., Where have All the Antibiotics Gone? *Can J Infect Dis Med Microbiol* **2006,** *17* (5), 287-290.
2. Gould, K., Antibiotics: from prehistory to the present day. *Journal of Antimicrobial Chemotherapy* **2016,** *71* (3), 572-575.
3. Morehead, M. S.; Scarbrough, C., Emergence of Global Antibiotic Resistance. *Prim Care* **2018,** *45* (3), 467-484.
4. Ventola, C. L., The antibiotic resistance crisis: part 1: causes and threats. *P T* **2015,** *40* (4), 277-283.
5. Hawkey, P. M., The origins and molecular basis of antibiotic resistance. *BMJ* **1998,** *317* (7159), 657-660.
6. Solomon, S. L.; Oliver, K. B., Antibiotic resistance threats in the United States: stepping back from the brink. In *Am Fam Physician*, United States, 2014; Vol. 89, pp 938-41.
7. CDC *Antibiotic Resistance Threats in the United States, 2019*; Atlanta, GA, 2019.
8. Ventola, C. L., The antibiotic resistance crisis: part 1: causes and threats. *P T* **2015,** *40* (4), 277-83.
9. Kohanski, M. A.; Dwyer, D. J.; Collins, J. J., How antibiotics kill bacteria: from targets to networks. *Nat Rev Microbiol* **2010,** *8* (6), 423-435.
10. Pham, T. D. M.; Ziora, Z. M.; Blaskovich, M. A. T., Quinolone antibiotics. *Medchemcomm* **2019,** *10* (10), 1719-1739.
11. Bush, K.; Bradford, P. A., β-Lactams and β-Lactamase Inhibitors: An Overview. *Cold Spring Harb Perspect Med* **2016,** *6* (8), a025247.
12. Begg, E. J.; Barclay, M. L., Aminoglycosides--50 years on. *Br J Clin Pharmacol* **1995,** *39* (6), 597-603.
13. Becker, B.; Cooper, M. A., Aminoglycoside Antibiotics in the 21st Century. *ACS Chemical Biology* **2013,** *8* (1), 105-115.
14. Silhavy, T. J.; Kahne, D.; Walker, S., The bacterial cell envelope. *Cold Spring Harb Perspect Biol* **2010,** *2* (5), a000414-a000414.

15. Vollmer, W.; Blanot, D.; De Pedro, M. A., Peptidoglycan structure and architecture. *FEMS Microbiology Reviews* **2008,** *32* (2), 149-167.

16. Abrahams, K. A.; Besra, G. S., Mycobacterial cell wall biosynthesis: a multifaceted antibiotic target. *Parasitology* **2018,** *145* (2), 116-133.

17. Dulberger, C. L.; Rubin, E. J.; Boutte, C. C., The mycobacterial cell envelope — a moving target. *Nature Reviews Microbiology* **2020,** *18* (1), 47-59.

18. Brown, L.; Wolf, J. M.; Prados-Rosales, R.; Casadevall, A., Through the wall: extracellular vesicles in Gram-positive bacteria, mycobacteria and fungi. *Nature Reviews Microbiology* **2015,** *13* (10), 620-630.

19. Barreteau, H.; Kovac, A.; Boniface, A.; Sova, M.; Gobec, S.; Blanot, D., Cytoplasmic steps of peptidoglycan biosynthesis. *FEMS Microbiol Rev* **2008,** *32* (2), 168-207.

20. Chung, B. C.; Zhao, J.; Gillespie, R. A.; Kwon, D. Y.; Guan, Z.; Hong, J.; Zhou, P.; Lee, S. Y., Crystal structure of MraY, an essential membrane enzyme for bacterial cell wall synthesis. *Science* **2013,** *341* (6149), 1012-1016.

21. Mohammadi, T.; Karczmarek, A.; Crouvoisier, M.; Bouhss, A.; Mengin-Lecreulx, D.; den Blaauwen, T., The essential peptidoglycan glycosyltransferase MurG forms a complex with proteins involved in lateral envelope growth as well as with proteins involved in cell division in Escherichia coli. *Mol Microbiol* **2007,** *65* (4), 1106-1121.

22. Sham, L.-T.; Butler, E. K.; Lebar, M. D.; Kahne, D.; Bernhardt, T. G.; Ruiz, N., Bacterial cell wall. MurJ is the flippase of lipid-linked precursors for peptidoglycan biogenesis. *Science (New York, N.Y.)* **2014,** *345* (6193), 220-222.

23. Cabeen, M. T.; Jacobs-Wagner, C., Bacterial cell shape. *Nat Rev Microbiol* **2005,** *3* (8), 601-10.

24. Lupoli, T. J.; Tsukamoto, H.; Doud, E. H.; Wang, T.-S. A.; Walker, S.; Kahne, D., Transpeptidase-mediated incorporation of D-amino acids into bacterial peptidoglycan. *Journal of the American Chemical Society* **2011,** *133* (28), 10748-10751.

25. Buynak, J. D., Cutting and stitching: the cross-linking of peptidoglycan in the assembly of the bacterial cell wall. *ACS Chem Biol* **2007,** *2* (9), 602-5.

26. Mainardi, J. L.; Fourgeaud, M.; Hugonnet, J. E.; Dubost, L.; Brouard, J. P.; Ouazzani, J.; Rice, L. B.; Gutmann, L.; Arthur, M., A novel peptidoglycan cross-linking

enzyme for a beta-lactam-resistant transpeptidation pathway. *J Biol Chem* **2005,** *280* (46), 38146-52.

27. Mainardi, J.-L.; Villet, R.; Bugg, T. D.; Mayer, C.; Arthur, M., Evolution of peptidoglycan biosynthesis under the selective pressure of antibiotics in Gram-positive bacteria. *FEMS Microbiology Reviews* **2008,** *32* (2), 386-408.

28. Macheboeuf, P.; Contreras-Martel, C.; Job, V.; Dideberg, O.; Dessen, A., Penicillin binding proteins: key players in bacterial cell cycle and drug resistance processes. *FEMS Microbiol Rev* **2006,** *30* (5), 673-91.

29. Nikolaidis, I.; Favini-Stabile, S.; Dessen, A., Resistance to antibiotics targeted to the bacterial cell wall. *Protein Sci* **2014,** *23* (3), 243-59.

30. Wivagg, C. N.; Bhattacharyya, R. P.; Hung, D. T., Mechanisms of β-lactam killing and resistance in the context of Mycobacterium tuberculosis. *J Antibiot (Tokyo)* **2014,** *67* (9), 645-54.

31. Nikaido, H.; Pagès, J.-M., Broad-specificity efflux pumps and their role in multidrug resistance of Gram-negative bacteria. *FEMS Microbiology Reviews* **2012,** *36* (2), 340-363.

32. Lim, D.; Strynadka, N. C., Structural basis for the beta lactam resistance of PBP2a from methicillin-resistant Staphylococcus aureus. *Nat Struct Biol* **2002,** *9* (11), 870-6.

33. Lecoq, L.; Dubée, V.; Triboulet, S.; Bougault, C.; Hugonnet, J.-E.; Arthur, M.; Simorre, J.-P., Structure of Enterococcus faeciuml,d-Transpeptidase Acylated by Ertapenem Provides Insight into the Inactivation Mechanism. *ACS Chemical Biology* **2013,** *8* (6), 1140-1146.

Chapter 2 Bacterial Cell Wall Probes

2.1 *Introduction*

As described in the previous chapter, the bacterial cell wall is a primary antibiotic target, as it provides cellular rigidity, and its compromise can lead to lysis and death. In this chapter, recently used and discovered chemical tools from the field to study metabolic processes of cell wall machinery will be summarized. These tools have provided researchers with the ability to describe and understand aspects of several bacterial processes (e.g., growth, secretion, division).[1]

The technique, referred to as “metabolic labeling,” describes the process by which a chemically modified precursor, termed a probe, becomes incorporated into a cell by use of the endogenous enzymatic machinery. The probe can be radioactive, contain a stable isotope, or display a bioorthogonal handle or a fluorophore. The use of radio- or isotopic labels in this scenario can be challenging as particular equipment is needed, the expenses to work with such labels can be cumbersome, and often, necessary precursors are not commercially available. In the case of bioorthogonal chemistry, an enzymatic precursor mimicking the natural substrate has a chemical reporter that does not interfere with the activity of the enzyme of interest. Then, the presence of the probe within the cell is tested by use of an exogenous label (e.g., a fluorophore or affinity tag) that specifically reacts with the chemical reporter.[1] This is considered a two-step label (**Figure 2.1**).[2] Alternatively, direct labeling occurs when the enzymatic precursor is conjugated to the exogenous label and becomes incorporated into the cell. This can be a challenge if the label is too large for the targeted enzymatic machinery to afford.

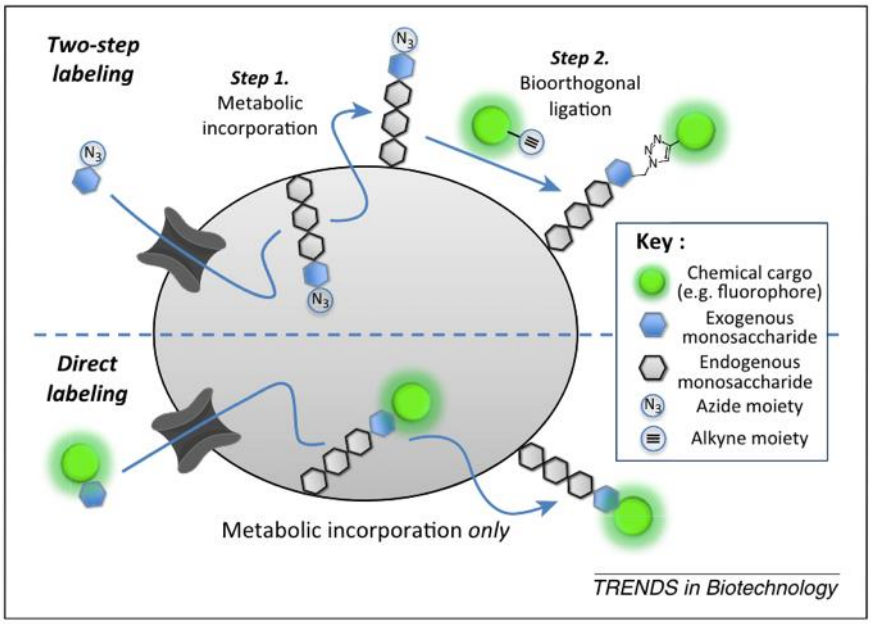

Figure 2.1 *Metabolic Labeling of a Bacterial Cell using Two-step or Direct Labeling. Reproduced with permission from*[2]*.*

In two-step labeling, an enzymatic substrate (blue hexagon, here, a monosaccharide) displaying a bioorthogonal handle (here, N_3) is incorporated through an endogenous pathway utilized by bacterial cells. Then, a chemical cargo (e.g., fluorophore) displaying a reactive partner (here, an alkyne) becomes covalently displayed due to the chemical reaction with a surface-displayed handle. In direct labeling, the enzymatic substrate is already modified with the chemical cargo and is displayed on the surface of the bacterial cell.

This thesis will focus largely on probes that contain a fluorescent moiety and are metabolized by cell wall synthesis enzymes.

2.2 *Metabolic Labeling of PG in Bacterial Cells*

D-amino acids were shown to be important to bacterial cells as they play a role in the PG strength and composition, and were found to be released into the surrounding environment at millimolar concentrations.[3] In early studies, single D-amino acids that were not native to the cell were demonstrated to be incorporated into the bacterial cell wall by

transpeptidase enzymes[4] that later allowed for the visualization of PG biosynthetic machinery dynamics in live cells. Fluorescently modifying single D-amino acids and subsequently monitoring fluorescent read-out with microscopy provided a novel method to monitor PG as it was being synthesized. Importantly, the labeling pattern observed was specific to D-amino acids, as the L-enantiomer showed near-background fluorescence.[5] This sparked an effort made by the field to use these tools to better understand bacterial cell wall processes. For example, D-amino acids displaying alkynes or azides, coupled with their complementary fluorescent dye for two-step metabolic labeling inside of a macrophage, aimed to aid in understanding the PG metabolism in an infection model.[6] Similarly, the presence PG in *Chlamydia trachomatis* (*C. trachomatis*) was confirmed by using a dipeptide (D-Ala-D-Ala) probe and click chemistry with a fluorophore that labeled the cells throughout multiple phases. This probe allowed the field to see, for the first time, the PG in an organism that was previously questioned for its presence.[7] Additionally, synthesized cell wall precursors (UDP-MurNAc pentapeptide modified with a fluorescein) were incorporated into Gram-positive and -negative organisms.[8] These studies hijacked native bacterial cell wall enzymatic machinery and paved the way for the field to use non-native D-amino acids and short peptides to probe bacterial cell wall processes.

Once these preliminary studies were established, researchers pushed to expand the chemical toolbox to relevant studies involving living systems and bacterial cells. The Bertozzi group developed near-infrared (NIR) probes with alkynes or azides that were activatable upon triazole formation, allowing for alkyne detection on cells without the need for washing. This study aimed to set the stage for *in vivo* (e.g., host cells or living organisms) imaging of PG in pathogenic bacteria.[9] With the idea in mind to reduce washing steps in order to generate techniques for high-throughput screens for potential TP inhibitors, a molecular-rotor based fluorescent D-amino acid was reported. Incorporation of the amino acid into the PG created a rigid environment to where the probe was rotationally inhibited and resulted in a turn-on fluorescent signal without the need to wash the cells.[10] Our group reported on imaging bacterial cells in a host by use of *Caenorhabditis elegans* (*C. elegans*) infected with *S. aureus*. The system was treated with a tetrazine-containing D-amino acid followed by a *trans*-cyclooctene (TCO) modified

fluorophore for an inverse electron-demand Diels-Alder (IED-DA) reaction.[11] Fluorescent D-amino acid probes used by Boersma et al. provided visualization of *Streptococcus pneumoniae* (*S. pneumoniae*) PG processing in biofilms on epithelial cells. *S. pneumoniae* is an organism that readily forms a biofilm and that can become pathogenic in compromised individuals.[12] Additionally, the PG of anaerobic commensal bacteria in a murine model was labeled for the first time by use of a coumarin D-amino acid.[13]

Metabolic labeling of PG was probed further by evaluation of TP substrate specificity and localization. Since these non-native amino acids were being processed by PG biosynthesis machinery, research by our group aimed to understand the TP preference for *C*-terminus variability in single amino acid probes.[14] Additionally, Pidgeon and coworkers developed stem peptide mimetic probes that provided a means to study Ldt preferences by modulating specific residues within the stem peptide sequence.[15] Work by the Spiegel group highlighted a stem peptide mimic (L-Lys-D-Ala-D-Ala) with a fluorophore to identify the PBP responsible for crosslinking this probe into the PG of *S. aureus* (PBP4) and to localize the regions where the probe was incorporated (and thus, to identify where PBP4 was active).[16, 17] To further understand bacterial growth and division, cells were visualized during cytokinesis with fluorescent D-amino acids in conjunction with fluorescent fusion proteins to elucidate the movement of FtsZ and FtsA filaments.[18] A combination of single D-amino acids and dipeptides used by the Siegrist and Swarts groups showed mycobacterial PG synthesis occurring at the sidewall in addition to the previously demonstrated division from the poles (rather than the septal region).[19]

2.3 *Glycan Labeling*

Aside from D-amino acid probes, dipeptides, and stem peptide mimics, the glycan portion of the PG has also been utilized for studying GlcNAc and MurNAc which can play a role in not only PG synthesis but also in host immune recognition.[20] The Grimes group installed a biorthogonal handle (either an alkyne or azide) onto MurNAc to harness metabolic labeling of the PG. Modification at the 2-*N* position afforded tolerance by PG

biosynthetic machinery and subsequent copper (I)-catalyzed azide-alkyne cycloaddition (CuAAC) with a corresponding fluorophore allowed visualization of bacterial cells by use of microscopy. Further, bacterial invasion and breakdown inside of macrophages was studied using these probes.[21] Since then, the Grimes group has developed their synthetic strategy for these probes and explored promiscuity of anomeric kinase (AmgK) and uridylyl transferase (MurU), MurNAc/GlcNAc recycling enzymes, by altering the 3-OH position of MurNAc.[22] Perley-Robertson et al. prepared a GlcNAc-1,6-anhydroMurNAc-fluorophore conjugate that was transported by a cellular enzyme in *Escherichia coli* (*E. coli*) spheroplasts, which aimed to aid in understanding of PG recycling and to investigate inhibitors of the transport enzyme involved.[23] Glycan labeling in the field was spearheaded by Bertozzi and Kiessling.[24]

More narrowly, mycobacterial glycans have been extensively studied. Of note, these glycans are essential for growth as well as infection, which makes them targets of interest for potential antibiotics. The majority of the probes reported are intended to report on trehalose, mycolate-containing glycolipids, and arabinose. In the category of mycolate-containing glycolipids, arabinogalactan-linked mycolates (AGM) and trehalose mono- and dimycolate (TMM and TDM) are the main contributors. The biosynthesis of AGM, TMM, and TDM is generally understood, and many chemical reporters mimic substrates of the treaholse-mediated glycolipid biosynthetic pathway. The first probe of this kind was a trehalose that was directly modified with a fluorescent moiety (“FITC-Tre”), that allowed the researchers to visualize *Mycobacterium tuberculosis* (*M. tuberculosis*) cells, as well as macrophages containing *M. tuberculosis*.[25] This work was expanded upon by the Bertozzi group, where they added the fluorescent moiety to different positions on trehalose and labeled other mycobacterial strains.[26] They built upon their own work by developing clickable trehalose derivatives, where the fluorescent residue was not directly attached, but rather clicked on after metabolic processing by cells, using CuAAC or strain-promoted alkyne-azide cycloaddition (SPAAC) chemistries.[27] These pioneering trehalose probes were used in many later studies to elucidate information related to trehalose recycling and incorporation into the mycobacterial cell envelope. To add to the knowledge base that these probes have provided, additional studies with positron emission

tomography (PET)-capable trehalose probes were reported,[28] as well as probes to identify potential inhibitors of trehalose synthesis.[25, 29, 30]

2.4 *Metabolic Labeling of Bacterial Glycoproteins, Teichoic Acids, and LPS*

Similar to glycosylation of eukaryotic proteins, bacterial proteins become glycosylated at asparagine or serine/threonine residues. Glycosylation in bacterial cells is important for immune evasion, motility, adhesion, and host colonization, all of which aid the organisms in causing disease or infection.[31] Because glycosylation is fundamental to virulence, an understanding of its function is important and probes to study it can be beneficial. Studies by the Dube lab over the years have involved probes based on GlcNAc to study glycosylation of proteins in *Helicobacter pylori* (*H. pylori*), an organism that infects the gastrointestinal tract. Their probes were azidoacetamide-modified GlcNAc, termed GlcNAz, and peracetylated GlcNAc, Ac_4GlcNAz, and allowed the identification of over 100 glycosylated proteins in *H. pylori*, many of which were associated with virulence.[32] Using this probe, the Dube group reacted a phosphine-dinitrophenyl (DNP) group and further exploited GlcNAz labeling to recruit fluorophore-conjugated anti-DNP antibodies to *H. pylori*.[33] Other analogues of such a probe were made to replicate more unique sugars such as FucNAc (found in *Pseudomonas*), Bac, and DATDH (for targeting *Neisseria*).[34]

As discussed in Section **1.3** Bacterial Cell Wall Gram-positive organisms have teichoic acids that account for more than half of the cell wall mass. While this is a feature shared amongst species classified as Gram-positive, the structure of teichoic acids tends to vary amongst specific organisms.[35] Teichoic acids play a large role bacterial cell adhesion and colonization, as well as the cellular shape and rigidity. As such, understanding teichoic acid biosynthesis is integral to aid in development of potential antibiotic targets.[36] Given the diversified and complex structure of teichoic acids across species, many metabolic probes could exist, but only probes that modify phosphocholine in teichoic acids from *Streptococcus pneumoniae* (*S. pneumoniae*) currently exist. This type of probe involves the use of choline modified with handles compatible for click

chemistry (both CuAAC[37] and SPAAC[38]), that promoted imaging experiments to visualize teichoic acids in *S. pneumoniae*. Choline is used by the cell only for teichoic acids when exogenously supplied (not for membrane phosphatidylcholine).[39] These modified choline probes are useful for studying a specific window of teichoic acids in bacterial cells, but more work is needed in this area to expand the metabolic labeling tools available.

For Gram-negative organisms, LPS (discussed in Section **1.3** Bacterial Cell Wall is targeted as a potential source of metabolic labeling. The basic, conserved structure of LPS involves lipid A, outer and inner core oligosaccharides, and a surface-exposed O-antigen polysaccharide. LPS is essential for Gram-negative organisms to survive.[40] Most of the probes developed thus far for targeting LPS are geared towards the core oligosaccharides (namely, keto-deoxyoctulosonate, KDO which is found only in Gram-negative organisms) and the O-antigen (where probes can be tailored to specific species, as this region varies amongst them). A KDO-N_3 probe was established by the Vauzeilles and Dukan groups, where they demonstrated cellular fluorescence after treatment of *E. coli* with KDO-N_3 followed by CuAAC with alkyne-488.[41] Since then, this probe has been used with SPAAC-compatible chemistry,[42] to identify Gram-negative organisms from a mixture containing both Gram-negative and Gram-positive species,[43, 44] and to label Gram-negative organisms in the intestinal tract of a live murine model.[13] Of the chemical probes that intend to label the O-antigen, there are many different types including fucose,[45] legionaminic acid,[46] pseudaminic acid,[47] and lipooligosaccharide (LOS)[48] targets. These involve azide-based handles that can be used for click-chemistry with a fluorescently compatible probe.

2.5 *Conclusion*

The work summarized in this Chapter highlights the versatility of metabolic labeling for bacterial cell processes. While this summary is extensive, there are many chemical probes that have been reported but are not discussed here. This Chapter encompasses the details of several metabolic reporters for peptidoglycan, glycan, glycoproteins, teichoic acids, and LPS biosynthesis and metabolic pathways. Many of these areas have

been explored deeply, but the overall number of probes to study these processes is limited, and there is still critical information that can be uncovered. The production of more specific and applicable compounds to understand bacterial pathways can tremendously aid in our knowledge base of methods for therapeutic avenues. The focus of the remainder of this thesis will be on chemical probes for metabolically labeling bacterial peptidoglycan.

2.6 *References*

1. Siegrist, M. S.; Swarts, B. M.; Fox, D. M.; Lim, S. A.; Bertozzi, C. R., Illumination of growth, division and secretion by metabolic labeling of the bacterial cell surface. *FEMS Microbiol Rev* **2015,** *39* (2), 184-202.

2. Gautam, S.; Gniadek, T. J.; Kim, T.; Spiegel, D. A., Exterior design: strategies for redecorating the bacterial surface with small molecules. *Trends Biotechnol* **2013,** *31* (4), 258-67.

3. Lam, H.; Oh, D.-C.; Cava, F.; Takacs Constantin, N.; Clardy, J.; de Pedro Miguel, A.; Waldor Matthew, K., D-Amino Acids Govern Stationary Phase Cell Wall Remodeling in Bacteria. *Science* **2009,** *325* (5947), 1552-1555.

4. Cava, F.; de Pedro, M. A.; Lam, H.; Davis, B. M.; Waldor, M. K., Distinct pathways for modification of the bacterial cell wall by non-canonical D-amino acids. *EMBO J* **2011,** *30* (16), 3442-3453.

5. Kuru, E.; Hughes, H. V.; Brown, P. J.; Hall, E.; Tekkam, S.; Cava, F.; de Pedro, M. A.; Brun, Y. V.; VanNieuwenhze, M. S., In Situ probing of newly synthesized peptidoglycan in live bacteria with fluorescent D-amino acids. *Angew Chem Int Ed Engl* **2012,** *51* (50), 12519-23.

6. Siegrist, M. S.; Whiteside, S.; Jewett, J. C.; Aditham, A.; Cava, F.; Bertozzi, C. R., d-Amino Acid Chemical Reporters Reveal Peptidoglycan Dynamics of an Intracellular Pathogen. *ACS Chemical Biology* **2013,** *8* (3), 500-505.

7. Liechti, G. W.; Kuru, E.; Hall, E.; Kalinda, A.; Brun, Y. V.; VanNieuwenhze, M.; Maurelli, A. T., A new metabolic cell-wall labelling method reveals peptidoglycan in Chlamydia trachomatis. *Nature* **2014,** *506* (7489), 507-510.

8. Sadamoto, R.; Niikura, K.; Sears, P. S.; Liu, H.; Wong, C.-H.; Suksomcheep, A.; Tomita, F.; Monde, K.; Nishimura, S.-I., Cell-Wall Engineering of Living Bacteria. *Journal of the American Chemical Society* **2002,** *124* (31), 9018-9019.

9. Shieh, P.; Siegrist, M. S.; Cullen, A. J.; Bertozzi, C. R., Imaging bacterial peptidoglycan with near-infrared fluorogenic azide probes. *Proceedings of the National Academy of Sciences* **2014,** *111* (15), 5456.

10. Hsu, Y. P.; Hall, E.; Booher, G.; Murphy, B.; Radkov, A. D.; Yablonowski, J.; Mulcahey, C.; Alvarez, L.; Cava, F.; Brun, Y. V.; Kuru, E.; VanNieuwenhze, M. S., Fluorogenic D-amino acids enable real-time monitoring of peptidoglycan biosynthesis and high-throughput transpeptidation assays. *Nat Chem* **2019,** *11* (4), 335-341.

11. Pidgeon, S. E.; Pires, M. M., Cell Wall Remodeling of Staphylococcus aureus in Live Caenorhabditis elegans. *Bioconjugate Chemistry* **2017,** *28* (9), 2310-2315.

12. Boersma, M. J.; Kuru, E.; Rittichier, J. T.; VanNieuwenhze, M. S.; Brun, Y. V.; Winkler, M. E., Minimal Peptidoglycan (PG) Turnover in Wild-Type and PG Hydrolase and Cell Division Mutants of Streptococcus pneumoniae D39 Growing Planktonically and in Host-Relevant Biofilms. *J Bacteriol* **2015,** *197* (21), 3472-85.

13. Hudak, J. E.; Alvarez, D.; Skelly, A.; von Andrian, U. H.; Kasper, D. L., Illuminating vital surface molecules of symbionts in health and disease. *Nat Microbiol* **2017,** *2*, 17099-17099.

14. Pidgeon, S. E.; Fura, J. M.; Leon, W.; Birabaharan, M.; Vezenov, D.; Pires, M. M., Metabolic Profiling of Bacteria by Unnatural C-terminated D-Amino Acids. *Angew Chem Int Ed Engl* **2015,** *54* (21), 6158-62.

15. Pidgeon, S. E.; Apostolos, A. J.; Nelson, J. M.; Shaku, M.; Rimal, B.; Islam, M. N.; Crick, D. C.; Kim, S. J.; Pavelka, M. S.; Kana, B. D.; Pires, M. M., L,D-Transpeptidase Specific Probe Reveals Spatial Activity of Peptidoglycan Cross-Linking. *ACS Chemical Biology* **2019,** *14* (10), 2185-2196.

16. Gautam, S.; Kim, T.; Shoda, T.; Sen, S.; Deep, D.; Luthra, R.; Ferreira, M. T.; Pinho, M. G.; Spiegel, D. A., An Activity-Based Probe for Studying Crosslinking in Live Bacteria. *Angew Chem Int Ed Engl* **2015,** *54* (36), 10492-6.

17. Gautam, S.; Kim, T.; Spiegel, D. A., Chemical Probes Reveal an Extraseptal Mode of Cross-Linking in Staphylococcus aureus. *Journal of the American Chemical Society* **2015,** *137* (23), 7441-7447.

18. Bisson-Filho, A. W.; Hsu, Y.-P.; Squyres, G. R.; Kuru, E.; Wu, F.; Jukes, C.; Sun, Y.; Dekker, C.; Holden, S.; VanNieuwenhze, M. S.; Brun, Y. V.; Garner, E. C., Treadmilling by FtsZ filaments drives peptidoglycan synthesis and bacterial cell division. *Science (New York, N.Y.)* **2017,** *355* (6326), 739-743.

19. García-Heredia, A.; Pohane, A. A.; Melzer, E. S.; Carr, C. R.; Fiolek, T. J.; Rundell, S. R.; Lim, H. C.; Wagner, J. C.; Morita, Y. S.; Swarts, B. M.; Siegrist, M. S., Peptidoglycan precursor synthesis along the sidewall of pole-growing mycobacteria. *Elife* **2018,** *7*.

20. Davis, K. M.; Weiser, J. N., Modifications to the peptidoglycan backbone help bacteria to establish infection. *Infect Immun* **2011,** *79* (2), 562-570.

21. Liang, H.; DeMeester, K. E.; Hou, C. W.; Parent, M. A.; Caplan, J. L.; Grimes, C. L., Metabolic labelling of the carbohydrate core in bacterial peptidoglycan and its applications. *Nat Commun* **2017,** *8*, 15015.

22. DeMeester, K. E.; Liang, H.; Jensen, M. R.; Jones, Z. S.; D'Ambrosio, E. A.; Scinto, S. L.; Zhou, J.; Grimes, C. L., Synthesis of Functionalized N-Acetyl Muramic Acids To Probe Bacterial Cell Wall Recycling and Biosynthesis. *Journal of the American Chemical Society* **2018,** *140* (30), 9458-9465.

23. Perley-Robertson, G. E.; Yadav, A. K.; Winogrodzki, J. L.; Stubbs, K. A.; Mark, B. L.; Vocadlo, D. J., A Fluorescent Transport Assay Enables Studying AmpG Permeases Involved in Peptidoglycan Recycling and Antibiotic Resistance. *ACS Chem Biol* **2016,** *11* (9), 2626-35.

24. Bertozzi, C. R.; Kiessling, L. L., Chemical glycobiology. (0036-8075 (Print)).

25. Backus, K. M.; Boshoff, H. I.; Barry, C. S.; Boutureira, O.; Patel, M. K.; D'Hooge, F.; Lee, S. S.; Via, L. E.; Tahlan, K.; Barry, C. E., 3rd; Davis, B. G., Uptake of unnatural trehalose analogs as a reporter for Mycobacterium tuberculosis. *Nat Chem Biol* **2011,** *7* (4), 228-35.

26. Rodriguez-Rivera, F. P.; Zhou, X.; Theriot, J. A.; Bertozzi, C. R., Visualization of mycobacterial membrane dynamics in live cells. *Journal of the American Chemical Society* **2017,** *139* (9), 3488-3495.

27. Swarts, B. M.; Holsclaw, C. M.; Jewett, J. C.; Alber, M.; Fox, D. M.; Siegrist, M. S.; Leary, J. A.; Kalscheuer, R.; Bertozzi, C. R., Probing the Mycobacterial Trehalome with Bioorthogonal Chemistry. *Journal of the American Chemical Society* **2012,** *134* (39), 16123-16126.

28. Rundell, S. R.; Wagar, Z. L.; Meints, L. M.; Olson, C. D.; O'Neill, M. K.; Piligian, B. F.; Poston, A. W.; Hood, R. J.; Woodruff, P. J.; Swarts, B. M., Deoxyfluoro-d-trehalose

(FDTre) analogues as potential PET probes for imaging mycobacterial infection. *Org Biomol Chem* **2016,** *14* (36), 8598-609.

29. Ojha, A. K.; Trivelli, X.; Guerardel, Y.; Kremer, L.; Hatfull, G. F., Enzymatic hydrolysis of trehalose dimycolate releases free mycolic acids during mycobacterial growth in biofilms. *J Biol Chem* **2010,** *285* (23), 17380-9.

30. Lee, J. J.; Lee, S. K.; Song, N.; Nathan, T. O.; Swarts, B. M.; Eum, S. Y.; Ehrt, S.; Cho, S. N.; Eoh, H., Transient drug-tolerance and permanent drug-resistance rely on the trehalose-catalytic shift in Mycobacterium tuberculosis. *Nat Commun* **2019,** *10* (1), 2928.

31. Benz, I.; Schmidt, M. A., Never say never again: protein glycosylation in pathogenic bacteria. *Mol Microbiol* **2002,** *45* (2), 267-76.

32. Champasa, K.; Longwell, S. A.; Eldridge, A. M.; Stemmler, E. A.; Dube, D. H., Targeted identification of glycosylated proteins in the gastric pathogen Helicobacter pylori (Hp). *Mol Cell Proteomics* **2013,** *12* (9), 2568-86.

33. Kaewsapsak, P.; Esonu, O.; Dube, D. H., Recruiting the host's immune system to target Helicobacter pylori's surface glycans. *Chembiochem* **2013,** *14* (6), 721-6.

34. Clark, E. L.; Emmadi, M.; Krupp, K. L.; Podilapu, A. R.; Helble, J. D.; Kulkarni, S. S.; Dube, D. H., Development of Rare Bacterial Monosaccharide Analogs for Metabolic Glycan Labeling in Pathogenic Bacteria. *ACS Chemical Biology* **2016,** *11* (12), 3365-3373.

35. Neuhaus, F. C.; Baddiley, J., A continuum of anionic charge: structures and functions of D-alanyl-teichoic acids in gram-positive bacteria. *Microbiol Mol Biol Rev* **2003,** *67* (4), 686-723.

36. Swoboda, J. G.; Campbell, J.; Meredith, T. C.; Walker, S., Wall teichoic acid function, biosynthesis, and inhibition. *Chembiochem* **2010,** *11* (1), 35-45.

37. Di Guilmi, A. M.; Bonnet, J.; Peiβert, S.; Durmort, C.; Gallet, B.; Vernet, T.; Gisch, N.; Wong, Y. S., Specific and spatial labeling of choline-containing teichoic acids in Streptococcus pneumoniae by click chemistry. *Chem Commun (Camb)* **2017,** *53* (76), 10572-10575.

38. Bonnet, J.; Wong, Y.-S.; Vernet, T.; Di Guilmi, A. M.; Zapun, A.; Durmort, C., One-Pot Two-Step Metabolic Labeling of Teichoic Acids and Direct Labeling of

Peptidoglycan Reveals Tight Coordination of Both Polymers Inserted into Pneumococcus Cell Wall. *ACS Chemical Biology* **2018,** *13* (8), 2010-2015.

39. Sohlenkamp, C.; López-Lara, I. M.; Geiger, O., Biosynthesis of phosphatidylcholine in bacteria. *Prog Lipid Res* **2003,** *42* (2), 115-62.

40. Zhang, G.; Meredith, T. C.; Kahne, D., On the essentiality of lipopolysaccharide to Gram-negative bacteria. *Curr Opin Microbiol* **2013,** *16* (6), 779-85.

41. Dumont, A.; Malleron, A.; Awwad, M.; Dukan, S.; Vauzeilles, B., Click-mediated labeling of bacterial membranes through metabolic modification of the lipopolysaccharide inner core. *Angew Chem Int Ed Engl* **2012,** *51* (13), 3143-6.

42. Nilsson, I.; Grove, K.; Dovala, D.; Uehara, T.; Lapointe, G.; Six, D. A., Molecular characterization and verification of azido-3,8-dideoxy-d-manno-oct-2-ulosonic acid incorporation into bacterial lipopolysaccharide. *J Biol Chem* **2017,** *292* (48), 19840-19848.

43. Fugier, E.; Dumont, A.; Malleron, A.; Poquet, E.; Mas Pons, J.; Baron, A.; Vauzeilles, B.; Dukan, S., Rapid and Specific Enrichment of Culturable Gram Negative Bacteria Using Non-Lethal Copper-Free Click Chemistry Coupled with Magnetic Beads Separation. *PLoS One* **2015,** *10* (6), e0127700.

44. Sherratt, A. R.; Rouleau, Y.; Luebbert, C.; Strmiskova, M.; Veres, T.; Bidawid, S.; Corneau, N.; Pezacki, J. P., Rapid Screening and Identification of Living Pathogenic Organisms via Optimized Bioorthogonal Non-canonical Amino Acid Tagging. *Cell Chem Biol* **2017,** *24* (8), 1048-1055.e3.

45. Yi, W.; Liu, X.; Li, Y.; Li, J.; Xia, C.; Zhou, G.; Zhang, W.; Zhao, W.; Chen, X.; Wang, P. G., Remodeling bacterial polysaccharides by metabolic pathway engineering. *Proc Natl Acad Sci U S A* **2009,** *106* (11), 4207-4212.

46. Mas Pons, J.; Dumont, A.; Sautejeau, G.; Fugier, E.; Baron, A.; Dukan, S.; Vauzeilles, B., Identification of living Legionella pneumophila using species-specific metabolic lipopolysaccharide labeling. *Angew Chem Int Ed Engl* **2014,** *53* (5), 1275-8.

47. Andolina, G.; Wei, R.; Liu, H.; Zhang, Q.; Yang, X.; Cao, H.; Chen, S.; Yan, A.; Li, X. D.; Li, X., Metabolic Labeling of Pseudaminic Acid-Containing Glycans on Bacterial Surfaces. *ACS Chemical Biology* **2018,** *13* (10), 3030-3037.

48. Heise, T.; Langereis, J. D.; Rossing, E.; de Jonge, M. I.; Adema, G. J.; Büll, C.; Boltje, T. J., Selective Inhibition of Sialic Acid-Based Molecular Mimicry in Haemophilus influenzae Abrogates Serum Resistance. *Cell Chem Biol* **2018,** *25* (10), 1279-1285.e8.

Chapter 3 Remodeling of Crossbridges Controls Peptidoglycan Crosslinking Levels in Bacterial Cell Walls

Adapted from: Apostolos, A. J.; Pidgeon, S. E.; Pires, M. M., Remodeling of Cross-bridges Controls Peptidoglycan Cross-linking Levels in Bacterial Cell Walls. *ACS Chemical Biology* **2020**, *15* (5), 1261-1267.

3.1 *Abstract*

Cell walls are barriers found in almost all known bacterial cells. These structures establish a controlled interface between the external environment and vital cellular components. A primary component of cell wall is a highly cross-linked matrix called peptidoglycan (PG). PG cross-linking, carried out by transglycosylases and transpeptidases, is necessary for proper cell wall assembly. Transpeptidases, targets of β-lactam antibiotics, stitch together two neighboring PG stem peptides (acyl-donor and acyl-acceptor strands). We recently described a novel class of cellular PG probes that were processed exclusively as acyl-donor strands. Herein, we have accessed the other half of the transpeptidase reaction by developing probes that are processed exclusively as acyl-acceptor strands. The critical nature of the cross-bridge on the PG peptide was demonstrated in live bacterial cells, and surprising promiscuity in cross-bridge primary sequence was found in various bacterial species. Additionally, acyl-acceptor probes provided insight into how chemical remodeling of the PG cross-bridge (e.g., amidation) can modulate cross-linking levels, thus establishing a physiological role of PG structural variations. Together, the acyl-donor and -acceptor probes will provide a versatile platform to interrogate PG cross-linking in physiologically relevant settings.

3.2 *Introduction*

Gram-positive pathogens continue to impose a significant global public health burden.[1] Among these organisms, Enterococci are one of the leading causes of nosocomial infections.[2] With the rise in antibiotic drug resistance, it has become clear that more

bacterial targets are needed to improve the therapeutic options to fight Enterococci infections. Peptidoglycan (PG), an essential component of bacterial cell walls, is one of the most important targets of antibiotics. Disaccharides of *N*-acetylglucosamine (GlcNAc) and *N*-acetylmuramic acid (MurNAc) make up the basic PG unit, which is further decorated with a pentameric stem peptide (e.g., L-Ala-D-isoGlx-L-Lys-D-Ala-D-Ala).[3, 4] PG units are polymerized and crosslinked via transglycosylation and transpeptidation (TP) reactions that assemble the sugars and peptides, respectively. PG crosslinking is essential, and, therefore, molecules that block this reaction are traditionally valuable antibiotics (e.g., β-lactams and vancomycin) and continue to result in promising drug leads (e.g., teixobactin).[5-7]

Intense efforts have led to a greater understanding of the chemical makeup, mechanism of assembly, and essential proteins that construct the PG network. Moreover, there is some evidence that small structural modifications within the PG matrix can alter the overall plasticity and physical properties of the cell wall (e.g., resistance to lysozyme).[8-10] Chemical composition of the stem peptide primary sequence can vary by the amidation/methylation of carboxylic groups, removal of amino acids, variation of amino acid character, and extensive alteration to the central lysine group. Yet, for the most part, their physiological impact remains elusive.[11-14]

The 3rd position with the PG stem peptide has defining structural characteristics. As an example, the difference of a carboxylic acid group on L-Lys versus *meso*-2,6-diaminopimelic acid (*m*-DAP) has important implications in the activation of the human innate immune system.[15] In *Enterococcus faecium* (*E. faecium*), the lysine sidechain is modified with D-iAsx while *Enterococcus faecalis* (*E. faecalis*) displays L-Ala-L-Ala. In addition, the nature of the crossbridge (the amino acids anchored onto the lysine residues) is critical based on its role in the nucleophilic step during crosslinking reactions. There are two main classes of PG crosslinking enzymes: D,D-TPs and L,D-TPs (**Figure 3.1**). Crosslinking by Penicillin Binding Protein (PBP) D,D-TPs generate 4-3 peptide crosslinks and L,D-TPs (Ldts) create 3-3 crosslinks within PG.

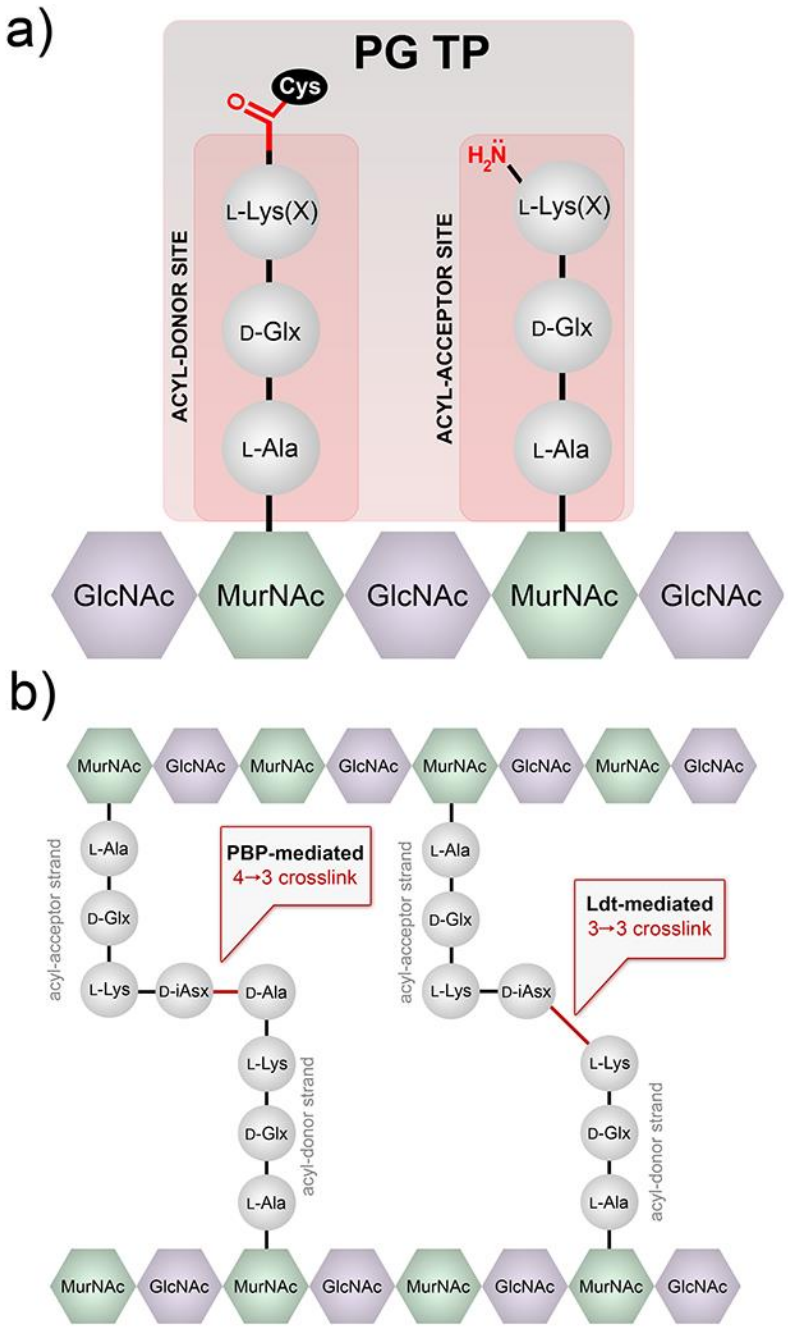

Figure 3.1 *Crosslinking reaction by TPs.*

(a) Example of two binding sites (acyl-donor and -acceptor) at the intermediate step of the crosslinking reaction are depicted. The acyl-chain is covalently anchored on the TP, which is subsequently transferred to the amino group on the acyl-acceptor strand. X represents the crossbridging amino acids. (b) Schematic of PG crosslinking in *E. faecium* showing the 2 types of crosslinks observed.

Fundamental understanding of PG crosslinking is key to define the processes that control PG structure and may provide novel drug targets. Single D-amino acid PG probes have spurred valuable insight into PG crosslinking in live bacterial cells.[16-21] Furthermore, elegant prior *in vitro* studies using synthetic PG analogs have provided insight into the substrate structural requirements of TPs.[12, 22-25] However, fewer reports have described probes that decipher TP substrate requirements in live bacterial cells. A recent example of a synthetic L-Lys-D-Ala-D-Ala stem peptide mimic led to the demonstration of extraseptal TP activity in *Staphylococcus aureus* (*S. aureus*).[26] Likewise, we recently reported the use of synthetic PG probes to establish crosslinking parameters based on the acyl-donor strand of Ldts.[27] We have now built on those findings by developing complementary probes that selectively track and dissect acyl-acceptor strand processing by TPs in live bacterial cells.

We initially hypothesized that structural analogs of the two TP substrates could be developed to control active site loading.

In designing our previous acyl-donor probe **1**, we mimicked the stem peptide fragment as a tetrapeptide and blocked the nucleophilic site on the acyl-acceptor strand (**Figure 3.2a**). In this work, the acyl-acceptor specific probe **2** was designed by installing the acyl-acceptor fragment (crossbridging D-iAsx in the case of *E. faecium*) and removing the terminal fragment recognized by the acyl-donor site (terminal D-Ala and/or D-Ala-D-Ala). Therefore, PG probes with the basic scaffold of tripeptide **2** should act solely as an acyl-acceptor strand. To track incorporation into the PG, a fluorescent handle was added to the *N*-terminus of the stem tripeptide analogs. Incubation of live bacterial cells with tripeptide probes is expected to result in their covalent incorporation into the PG scaffold by TPs (**Figure 3.2b**). Crosslinking can then be readily quantified and analyzed using standard fluorescence-based techniques, thus providing a mode to interrogate how primary sequences of the acyl-acceptor strand modulate PG crosslinking (**Figure 3.2c**).

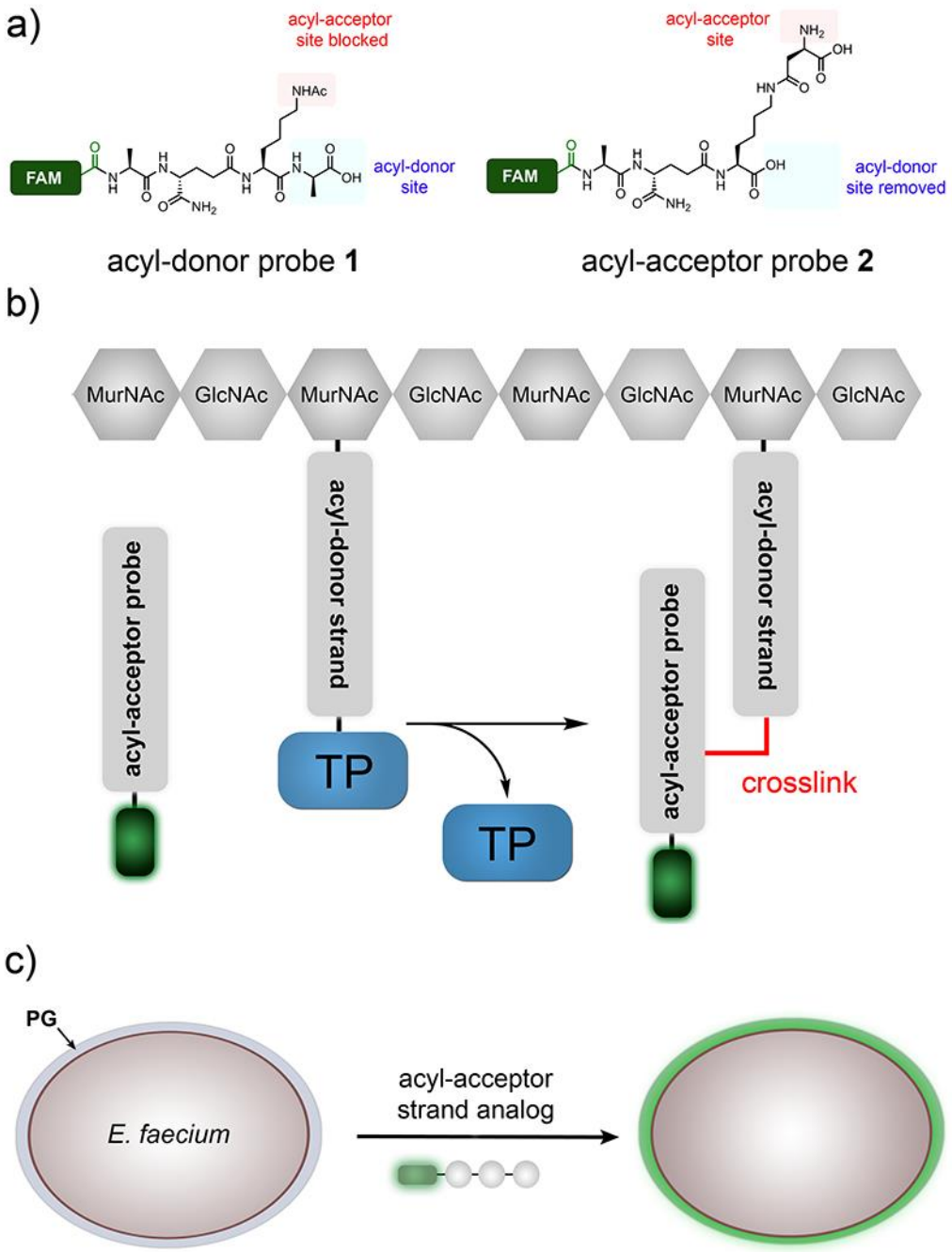

Figure 3.2 *Design of tripeptide probes and the assay to assess acyl-acceptor strands in live cells.*

(a) Structure-based design of acyl-donor and -acceptor probes. (b) Schematic diagram showing how the fluorescently tagged tripeptide probe gets covalently crosslinked into the bacterial PG scaffold. (c) Schematic of the whole cell analysis that can be accessed by the tripeptide probes.

3.3 *Results and Discussion*

3.3.1 *Tripeptide probes as acyl-acceptor strands in E. faecium*

At first, we synthesized a panel of tripeptide probes that were designed to investigate acyl-acceptor strand recognition in live *E. faecium* (**Figure 3.3**). D-iAsx is the canonical crossbridge amino acid in *E. faecium*, where a nucleophilic attack by the sidechain *N*-terminus nitrogen leads to formation of PG crosslinks. All probes were synthesized using standard solid phase peptide chemistry and included a carboxy-fluorescein tag (FAM). *E. faecium* cells were treated with individual probes and cellular fluorescence levels were measured after overnight incubation. The first two stem peptide mimics, **TriQK** and **TriQD**, were designed to test the role of crossbridging amino acids is the acyl-capture step of TP. Our results showed that when cells were treated with **TriQK**, which lacks the crossbridging amino acid, fluorescence levels were near background (**Figure 3.3a**). Introduction of the crossbridge D-iAsp (**TriQD**) led to ~7- fold fluorescence increase over background. These results provide *in vivo* evidence for the importance of the crossbridge for robust crosslinking of the PG scaffold and suggest that the enzyme responsible for D-iAsp installation, Asl_{fm},[28] is a potential narrow-spectrum drug target. Given that only approximately 60% of the lysines are modified with D-iAsx in *E. faecium*[29], and that we have evidence that unmodified lysine residues do not participate in TP reactions as acyl acceptors, these results also suggest a mode of controlling PG crosslinking based on Asl_{fm} processing of PG precursors in the cytosol of cells prior to exposure to TPs.

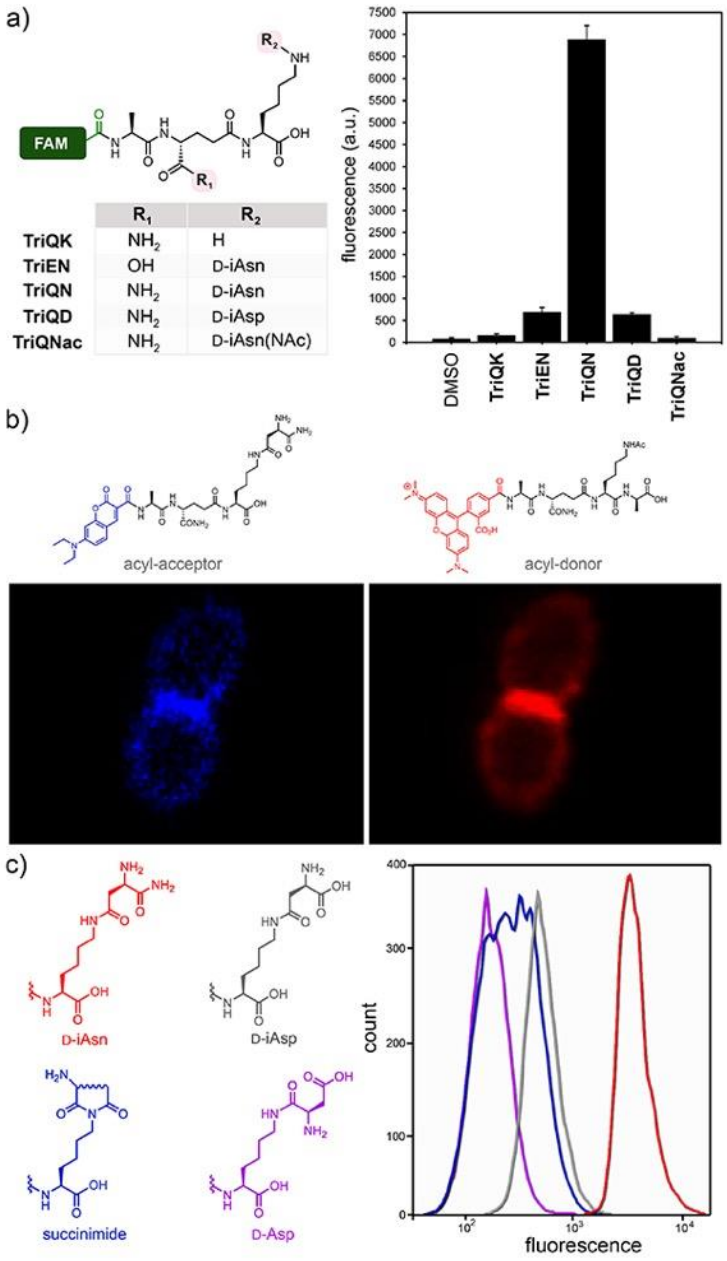

Figure 3.3 *Crosslinking of tripeptide probes in live E. faecium cells.*

(a) Chemical series tripeptide probes based on the modifications at the D-iGlx and lysine sidechain; FAM = carboxyfluorescein. Flow cytometry analysis of *E. faecium* (D344s) treated overnight with 100 μM of tri-peptide probes. Data are represented as mean + SD (n = 3). (b) Confocal microscopy of *E. faecium* cells labeled with the designated probes (100 μM) for 5 min. Scale bar = 2 μm. (c) Labeling of cells similar to (a) with a focused library of re-arranged crossbriges.

We then analyzed the role of amidation in the 2nd position D-iGlu in the crosslinking step. Recent genetic analyses revealed the essential nature of the genes encoding the enzymes that carry out the amidation of D-iGlu to D-iGln in *S. aureus* and *Streptococcus pneumoniae*.[30, 31] Subsequent *in vitro* characterization suggested that lack of D-iGlu amidation impairs PG crosslinking.[11, 23] Yet, it remained unresolved whether D-iGlu amidation impacts processing at the acyl-donor, acyl-acceptor, or both sites. We recently demonstrated that amidation of D-iGlu is critical for the acyl-donor strand for both classes of TPs.[27] To test these concepts in the acyl-acceptor substrate, *E. faecium* cells were treated with **TriEN**. In sharp contrast to the D-iGln variant (**TriQN**), cellular fluorescence levels were significantly lower in cells treated with the D-iGlu variant (**TriEN**).

We next evaluated how chemical remodeling of the acyl-acceptor strand may influence TP crosslinking in *E. faecium*. While the sidechain of the 3rd position lysine is initially loaded with a D-iAsp crossbridge, its carboxylic acid can be biochemically amidated to generate D-iAsn crossbridges to varying levels in *E. faecium*.[29] In fact, for similar organisms like *Lactococcus lactis* (*L. lactis*) it has been estimated that ~75% of crossbridges D-iAsp are amidated to D-iAsn.[32] Yet, the physiological and TP-processing consequences of D-iAsp amidation remain unresolved. We hypothesized that we could establish the role of amidation using synthetic analogs in live bacteria. Quite strikingly, treatment of *E. faecium* with **TriQN** resulted in considerably higher crosslinking levels relative to **TriQD** (**Figure 3.3a**). These results suggest that amidation of D-iAsp within the acyl-acceptor strand play a critical role in controlling PG crosslinking levels. Moreover, we demonstrated that the crossbridge of **TriQN** is, in fact, the acyl-acceptor site by building a control probe (**TriQNAc**) in which the nucleophilic amino group is acetylated to block acyl-capture. Fluorescence levels for cells treated with **TriQNAc** were near background, a result that is consistent with the site of acyl-capture.

A different strain of *E. faecium* showed a similar labeling profile as the parental drug-sensitive strain (**Figure 3.4**), which suggests that a different strain within type of bacteria has similar acyl-acceptor substrate preferences. Moreover, cell labeling was not

entirely disrupted in an isogenic strain lacking Ldt TP gene (ldt_{fm}), which suggests that the tripeptide probe is likely incorporated into the PG scaffold *via* L,D-TPs and D,D-TPs (**Figure 3.4**). Confocal microscopy was then used to delineate the incorporation of the probes within the PG scaffold of live cells. For these experiments, a short pulse labeling step was performed with the acyl-acceptor probe modified with a blue fluorophore and the acyl-donor probe modified with a red fluorophore (**Figure 3.3b**). From our results, it is clear that there is some overlap between PG incorporation of these probes, and we established that the septal region is the primary site of PG incorporation.

Having shown that amidation of the crossbridge (D-iAsp to D-iAsn) had significant consequences in crosslinking levels in *E. faecium*, we tested the commonality these observations across other species with similarly structured crossbridges.[32] Consistently, labeling levels in *L. lactis* and *Lactococcus casei* (*L. casei*) were considerably lower with **TriQD** relative to **TriQN** (**Figure 3.5**). Interestingly, a recent transposon mutagenesis screen revealed a single gene responsible for the immune-augmenting activity of *L. casei*:*asnH* whose protein product amidates D-iAsp to D-iAsn.[33] It was observed that the mutant strain not expressing AsnH lacked thick peptidoglycan in electron microscopy analysis, a finding that is consistent with D-iAsp amidation having an significant effect in PG crosslinking. Together, our data point to a three-level biochemical control (addition of crossbridge, D-iGlu to D-iGln, and D-iAsp to D-iAsn) of the acyl-acceptor substrate structure that likely combine to tune crosslinking level in *E. faecium*.

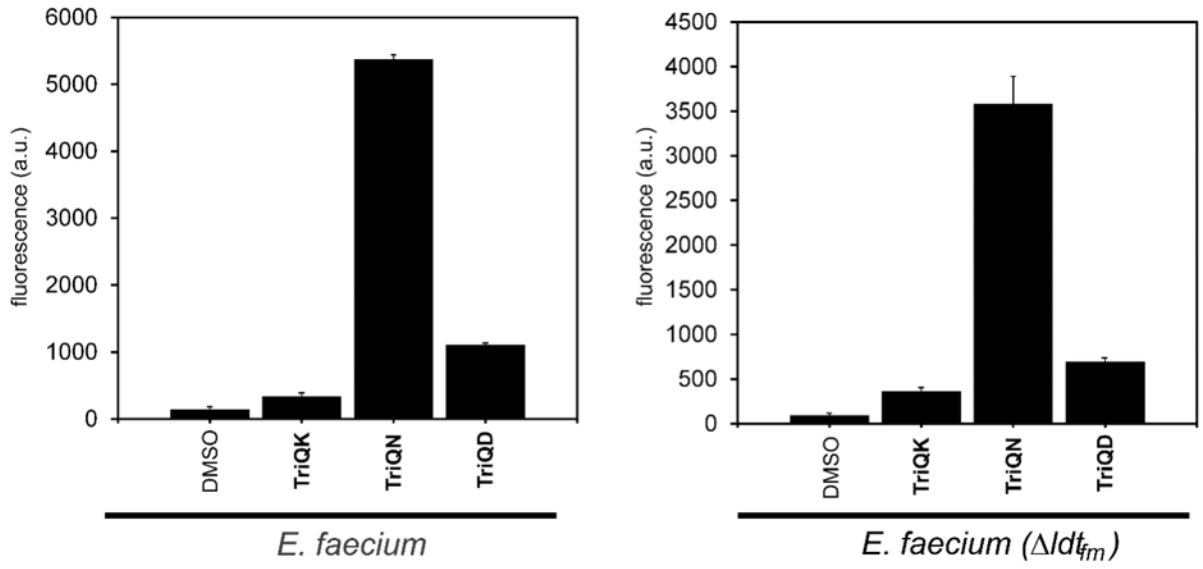

Figure 3.4 *Flow cytometry analysis of an additional E. faecium strain and isogenic strain lacking Ldt TP gene (ldt$_{fm}$) incubated overnight with 100 μM* ***TriQK****,* ***TriQN****, or* ***TriQD****. Data are represented as mean + SD (n = 3).*

A possible consequence of D-iAsp amidation is spontaneous re-arrangement of isoasparagine. These types of re-arrangements are well documented in mammalian proteins and also play important roles in intein splicing.[34-37] Isoasparagine re-arrangement is initiated by the internal attack of the amide nitrogen onto the carboxamide of isoasparagine yielding a cyclic succinimide intermediate, which can be hydrolyzed into either aspartic acid or isoaspartic acid. A solid-state NMR analysis of *E. faecium* PG revealed fingerprints consistent with all such re-arrangement products.[29] We wondered if spontaneous D-iAsn re-arrangement products could still serve as competent crossbridges for PG crosslinking, and, therefore, built a secondary library that mapped out three of the possible products (**Figure 3.3c** and **Figure 3.6**). *E. faecium* labeling results showed that all re-arranged products were considerably poorer TP substrates. It is intriguing to speculate about the biological impact in the nonenzymatic deamidation of D-iAsn considering its potential deleterious effect in PG crosslinking. Perhaps, it could serve as a molecular timer in a similar context as what has been described to deamidation of asparagine in human proteins. A possibility may be that D-iAsn re-arrangement could

provide a competitive advantage by reducing susceptibility against bacteriophage endolysins that specifically cleave D-iAsn but not D-Asp crosslinks.[38]

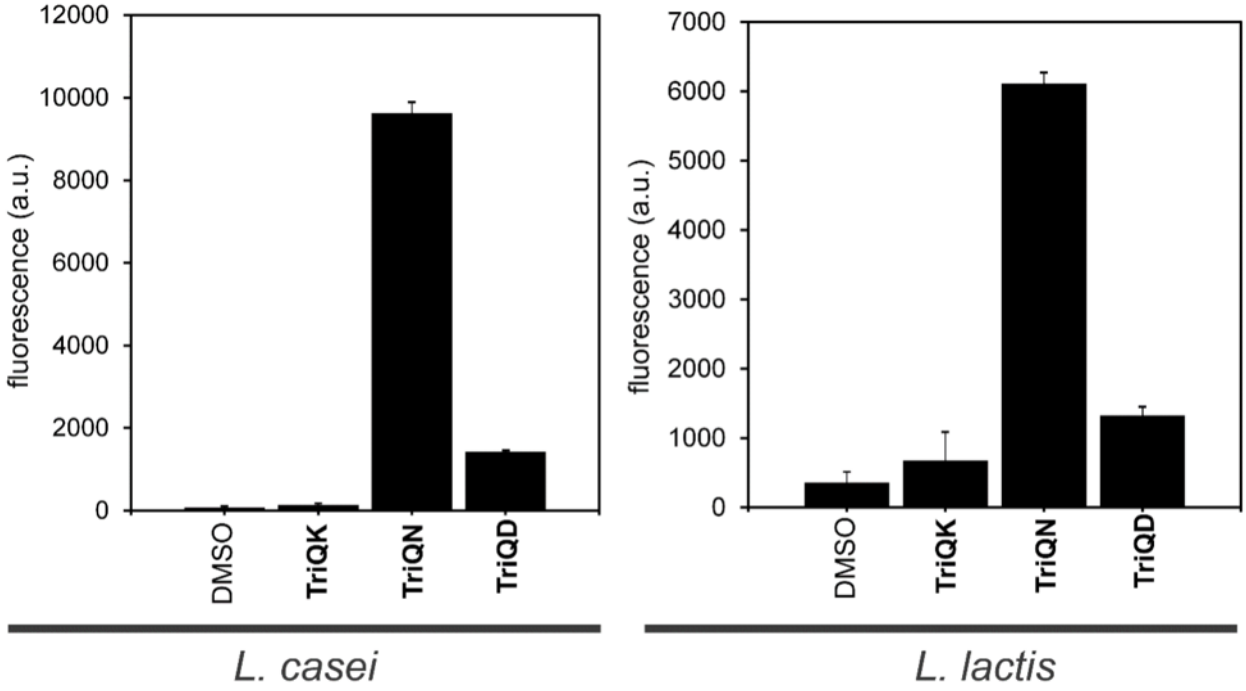

Figure 3.5 *Flow cytometry analysis of L. casei and L. lactis (ATCC 11454) strains, which have similarly structured PG crossbridges as E. faecium, incubated overnight with 100 μM* ***TriQK****,* ***TriQN****, or* ***TriQD****. Data are represented as mean + SD (n = 3).*

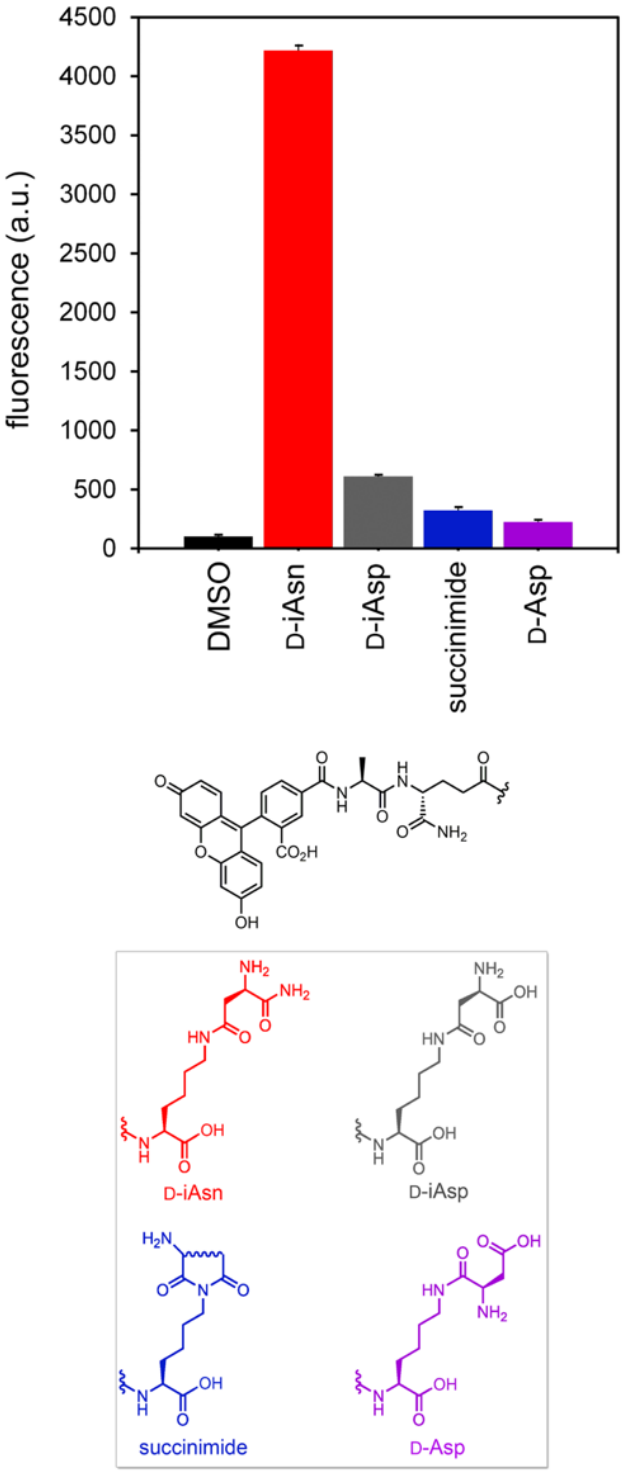

Figure 3.6 *Flow cytometry analysis of E. faecium D344s incubated overnight with 100 μM* ***D-iAsn***, ***D-iAsp***, ***succinimide***, *or* ***D-Asp****. Data are represented as mean + SD (n = 3). The structure of each is shown below flow cytometry data.*

3.3.2 *Tripeptide probes as acyl-acceptor strands in E. faecalis*

To extend our results to another type of Enterococci, acyl-acceptors probes were adopted for *E. faecalis*. In the case of *E. faecalis*, ligases BppA1 and BppA2 are responsible for transferring L-Ala from Ala-*t*RNA to the first and 2nd positions of the ε-amino group of lysine of PG precursors, respectively.[39] We synthesized **TriQAA**, which mimics the crossbridge in *E. faecalis,* to initially test acyl-acceptor processing (**Figure 3.7a**). Incubation of *E. faecalis* cells with **TriQAA** led to a ~10.5 fold increase over the unmodified lysine side chain **TriQK**, thus again demonstrating the necessity for a crossbridging unit for proper acyl capture strand in Enterococci PG crosslinking. Inverting the stereochemistry of the crossbridge in **TriQAA** to **TriQaa** also led to baseline fluorescence, indicating that TPs are stereospecific at the acyl-acceptor position. Acetylation of the *E. faecalis* probe, **TriQAAac**, which blocks acyl-acceptor nucleophilic site, led to baseline fluorescence levels. This finding is consistent with the amino group of the terminal L-alanine as the nucleophile for covalent crosslinking into the PG scaffold. Surprisingly, lack of amidation at the second position (**TriEAA**) only resulted in a ~1.3-fold decrease in fluorescence, showing that amidation may not be an absolute requirement for the acyl-acceptor recognition in *E. faecalis*.

3.3.3 *Tripeptide probes as acyl-acceptor strands in S. aureus*

We next turned our attention to the problematic human pathogen *S. aureus*. In *S. aureus*, peptidyl transferases FemX, FemA, and FemB catalyze the stepwise addition of five glycines to the lysine residue on the 3rd position of the PG precursor.[40-42] Recently, Walker and co-workers isolated PG precursors corresponding to one, three, and five glycine units and showed *in vitro* that PBP transpeptidases have varying levels of preference for the length of the glycine chain.[12] We built a library of tripeptide *S. aureus* probes that complement their approach by assessing the acyl-acceptor preference in live bacterial cells. We synthesized **TriQG1-6** (**Figure 3.7b**), corresponding to glycine chains from 1 to 6 units, and measured their incorporation into the PG scaffold of *S. aureus* cells.

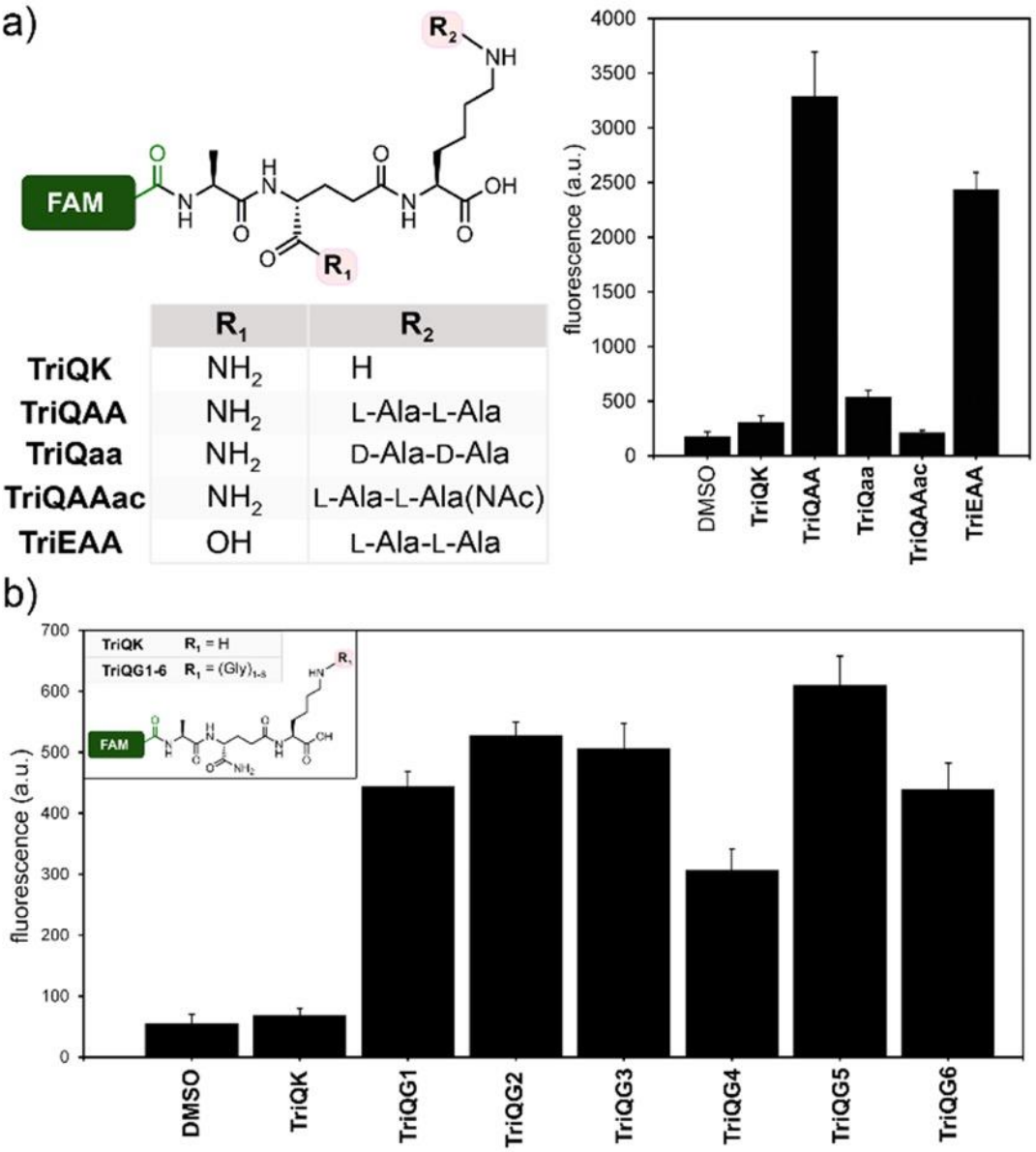

Figure 3.7 *Crosslinking of tripeptide probes in live E. faecalis and S. aureus cells.*

Chemical series tripeptide probes based corresponding to the stem peptide of (a) *E. faecalis* and (b) *S. aureus*. Flow cytometry analysis of cells treated overnight with 100 µM of tri-peptide probes. Data are represented as mean + SD (n = 3).

Consistent with our previous results, the absence of glycine modification (**TriQK**) resulted in background levels of PG incorporation. Interestingly, addition of a single glycine (**TriQG1**) led to ~7-fold increase in cellular fluorescence levels.

These results are consistent with a previously reported viable *S. aureus femAB*-null strain in which one glycine crossbridges were observed, albeit with severe crosslinking defects and impaired growth.[42, 43] Our results clearly demonstrate the physiological consequence of a lack of a single glycine unit and point to FemX is an particularly attractive target for therapeutic development, something that had been suggested but had not been observed in live bacterial cells due to the lethality of *femX*-deletion.[44] Crossbridges of 2 to 5 glycine resulted in comparable labeling levels. Extending beyond the natural pentaglycine chain (**TriQG6**) did not significantly impact crosslinking, which suggests that there is a high level of flexibility by the acyl-acceptor strand in *S. aureus*.

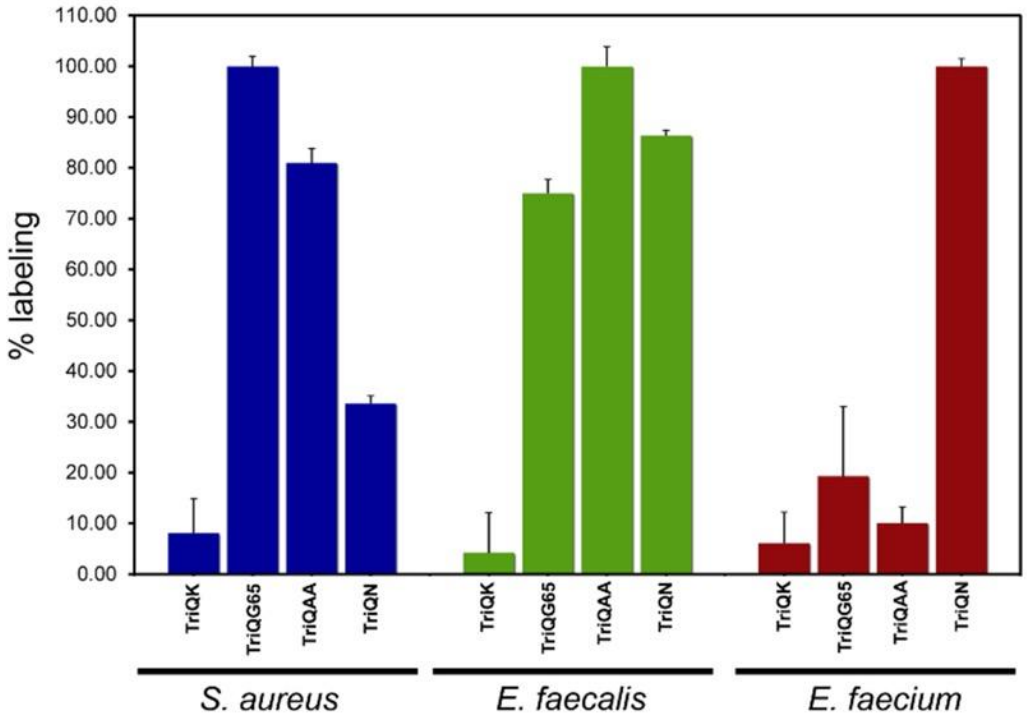

Figure 3.8 *Crossbridge preferences across bacterial species. Flow cytometry analysis of cells treated overnight with 100 μM of tri-peptide probes. Data are represented as mean + SD (n = 3).*

3.3.4 *Examining crossbridge preferences across species*

Having individually established the structural preference of the acyl-acceptor strand for various bacteria, we next set out to examine how crossbridges are tolerated by TPs across different species. Because TPs are frequent targets of β-lactams and other potent antibiotics, these enzymes play central roles in the drug resistance among several classes of medically relevant bacteria.[45] Moreover, mobile elements carrying TP genetic information can be a powerful modality for the acquisition of drug resistant phenotypes. The *mecA* gene underpinning the drug resistant phenotype of Methicillin-resistant *Staphylococcus aureus* (MRSA) has been proposed to originate from *Staphylococcus sciuri* (*S. sciuri*).[46] Therefore, the ability of TPs to process diverse PG architectures may have implications on the potential of TP to cross polinate drug resistance phenotypes. As an example, it was recently shown that commensal streptococci can serve as a reservoir for PBPs that can cross pollinate drug resistant phenotypes.[47]

To investigate the tolerance of non-native crossbridges in PG crosslinking reactions, the three canonical crossbridges (**TriQN**, **TriQAA**, and **TriQG5**) were incubated with *E. faecium*, *E. faecalis*, and *S. aureus*. *S. aureus* showed some promiscuity in accepting both **TriQAA** and **TriQN** (**Figure 3.8**) while still demonstrating some preference for pentaglycine crossbridge. Conversely, *E. faecium* showed strong preference for its natural acyl-acceptor strand **TriQN**. Treatment of *E. faecium* cells with **TriQAA** or **TriQG5** led to background fluorescence levels. Strikingly, *E. faecalis* showed little preference in the acyl-acceptor side chain and labeled well with all three tripeptide probes. These findings are consistent with previous *in vitro* studies that illustrated the promiscuity of *E. faecalis* TPs in accepting non-native crossbridges.[48, 49] Our results provide *in vivo* evidence that some bacterial strains possess a high degree of tolerance for exogenous crossbridges, which may ultimately provide a potentially viable drug resistance modality.

3.4 *Conclusion*

Targeting the enzymatic processes that control PG assembly is a powerful method of disabling bacterial pathogens. Overall, our results demonstrate the requirement of the crossbridge in acyl-acceptors for proper crosslinking by TPs in three different types of bacteria, thus reinforcing the concept that lysine modification is pivotal in tuning the PG crosslinking machinery. Future investigations will center on finding out how flexibility in PG crosslinking may promote the evolution of drug resistance. In developing a comprehensive structural analysis of both the acyl-donor and -acceptor strands, we anticipate that these results may guide drug design and open new avenues of therapeutic modalities.

3.5 *Materials and Methods*

Materials. All peptide related reagents (resin, coupling reagent, deprotection reagent, amino acids, and cleavage reagents) were purchased from ChemImpex. Bacterial strains *E. faecium* D344s and *E. faecalis* ATCC 29212 were grown in brain heart infusion broth for all experiments. *S. aureus* SC01 was grown in lysogeny broth.

Flow cytometry analysis of bacteria labeling with *E. faecium*. Brain heart infusion (BHI) broth containing 100 μM **TriQK**, **TriEN**, **TriQN**, **TriQD**, or **TriQNac** were prepared. *E. faecium* D344s, *E. faecium* WT, or isogenic strain lacking the Ldt TP gene (ldt_{fm}) from an overnight culture were added to the medium (1:100 dilution) and allowed to grow overnight at 37^{o}C with shaking at 250 rpm. The bacteria were harvested at 6,000g and washed three times with original culture volume of 1x PBS followed by fixation with 2% formaldehyde in 1x PBS for 30 min at ambient temperature. The cells were washed once more to remove formaldehyde and then analyzed using a BDFacs Canto II flow cytometer using a 488nm argon laser (L1) and a 530/30 bandpass filter (FL1). A minimum of 10,000 events were counted for each data set. The data was analyzed using the FACSDiva version 6.1.1. Standard deviation shown is derived from technical replicates.

Flow cytometry analysis of bacteria labeling with *E. faecalis*. Brain heart infusion (BHI) broth containing 100 µM **TriQK**, **TriQAA**, **TriQaa**, **TriQAAac**, or **TriEAA** were prepared. *E. faecalis* ATCC 29212 from an overnight culture was added to the medium (1:100 dilution) and allowed to grow overnight at 37ºC with shaking at 250 rpm. The bacteria were harvested at 6,000g and washed three times with original culture volume of 1x PBS followed by fixation with 2% formaldehyde in 1x PBS for 30 min at ambient temperature. The cells were washed once more to remove formaldehyde and then analyzed using a BDFacs Canto II flow cytometer using a 488nm argon laser (L1) and a 530/30 bandpass filter (FL1). A minimum of 10,000 events were counted for each data set. The data was analyzed using the FACSDiva version 6.1.1. Standard deviation shown is derived from technical replicates.

Flow cytometry analysis of bacteria labeling with *S. aureus*. Lysogeny broth (LB) broth containing 100 µM **TriQK**, **TriQG1**, **TriQG2**, **TriQG3**, **TriQG4**, **TriQG5**, or **TriQG6** were prepared. *S. aureus* SC01 from an overnight culture was added to the medium (1:100 dilution) and allowed to grow overnight at 37ºC with shaking at 250 rpm. The bacteria were harvested at 6,000g and washed three times with original culture volume of 1x PBS followed by fixation with 2% formaldehyde in 1x PBS for 30 min at ambient temperature. The cells were washed once more to remove formaldehyde and then analyzed using a BDFacs Canto II flow cytometer using a 488nm argon laser (L1) and a 530/30 bandpass filter (FL1). A minimum of 10,000 events were counted for each data set. The data was analyzed using the FACSDiva version 6.1.1. Standard deviation shown is derived from technical replicates.

Flow cytometry analysis of bacteria labeling with *L. casei*. Difco Lactobacilli MRS broth containing 100 µM **TriQK**, **TriQN**, or **TriQD** were prepared. *L. casei* from an overnight culture was added to the medium (1:100 dilution) and allowed to grow overnight at 37ºC with shaking at 250 rpm. The bacteria were harvested at 6,000g and washed three times with original culture volume of 1x PBS followed by fixation with 2% formaldehyde in 1x PBS for 30 min at ambient temperature. The cells were washed once more to remove formaldehyde and then analyzed using a BDFacs Canto II flow cytometer

using a 488nm argon laser (L1) and a 530/30 bandpass filter (FL1). A minimum of 10,000 events were counted for each data set. The data was analyzed using the FACSDiva version 6.1.1. Standard deviation shown is derived from technical replicates.

Flow cytometry analysis of bacteria labeling with *L. lactis*. BHI broth containing 100 µM **TriQK**, **TriQN**, or **TriQD** were prepared. *L. lactis* ATCC 11454 from an overnight culture was added to the medium (1:100 dilution) and allowed to grow overnight at 37ºC with shaking at 250 rpm. The bacteria were harvested at 6,000g and washed three times with original culture volume of 1x PBS followed by fixation with 2% formaldehyde in 1x PBS for 30 min at ambient temperature. The cells were washed once more to remove formaldehyde and then analyzed using a BDFacs Canto II flow cytometer using a 488nm argon laser (L1) and a 530/30 bandpass filter (FL1). A minimum of 10,000 events were counted for each data set. The data was analyzed using the FACSDiva version 6.1.1. Standard deviation shown is derived from technical replicates.

Confocal microscopy analysis of *E. faecium* labeled with acyl-acceptor and acyl-donor. Brain heart infusion (BHI) broth containing 500 µM **Coumarin-TriQN** (acyl acceptor), and 500 µM **TetraRh(Ac)** (acyl donor) was prepared. *E. faecium* (D344s) from an overnight growth was added to the medium (1:10 dilution) and incubated at 37ºC with shaking at 250 rpm for 5 minutes. The bacteria were immediately harvested at 6,000g and washed three times with original culture volume of 1x PBS followed by fixation with 2% formaldehyde in 1x PBS for 30 min at ambient temperature. The cells were washed once more to remove formaldehyde and then analyzed using a Nikon C2 confocal microscope.

Peptidoglycan Isolation. BHI medium (200 mL) containing 500 µM **TriQN** modified with a rhodamine fluorophore was prepared. *E. faecium* D344S bacteria were added to the BHI medium (1:100) and allowed to grow overnight at 37°C with shaking at 250 rpm. The cells were harvested and washed with 1x with cold 0.025 M potassium phosphate buffer, pH 7.0. Washed cells were pelleted, resuspended in sterile H_2O and lyophilized. The cells were then resuspended in sterile H_2O added, dropwise to boiling water with 4% (w/v)

sodium dodecyl sulfate (SDS). The sample was boiled for 30 minutes, and was then cooled for 2 hours with stirring, and was allowed to stand overnight (unstirred) at room temperature. The sample was sedimented by centrifugation at 60,000g for 20 minutes at room temperature, and washed three times, using the same centrifugation parameters, with sterile H_2O. The pellet was then incubated at 37°C with shaking at 110 rpm for 16 hours in 20 mL of 20 mM potassium phosphate buffer pH 7.8 with 200 μg/mL Trypsin and 83 μg/mL DNase. Following, the sample was sedimented by centrifugation at 100,000g for 1 hour at 20°C and washed three times, using the same centrifugation parameters, with sterile H_2O. The pellet was then incubated at 37°C with shaking at 110 rpm in 2mL of 25 mM potassium phosphate buffer pH 6.5/10 mM $MgCl_2$ with 200 μg/mL lysozyme and 250 μg/mL mutanolysin. After 16 hours, the samples were boiled for 3 minutes to inactivate the enzymes and centrifuged at 12,000g for 5 minutes. The supernatant was salvaged, filtered with a 25 mm 0.45 μm Nylon membrane, and applied to an Aeris 250 x 21.2 mm reverse-phase C18 column using a Waters 600 HPLC pumped with 100% H_2O with 0.1% Trifluoroacetic acid (TFA) for 20 minutes, followed collection of the elutant with a linear methanol gradient (0-100% with 0.1% TFA) for 20 minutes, and an isocratic 10 minute hold at 100% methanol. The collection was rotovaped, lyophilized, and analyzed using an Agilent 1260 Infinity II Prime LC and Agilent 6545B QTOF with a Luna 30 x 2.00 mm reverse-phase C18(2) column, eluted at a flow rate of 0.5 mL/min for 10 minutes with 0.1% formic acid (v/v) in water and subsequently with a 90 minute linear acetonitrile gradient (0-20%) in 0.1% formic acid. The column temperature was maintained at 40°C.

PG Digestion/Lysozyme Treatment of Labeled Peptidoglycan. *E. faecium* D344S (1:100) were added to the BHI medium or BHI medium containing 100 μM **TriQN** and allowed to grow overnight at 37°C with shaking. The bacteria were harvested at 6,000g and washed three times with original culture volume of 1x PBS followed by fixation with 2% formaldehyde in 1x PBS for 30 min at ambient temperature. Cells were washed four times with 1x PBS to remove the formaldehyde. The bacteria were resuspended in 1x PBS containing 1 mg/mL lysozyme (MP biomedicals) and incubated at 37°C. A portion of the cells were taken at 1, 5, 30, 60, and 120 min. At each time point, the collected bacteria

were washed three times with 1x PBS and resuspended in a final solution of 1x PBS containing 4% formaldehyde to quench the lysozyme reaction. Cells were analyzed using a Life Technologies Attune Nxt instrument. A minimum of 10,000 events were counted for each data set. The data was analyzed using FCS Express 7.

Flow Cytometry Analysis of Antibiotic Treated *E. faecium* D344S

Brain heart infusion (BHI) broth containing 100 μM **TriQN** was prepared. To the medium was added antibiotics ampicillin or Meropenem at varying sub-MIC concentrations. *E. faecium* D344S was added to the corresponding medium (1:100 dilution) and allowed to grow overnight at 37 °C with shaking at 250 rpm. The bacteria were harvested at 6,000g and washed three times with original culture volume of 1× PBS followed by fixation with 2% formaldehyde in 1×PBS for 30 min at ambient temperature. The cells were washed once more to remove formaldehyde and then analyzed using a Life Technologies Attune Nxt instrument.

3.6 *References*

1. Andersson, D. I.; Hughes, D., Antibiotic resistance and its cost: is it possible to reverse resistance? *Nat Rev Microbiol* **2010,** *8* (4), 260-71.

2. Arias, C. A.; Murray, B. E., The rise of the Enterococcus: beyond vancomycin resistance. *Nat Rev Microbiol* **2012,** *10* (4), 266-78.

3. Vollmer, W.; Blanot, D.; De Pedro, M. A., Peptidoglycan structure and architecture. *FEMS Microbiology Reviews* **2008,** *32* (2), 149-167.

4. Silhavy, T. J.; Kahne, D.; Walker, S., The bacterial cell envelope. *Cold Spring Harb Perspect Biol* **2010,** *2* (5), a000414-a000414.

5. Ling, L. L.; Schneider, T.; Peoples, A. J.; Spoering, A. L.; Engels, I.; Conlon, B. P.; Mueller, A.; Schäberle, T. F.; Hughes, D. E.; Epstein, S.; Jones, M.; Lazarides, L.; Steadman, V. A.; Cohen, D. R.; Felix, C. R.; Fetterman, K. A.; Millett, W. P.; Nitti, A. G.; Zullo, A. M.; Chen, C.; Lewis, K., A new antibiotic kills pathogens without detectable resistance. *Nature* **2015,** *517* (7535), 455-9.

6. Breukink, E.; de Kruijff, B., Lipid II as a target for antibiotics. *Nat Rev Drug Discov* **2006,** *5* (4), 321-32.

7. Bugg, T. D.; Braddick, D.; Dowson, C. G.; Roper, D. I., Bacterial cell wall assembly: still an attractive antibacterial target. *Trends Biotechnol* **2011,** *29* (4), 167-73.

8. Wang, G.; Lo, L. F.; Forsberg, L. S.; Maier, R. J., Helicobacter pylori peptidoglycan modifications confer lysozyme resistance and contribute to survival in the host. *mBio* **2012,** *3* (6), e00409-e412.

9. Juan, C.; Torrens, G.; Barceló, I. M.; Oliver, A., Interplay between Peptidoglycan Biology and Virulence in Gram-Negative Pathogens. *Microbiol Mol Biol Rev* **2018,** *82* (4).

10. Vijayrajratnam, S.; Pushkaran, A. C.; Balakrishnan, A.; Vasudevan, A. K.; Biswas, R.; Mohan, C. G., Bacterial peptidoglycan with amidated meso-diaminopimelic acid evades NOD1 recognition: an insight into NOD1 structure-recognition. *Biochem J* **2016,** *473* (24), 4573-4592.

11. Zapun, A.; Philippe, J.; Abrahams, K. A.; Signor, L.; Roper, D. I.; Breukink, E.; Vernet, T., In vitro Reconstitution of Peptidoglycan Assembly from the Gram-Positive Pathogen Streptococcus pneumoniae. *ACS Chemical Biology* **2013,** *8* (12), 2688-2696.

12. Srisuknimit, V.; Qiao, Y.; Schaefer, K.; Kahne, D.; Walker, S., Peptidoglycan Cross-Linking Preferences of Staphylococcus aureus Penicillin-Binding Proteins Have Implications for Treating MRSA Infections. *Journal of the American Chemical Society* **2017,** *139* (29), 9791-9794.

13. Morlot, C.; Straume, D.; Peters, K.; Hegnar, O. A.; Simon, N.; Villard, A. M.; Contreras-Martel, C.; Leisico, F.; Breukink, E.; Gravier-Pelletier, C.; Le Corre, L.; Vollmer, W.; Pietrancosta, N.; Håvarstein, L. S.; Zapun, A., Structure of the essential peptidoglycan amidotransferase MurT/GatD complex from Streptococcus pneumoniae. *Nat Commun* **2018,** *9* (1), 3180.

14. Kumar, J. K., Lysostaphin: an antistaphylococcal agent. *Appl Microbiol Biotechnol* **2008,** *80* (4), 555-61.

15. Franchi, L.; Warner, N.; Viani, K.; Nuñez, G., Function of Nod-like receptors in microbial recognition and host defense. *Immunol Rev* **2009,** *227* (1), 106-128.

16. Kuru, E.; Hughes, H. V.; Brown, P. J.; Hall, E.; Tekkam, S.; Cava, F.; de Pedro, M. A.; Brun, Y. V.; VanNieuwenhze, M. S., In Situ probing of newly synthesized peptidoglycan in live bacteria with fluorescent D-amino acids. *Angew Chem Int Ed Engl* **2012,** *51* (50), 12519-23.

17. Kuru, E.; Tekkam, S.; Hall, E.; Brun, Y. V.; Van Nieuwenhze, M. S., Synthesis of fluorescent D-amino acids and their use for probing peptidoglycan synthesis and bacterial growth in situ. *Nat Protoc* **2015,** *10* (1), 33-52.

18. Siegrist, M. S.; Whiteside, S.; Jewett, J. C.; Aditham, A.; Cava, F.; Bertozzi, C. R., d-Amino Acid Chemical Reporters Reveal Peptidoglycan Dynamics of an Intracellular Pathogen. *ACS Chemical Biology* **2013,** *8* (3), 500-505.

19. Siegrist, M. S.; Swarts, B. M.; Fox, D. M.; Lim, S. A.; Bertozzi, C. R., Illumination of growth, division and secretion by metabolic labeling of the bacterial cell surface. *FEMS Microbiol Rev* **2015,** *39* (2), 184-202.

20. Lebar, M. D.; May, J. M.; Meeske, A. J.; Leiman, S. A.; Lupoli, T. J.; Tsukamoto, H.; Losick, R.; Rudner, D. Z.; Walker, S.; Kahne, D., Reconstitution of Peptidoglycan Cross-Linking Leads to Improved Fluorescent Probes of Cell Wall Synthesis. *Journal of the American Chemical Society* **2014,** *136* (31), 10874-10877.

21. Lupoli, T. J.; Tsukamoto, H.; Doud, E. H.; Wang, T.-S. A.; Walker, S.; Kahne, D., Transpeptidase-mediated incorporation of D-amino acids into bacterial peptidoglycan. *Journal of the American Chemical Society* **2011,** *133* (28), 10748-10751.

22. Lebar, M. D.; Lupoli, T. J.; Tsukamoto, H.; May, J. M.; Walker, S.; Kahne, D., Forming Cross-Linked Peptidoglycan from Synthetic Gram-Negative Lipid II. *Journal of the American Chemical Society* **2013,** *135* (12), 4632-4635.

23. Ngadjeua, F.; Braud, E.; Saidjalolov, S.; Iannazzo, L.; Schnappinger, D.; Ehrt, S.; Hugonnet, J. E.; Mengin-Lecreulx, D.; Patin, D.; Ethève-Quelquejeu, M.; Fonvielle, M.; Arthur, M., Critical Impact of Peptidoglycan Precursor Amidation on the Activity of l,d-Transpeptidases from Enterococcus faecium and Mycobacterium tuberculosis. *Chemistry* **2018,** *24* (22), 5743-5747.

24. Welsh, M. A.; Taguchi, A.; Schaefer, K.; Van Tyne, D.; Lebreton, F.; Gilmore, M. S.; Kahne, D.; Walker, S., Identification of a Functionally Unique Family of Penicillin-Binding Proteins. *Journal of the American Chemical Society* **2017,** *139* (49), 17727-17730.

25. Triboulet, S.; Bougault, C. M.; Laguri, C.; Hugonnet, J. E.; Arthur, M.; Simorre, J. P., Acyl acceptor recognition by Enterococcus faecium L,D-transpeptidase Ldtfm. *Mol Microbiol* **2015,** *98* (1), 90-100.

26. Gautam, S.; Kim, T.; Shoda, T.; Sen, S.; Deep, D.; Luthra, R.; Ferreira, M. T.; Pinho, M. G.; Spiegel, D. A., An Activity-Based Probe for Studying Crosslinking in Live Bacteria. *Angew Chem Int Ed Engl* **2015,** *54* (36), 10492-6.

27. Pidgeon, S. E.; Apostolos, A. J.; Nelson, J. M.; Shaku, M.; Rimal, B.; Islam, M. N.; Crick, D. C.; Kim, S. J.; Pavelka, M. S.; Kana, B. D.; Pires, M. M., L,D-Transpeptidase Specific Probe Reveals Spatial Activity of Peptidoglycan Cross-Linking. *ACS Chemical Biology* **2019,** *14* (10), 2185-2196.

28. Bellais, S.; Arthur, M.; Dubost, L.; Hugonnet, J. E.; Gutmann, L.; van Heijenoort, J.; Legrand, R.; Brouard, J. P.; Rice, L.; Mainardi, J. L., Aslfm, the D-aspartate ligase responsible for the addition of D-aspartic acid onto the peptidoglycan precursor of Enterococcus faecium. *J Biol Chem* **2006,** *281* (17), 11586-94.

29. Patti, G. J.; Kim, S. J.; Schaefer, J., Characterization of the peptidoglycan of vancomycin-susceptible Enterococcus faecium. *Biochemistry* **2008,** *47* (32), 8378-85.

30. Figueiredo, T. A.; Sobral, R. G.; Ludovice, A. M.; Almeida, J. M.; Bui, N. K.; Vollmer, W.; de Lencastre, H.; Tomasz, A., Identification of genetic determinants and enzymes involved with the amidation of glutamic acid residues in the peptidoglycan of Staphylococcus aureus. *PLoS Pathog* **2012,** *8* (1), e1002508.

31. Liu, X.; Gallay, C.; Kjos, M.; Domenech, A.; Slager, J.; van Kessel, S. P.; Knoops, K.; Sorg, R. A.; Zhang, J. R.; Veening, J. W., High-throughput CRISPRi phenotyping identifies new essential genes in Streptococcus pneumoniae. *Mol Syst Biol* **2017,** *13* (5), 931.

32. Courtin, P.; Miranda, G.; Guillot, A.; Wessner, F.; Mézange, C.; Domakova, E.; Kulakauskas, S.; Chapot-Chartier, M. P., Peptidoglycan structure analysis of Lactococcus lactis reveals the presence of an L,D-carboxypeptidase involved in peptidoglycan maturation. *J Bacteriol* **2006,** *188* (14), 5293-8.

33. Ito, M.; Kim, Y. G.; Tsuji, H.; Takahashi, T.; Kiwaki, M.; Nomoto, K.; Danbara, H.; Okada, N., Transposon mutagenesis of probiotic Lactobacillus casei identifies asnH, an asparagine synthetase gene involved in its immune-activating capacity. *PLoS One* **2014,** *9* (1), e83876.

34. Corti, A.; Curnis, F., Isoaspartate-dependent molecular switches for integrin-ligand recognition. *J Cell Sci* **2011,** *124* (Pt 4), 515-22.

35. Weintraub, S. J.; Manson, S. R., Asparagine deamidation: a regulatory hourglass. In *Mech Ageing Dev*, Ireland, 2004; Vol. 125, pp 255-7.

36. Yang, H.; Zubarev, R. A., Mass spectrometric analysis of asparagine deamidation and aspartate isomerization in polypeptides. *Electrophoresis* **2010,** *31* (11), 1764-72.

37. Liu, Z.; Frutos, S.; Bick, M. J.; Vila-Perelló, M.; Debelouchina, G. T.; Darst, S. A.; Muir, T. W., Structure of the branched intermediate in protein splicing. *Proc Natl Acad Sci U S A* **2014,** *111* (23), 8422-7.

38. Regulski, K.; Courtin, P.; Kulakauskas, S.; Chapot-Chartier, M. P., A novel type of peptidoglycan-binding domain highly specific for amidated D-Asp cross-bridge, identified in Lactobacillus casei bacteriophage endolysins. *J Biol Chem* **2013,** *288* (28), 20416-26.

39. Bouhss, A.; Josseaume, N.; Severin, A.; Tabei, K.; Hugonnet, J.-E.; Shlaes, D.; Mengin-Lecreulx, D.; van Heijenoort, J.; Arthur, M., Synthesis of the l-Alanyl-l-alanine

Cross-bridge of Enterococcus faecalis Peptidoglycan*. *Journal of Biological Chemistry* **2002,** *277* (48), 45935-45941.

40. Maidhof, H.; Reinicke, B.; Blümel, P.; Berger-Bächi, B.; Labischinski, H., femA, which encodes a factor essential for expression of methicillin resistance, affects glycine content of peptidoglycan in methicillin-resistant and methicillin-susceptible Staphylococcus aureus strains. *J Bacteriol* **1991,** *173* (11), 3507-13.

41. Henze, U.; Sidow, T.; Wecke, J.; Labischinski, H.; Berger-Bächi, B., Influence of femB on methicillin resistance and peptidoglycan metabolism in Staphylococcus aureus. *Journal of Bacteriology* **1993,** *175* (6), 1612-1620.

42. Monteiro, J. M.; Covas, G.; Rausch, D.; Filipe, S. R.; Schneider, T.; Sahl, H. G.; Pinho, M. G., The pentaglycine bridges of Staphylococcus aureus peptidoglycan are essential for cell integrity. *Sci Rep* **2019,** *9* (1), 5010.

43. Strandén, A. M.; Ehlert, K.; Labischinski, H.; Berger-Bächi, B., Cell wall monoglycine cross-bridges and methicillin hypersusceptibility in a femAB null mutant of methicillin-resistant Staphylococcus aureus. *Journal of Bacteriology* **1997,** *179* (1), 9-16.

44. Tschierske, M.; Mori, C.; Rohrer, S.; Ehlert, K.; Shaw, K. J.; Berger-Bächi, B., Identification of three additional femAB-like open reading frames in Staphylococcus aureus. *FEMS Microbiol Lett* **1999,** *171* (2), 97-102.

45. Waxman, D. J.; Strominger, J. L., Penicillin-binding proteins and the mechanism of action of beta-lactam antibiotics. *Annu Rev Biochem* **1983,** *52*, 825-69.

46. Wu, S.; Piscitelli, C.; de Lencastre, H.; Tomasz, A., Tracking the evolutionary origin of the methicillin resistance gene: cloning and sequencing of a homologue of mecA from a methicillin susceptible strain of Staphylococcus sciuri. *Microb Drug Resist* **1996,** *2* (4), 435-41.

47. Jensen, A.; Valdórsson, O.; Frimodt-Møller, N.; Hollingshead, S.; Kilian, M., Commensal streptococci serve as a reservoir for β-lactam resistance genes in Streptococcus pneumoniae. *Antimicrob Agents Chemother* **2015,** *59* (6), 3529-40.

48. Magnet, S.; Arbeloa, A.; Mainardi, J. L.; Hugonnet, J. E.; Fourgeaud, M.; Dubost, L.; Marie, A.; Delfosse, V.; Mayer, C.; Rice, L. B.; Arthur, M., Specificity of L,D-transpeptidases from gram-positive bacteria producing different peptidoglycan chemotypes. *J Biol Chem* **2007,** *282* (18), 13151-9.

49. Arbeloa, A.; Hugonnet, J. E.; Sentilhes, A. C.; Josseaume, N.; Dubost, L.; Monsempes, C.; Blanot, D.; Brouard, J. P.; Arthur, M., Synthesis of mosaic peptidoglycan cross-bridges by hybrid peptidoglycan assembly pathways in gram-positive bacteria. *J Biol Chem* **2004,** *279* (40), 41546-56.

Chapter 4 Facile Synthesis and Metabolic Incorporation of *m*-DAP Bioisosteres Into Cell Walls of Live Bacteria

Adapted From: Apostolos, A. J., Nelson, J. M., Silva, J. R. A., Lameira, J., Achimovich, A. M., Gahlmann, A., Alves, C. N., and Pires, M. M. Facile Synthesis and Metabolic Incorporation of m-DAP Bioisosteres Into Cell Walls of Live Bacteria, *ACS Chemical Biology* **2020,** *15*, 2966-2975.

4.1 *Abstract*

Bacterial cell walls contain peptidoglycan (PG), a scaffold that provides proper rigidity to resist lysis from internal osmotic pressure and a barrier to protect cells against external stressors. It consists of repeating sugar units with a linkage to a stem peptide that becomes highly crosslinked by cell wall transpeptidases (TP). While synthetic PG fragments containing L-Lysine in the 3rd position on the stem peptide are easier to access, those with *meso*-diaminopimelic acid (*m*-DAP) pose a severe synthetic challenge. Herein, we describe a solid phase synthetic scheme based on widely available building blocks to assemble *meso*-cystine (*m*-CYT), which mimics key structural features of *m*-DAP. To demonstrate proper mimicry of *m*-DAP, cell wall probes were synthesized with *m*-CYT in place of *m*-DAP and evaluated for their metabolic processing in live bacterial cells. We found that *m*-CYT-based cell wall probes were properly processed by TPs in various bacterial species that endogenously contain *m*-DAP in their PG. Additionally, we have used hybrid Quantum Mechanical/Molecular Mechanical (QM/MM) and Molecular Dynamics (MD) simulations to explore the influence of *m*-DAP analogs on the PG crosslinking. The results showed that crosslinking mechanism of transpeptidases occurred through a concerted process. We anticipate that this strategy, which is based on the use of inexpensive and commercially available building blocks, can be widely adopted to provide greater accessibility of PG mimics for *m*-DAP containing organisms.

4.2 *Introduction*

Peptidoglycan (PG) is a structurally integral part of the bacterial cell wall that provides cellular rigidity and prevents lysis from osmotic stress. The primary monomeric unit of PG includes a disaccharide of *N*-acetylglucosamine (GlcNAc) and *N*-acetylmuramic acid (MurNAc) sugars, with linkage to a stem peptide, typically a pentamer with the sequence L-Ala-iso-D-Glu-L-Lys-D-Ala-D-Ala or with *meso*-diaminopimelic acid (*m*-DAP) in place of L-Lys at the 3rd position. Nascent PG units are imbedded within the existing PG scaffold by the transglycosylation of the disaccharides and the crosslinking of neighboring stem peptides, carried out by transpeptidase (TP) enzymes.[1]

There are considerable similarities in PG structure across different types of bacteria and, yet, slight structural variations can alter cell wall physiochemical properties and can tune interaction with neighboring cells including host organisms. Today, we know that fragments of PG are released into surrounding environments as by-products of cell wall metabolism or as a component of signaling systems to modulate the response from a neighboring bacteria or a host organism.[2] A prominent difference in PG primary structure occurs at the 3rd position on the stem peptide, which is also the site for PG crosslinking and Braun's lipoprotein attachment (**Figure 4.1a**).[3, 4] The difference of a single carboxylic acid between *m*-DAP and L-Lys can play a major role in how PG is sensed. As an example, vegetative *Bacillus subtilis* (*B. subtilis*) cells release PG fragments to communicate the initiation of a synchronized germination event from spores using the sensor protein PrkC.[5, 6] The specificity in this communication is dictated by the complete lack of PrkC response to L-Lys containing PG fragments, which are nonnative to the *m*-DAP based PG of *B. subtilis*.[7] Similarly, bacteria release biomacromolecules (e.g., PG) that are collectively known as pathogen-associated molecular patterns (PAMPs), which can be sensed by human immune cells indicating that there may be an infection.[8] NOD1, from the family of PAMP receptors, is known to be activated by the minimal agonist D-Glu-*m*-DAP (iE-DAP).[9] It was recently demonstrated that several bacterial species amidate *m*-DAP to evade NOD1 activation.[10, 11] Together, these

examples highlight how alterations to the PG stem peptide structure can regulate sensing and metabolism of PG fragments.

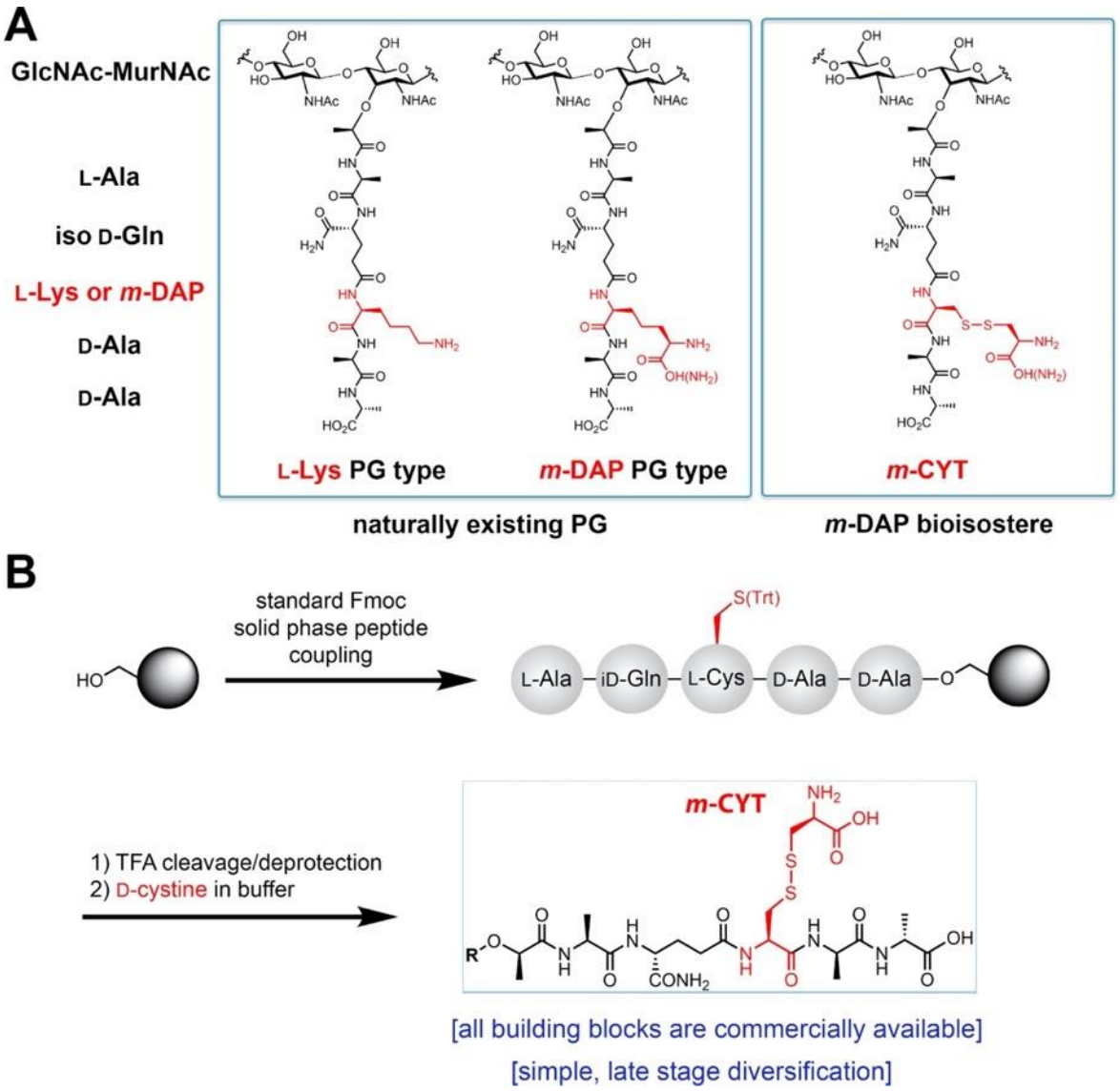

Figure 4.1 *(A) Chemical structure of the basic unit of PG (disaccharide attached to the stem pentapeptide). A major difference between bacterial species occurs at the 3rd position (L-Lys and m-DAP). This schematic diagram shows how the bioisostere m-CYT mimics key structural features of m-DAP. (B) Proposed synthetic route to assemble m-CYT containing PG fragments.*

A large number of pathogenic and commensal bacteria have *m*-DAP based PG. Therefore, it is critically important to be able to synthesize homogeneous *m*-DAP based PG fragments (as opposed to heterogenous isolated PG fragments from live bacteria) to systematically dissect the biological consequences of alterations to the PG stem peptide found in these organisms.[12, 13] While Fmoc-protected L-Lys building blocks are readily available and highly compatible with standard solid phase peptide chemistry, *m*-DAP is not commercially available and this poses a significant synthetic barrier. The internal symmetry of *m*-DAP coupled with the need to have differentiated, orthogonally protected stereocenters, makes its synthesis and that of its protected counterparts highly challenging.[14-19] Instead of the difficult-to-synthesize *m*-DAP, an alternative strategy involves the utilization of *m*-DAP analogs that mimic the key components and are functionally similar to *m*-DAP. Examples of a such analogs include *meso*-lanthionine (*m*-LAN)[20-22] and *meso*-oxa-DAP.[23-26] While both of these analogs recapitulate aspects of *m*-DAP as demonstrated by their processing by enzymes that recognize *m*-DAP residues, their synthesis still involves several solution phase chemistry steps and they are not readily adaptable to Fmoc-based solid phase chemistry. We envisioned that we could use widely available Fmoc-protected L-Cys as a precursor to the synthesis of *meso*-cystine (*m*-CYT) analogs (**Figure 4.1b**). *m*-CYT preserves critical structural features at the terminal end of the sidechain, and this building block can easily be diversified using commercially available amino acids to build homogenous PG fragments and their naturally occurring derivatives. We leveraged our synthetic strategy to access variants of *m*-DAP bioisosteres and showed that naturally existing modifications to the PG structure can alter their metabolism and processing by cell wall biosynthetic machinery.

We anticipated that we could leverage the mimicry of *m*-DAP by *m*-CYT to study PG crosslinking, which is an essential step in the biosynthesis of properly structured bacterial cell walls. PG crosslinking is mainly carried out by Penicillin Binding Protein transpeptidases (D,D-TP) and L,D-transpeptidases (Ldts) to generate distinct connectivity patterns (**Figure 4.2a**). The importance of these two TP classes of enzymes is illustrated by the general lack of sensitivity of Ldts against most β-lactam antibiotics (e.g., penicillins and cephalosporins). A large number of clinically relevant antibiotics interfere with PG

crosslinking and, therefore, probes that track cell wall crosslinking dynamics can potentially reveal novel targets for drug discovery. Single D-amino acid PG probes have now become essential tools to image PG biosynthesis.[27-32] Yet, single D-amino acid PG probes cannot interrogate how the stem peptide structure (or its many chemical modifications) can control PG crosslinking or processing. We[33, 34], and others[35-38], have recently demonstrated that fluorescently tagged structural mimics of nascent TP substrates can be crosslinked into the growing PG scaffold of live cells, thus hijacking the cell wall machinery (**Figure 4.2b**). Indeed, we have shown that penta-, tetra-, and tri-peptides that are analogs of the PG stem peptide are accepted by TPs to varying extents.[33, 34] However, to this point we had been unable to investigate the role of *m*-DAP (and its modifications) because of the challenge in building *m*-DAP containing peptides.

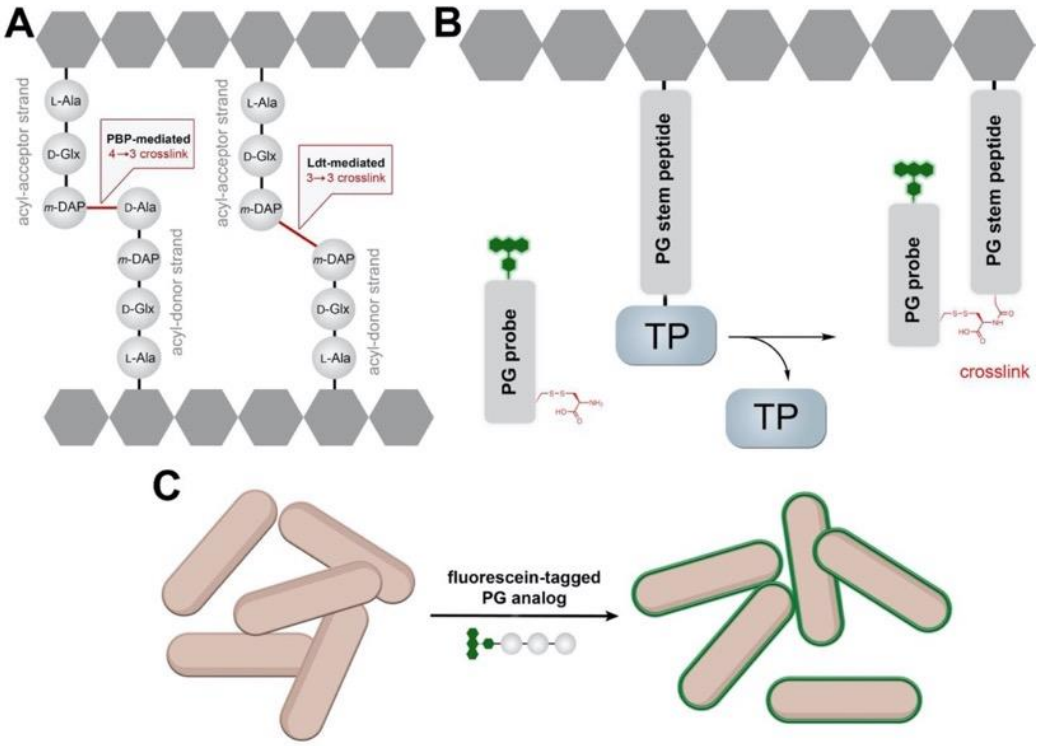

Figure 4.2 *Cartoon representation of the two primary modes of PG crosslinking carried about by D,D- and L,D-transpeptidases. (B) Snapshot representation of the acyl-intermediate of the TP reaction showing the hijacking of this step in the installation of the fluorescently tagged PG probe into the existing PG scaffold. (C) Probe incorporation on the cell surface can be readily measured using flow cytometry cell analysis.*

4.3 *Results and Discussion*

4.3.1 *Synthesis of m-CYT probes and labeling in live M. smegmatis cells*

At first, we set out to establish a potential route to build *m*-CYT containing PG fragments that involved a post-cleavage modification with the crude peptide. Fmoc-L-Cys(Trt)-OH was coupled into the 3rd position of the pentapeptide using conventional peptide coupling conditions. Following the concomitant global deprotection and release from the solid support, the crude material was treated with D-cystine to promote the installation of D-Cys onto the free sulfhydryl of the L-Cys containing peptide *via* disulfide exchange to generate *m*-CYT. The lack of cysteine residues in naturally existing PG will ensure the chemoselective modification of L-Cys in synthesizing *m*-CYT containing PG fragments. Tripeptides were chosen to establish the recognition of the sidechain since tripeptides cannot act as acyl-donors in the TP reaction (they lack the D-Ala necessary for the acyl-donor step) and, instead, operate solely as acyl-acceptors. In this configuration, the amino group on the *m*-CYT tripeptide acts as the nucleophile in the PG crosslinking reaction (**Figure 4.2b**). Fluorescein was conjugated to the *N*-terminus to track incorporation into the PG *via* TPs and fluorescence can be readily quantified using flow cytometry (**Figure 4.2c**). A panel of probes was assembled based on analogs of the PG stem peptide that incorporated naturally existing chemical modifications to the backbone and sidechain (**Figure 4.3a**).

We first chose to evaluate the metabolic labeling of *Mycobacterium smegmatis* (*M. smegmatis*), whose PG biosynthesis tracks similarly with the pathogenic *Mycobacterium tuberculosis*, the causative agent of Tuberculosis (TB).[39-41] TB continues to impose a tremendous health burden across the globe and the unique composition of the *Mycobacterium* cell wall provides an opportunity for the elucidation of novel drug targets. For this set of experiments, *M. smegmatis* growing in early lag-phase were treated with exogenously supplied probes and incubated overnight. Supplementation of *M. smegmatis* cells with **Tri$_E$*m*CYT** (a tripeptide probe that contains iso-D-Glu on the

second position and *m*-CYT on the 3rd position) resulted in cellular fluorescence levels that were ~50-fold higher than control cells, a clear indication that *m*-CYT satisfactorily mimics *m*-DAP and is recognized by the native TP (**Figure 4.3b**). While PG precursors are initially biosynthesized with an iso-D-Glu in the 2nd position of the stem peptide, it is now established that for several Gram-positive organisms, iso-D-Glu is converted to iso-D-Gln.[37, 42, 43] In fact, the gene encoding the tandem enzyme MurT-GatD, responsible for iso-D-Glu amidation, is essential in *Staphylococcus aureus* and *Streptococcus pneumoniae*.[44, 45] It was demonstrated, *in vitro*, that absence of iso-D-Glu amidation resulted in undetectable levels of PG crosslinking.[37, 42] Yet, PG crosslinking reactions utilize two PG strands and it was not established if iso-D-Glu amidation was required on both acyl-acceptor and acyl-donor strands. Our group recently showed that iso-D-Glu amidation plays an important role in controlling PG crosslinking in the acyl-donor strand of *M. smegmatis* and *M. tuberculosis*.[34] Amidation of the second position to iso-D-Glu (**Tri$_Q$*m*CYT**) resulted in the doubling of PG incorporation as evident by the increase in cellular fluorescence, which indicates a preference for amidated iso-D-Glu but not an absolute requirement. Our new results indicate that iso-D-Glu amidation in the acyl-acceptor strand may not be an absolute requirement for PG crosslinking in *M. smegmatis*.

The sidechain of the 3rd position (L-Lys or *m*-DAP, **Figure 4.2**) in naturally existing PG contains the critical amine nucleophile and it is, theoretically, possible that PG strands lacking the carboxylic acid could be competent acyl-strand acceptors in the TP crosslinking reactions. To test the essentiality of the carboxylic acid moiety in *m*-CYT, two control probes were designed and synthesized: **Tri$_Q$LLys** and **Tri$_Q$Cystamine**. However, our results showed that the carboxylic acid moiety is essential for the acyl-acceptor strand to crosslink into the PG scaffold as the analogous probes lacking the carboxylic acid group led to minimal cellular fluorescence regardless of the linker composition (methylene and disulfide, **Figure 4.3a**). Critically, these results also indicate that the increase in cellular fluorescence is not purely due to disulfide exchange at the cell surface based on the low labeling levels with **Tri$_Q$Cystamine**. A major advantage of our strategy is the ability to access derivatives of *m*-DAP that are known to be naturally occurring such as amidation of the carboxylic acid. Currently, there is little known about *m*-DAP amidation in *M.*

smegmatis and *M. tuberculosis*, whereas it was previously reported that the PG of *Mycobacterium abscessus* contains about 20 percent of amidated *m*-DAP.[46] Some plausible biological roles of *m*-DAP amidation have been proposed. In a transposon screen for lysozyme potentiation in a *m*-DAP containing organism, *Rhodococcus erythropolis*, a gene was identified that is related to *m*-DAP amidation.[47] Later, the same gene was found to play a role in β-lactam antibiotic sensitivity in *Corynebacterium glutamicum* (*C. glutamicum*)[48] and *B. subtilis*.[49] The absence of live cell PG probes has hampered our ability to establish the effect of *m*-DAP amidation on PG crosslinking. To gain insight into this open question, we investigated how *m*-DAP amidation impacts TP crosslinking levels by building **Tri$_E$*m*CYT$_{NH2}$** and **Tri$_Q$*m*CYT$_{NH2}$**. Interestingly, amidation of the *m*-DAP crossbridge in combination with iso-D-Glu (**Tri$_E$*m*CYT$_{NH2}$**) led to similar TP-based incorporation as **Tri$_Q$*m*CYT**. These results suggest the possibility that *m*-DAP amidation serves as a compensatory modification to the lack of iso-D-Glu amidation. The double amidation in **Tri$_Q$*m*CYT$_{NH2}$** led to fluorescence levels equivalent to with **Tri$_E$*m*CYT**. 3D lattice light sheet imaging revealed that fluoresence was concentrated at the cell boundaries, but could also be observed to be concentrated at the cell poles and division septa (**Figure 4.3c**). Reversing the peptide sequence of the stem peptide analog led to a dramatic decrease in labeling levels (**Figure 4.4**).

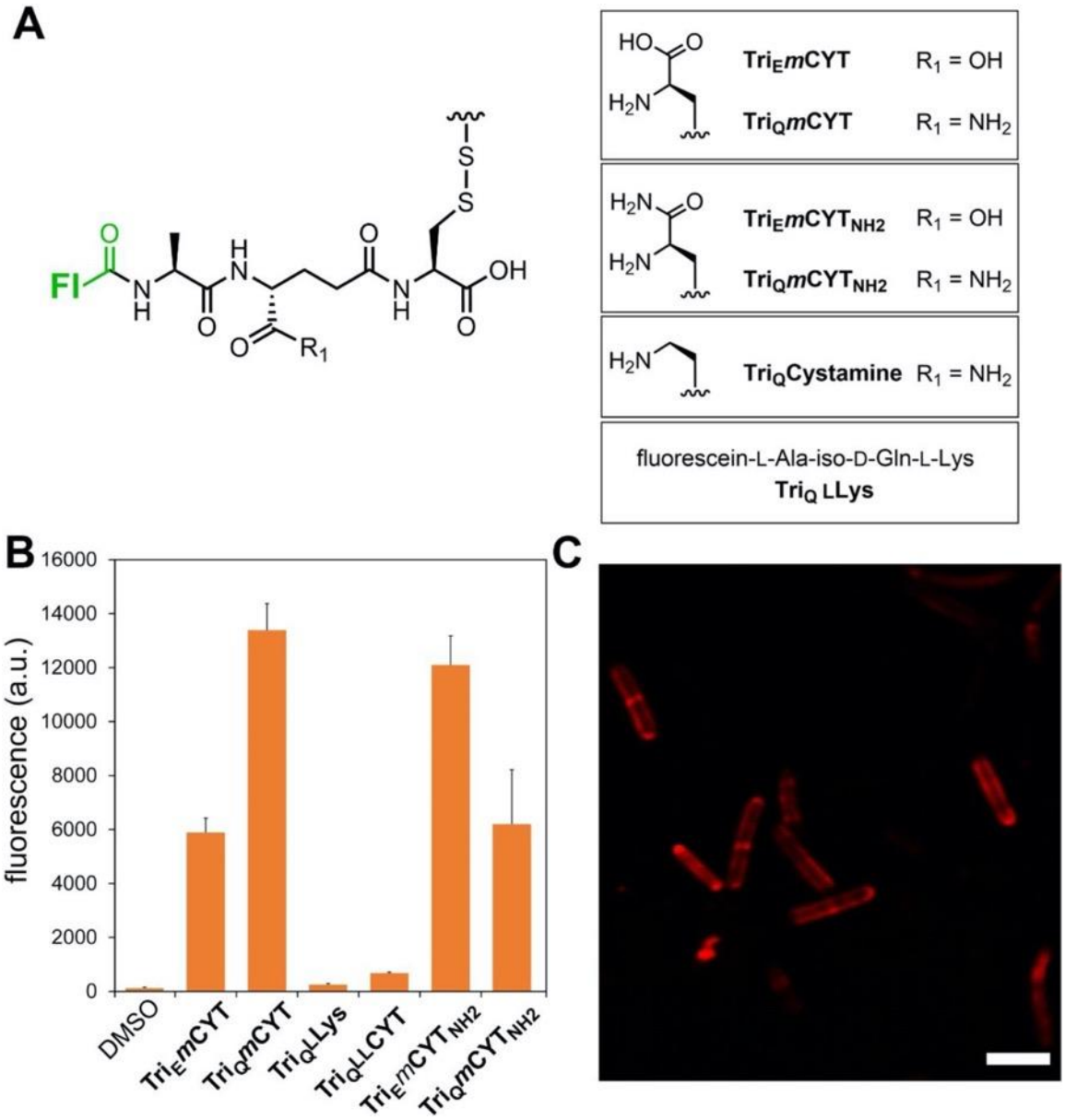

Figure 4.3 *(A) Chemical structures for tripeptide-based probes. Fl = carboxyfluorescein. (B) Flow cytometry analysis of M. smegmatis treated overnight with 100 μM of tri-peptide probes. Data are represented as mean + SD (n = 3). (C) XY slice through a 3D fluorescence image of M. smegmatis treated overnight with 100 μM of TAMRA modified* ***Tri$_E$mCYT$_{NH2}$****. Scale bar = 5 μm.*

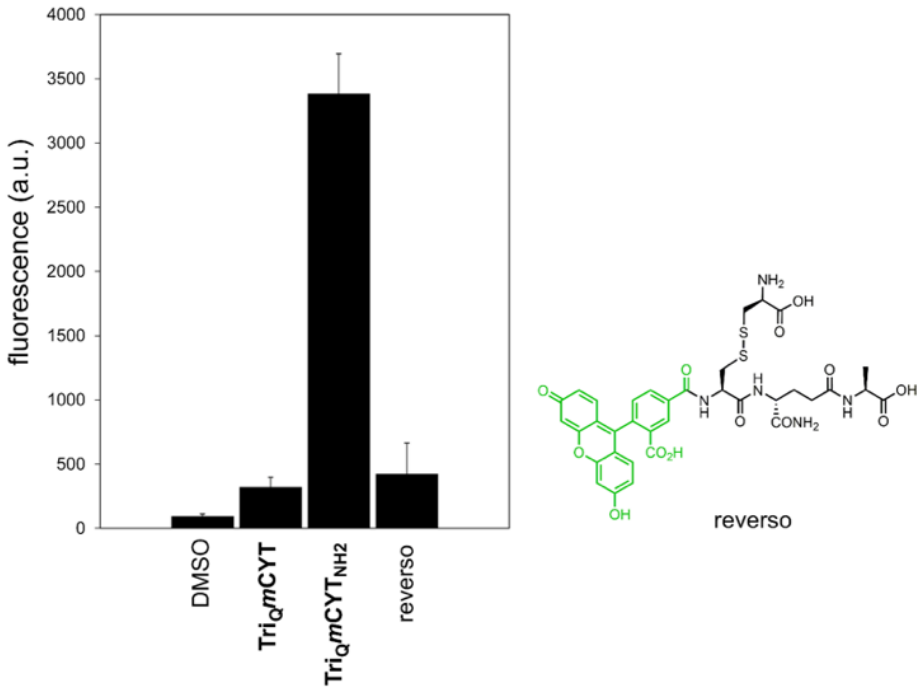

Figure 4.4 *Flow cytometry analysis of M. smegmatis (WT) untreated or treated overnight with 100 µM* ***TriQmCYT****,* ***TriQmCYTNH₂*** *or the scrambled sequence. Data are represented as mean + SD (n=3).*

4.3.2 *Defining the mode of m-CYT probe incorporation*

Having demonstrated that tripeptide probes displaying *m*-CYT residues are functional in live bacterial cells, we next performed several additional experiments to further define the mode of probe incorporation into the bacterial PG scaffold. Incorporation of tripeptide-based probes can potentially be processed by two distinct classes of TPs. We attempted to determine if an individual TP class contributed more prominently to the crosslinking of the *m*-CYT probe into the PG scaffold by using antibiotics to interfere with specific TP function. As a point of comparison, we also assessed incorporation of two probes that we had previously disclosed to be D,D-TP specific (**Penta$_Q$LLys**) and Ldt-specific (**Tetra$_Q$LLys**).[34] Co-incubation of ampicillin, a β-lactam that does not inhibit Ldts[50], with **Tri$_Q$*m*CYT** led to a slight increase in cellular labeling in a concentration dependent manner consistent with Ldt-mediated PG incorporation and similar to the Ldt-specific **Tetra$_Q$LLys** (**Figure 4.5**). The increase in cellular fluorescence may be

interpreted as a response mechanism to the inactivation of parts of the cell wall biosynthetic machinery, a feature that we previously observed with *Enterococcus faecium*[34] and we are exploring further. As expected, ampicillin treatment led to a decrease in cellular labeling with the D,D-TP specific **Penta$_Q$LLys**. Treatment with sub-lethal concentrations of meropenem, an inhibitor of both TP classes[51], resulted in a decrease of **Tri$_Q$*m*CYT** labeling. The mechanism of PG incorporation was further interrogated by using Ldt-deletion strains. Whereas deletion of two individual Ldts did not impact cellular labeling, the deletion of the five primary Ldts led to near background cellular fluorescence (**Figure 4.6**). Together, these results principally established that *m*-CYT is a functional substitute for native *m*-DAP in TP processing in live bacterial cells.

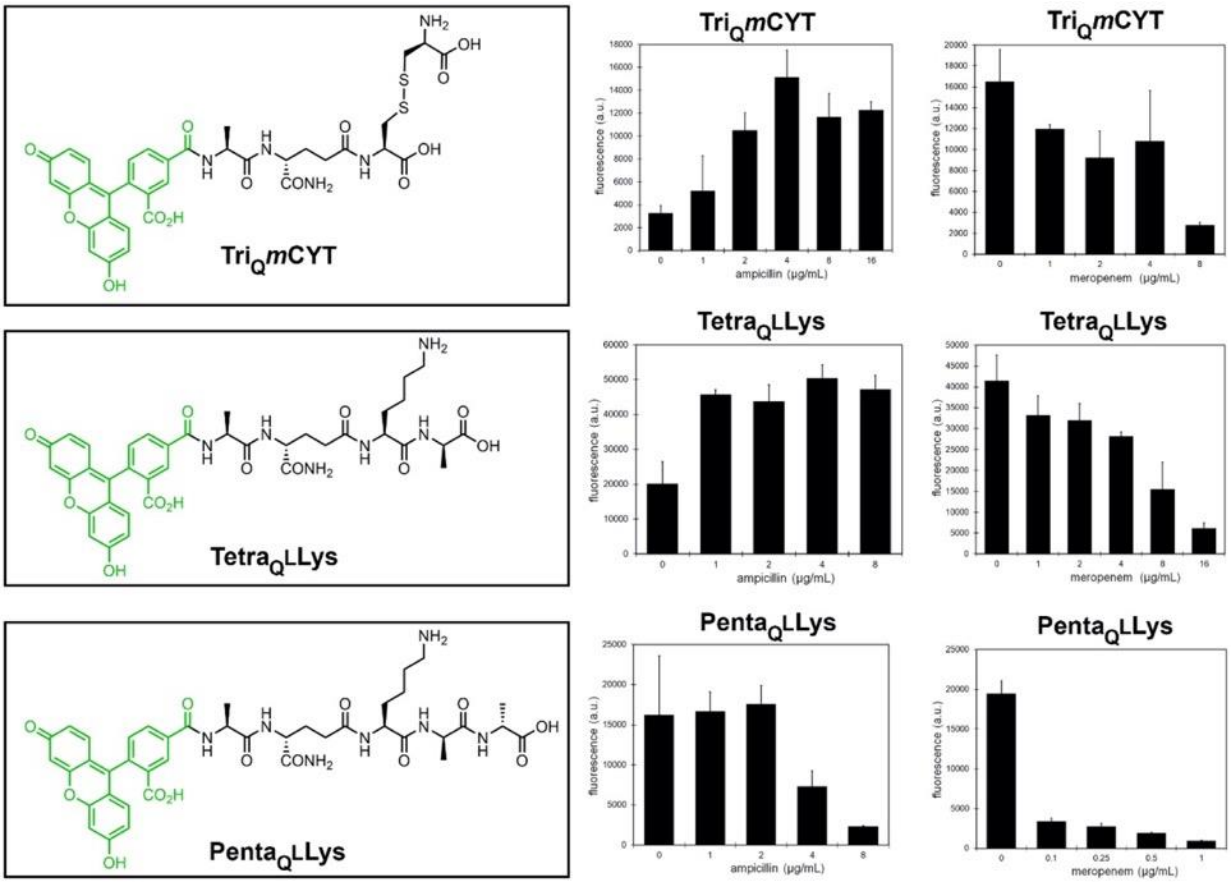

Figure 4.5 *Flow cytometry analysis of M. smegmatis treated overnight with 100 μM of each probe and increasing concentrations of ampicillin or meropenem. Data are represented as mean + SD (n=3).*

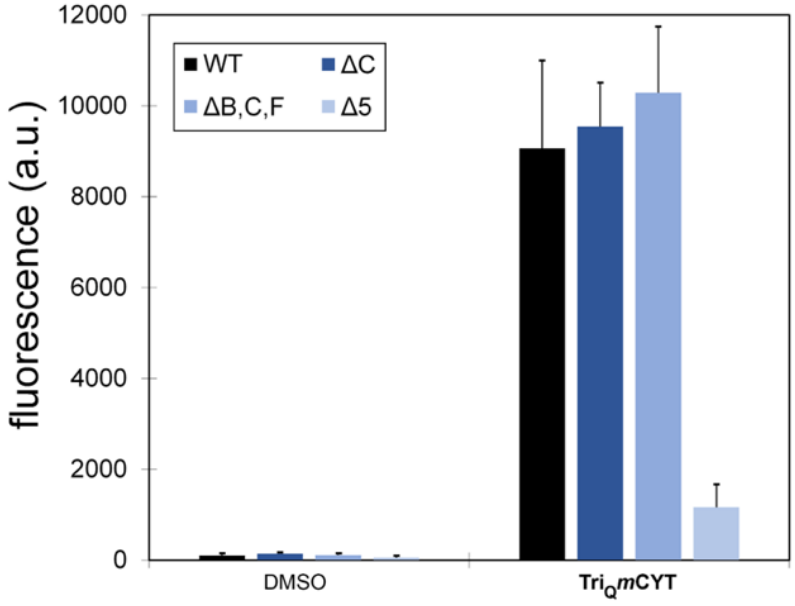

Figure 4.6 *Flow cytometry analysis of M. smegmatis (WT) and Ldt knockout mutants untreated or treated overnight with 100 µM* ***TriQmCYT****. Data are represented as mean + SD (n=3).*

4.3.3 *Computational model of m-CYT in the active site of a Ldt*

We next sought to use computational simulations to assess the mimicry of *m*-CYT for *m*-DAP in the context of their recognition in the active site of Ldts. Initially, it should be pointed out that a classification of Ldts enzymes from *M. tuberculosis* and *M. smegmatis* was proposed taking into account the homology sequence of Ldts into 18 mycobacterial genomes.[52] A phylogenetic and biochemical study to distinguish mycobacterial Ldts was recently carried out by Zandi and co-workers in which the class 2 (LdtB) of Ldt_{Msm} was identified as homologue of Ldt_{Mt2}.[51] They established a theoretical model of Ldt_{Msm} (LdtB) by a homology modelling approach using the SWISS-MODEL server.[53, 54] Here, we applied a similar procedure to the theoretical model of Ldt_{Msm} which has 70% of sequence identity with the selected template (Ldt_{Mt2}, PDB CODE: 5K69). This model had a RMSD of 0.064 Å after by overlapping template (Ldt_{Mt2}) and target (Ldt_{Msm}) structures, consistent with what was observed by Zandi and co-workers.[51] Therefore, our

theoretical model of Ldt_{Msm} was appropriately used for classical and mechanical-quantum simulations.

Our previous QM/MM computational studies revealed that catalytic mechanism of Ldt_{Mt2} starts with a proton transfer from Cys346 to His328, where the ionic-pair is more stable than neutral form.[55, 56] Here, the computational simulations start from product state of Ldt-PG reaction with ionic-pair of Cys364 and His328 catalytic residues. To explore the influence of *m*-DAP analogs during PG crosslinking three systems were built: (I) Ldt-*m*-DAP, (II) Ldt-L-Lys, and (III) Ldt-*m*-CYT. The structural and energetic parameters obtained from QM/MM umbrella sampling simulations are summarized on Table S1 (not included in this dissertation). Our results for the 2D-FES obtained by the RCX versus RCY for the systems I-III are shown in **Figure 4.7**. The crosslinking mechanism of Ldt_{Msm} occurs *via* a concerted reaction, which agree with catalytic mechanism of Ldt_{Mt2} proposed on our previous computational studies. Interestingly, the theoretical free energy barrier obtained for the synthetic PG (*m*-CYT) are close to the value obtained to native PG (*m*-DAP) (about 3 kcal/mol higher), making the reaction between *m*-CYT and Ldt kinetically favorable. These results confirm that *m*-CYT can adopt the proper configuration to mimic the endogenous *m*-DAP.

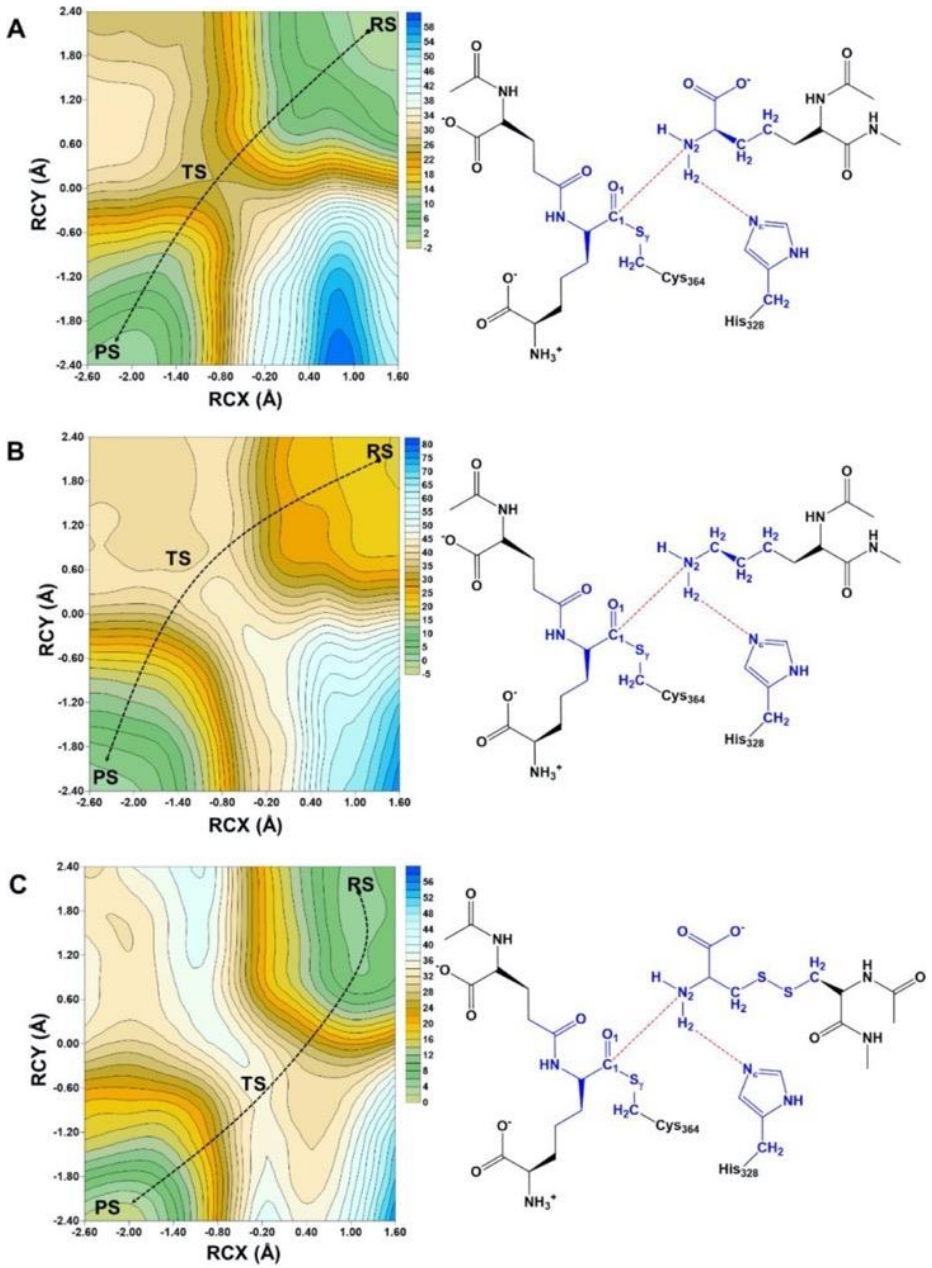

Figure 4.7 *Plots of 2D–FES calculated at DFTB/MM level (left) and combinations of RCX and RCY coordinates (right), describing the PG crosslinking mechanism of (A) Ldt-m-DAP, (B) Ldt-L-Lys, and (C) Ldt-m-CYT. QM atoms for each system are in blue color. The energy values are reported in kcal/mol.*

4.3.4 *m-CYT probes in other m-DAP-containing organisms*

Bacteria use modifications to the primary sequence of the PG stem peptide as an adaptation mechanism that is, likely, specific to its needs and niche.[1, 5] As such, it is possible that amidation of D-iGlu and *m*-DAP may not have the same consequence in all bacteria with *m*-DAP based PG. We became interested in leveraging our probes to investigate naturally occurring PG modifications in the probiotic organism *Lactobacillus plantarum* (*L. plantarum*).[57] Despite our lack of understanding of all the ways that probiotics modulate host immune responses, it is clear that PG fragments play an integral part *via* the modulation of NOD receptors.[58, 59] Chemical modifications to the PG stem peptide can, in turn, alter the level of activation by PG sensors as is evidenced by the muted response by NOD1 receptors when treated with PG fragments containing amidated D-iGlu[60] and *m*-DAP.[61] In fact, deletion of the gene responsible for *m*-DAP amidation in *L. plantarum* results in impaired cell growth and filamentation[62] and it is lethal in *B. subtilis*.[49] Incorporation of tripeptide based probes into the PG of *L. plantarum* was tested by supplementing the probes during cell culture (**Figure 4.8**). Similar to *M. smegmatis*, the carboxylic acid within the sidechain in the 3rd position of the stem peptide was critical for high cellular labeling levels. In contrast to *M. smegmatis*, there is less pronounced selectivity for D-iGlu amidation and, instead, *m*-DAP amidation alone is sufficient to yield high levels of PG incorporation (**Figure 4.8**). Interestingly, the supplementation of **Tri$_{Q}$*m*CYT$_{NH2}$** in *L. plantarum* led to the highest labeling levels our laboratory has ever observed with any cell wall probe and showed the expected labeling pattern. The high cell surface labeling levels observed could prove to be helpful in grafting epitopes (in place of fluorescein) on the surface of *L. plantarum* to promote specific adhesion to abiotic surfaces or targeted binding to pathogenic mammalian cells.

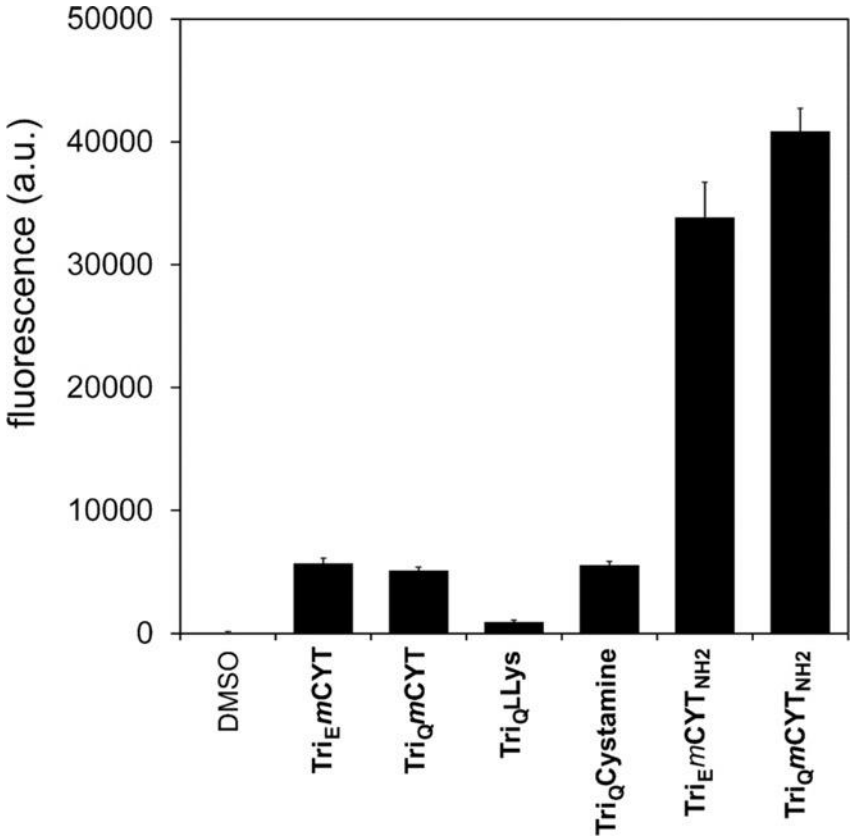

Figure 4.8 *Flow cytometry analysis of L. plantarum treated overnight with 100 μM of each probe. Data are represented as mean + SD (n=3).*

To confirm that the fluorescent signal in the flow cytometry experiments was, in fact, emitted from within the PG scaffold, a series of additional experiments were performed. First, *L. plantarum* cells were labeled with the tripeptide probe **Tri$_Q$*m*CYT$_{NH2}$**, fixed with formaldehyde to preserve the basic cellular structure, and subjected to a treatment with mutanolysin, which is expected to selectively depolymerize the PG scaffold.[62] We found that fluorescent signals were reduced in a time-dependent manner, consistent with embedment of the probes within the PG scaffold (**Figure 4.9**). As a control experiment, labeled cells were treated with lysozyme and no reduction in cellular fluorescence was observed, as *L. plantarum* is inherently resistant to lysozyme due to *O*-acetylation of GlnNAc.[62] As a complement to PG digestion, which releases the entire scaffold regardless of what the stem peptide structure is, we took advantage of the disulfide bond to delineate probe incorporation. *L. plantarum* cells were incubated

with **Tri$_{Q}$*m*CYT$_{NH2}$** and subsequently treated with dithiothreitol (DTT), which is expected to reduce the disulfide bond in the crosslinked *m*-CYT thus releasing the part of the probe containing fluorescein from the remaining PG scaffold (**Figure 4.10**). The observed decrease in cellular fluorescence is consistent with the proposed mode of incorporation and further suggests that the tripeptide probe is primarily incorporated as an acyl-acceptor strand because acyl-donor strands would not result in probe release from the PG. Finally, we performed PG analysis of **Tri$_{Q}$*m*CYT$_{NH2}$** treated *L. plantarum* cells and found evidence of dimeric crosslinked PG fragments that are entirely consistent with Ldt-mediated incorporation and no evidence of PBP-mediated incorporation (figure not included in this dissertation).

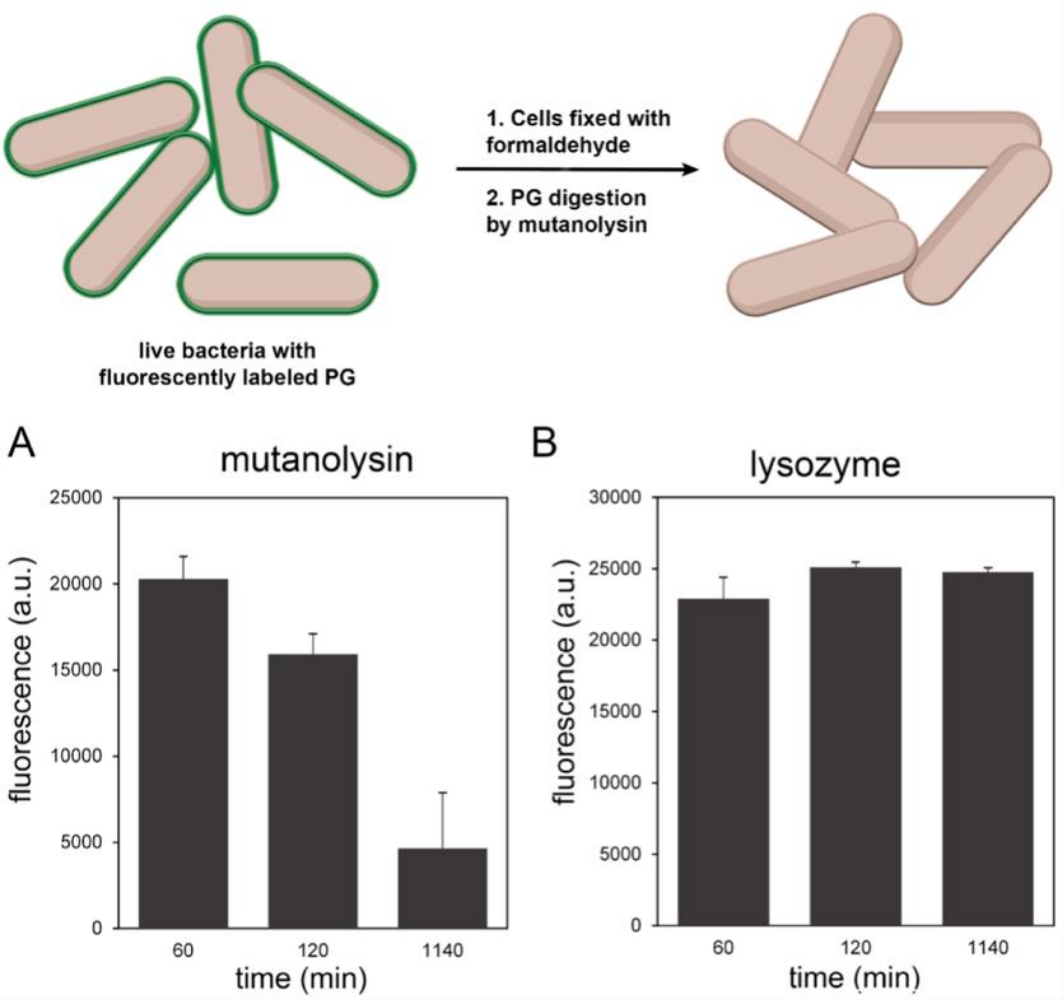

Figure 4.9 *Above: Schematic of cells labeled and fixed with fluorescent probe, then treated with mutanolysin for PG digestion. (A) Flow cytometry analysis of L. plantarum cells labeled overnight with 100 µM* ***TriQmCYT$_{NH2}$****, fixed with formaldehyde, washed 4X, and treated with 500 µg/mL mutanolysin at 37°C. At various time points, samples were collected and cells were analyzed by flow cytometry. Data are represented as mean + SD (n=3). (B) Flow cytometry analysis of L. plantarum cells labeled overnight with 100 µM* ***Tri$_Q$mCYT$_{NH2}$****, fixed with formaldehyde, washed 4X, and treated with 500 µg/mL lysozyme at 37°C. At various time points, samples were collected and cells were analyzed by flow cytometry. Data are represented as mean + SD (n=3).*

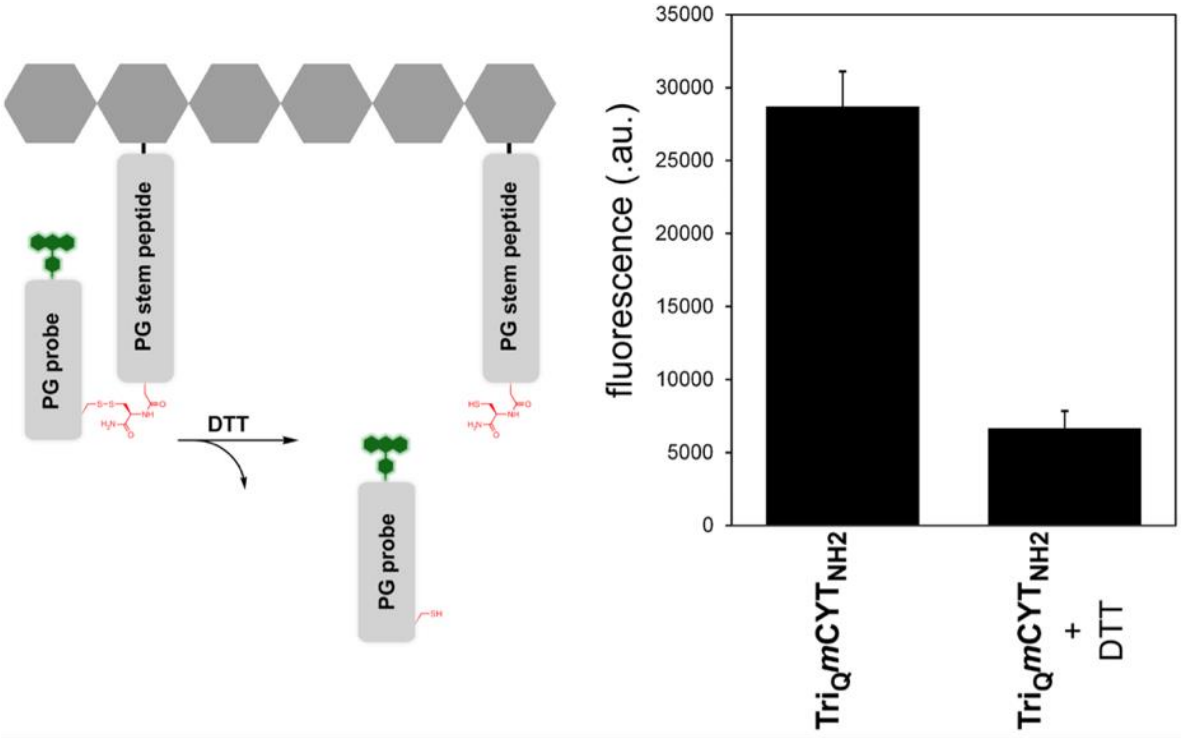

Figure 4.10 *(Left) Schematic of TriQmCYT probe crosslinked to the PG stem peptide, followed by treatment of DTT which is expected to reduce the cystine and lead to release of the fluorescent probe. (Right) Flow cytometry analysis of L. plantarum treated overnight with 100 μM* ***Tri$_Q$mCYT$_{NH2}$****, fixed with formaldehyde and, if noted, treated with 10 mM DTT for 10 min. Data are represented as mean + SD (n=3).*

Appreciating that the disulfide bond in *m*-CYT provides a unique chemical handle, we hypothesized that we could selectively assess the mode of probe incorporation by treatment with a reducing agent. Transpeptidases catalyze the crosslinking of two neighboring stem peptides, with one stem peptide acting as the acyl-donor and the other acting as the acyl-acceptor strand. We previously showed that tetramer and pentamer stem peptide analogs can potentially act as either acyl-donor or -acceptor strands owing to the inclusion of the nucleophilic crossbridge and the sacrificial *C*-terminal D-alanine.[33, 34] We reasoned that DTT reduction of the *m*-CYT containing probes after their metabolic incorporation within the PG scaffold would selectively release probes that were installed *via* the acyl-acceptor mode. On the other hand, probes should be retained if they

were incorporated into the PG scaffold *via* the acyl-acceptor mode. To test this idea, we treated *L. plantarum* cells with **Penta$_Q$*m*CYT** or **Penta$_Q$*m*CYT$_{NH2}$** overnight and then treated them with DTT. Our results showed that there was increased labeling upon amidation of the crossbridge to carboxamide and that *m*-CYT is also recognized by the PG machinery when installed onto a pentameric stem peptide analog (**Figure 4.11**). Moreover, there was a considerable decrease in cellular fluorescence following DTT treatment of cells labeled with **Penta$_Q$*m*CYT$_{NH2}$** but no change in cells labeled with **D-Lys(FITC)**. The decrease in fluorescence levels likely points to **Penta$_Q$*m*CYT$_{NH2}$** as a primary acyl-acceptor strand with the remaining fluorescence potentially describing the portion of incorporation as acyl-donor strands. Finally, PG incorporation was verified using standard PG analysis from cells treated with **Tri$_Q$*m*CYT$_{NH2}$**. Two additional bacterial species were tested for *m*-CYT labeling including *Listeria monocytogenes* (*L. monocytogenes*) and *Lactobacillus casei* (*L. casei*). *L. monocytogenes* possess an *m*-DAP type of PG structure while *L. casei* is a L-Lys type bacteria that typically contains a D-Asn crossbridge.[63] It was observed that *L. monocytogenes* labeled in a manner consistent with other *m*-DAP-based organisms (**Figure 4.12**) but, as expected, *L. casei* showed little labeling with the probe displaying *m*-CYT (**Figure 4.12**).

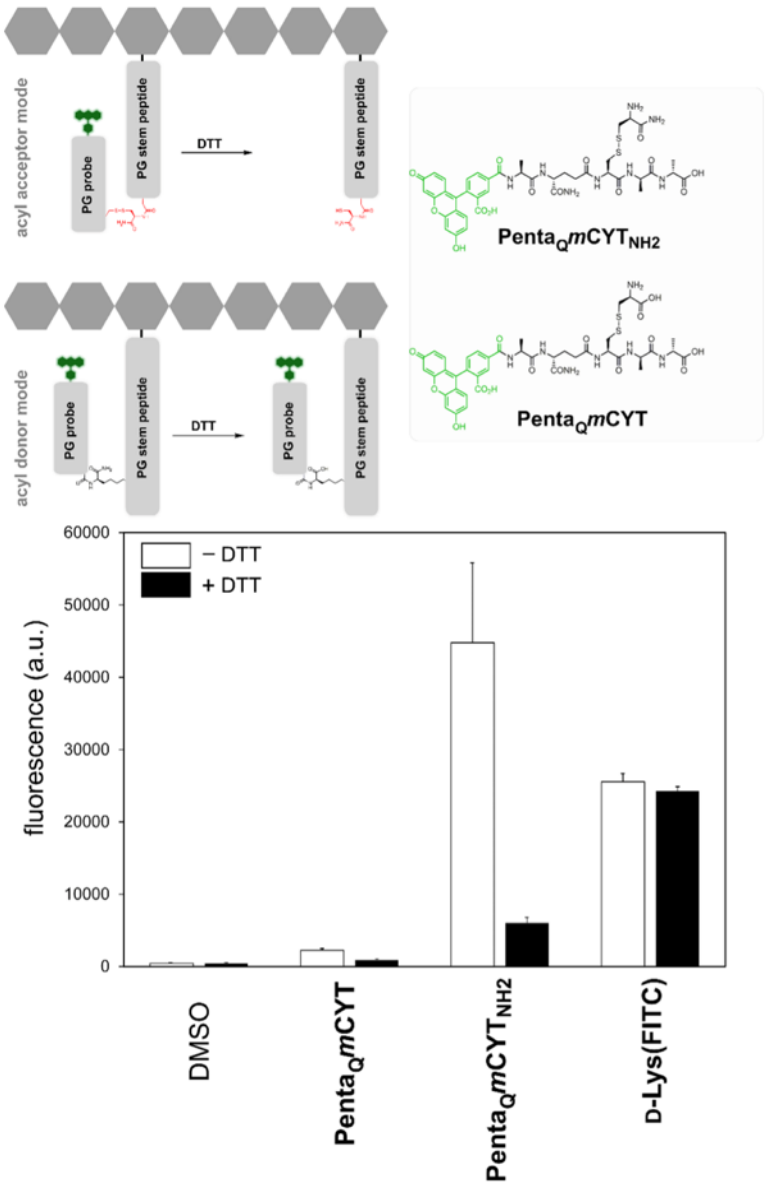

Figure 4.11 *Flow cytometry analysis of L. plantarum untreated or treated overnight with 100 µM* ***PentaQmCYT***, ***PentaQmCYT$_{NH2}$***, *or D-Lys(FITC) in the absence of presence of DTT (10 mM). Data are represented as mean + SD (n=3).*

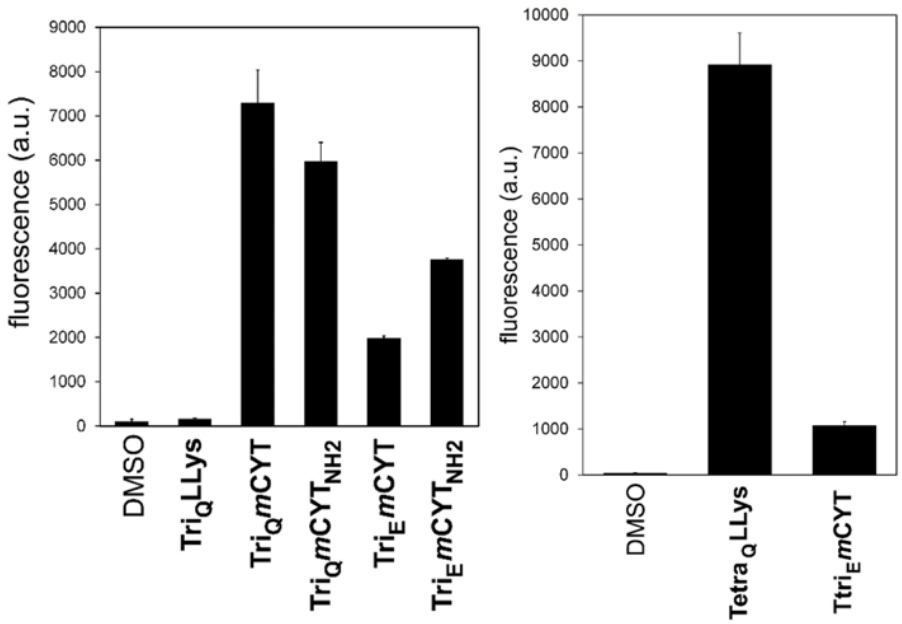

Figure 4.12 *(Left) Flow cytometry analysis of Listeria monocytogenes treated overnight with 100 µM of each probe. Data are represented as mean + SD (n=3). (Right) Flow cytometry analysis of Lactobacillus casei (L. casei) treated overnight with 100 µM of each probe. Data are represented as mean + SD (n=3).*

4.4 *Conclusion*

There is increasing interest in understanding the cell wall biosynthetic machinery in live bacterial cells. The principal driving force for *in vivo* analysis is the emerging paradigm of extensive protein-protein interactions that control components of the cell wall biosynthetic machinery to modulate the growth and remodeling of PG. Our group and others have previously described a class of L-Lys-based PG probes that operates by mimicking components of the PG stem peptide to metabolically label the PG of live cells by TP-mediated incorporation, thus providing a direct signal that reports on PG biosynthesis. And yet, the lack of facile synthetic routes to *m*-DAP building blocks or their derivatives to assemble PG analogs of *m*-DAP containing organisms has hampered fundamental studies using live bacteria. We describe a strategy that makes use of the simple and widely available Fmoc-protected L-Cys to build *m*-CYT, which recapitulates key structural

features of *m*-DAP. After demonstrating the ease of synthesizing *m*-CYT containing peptides, we showed that TPs accepted *m*-CYT in place of m-DAP by labeling live bacterial cells. More specifically, we installed *m*-CYT in a PG probe that can only be crosslinked into the bacterial PG scaffold by mimicking *m*-DAP. We anticipate that *m*-CYT will complement emerging tools to better understand cell wall biosynthesis in *m*-DAP containing organisms by providing a reliable route to a bioisostere that is biologically functional.

4.5 *Materials and Methods*

Materials. All peptide related reagents (resin, coupling reagent, deprotection reagent, amino acids, and cleavage reagents) were purchased from ChemImpex. Bacterial strains *M. smegmatis* WT and Δldt were grown in lysogeny broth supplemented with 0.05% Tween 80 for all experiments. *L. plantarum* and *L. casei* were grown in Lactobacilli MRS broth. *L. monocytogenes* was grown in brain heart infusion broth.

Flow cytometry analysis of bacterial labeling. Media containing 100 µM of each probe were prepared. Bacterial cells from an overnight culture were added to the medium (1:100 dilution) and allowed to grow overnight at 37°C with shaking at 250 rpm. The bacteria were harvested at 6,000g and washed three times with original culture volume of 1x PBS followed by fixation with 2% formaldehyde in 1x PBS for 30 min at room temperature. The cells were washed once more to remove formaldehyde and then analyzed using a BDFacs Canto II flow cytometer with a 488nm argon laser (L1) and a 530/30 bandpass filter (FL1). A minimum of 10,000 events were counted for each data set. The data was analyzed using the FACSDiva version 6.1.1.

Flow cytometry analysis of *L. plantarum* treated with DTT. *L. plantarum* cells from an overnight culture were added to blank media (1:100 dilution), media supplemented with 100 µM **Tri$_{Q}$*m*CYT$_{NH2}$**, or 100 µM **Tri$_{Q}$*m*CYT$_{NH2}$** that was pre-treated with 5 mM dithiothreitol (DTT). Cells were grown overnight at 37°C with shaking at 250 rpm. The bacterial cells were harvested at 6,000g and washed three times with original culture

volume of 1x PBS. Cells labeled with pre-reduced **Tri$_Q$*m*CYT$_{NH2}$** were fixed with formaldehyde. Cells labeled with **Tri$_Q$*m*CYT$_{NH2}$** were treated with 10 mM DTT for 10 min, washed twice, fixed with 4% formaldehyde and resuspended in 1x PBS for analysis by BDFacs Canto II flow cytometer, as previously described.

PG Digestion: Lysozyme/Mutanolysin Treatment of Labeled Peptidoglycan. *L. plantarum* (1:100) were added to Lactobacilli MRS broth or Lactobacilli MRS broth containing 100 mM **Tri$_Q$*m*CYT$_{NH2}$** and allowed to grow overnight at 37°C with shaking at 250 rpm. The bacteria were harvested at 6,000g and washed three times with original culture volume of 1x PBS followed by fixation with 2% formaldehyde in 1x PBS for 30 min at ambient temperature. Cells were washed once more to remove the formaldehyde. Cells were washed three times with 1x PBS. Cell pellets were resuspended in 1x PBS containing 500 mg/mL lysozyme (MP biomedicals) or 40 mg/mL mutanolysin (Sigma-Aldrich) and incubated at 37°C. A portion of the cells were taken at 1, 60, 120, 240, and 1140 min. At each time point, the collected bacteria were washed three times with 1x PBS and resuspended in a final solution of 1x PBS containing 4% formaldehyde to quench the lysozyme/mutanolysin reaction. Cells were analyzed using a BDFacs Canto II flow cytometer using the previously stated parameters.

Peptidoglycan Isolation. MRS medium (50 mL) containing 500 µM **Tri$_Q$*m*CYT$_{NH2}$** was prepared. *L. plantarum* bacteria were added to the MRS medium (1:100) and allowed to grow overnight at 37°C with shaking at 250 rpm. The cells were harvested and washed with 1x with cold 0.025 M potassium phosphate buffer, pH 7.0. Washed cells were pelleted, resuspended in sterile H_2O and lyophilized. The cells were then resuspended in sterile H_2O added, dropwise to boiling water with 4% (w/v) sodium dodecyl sulfate (SDS). The sample was boiled for 30 minutes, and was then cooled for 2 hours with stirring, and was allowed to stand overnight (unstirred) at room temperature. The sample was sedimented by centrifugation at 60,000g for 20 minutes at room temperature, and washed three times, using the same centrifugation parameters, with sterile H_2O. The pellet was then incubated at 37°C with shaking at 110 rpm for 16 hours in 20 mL of 20 mM potassium phosphate buffer pH 7.8 with 200 µg/mL Trypsin and 83 µg/mL DNase. Following, the

sample was sedimented by centrifugation at 100,000g for 1 hour at 20° C and washed three times, using the same centrifugation parameters, with sterile H_2O. The pellet was then incubated at 37°C with shaking at 110 rpm in 2mL of 25 mM potassium phosphate buffer pH 6.5/10 mM $MgCl_2$ with 200 µg/mL lysozyme and 250 µg/mL mutanolysin. After 16 hours, the samples were boiled for 3 minutes to inactivate the enzymes and centrifuged at 12,000g for 5 minutes. The supernatant was salvaged, filtered with a 25 mm 0.45 µm Nylon membrane, and applied to an Aeris 250 x 21.2 mm reverse-phase C18 column using a Waters 600 HPLC pumped with 100% H_2O with 0.1% Trifluoroacetic acid (TFA) for 20 minutes, followed collection of the elutant with a linear methanol gradient (0-100% with 0.1% TFA) for 20 minutes, and an isocratic 10 minute hold at 100% methanol. The collection was rotovaped, lyophilized, and analyzed using an Agilent 1260 Infinity II Prime LC and Agilent 6545B QTOF with a Luna 30 x 2.00 mm reverse-phase C18(2) column, eluted at a flow rate of 0.5 mL/min for 10 minutes with 0.1% formic acid (v/v) in water and subsequently with a 90 minute linear methanol gradient (0-20%) in 0.1% formic acid. The column temperature was maintained at 40°C.

Lattice Light Sheet Imaging of *M. smegmatis*

Mounting cells on chitosan coated coverslips

To promote adherence of cells (1,2), 5 mm round, chitosan-coated coverslips were used for mounting samples. Coverslips were covered with 1% (w/v) chitosan (ThermoFisher) in 1.5% (v/v) glacial acetic acid for 15 minutes at room temperature. The coverslips were then gently rinsed with water and allowed to dry at room temperature for at least 2 hours before use. Fixed, labeled cell suspensions of *M. smegmatis* were applied to the coated surface of the coverslip, and left unperturbed at room temperature for 1.5 hours to allow for adherence. Coverslips were then gently rinsed with PBS and mounted for imaging in the LLSM basin containing PBS as the imaging buffer.

LLSM image acquisition

Fluorescence imaging was performed on a home-built lattice light sheet microscope (3), as described previously (4, 5). **Tri$_{E}$*m*CYT$_{NH2}$** fluorescence was excited with 561 nm light

sheet excitation, using a time-averaged (dithered), square lattice pattern. 3D images were acquired by translating the sample through the optical light sheet in 200 nm steps using a piezo nano-positioning stage (Physik Instrumente P-621.1CD). Light intensity at the sample was < 1 W/cm^2. Widefield fluorescence images of each imaging plane were collected using an sCMOS detector (Hamamatsu ORCA Flash v2).

Raw Image Processing

Raw images were deskewed and deconvolved as described previously (3,6). Deconvolution was performed using 10 iterations of the Richardson-Lucy algorithm. An experimentally measured PSF of fluorescent beads (200 nm FluoSpheres®, ThermoFisher) was used as the deconvolution kernel.

4.6 *References*

1. Vollmer, W.; Blanot, D.; De Pedro, M. A., Peptidoglycan structure and architecture. *FEMS Microbiology Reviews* **2008,** *32* (2), 149-167.

2. Lam, H.; Oh, D.-C.; Cava, F.; Takacs Constantin, N.; Clardy, J.; de Pedro Miguel, A.; Waldor Matthew, K., D-Amino Acids Govern Stationary Phase Cell Wall Remodeling in Bacteria. *Science* **2009,** *325* (5947), 1552-1555.

3. Braun, V.; Bosch, V., Sequence of the murein-lipoprotein and the attachment site of the lipid. *Eur J Biochem* **1972,** *28* (1), 51-69.

4. Braun, V.; Wolff, H., Attachment of lipoprotein to murein (peptidoglycan) of Escherichia coli in the presence and absence of penicillin FL 1060. *J Bacteriol* **1975,** *123* (3), 888-97.

5. Dworkin, J., The medium is the message: interspecies and interkingdom signaling by peptidoglycan and related bacterial glycans. *Annu Rev Microbiol* **2014,** *68*, 137-54.

6. Shah, I. M.; Laaberki, M. H.; Popham, D. L.; Dworkin, J., A eukaryotic-like Ser/Thr kinase signals bacteria to exit dormancy in response to peptidoglycan fragments. *Cell* **2008,** *135* (3), 486-96.

7. Squeglia, F.; Marchetti, R.; Ruggiero, A.; Lanzetta, R.; Marasco, D.; Dworkin, J.; Petoukhov, M.; Molinaro, A.; Berisio, R.; Silipo, A., Chemical Basis of Peptidoglycan Discrimination by PrkC, a Key Kinase Involved in Bacterial Resuscitation from Dormancy. *Journal of the American Chemical Society* **2011,** *133* (51), 20676-20679.

8. Wolf, A. J.; Underhill, D. M., Peptidoglycan recognition by the innate immune system. *Nat Rev Immunol* **2018,** *18* (4), 243-254.

9. Chamaillard, M.; Hashimoto, M.; Horie, Y.; Masumoto, J.; Qiu, S.; Saab, L.; Ogura, Y.; Kawasaki, A.; Fukase, K.; Kusumoto, S.; Valvano, M. A.; Foster, S. J.; Mak, T. W.; Nuñez, G.; Inohara, N., An essential role for NOD1 in host recognition of bacterial peptidoglycan containing diaminopimelic acid. *Nat Immunol* **2003,** *4* (7), 702-7.

10. Girardin, S. E.; Travassos, L. H.; Hervé, M.; Blanot, D.; Boneca, I. G.; Philpott, D. J.; Sansonetti, P. J.; Mengin-Lecreulx, D., Peptidoglycan molecular requirements allowing detection by Nod1 and Nod2. *J Biol Chem* **2003,** *278* (43), 41702-8.

11. Vijayrajratnam, S.; Pushkaran, A. C.; Balakrishnan, A.; Vasudevan, A. K.; Biswas, R.; Mohan, C. G., Bacterial peptidoglycan with amidated meso-diaminopimelic acid evades NOD1 recognition: an insight into NOD1 structure-recognition. *Biochem J* **2016,** *473* (24), 4573-4592.

12. Irazoki, O.; Hernandez, S. B.; Cava, F., Peptidoglycan Muropeptides: Release, Perception, and Functions as Signaling Molecules. *Front Microbiol* **2019,** *10*, 500.

13. Cava, F.; de Pedro, M. A., Peptidoglycan plasticity in bacteria: emerging variability of the murein sacculus and their associated biological functions. *Curr Opin Microbiol* **2014,** *18*, 46-53.

14. Hernández, N.; Martín, V. S., General stereoselective synthesis of chemically differentiated alpha-diamino acids: synthesis of 2,6-diaminopimelic and 2,7-diaminosuberic acids. *J Org Chem* **2001,** *66* (14), 4934-8.

15. Lee, M.; Hesek, D.; Shah, I. M.; Oliver, A. G.; Dworkin, J.; Mobashery, S., Synthetic peptidoglycan motifs for germination of bacterial spores. *Chembiochem* **2010,** *11* (18), 2525-9.

16. Ross, A. C.; McKinnie, S. M. K.; Vederas, J. C., The Synthesis of Active and Stable Diaminopimelate Analogues of the Lantibiotic Peptide Lactocin S. *Journal of the American Chemical Society* **2012,** *134* (4), 2008-2011.

17. Roychowdhury, A.; Wolfert, M. A.; Boons, G. J., Synthesis and proinflammatory properties of muramyl tripeptides containing lysine and diaminopimelic acid moieties. *Chembiochem* **2005,** *6* (11), 2088-97.

18. Kawasaki, A.; Karasudani, Y.; Otsuka, Y.; Hasegawa, M.; Inohara, N.; Fujimoto, Y.; Fukase, K., Synthesis of diaminopimelic acid containing peptidoglycan fragments and tracheal cytotoxin (TCT) and investigation of their biological functions. *Chemistry* **2008,** *14* (33), 10318-30.

19. Kumar, S.; Roychowdhury, A.; Ember, B.; Wang, Q.; Guan, R.; Mariuzza, R. A.; Boons, G. J., Selective recognition of synthetic lysine and meso-diaminopimelic acid-type peptidoglycan fragments by human peptidoglycan recognition proteins I{alpha} and S. *J Biol Chem* **2005,** *280* (44), 37005-12.

20. Denoël, T.; Zervosen, A.; Gerards, T.; Lemaire, C.; Joris, B.; Blanot, D.; Luxen, A., Stereoselective synthesis of lanthionine derivatives in aqueous solution and their

incorporation into the peptidoglycan of Escherichia coli. *Bioorganic & Medicinal Chemistry* **2014,** *22* (17), 4621-4628.

21. Knerr, P. J.; van der Donk, W. A., Chemical Synthesis of the Lantibiotic Lacticin 481 Reveals the Importance of Lanthionine Stereochemistry. *Journal of the American Chemical Society* **2013,** *135* (19), 7094-7097.

22. Uehara, A.; Fujimoto, Y.; Kawasaki, A.; Kusumoto, S.; Fukase, K.; Takada, H., Meso-diaminopimelic acid and meso-lanthionine, amino acids specific to bacterial peptidoglycans, activate human epithelial cells through NOD1. *J Immunol* **2006,** *177* (3), 1796-804.

23. Cobb, S. L.; Vederas, J. C., A concise stereoselective synthesis of orthogonally protected lanthionine and beta-methyllanthionine. *Org Biomol Chem* **2007,** *5* (7), 1031-8.

24. Diaper, C. M.; Sutherland, A.; Pillai, B.; James, M. N.; Semchuk, P.; Blanchard, J. S.; Vederas, J. C., The stereoselective synthesis of aziridine analogues of diaminopimelic acid (DAP) and their interaction with dap epimerase. *Org Biomol Chem* **2005,** *3* (24), 4402-11.

25. Soni, A. S.; Lin, C. S.; Murphy, M. E. P.; Tanner, M. E., Peptides Containing meso-Oxa-Diaminopimelic Acid as Substrates for the Cell-Shape-Determining Proteases Csd6 and Pgp2. *Chembiochem* **2019,** *20* (12), 1591-1598.

26. Soni, A. S.; Vacariu, C. M.; Chen, J. Y.; Tanner, M. E., Synthesis of a meso-Oxa-Diaminopimelic Acid Containing Peptidoglycan Pentapeptide and Coupling to the GlcNAc-anhydro-MurNAc Disaccharide. *Organic Letters* **2020,** *22* (6), 2313-2317.

27. Kuru, E.; Hughes, H. V.; Brown, P. J.; Hall, E.; Tekkam, S.; Cava, F.; de Pedro, M. A.; Brun, Y. V.; VanNieuwenhze, M. S., In Situ probing of newly synthesized peptidoglycan in live bacteria with fluorescent D-amino acids. *Angew Chem Int Ed Engl* **2012,** *51* (50), 12519-23.

28. Kuru, E.; Tekkam, S.; Hall, E.; Brun, Y. V.; Van Nieuwenhze, M. S., Synthesis of fluorescent D-amino acids and their use for probing peptidoglycan synthesis and bacterial growth in situ. *Nat Protoc* **2015,** *10* (1), 33-52.

29. Siegrist, M. S.; Whiteside, S.; Jewett, J. C.; Aditham, A.; Cava, F.; Bertozzi, C. R., (D)-Amino acid chemical reporters reveal peptidoglycan dynamics of an intracellular pathogen. *ACS Chem Biol* **2013,** *8* (3), 500-5.

30. Siegrist, M. S.; Swarts, B. M.; Fox, D. M.; Lim, S. A.; Bertozzi, C. R., Illumination of growth, division and secretion by metabolic labeling of the bacterial cell surface. *FEMS Microbiol Rev* **2015,** *39* (2), 184-202.

31. Lebar, M. D.; May, J. M.; Meeske, A. J.; Leiman, S. A.; Lupoli, T. J.; Tsukamoto, H.; Losick, R.; Rudner, D. Z.; Walker, S.; Kahne, D., Reconstitution of Peptidoglycan Cross-Linking Leads to Improved Fluorescent Probes of Cell Wall Synthesis. *Journal of the American Chemical Society* **2014,** *136* (31), 10874-10877.

32. Lupoli, T. J.; Tsukamoto, H.; Doud, E. H.; Wang, T.-S. A.; Walker, S.; Kahne, D., Transpeptidase-Mediated Incorporation of d-Amino Acids into Bacterial Peptidoglycan. *Journal of the American Chemical Society* **2011,** *133* (28), 10748-10751.

33. Apostolos, A. J.; Pidgeon, S. E.; Pires, M. M., Remodeling of Cross-bridges Controls Peptidoglycan Cross-linking Levels in Bacterial Cell Walls. *ACS Chemical Biology* **2020,** *15* (5), 1261-1267.

34. Pidgeon, S. E.; Apostolos, A. J.; Nelson, J. M.; Shaku, M.; Rimal, B.; Islam, M. N.; Crick, D. C.; Kim, S. J.; Pavelka, M. S.; Kana, B. D.; Pires, M. M., L,D-Transpeptidase Specific Probe Reveals Spatial Activity of Peptidoglycan Cross-Linking. *ACS Chemical Biology* **2019,** *14* (10), 2185-2196.

35. Welsh, M. A.; Taguchi, A.; Schaefer, K.; Van Tyne, D.; Lebreton, F.; Gilmore, M. S.; Kahne, D.; Walker, S., Identification of a Functionally Unique Family of Penicillin-Binding Proteins. *Journal of the American Chemical Society* **2017,** *139* (49), 17727-17730.

36. Gautam, S.; Kim, T.; Shoda, T.; Sen, S.; Deep, D.; Luthra, R.; Ferreira, M. T.; Pinho, M. G.; Spiegel, D. A., An Activity-Based Probe for Studying Crosslinking in Live Bacteria. *Angew Chem Int Ed Engl* **2015,** *54* (36), 10492-6.

37. Ngadjeua, F.; Braud, E.; Saidjalolov, S.; Iannazzo, L.; Schnappinger, D.; Ehrt, S.; Hugonnet, J. E.; Mengin-Lecreulx, D.; Patin, D.; Ethève-Quelquejeu, M.; Fonvielle, M.; Arthur, M., Critical Impact of Peptidoglycan Precursor Amidation on the Activity of l,d-Transpeptidases from Enterococcus faecium and Mycobacterium tuberculosis. *Chemistry* **2018,** *24* (22), 5743-5747.

38. Gautam, S.; Kim, T.; Spiegel, D. A., Chemical Probes Reveal an Extraseptal Mode of Cross-Linking in Staphylococcus aureus. *Journal of the American Chemical Society* **2015,** *137* (23), 7441-7447.

39. Baranowski, C.; Welsh, M. A.; Sham, L. T.; Eskandarian, H. A.; Lim, H. C.; Kieser, K. J.; Wagner, J. C.; McKinney, J. D.; Fantner, G. E.; Ioerger, T. R.; Walker, S.; Bernhardt, T. G.; Rubin, E. J.; Rego, E. H., Maturing Mycobacterium smegmatis peptidoglycan requires non-canonical crosslinks to maintain shape. *Elife* **2018,** *7*.

40. Flores, A. R.; Parsons, L. M.; Pavelka, M. S., Genetic analysis of the beta-lactamases of Mycobacterium tuberculosis and Mycobacterium smegmatis and susceptibility to beta-lactam antibiotics. *Microbiology (Reading)* **2005,** *151* (Pt 2), 521-532.

41. Maitra, A.; Munshi, T.; Healy, J.; Martin, L. T.; Vollmer, W.; Keep, N. H.; Bhakta, S., Cell wall peptidoglycan in Mycobacterium tuberculosis: An Achilles' heel for the TB-causing pathogen. *FEMS Microbiol Rev* **2019,** *43* (5), 548-575.

42. Zapun, A.; Philippe, J.; Abrahams, K. A.; Signor, L.; Roper, D. I.; Breukink, E.; Vernet, T., In vitro Reconstitution of Peptidoglycan Assembly from the Gram-Positive Pathogen Streptococcus pneumoniae. *ACS Chemical Biology* **2013,** *8* (12), 2688-2696.

43. Mahapatra, S.; Yagi, T.; Belisle, J. T.; Espinosa, B. J.; Hill, P. J.; McNeil, M. R.; Brennan, P. J.; Crick, D. C., Mycobacterial lipid II is composed of a complex mixture of modified muramyl and peptide moieties linked to decaprenyl phosphate. *J Bacteriol* **2005,** *187* (8), 2747-57.

44. Figueiredo, T. A.; Sobral, R. G.; Ludovice, A. M.; de Almeida, J. M. F.; Bui, N. K.; Vollmer, W.; de Lencastre, H.; Tomasz, A., Identification of Genetic Determinants and Enzymes Involved with the Amidation of Glutamic Acid Residues in the Peptidoglycan of Staphylococcus aureus. *PLOS Pathogens* **2012,** *8* (1), e1002508.

45. Liu, X.; Gallay, C.; Kjos, M.; Domenech, A.; Slager, J.; van Kessel, S. P.; Knoops, K.; Sorg, R. A.; Zhang, J. R.; Veening, J. W., High-throughput CRISPRi phenotyping identifies new essential genes in Streptococcus pneumoniae. *Mol Syst Biol* **2017,** *13* (5), 931.

46. Lavollay, M.; Fourgeaud, M.; Herrmann, J. L.; Dubost, L.; Marie, A.; Gutmann, L.; Arthur, M.; Mainardi, J. L., The peptidoglycan of Mycobacterium abscessus is predominantly cross-linked by L,D-transpeptidases. *J Bacteriol* **2011,** *193* (3), 778-82.

47. Mitani, Y.; Meng, X.; Kamagata, Y.; Tamura, T., Characterization of LtsA from Rhodococcus erythropolis, an enzyme with glutamine amidotransferase activity. *J Bacteriol* **2005,** *187* (8), 2582-91.

48. Levefaudes, M.; Patin, D.; de Sousa-d'Auria, C.; Chami, M.; Blanot, D.; Hervé, M.; Arthur, M.; Houssin, C.; Mengin-Lecreulx, D., Diaminopimelic Acid Amidation in Corynebacteriales: NEW INSIGHTS INTO THE ROLE OF LtsA IN PEPTIDOGLYCAN MODIFICATION. *J Biol Chem* **2015,** *290* (21), 13079-94.

49. Dajkovic, A.; Tesson, B.; Chauhan, S.; Courtin, P.; Keary, R.; Flores, P.; Marlière, C.; Filipe, S. R.; Chapot-Chartier, M. P.; Carballido-Lopez, R., Hydrolysis of peptidoglycan is modulated by amidation of meso-diaminopimelic acid and Mg(2+) in Bacillus subtilis. *Mol Microbiol* **2017,** *104* (6), 972-988.

50. Mainardi, J. L.; Fourgeaud, M.; Hugonnet, J. E.; Dubost, L.; Brouard, J. P.; Ouazzani, J.; Rice, L. B.; Gutmann, L.; Arthur, M., A novel peptidoglycan cross-linking enzyme for a beta-lactam-resistant transpeptidation pathway. *J Biol Chem* **2005,** *280* (46), 38146-52.

51. Zandi, T. A.; Marshburn, R. L.; Stateler, P. K.; Brammer Basta, L. A., Phylogenetic and Biochemical Analyses of Mycobacterial l,d-Transpeptidases Reveal a Distinct Enzyme Class That Is Preferentially Acylated by Meropenem. *ACS Infect Dis* **2019,** *5* (12), 2047-2054.

52. Sanders, A. N.; Wright, L. F.; Pavelka, M. S., Genetic characterization of mycobacterial L,D-transpeptidases. *Microbiology (Reading)* **2014,** *160* (Pt 8), 1795-1806.

53. Waterhouse, A.; Bertoni, M.; Bienert, S.; Studer, G.; Tauriello, G.; Gumienny, R.; Heer, F. T.; de Beer, T. A. P.; Rempfer, C.; Bordoli, L.; Lepore, R.; Schwede, T., SWISS-MODEL: homology modelling of protein structures and complexes. *Nucleic Acids Res* **2018,** *46* (W1), W296-w303.

54. Bienert, S.; Waterhouse, A.; de Beer, T. A.; Tauriello, G.; Studer, G.; Bordoli, L.; Schwede, T., The SWISS-MODEL Repository-new features and functionality. *Nucleic Acids Res* **2017,** *45* (D1), D313-d319.

55. Silva, J. R.; Roitberg, A. E.; Alves, C. N., Catalytic mechanism of L,D-transpeptidase 2 from Mycobacterium tuberculosis described by a computational approach: insights for the design of new antibiotics drugs. *J Chem Inf Model* **2014,** *54* (9), 2402-10.

56. Silva, J. R.; Govender, T.; Maguire, G. E.; Kruger, H. G.; Lameira, J.; Roitberg, A. E.; Alves, C. N., Simulating the inhibition reaction of Mycobacterium tuberculosis L,D-transpeptidase 2 by carbapenems. *Chem Commun (Camb)* **2015,** *51* (63), 12560-2.

57. Bron, P. A.; van Baarlen, P.; Kleerebezem, M., Emerging molecular insights into the interaction between probiotics and the host intestinal mucosa. *Nat Rev Microbiol* **2011,** *10* (1), 66-78.

58. D'Ambrosio, E. A.; Drake, W. R.; Mashayekh, S.; Ukaegbu, O. I.; Brown, A. R.; Grimes, C. L., Modulation of the NOD-like receptors NOD1 and NOD2: A chemist's perspective. *Bioorg Med Chem Lett* **2019,** *29* (10), 1153-1161.

59. Griffin, M. E.; Hespen, C. W.; Wang, Y. C.; Hang, H. C., Translation of peptidoglycan metabolites into immunotherapeutics. *Clin Transl Immunology* **2019,** *8* (12), e1095.

60. Wolfert, M. A.; Roychowdhury, A.; Boons, G. J., Modification of the structure of peptidoglycan is a strategy to avoid detection by nucleotide-binding oligomerization domain protein 1. *Infect Immun* **2007,** *75* (2), 706-13.

61. Wang, Q.; Matsuo, Y.; Pradipta, A. R.; Inohara, N.; Fujimoto, Y.; Fukase, K., Synthesis of characteristic Mycobacterium peptidoglycan (PGN) fragments utilizing with chemoenzymatic preparation of meso-diaminopimelic acid (DAP), and their modulation of innate immune responses. *Org Biomol Chem* **2016,** *14* (3), 1013-23.

62. Bernard, E.; Rolain, T.; Courtin, P.; Hols, P.; Chapot-Chartier, M. P., Identification of the amidotransferase AsnB1 as being responsible for meso-diaminopimelic acid amidation in Lactobacillus plantarum peptidoglycan. *J Bacteriol* **2011,** *193* (22), 6323-30.

63. Billot-Klein, D.; Legrand, R.; Schoot, B.; van Heijenoort, J.; Gutmann, L., Peptidoglycan structure of Lactobacillus casei, a species highly resistant to glycopeptide antibiotics. *J Bacteriol* **1997,** *179* (19), 6208-12.

Chapter 5 Metabolic Processisng of Selenium-based Bioisostere of *meso*-diaminopimelic Acid in Live Bacteria

Apostolos, A.J., Ocius, K., Koyasseril-Yehiya, T.M., Santamaria, C., Silva, J.R.A., Lameira, J., Alves, C.N., Siegrist, M.S., Pires, M.M.

5.1 *Abstract*

A primary component of all known bacterial cell walls is the peptidoglycan (PG) layer, which is comprised of repeating units of sugars connected to short and unusual peptides. The various steps within PG biosynthesis are targets of potent antibiotics as proper assembly of the PG is essential for cellular growth and survival. Synthetic mimics of PG have proven to be indispensable tools to study bacterial cell structure, growth and remodeling. Yet, a common component of PG, *meso*-diaminopimelic acid (*m*-DAP) at the third position of the stem peptide, remains challenging to access synthetically and is not commercially available. Here, we describe the synthesis and metabolic processing of a selenium-based bioisostere mimic of *m*-DAP, selenolanthionine and show that selenolanthionine is installed within the PG of live bacteria by the native cell wall crosslinking machinery in mycobacterial species. This PG probe has an orthogonal release mechanism that could be important for downstream proteomics studies. Finally, we describe a bead-based assay that is compatible with high-throughput screening of cell wall enzymes. We envision that this probe will supplement the current methods available for investigating PG crosslinking in *m*-DAP containing organisms.

5.2 *Introduction*

The bacterial cell envelope is highly complex and its overall architecture can vary among the different classifications of bacteria (e.g., Gram-positive, Gram-negative, and mycobacteria); however, all known bacteria possess a peptidoglycan (PG) layer. PG is a large biomacromolecule that encompasses the inner membrane of bacteria.[1] It is essential to the viability of bacterial cells; a feature that is tied to the structural support it provides by maintaining cellular shape and rigidity. For almost all known bacteria, PG is

composed of a backbone glycan strand connected to short and highly unusual peptides (often referred to as stem peptides). While there can be variability in the primary sequence of the stem peptide, some features remain constant. For example, stem peptides are initially biosynthesized as pentamers and most often contain the sequence L-Ala-D-iGlu-X-D-Ala-D-Ala, whereby X can be *meso*-diaminopimelic acid (*m*-DAP) or L-Lys (typically modified with a crossbridge).

The most varied position within the stem peptide is the third amino acid.[1] Bacteria whose PG contain *m*-DAP (**Figure 5.1a**) are diverse, ranging across Gram-positive bacteria such as *Bacillus subtilis* (*B. subtilis*) and *Lactobacillus plantarum* (*L. plantarum)*, Gram-negative bacteria such as *Escherichia coli* (*E. coli*) and *Pseudomonas aeruginosa* (*P. aeruginosa*), and mycobacteria such as *Mycobacterium tuberculosis* (*M. tuberculosis*).[2, 3] Many of these bacteria are important for human health as these organisms can be dangerous pathogens and/or part of the microbial community that colonize humans. The difference between *m*-DAP and L-Lys may be structurally subtle (a carboxyl on the ε carbon) but this variation can impose a significant impact on how PG fragments are sensed or metabolized.[4-6] For instance, fragments of PG and other macromolecules released by bacterial cells are recognized by the human immune system as pathogen-associated molecular patterns (PAMPs), which are biomolecules that signal the presence of bacterial cells (a potential danger signal).[7] A prominent PAMP receptor in human immune cells, NOD1, is activated by the minimal PG motif, D-iGlu-*m*-DAP (iE-DAP).[8] However, the analogous PG fragment from L-Lys containing bacteria, D-iGlu-L-Lys, does not activate NOD1. Moreover, recent studies have demonstrated that amidation of *m*-DAP can greatly attenuate NOD1 activation, which suggests a potential pathway for *m*-DAP containing bacteria to edit the PG layer to reduce recognition by the host immune system.[9, 10] A similar strict preference for *m*-DAP containing PG fragments has also been observed for the resuscitation receptors on *B. subtilis*.[11-13] Given the significant role *m*-DAP can play in microbiology and host-bacteria interactions, there is a need for access to *m*-DAP based chemical probes to interrogate processes related to PG remodeling, biosynthesis, and sensing.[14, 15]

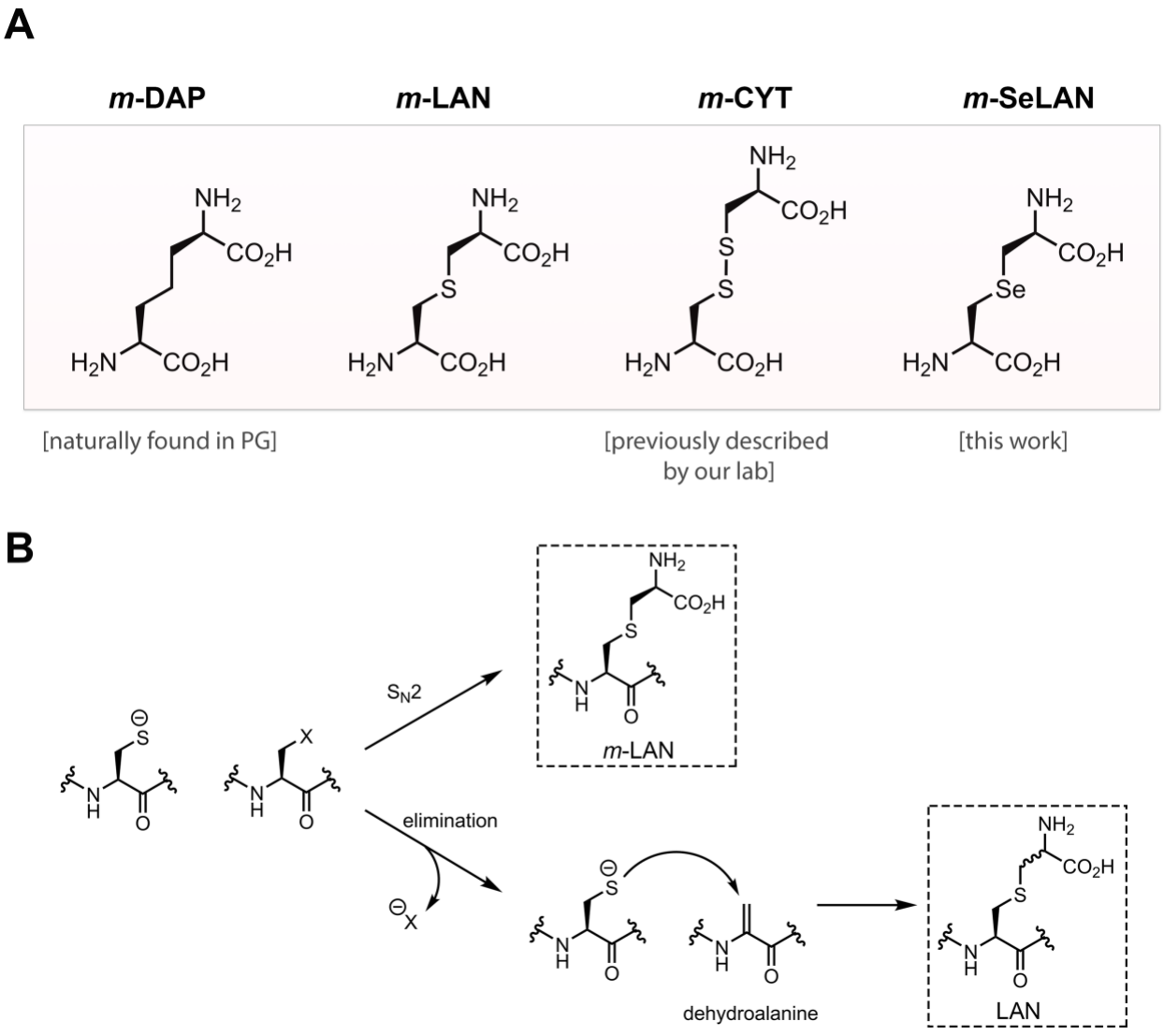

Figure 5.1 *(A) Chemical structure of m-DAP and its three bioisosteres (m-LAN, m-CYT, and m-SeLAN). (B) Chemical synthesis of m-LAN from commercially available precursors often results in the racemization of the sidechain stereocenter due to a competing elimination reaction that occurs in the higher pH conditions required to deprotonate the sidechain of Cys.*

As of today, *m*-DAP building blocks compatible with standard Fmoc- or Boc-based solid phase peptide synthesis are not commercially available. The general lack of commercial accessibility to these reagents has hampered the development of *m*-DAP based probes[11, 16-20] and has, in effect, unbalanced the focus towards L-Lys containing

bacterial species. A major bottleneck to the generation of *m*-DAP building blocks is the presence of an internal plane of symmetry, which needs to be orthogonally protected for Fmoc-based peptide synthesis.[18] Due to this synthetic barrier, *m*-DAP analogues, such as *meso*-lanthionine (*m*-LAN)[21-23] and *meso*-oxa-DAP, that mimic the key structural features have been described (**Figure 5.1a**).[23-26] Despite retaining critical structural mimicry of *m*-DAP, both *m*-LAN and *meso*-oxa-DAP have drawbacks related to complicated preparation of starting materials.

In response to this gap in readily accessible bioisosteres, we previously reported on a *m*-DAP analogue that utilized commercially available building blocks and solid-phase peptide synthesis to generate *meso*-cystine (*m*-CYT, **Figure 5.1a**).[27] While *m*-CYT was well tolerated as a surrogate for *m*-DAP in live bacteria, as demonstrated by its metabolic incorporation into the PG, we recognized that it may be beneficial to retain the same number of atoms in the sidechain, which *m*-CYT does not. Moreover, the reducibility of the disulfide bond in *m*-CYT may prove to be a challenge in assays that require reducing agents and in intracellular compartments of mammalian cells. Motivated by the shortcomings of current bioisosteres, we sought to leverage the unique reactivity of selenium to assemble a novel *m*-DAP analog, selenolanthionine (*m*-SeLAN, **Figure 5.1a**) using commercially available reagents.

5.3 *Results and Discussion*

5.3.1 *Synthesis of a stem tripeptide containing SeLAN*

Nature has taken advantage of the sulfhydryl on the sidechain of cysteine to diversify natural products, including in the biosynthesis of lantibiotics. While lanthionines within lantibiotics are precisely constructed by enzymes, it has proven to be considerably more challenging to control the stereochemical configuration using synthetic organic chemical methods. Prior synthetic efforts towards *m*-LAN using commercially available building blocks suffered from racemization problems[28], stemming from elimination and subsequent Michael addition, and formation of isomeric products that are challenging to separate (**Figure 5.1b**)[21] For these reasons, we envisioned that we could substitute the

L-Cys precursor to *m*-CYT with selenocysteine (Sec). A key component to this strategy is the lower selenol *p*Ka value in Sec of ~5 relative to the *p*Ka value of thiol in Cys, which is ~8.[29] The reduced *p*Ka means that the pH of the solution can be made more acidic, which will greatly suppress the elimination of β-chloro-D-Ala to dehydroalanine.[30]

We reasoned that access to an *m*-DAP analog (*m*-SeLAN) could allow us to expand our toolbox of probes to investigate PG biosynthesis and remodeling. A prominent PG structural feature of all known bacteria is the crosslinked stem peptides that afford stable covalent linkages. Disruption to the PG structure can be lethal to bacterial cells, as evidenced by the number of small molecule antibiotics (e.g., β-lactams, teixobactin) and immune system components (e.g., lysozyme) that target various steps in the PG assembly.[7, 30, 31] A better understanding of the key biological features of PG crosslinking could reveal under-explored modes of bactericidal agents and/or potentiating adjuvants. PG crosslinking is mediated by PG-associated transpeptidases, namely Penicillin Binding Proteins (PBPs) and L,D-transpeptidases (Ldts). After forming an acyl-intermediate between its active site residue and a nearby stem peptide, the transpeptidase promotes a nucleophilic attack by the 3rd position *m*-DAP residue of a neighboring stem peptide strand (**Figure 5.2a**). Our laboratory and others have previously demonstrated that synthetic stem peptide mimetics with fluorescent handles on the *N*-terminus can be processed by PG transpeptidases in live bacterial cells, thereby becoming metabolically incorporated into the PG.[32-35]

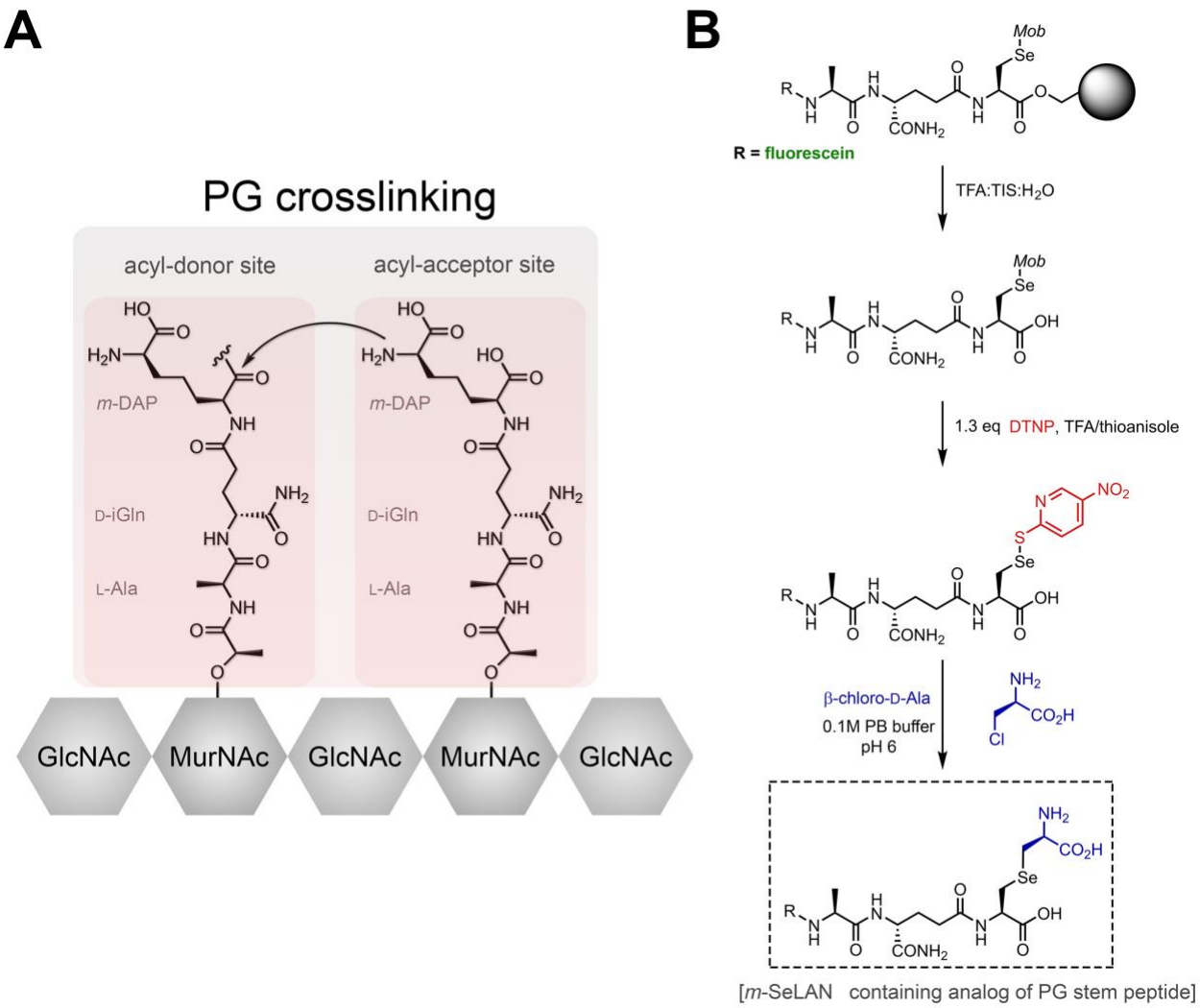

Figure 5.2 *(A) In the final step of PG crosslinking by transpeptidases, an amino group from the acyl-acceptor strand performs an attack on the acyl-donor strand. Shown is one potential configuration whereby this reaction would result in a 3-3 crosslink. Other reactions are possible that can result in altered crosslinking configurations. (B) Synthetic route to obtain m-SeLAN containing peptides.*

We opted to initially synthesize a tripeptide version of the stem peptide as tripeptides cannot act as acyl-donors in the PG crosslinking reactions (since they lack a terminal D-Ala necessary for the first step of the reaction) and will only participate as acyl-acceptors. Therefore, these probes should act solely as acyl-acceptor strands, which would demonstrate the potential mimicry of *m*-DAP by *m*-SeLAN. We aimed to devise a

synthetic route using entirely commercially available reagents. To this end, the installation of Fmoc-L-Sec(Mob) at the third position of the stem peptide mimic could provide a site for the post-cleavage modification to provide *m*-SeLAN (**Figure 5.2b**). Using standard solid-phase peptide synthesis, Fmoc-L-Sec(Mob) was incorporated at the third position and the *N*-terminus was modified with a fluorescein to track incorporation into the PG (fluorescence readout can be quantified by flow cytometry or confocal microscopy). After building the peptide on solid support, the Sec-containing tripeptide was released from resin, leaving the methoxybenzyl (Mob) protecting group intact. The crude peptide was then reacted *in situ* to switch the Mob group for thio-5-nitropyridine (TNP).[36] This intermediate was then allowed to react with β-chloro-D-Ala in phosphate buffer at pH 6[30] in the presence of dithiothreitol (DTT) to yield the final product (**TriSeLAN**, **Figure 5.2b**). In addition to **TriSeLAN**, we synthesized a peptide with a selenocystamine (**TriSeLys**) at the third position to have the ability to test the essentiality of the carboxylic acid on the side chain in live cells. The synthesis was similarly performed with the main exception being that the Sec was reacted with 2-chloro-ethylamine instead of β-chloro-D-Ala.

5.3.2 *TriSeLAN incorporation in live bacterial cells*

With the initial seleno-bioisosteres in hand (**Figure 5.3a**), we sought to evaluate the metabolic labeling of *Mycobacterium smegmatis* (*M. smegmatis*), an organism that contains *m*-DAP in its PG.[37] *M. smegmatis* is also a model organism for the infectious *Mycobacterium tuberculosis*, the causative agent of Tuberculosis (TB) that is estimated to infect one third of the world's population.[38-40] To test the functional mimicry of *m*-SeLAN, bacterial cells were cultured in the presence of the various tripeptide probes to promote their metabolic incorporation into the PG scaffold during cellular growth (**Figure 5.3b**). When cells were treated with **TriSeLAN**, a marked increase in cellular fluorescence of ~ 22-fold was observed relative to untreated cells. We had previously shown that the carboxylic acid on the sidechain of the acyl-acceptor was critical for recognition and crosslinking in *M. smegmatis*.[27] To confirm those results in the context of the seleno-based probes, we synthesized two additional stem peptide analogs (**TriLys** and **TriSeLys**), in which the acyl-acceptor amino group is retained. Consistently, cellular

fluorescence labeling decreased considerably for both probes (**Figure 5.3b**). Furthermore, similar confocal analysis with another bacterium within the same genus, *Mycobacterium bovis* bacillus Calmette-Guérin (BCG), revealed extensive labeling with **TriSeLAN** (**Figure 5.4**). Metabolic tagging was also observed for another bacterial species whose PG scaffold contains *m*-DAP, *Lactobacillus plantarum* (**Figure 5.5**). Taken together, these results are suggestive of proper mimicry of *m*-SeLAN in the context of transpeptidase processing in live cells and that the carboxylic acid is critical for metabolic labeling.

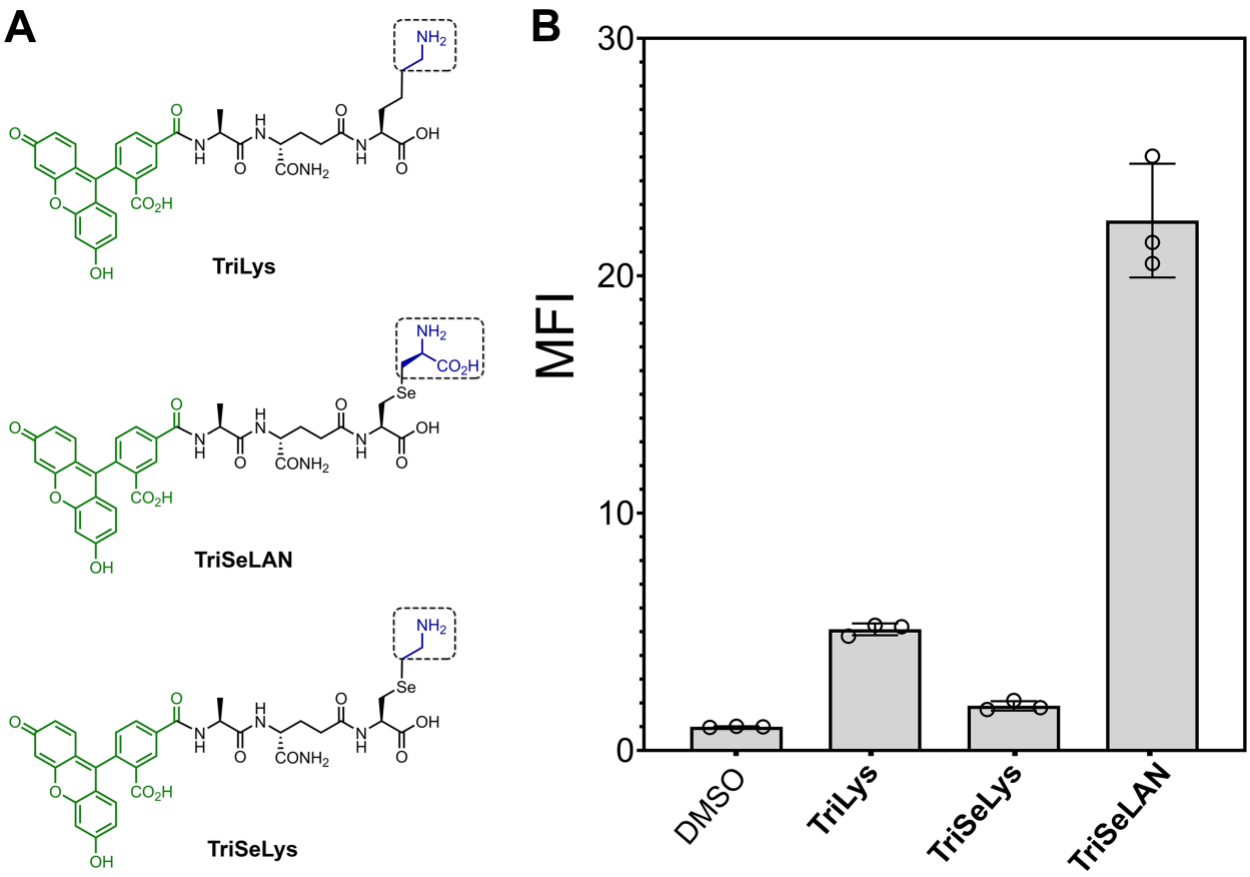

Figure 5.3 *(A) Chemical structures of the tripeptide probes used in the study. The box highlights the structural differences at the crossbridge. Fluorescein is present for quantification of incorporation. (B) Flow cytometry analysis of M. smegmatis treated overnight with DMSO or 100 μM of designated tripeptide probes. Data are represented as mean + SD (n = 3). MFI, median fluorescence intensity.*

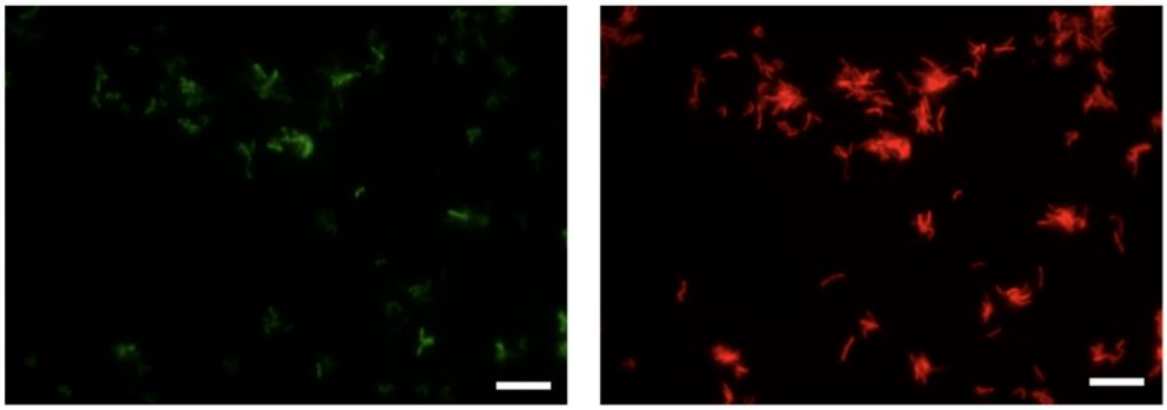

Figure 5.4 *Confocal microscopy image of M. bovis BCG cells treated with* ***TriSeLAN*** *(200 µM). Cells express mCherry. Green fluorescence images (left) show that the probe is associated with cells. Scale bar = 10 µm.*

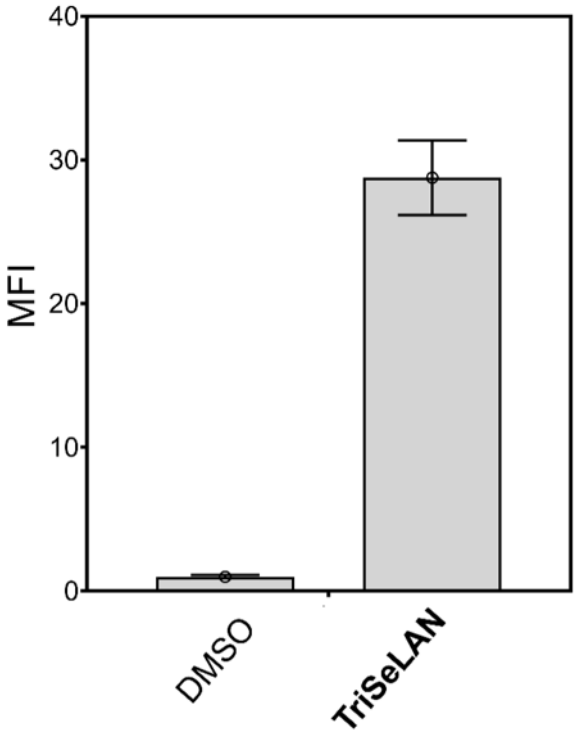

Figure 5.5 *Flow cytometry analysis of L. plantarum treated overnight with DMSO or 100 µM of designated tripeptide probes. Data are represented as mean + SD (n = 3).*

Additionally, a number of experiments were performed to demonstrate the incorporation of the synthetic stem peptide analog within the PG of cells. We initially turned to SaccuFlow, a protocol we described recently to quantitatively measure the fluorescence of isolated PG (sacculi, **Figure 5.6a**).[41] Sacculi from *M. smegmatis* treated with **TriSeLAN** showed high levels of fluorescence, which was consistent with the results obtained with whole cells (**Figure 5.6b**). The sacculi isolation protocol is expected to remove all biomacromolecules outside of PG, which indicates that the fluorescence signal is retained even after performing the individual isolation steps. Metabolic incorporation into the PG scaffold was confirmed by directly analyzing muropeptides. *M. smegmatis* cultures supplemented with **TriSeLAN** were subjected to PG isolation and analyzed for potential crosslinks of the fluorescent probe to endogenous PG stem peptides. We identified natural muropeptides with *N*-acetylated muramic acid as well as the *N*-glycosylated muramic sugar that is found in the native PG of *M. smegmatis*.[42] The GlcNAc-MurNAc tetrapeptide (with iso-D-Glu and non-amidated *m*-DAP) as well as the *N*-glycosylated MurNAc tetrapeptide (with either iso-D-Glu and amidated *m*-DAP or iso-D-Gln and non-amidated *m*-DAP) were identified to be crosslinked to the fluorescent seleno-containing tripeptide, with isotopic patterns representative of selenium.

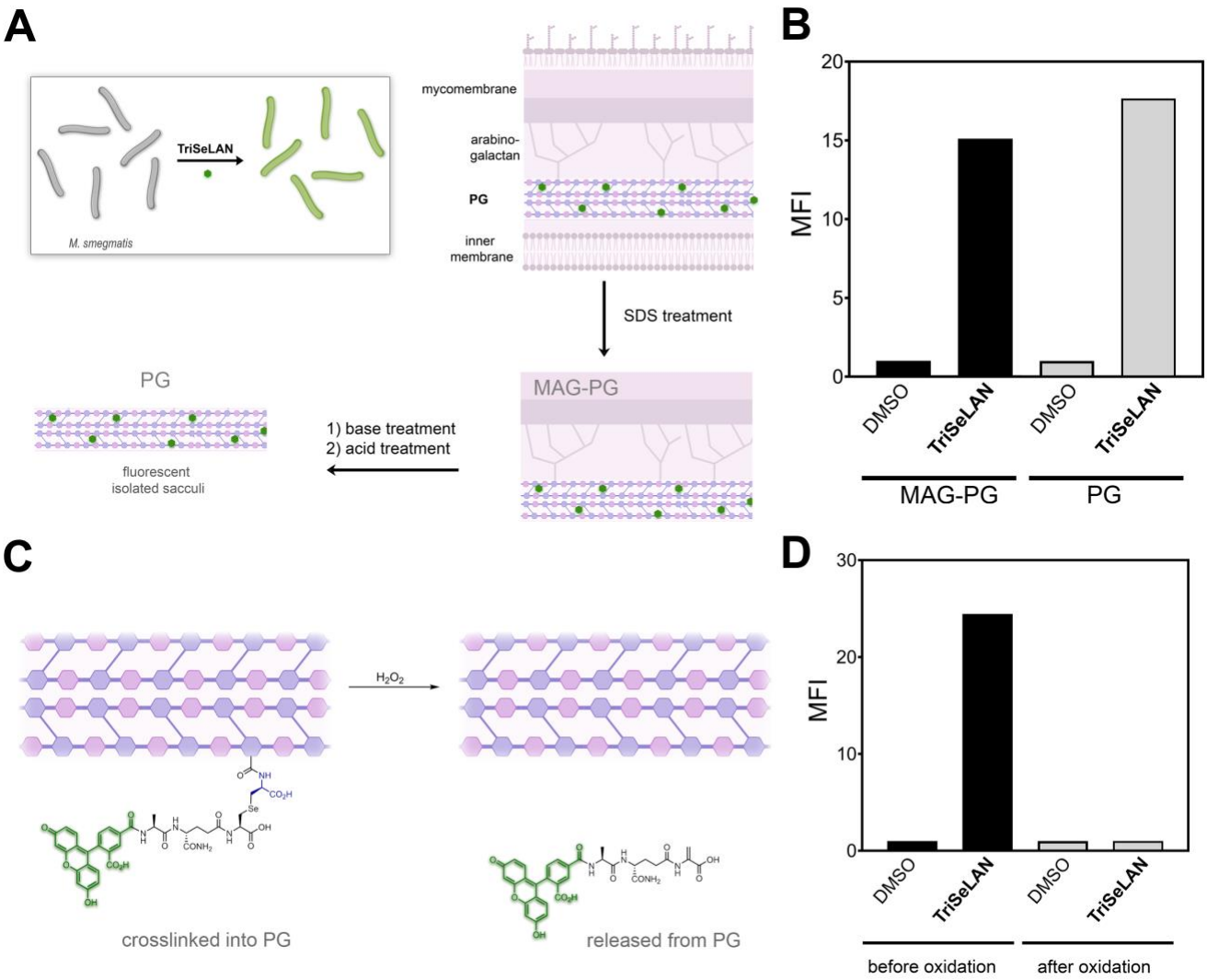

Figure 5.6 *(A) Treatment of M. smegmatis with* ***TriSeLAN*** *should result in PG tagging with a fluorescent handle. Cells are subjected to a series of PG isolation steps, yielding an intermediate mycolylarabinogalactan-peptidoglycan (MAG-PG) and the intact final PG scaffold. (B) M. smegmatis treated overnight with DMSO or 100 μM of designated tripeptide probes. Flow cytometry measurements were made at intermediate points and at the final isolated PG. Data are shown as average of individual sacculi. (C) Schematic diagram showing the crosslinked probe prior to and after the oxidation by hydrogen peroxide to yield a dehydroalanine (and other released products). (D) Flow cytometry analysis of metabolically tagged sacculus before and after oxidation. Data are shown for individual sacculus. MFI, median fluorescence intensity.*

A unique feature of selenoether (as in the one found in *m*-SeLAN) is its ability to be cleaved using orthogonal oxidation conditions to yield dehydroalanine (**Figure 5.6a**).[43, 44] To further confirm the presence of our probe within the PG, metabolically tagged sacculi was treated with hydrogen peroxide to induce the release of the fluorescent tag. A marked decrease in sacculi fluorescence was measured after hydrogen peroxide treatment (**Figure 5.6b**). As a control, sacculi from *M. smegmatis* treated with a non-releasable stem peptide analog did not change after exposure to the same oxidation step (**Figure 5.7**). This selective oxidative cleavage in the background of all other biological functional groups has been exploited in chemoproteomics programs.[45] Likewise, we envision that *m*-SeLAN may provide a handle to reverse the PG crosslinking in isolated sacculi, and potentially in live bacteria cells.

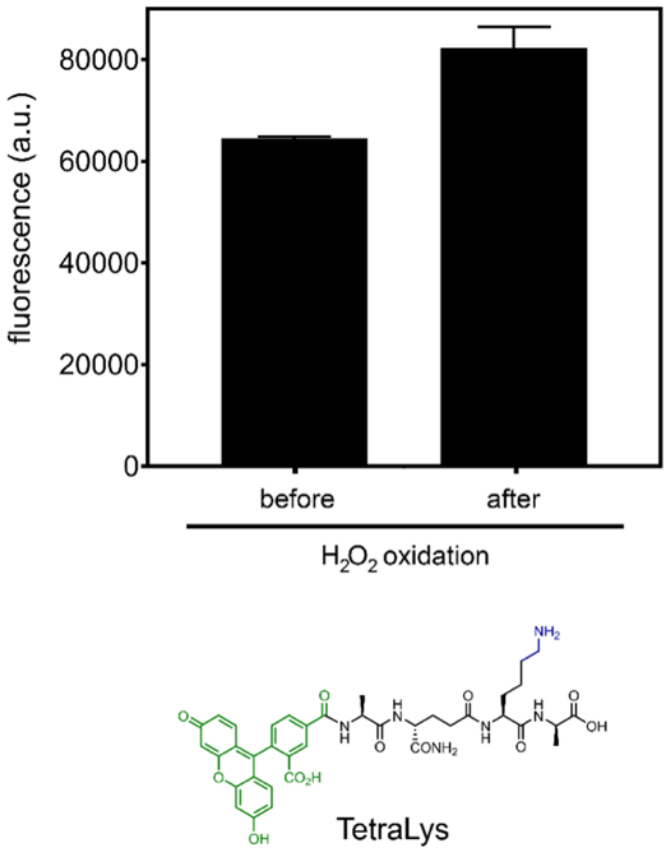

Figure 5.7 *Flow cytometry analysis of sacculi isolated from M. smegmatis treated overnight with DMSO or 100 μM of* ***Fl-TetraLys****. Data are represented as mean + SD (n = 3).*

5.3.3 *Computational model of SeLAN in the active site of a Ldt*

To explore the influence of *m*-SeLAN on PG crosslinking, we constructed three computational models to examine the configuration (and its impact) of natural *m*-DAP as compared to *m*-CYT and *m*-SeLAN in the active site of an L,D-transpeptidase from *M. smegmatis*. The starting points for MM and QM/MM simulations were obtained from our previous study.[27] As we previously described in a QM/MM mechanistic study involving Ldt systems,[46] the analysis starts with the formation of the ionic-pair, by a proton transfer from Cys346 to His328. To test the influence of *m*-DAP bioisosteres, three systems were built: (I) Ldt-*m*-DAP, (II) Ldt-*m*-CYT and (III) Ldt-*m*-SeLAN (**Figure 5.8a**).

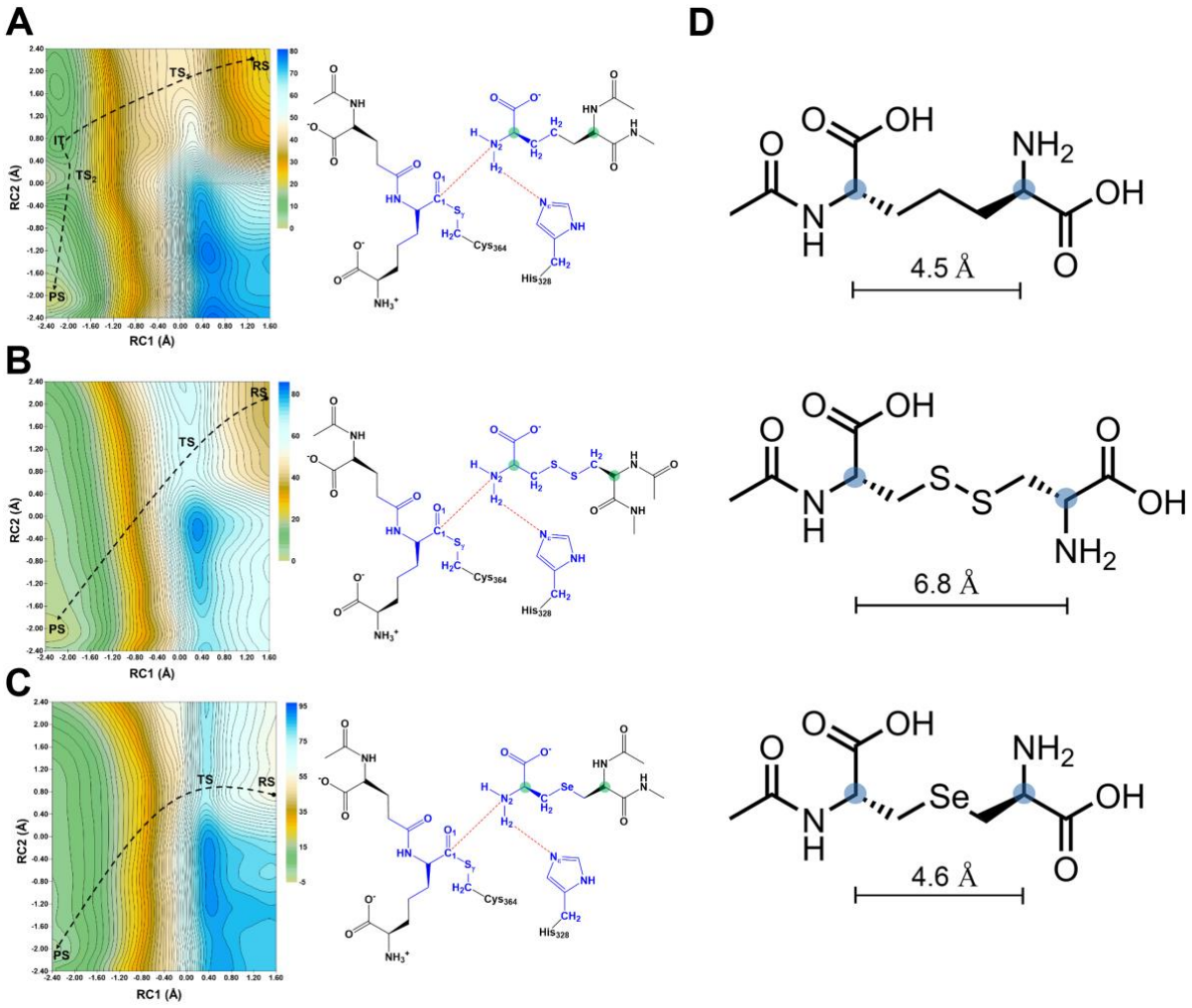

Figure 5.8 *Plots of 2D-PMF at PM3/MM level (left) and combinations of RC1 and RC1 reaction coordinates (right), describing the PG cross-linking mechanism of (A) Ldt-m-DAP system I, (B) Ldt-m-CYT system II, and (C) Ldt-m-SeLAN system III. QM atoms for each system are in blue. Alpha carbons of the peptide sidechain are highlighted in green. The energy values are reported in kcal/mol. (D) Average distances from QM/MM for the designated atoms in the three bioisosteres studied.*

The most relevant structural and energetic values obtained from QM/MM umbrella sampling simulations are summarized (Table S1, not shown in this dissertation). As shown in **Figure 5.8** and summarized in Table S1, the crosslinking mechanism of Ldt_{Msm} at PM3/MM level occurs *via* a concerted reaction for the *m*-CYT and *m*-SeLAN systems. However, for the *m*-DAP system, the reaction occurs by stepwise mechanism. In the first

step, we can observe a nucleophilic attack from amine nucleophile (N_2 atom) to carbonyl group of acyl-enzyme (C_1 atom), which shows a theoretical free energy barrier equal to 22 kcal/mol. After, a proton transfer from amine nucleophile to imidazole group of catalytic His328 with a very small free energy barrier (about 3.4 kcal/mol). The first step of *m*-DAP system mechanism is energetically and structurally similar to reaction for the *m*-CYT and *m*-SeLAN systems.

Interestingly, from the thermodynamics perspective of the computed reaction, we observe that ΔG^R of *m*-SeLAN system (–55.4 kcal/mol) is much more favorable than for *m*-DAP and *m*-CYT systems (–22.7 and –37.0 kcal/mol, respectively). To explain the differences in the ΔG^R's, we computed the Mulliken charges (averaged over PM3/MM US frames) in the chemical species of the reactions (Table S1, not shown in this dissertation). The charges of the S_γ and C_1 atom are similar for all systems when the RS configuration is considered. However, the charge of the N_2 atom (amine nucleophile) has a larger electron density for *m*-SeLAN system, which allows a more favorable nucleophilic attack. At the end of reaction (PS) in all 3 systems, N_2 atom has the same electron density. Additionally, it was observed that the distance between alpha carbons (**Figure 5.8a**) are quite similar in *m*-DAP and *m*-SeLAN systems, which may explain the tolerability of PG crosslinking enzymes to this bioisostere (**Figure 5.8b**).

5.3.4 *In vitro enzymatic reaction to examine SeLAN mimicry of m-DAP*

We next explored the possibility of testing the suitability of *m*-SeLAN in mimicking *m*-DAP in the context of a purified enzymatic reaction. While there has been tremendous amount of effort devoted to assessing the acylation sensitivity of transpeptidases (PBPs and Ldts) to antibiotics[47-50], it has proven to be much more difficult to study the native transpeptidation reaction *in vitro*. This challenge stems from two primary features: the difficulty in obtaining purified substrates that correspond to the desired muropeptide and the general lack of bioanalytical tools to track transpeptidation in solution. While synthetic approaches can address the need for pure muropeptides, fewer advances have been observed in the determination of transpeptidase products. Previous efforts have focused on the use of radioactive labeled muropeptides,[51, 52] Western blotting against a biotin

modified D-amino acid,[53] HPLC analysis,[54, 55] and most recently a fluorogenic D-amino acid.[56] We hypothesized that it would be possible to quantitatively assess transpeptidation *in vitro* by performing the reaction on the surface of a bead, which can be readily analyzed by flow cytometry in a 96-well plate format. The concept relies on the conjugation of a synthetic PG mimetic strand (acyl-donor or -acceptor) onto a solid support, followed by incubation with a transpeptidase and the corresponding crosslinking partner covalently linked to a fluorophore (**Figure 5.9a**). When the acyl-donor strand is anchored onto the bead, the transpeptidation reaction covalently installs the fluorescent acyl-acceptor strand.

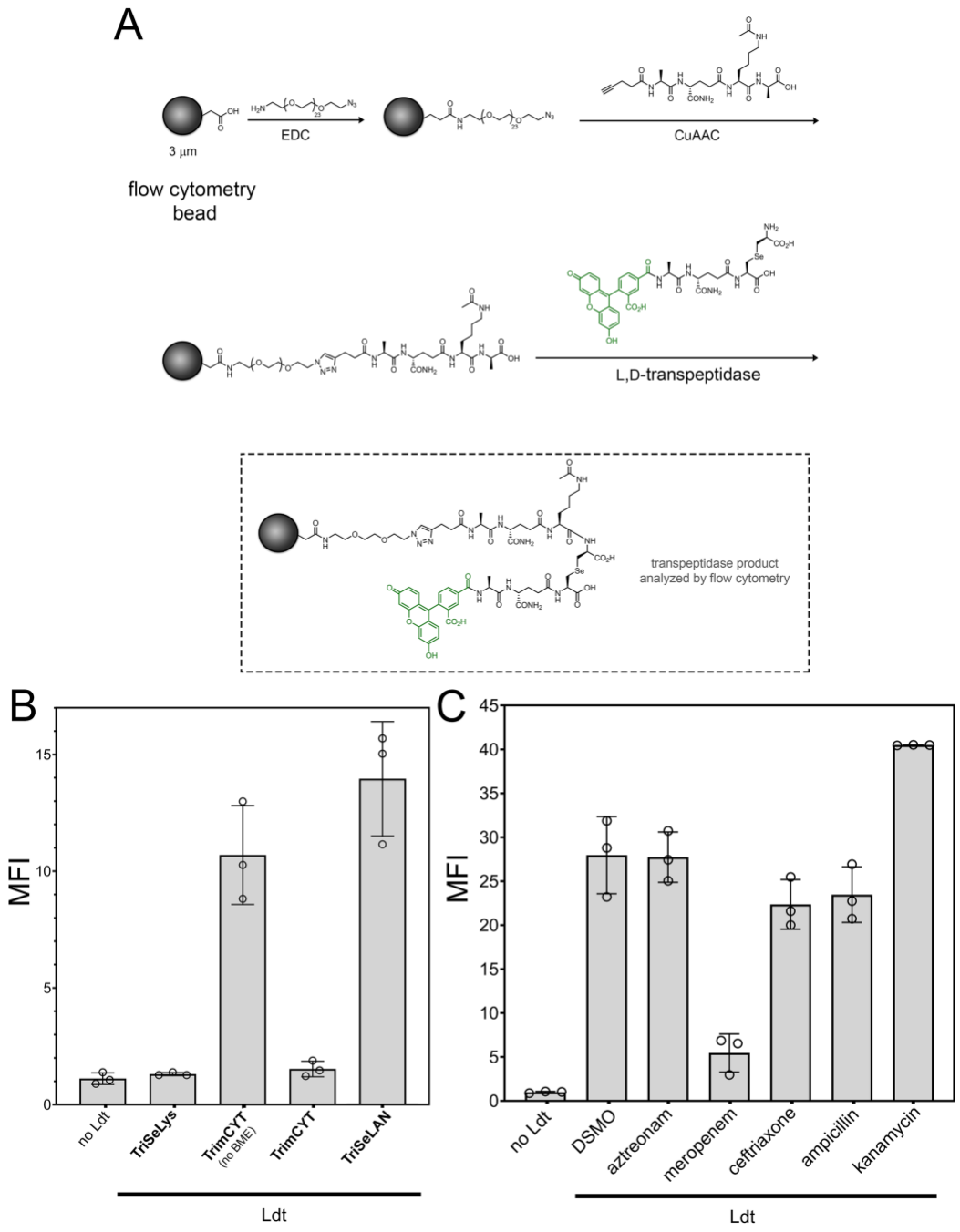

Figure 5.9 *(A) Schematic representation of the assay of transpeptidation on the bead. (B) Flow cytometry analysis of stem peptide modified beads incubated in the presence of* Ldt_{Mt2}*, reducing agent, and various fluorescently labeled synthetic stem peptide analogs. (C) Flow cytometry analysis of stem peptide modified beads incubated in the presence of* Ldt_{Mt2}*, the substrate* ***TriSeLAN****, in the presence of antibiotics. MFI, median fluorescence intensity.*

We tested how the primary structure of the tripeptide mimic of the stem peptide could impact Ldt processing by using Ldt_{Mt2}, a prominent Ldt from *Mycobacterium tuberculosis* (**Figure 5.9b**). Similar to the whole cell labeling results, a strong preference in transpeptidation activity was observed for the tripeptide containing the *m*-DAP mimicking amino acid at the 3rd position. In the presence of reducing agent, **Tri*m*CYT** was not able to be processed by Ldt_{Mt2}, as noted by a low fluorescent readout. In the future, we plan to fully expand the acyl-donor strand and acyl-acceptor chain to perform a comprehensive structure-activity relationship that will, for the first time, reveal how the primary structure of the two substrates may control crosslinking activity. We then evaluated a panel of antibiotics, ranging from the four main classes of β-lactams and a non-cell wall targeting agent, for their ability to inhibit Ldt-processing using the same bead assay (**Figure 5.9c**). Consistent with prior studies using Ldt_{Mt2}, there was minimum disruption to the transpeptidation reaction observed when monobactam (aztreonam), penicillin (ampicillin), and cephalosporin (ceftriaxone) β-lactams were included in the reaction mixture.[47, 48] Similarly, the addition of an aminoglycoside kanamycin, resulted in no reduction in fluorescence levels. Upon the addition of meropenem, a carbapenem, there was a marked decrease in fluorescence levels that is consistent with full inhibition of Ldt_{Mt2}. Together, these results suggest that this assay may provide a unique platform to determine the antibiotic sensitivities of transpeptidases in a way that is readily scalable and competitive with high-throughput analyses, and that **TriSeLAN** is a suitable acyl-acceptor for Ldt_{Mt2} *in vitro*.

5.3.5 *Treatment of m-DAP auxotrophs with SeLAN*

We finally evaluated the tolerability of mycobacteria to the new *m*-DAP bioisostere by supplementing a single amino acid *m*-SeLAN to cells that are auxotrophic for *m*-DAP. Uniquely, the metabolism of single amino acid *m*-DAP bioisosteres requires that every biosynthetic step (starting with MurE ligase) within the PG biosynthesis accommodates the synthetic analog. There is precedence in *E. coli* that are auxotrophic for *m*-DAP to have growth rescued with lanthionine (and cystathionine) supplementation.[57, 58] Moreover,

an unusual mutation led to a *m*-DAP auxotrophic strain of *M. smegmatis* to biosynthesize lanthionine and utilize it in place of *m*-DAP for PG biosynthesis.[59] Cell growth rescue experiments were performed with *m*-DAP auxotrophic *M. smegmatis* cells by adopting prior protocols (**Figure 5.10**). Briefly, cells were grown to early log phase (OD_{600} ~0.2), then the media was supplemented with *m*-DAP alone or a combination of *m*-DAP and *m*-SeLAN. In the absence of supplementation of *m*-DAP, the optical density does not change over 24 h post media exchange. As expected, addition of *m*-DAP to the media rescues growth at both 5 and 10 μg/mL. Supplementation of *m*-SeLAN led to a modest but reproducible increase in optical density when co-incubated with 5 μg/mL of *m*-DAP, which indicates the proper utilization of this bioisostere in *M. smegmatis m*-DAP auxotrophs. Additionally, we isolated and analyzed the PG and found *m*-SeLAN incorporated into the endogenous stem peptide.

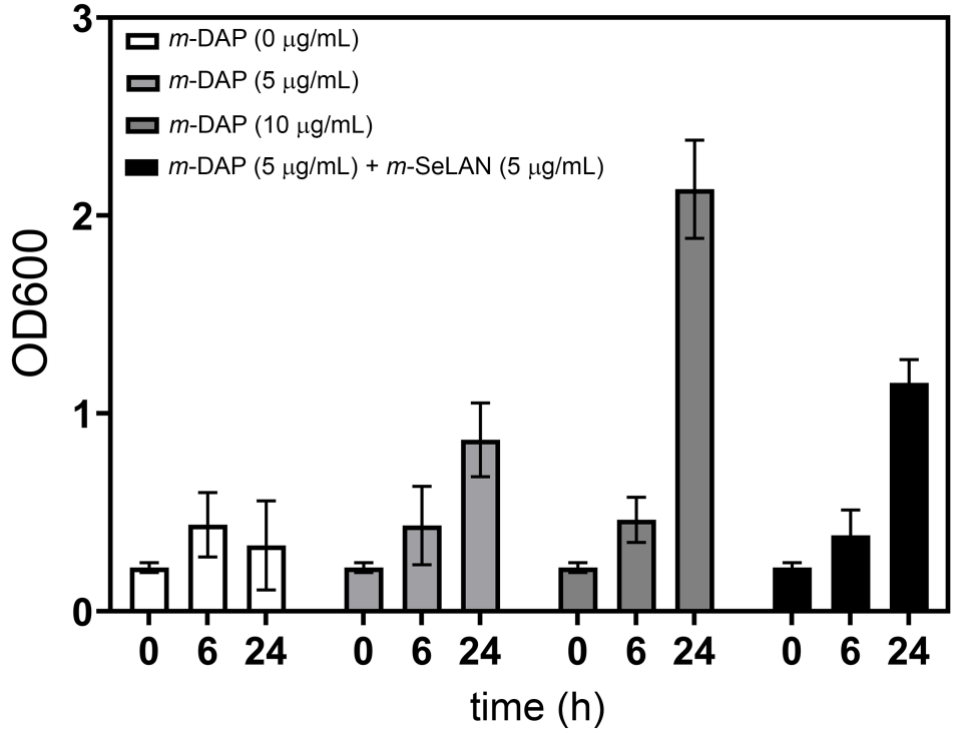

Figure 5.10 *m-DAP auxotrophic M. smegmatis were grown to OD600 of 0.25 in media supplemented with exogenous m-DAP, at which point the media was exchanged with the media described for each condition. The OD600 was then measured at time 0, 6, and 24 h post media exchange. Data are represented as mean + SD (n = 3).*

5.4 *Conclusion*

Here, we described a strategy that uses solid-phase peptide synthesis to construct a selenolanthionine *m*-DAP mimic. This probe was tolerated by endogenous PG crosslinking machinery in live *M. smegmatis* and BCG cells, as investigated by the use of flow cytometry and confocal microscopy. Importantly, the *m*-SeLAN tripeptide probe specifically suggests proper *m*-DAP mimicry, as it acts as an acyl-acceptor in the PG crosslinking step. The incorporation of selenolanthionine based probes was also observed in other organisms that incorporate *m*-DAP within their PG. A number of lines of evidence pointed to the specific incorporation of this probe within the PG of mycobacteria, including an assay in which the selenolanthionine was selectively released from the isolated PG. *m*-SeLAN was further shown to have *m*-DAP mimicry when *m*-DAP auxotrophs were rescued by supplementation of single amino acid *m*-SeLAN and *m*-DAP into the media. We envision that this building block can provide an alternate synthetic route for various *m*-DAP bioisosteres that involve a selenoether linkage (established by the use of completely commercial reagents) which prevents the possibility of reduction and maintains the approximate length of the *m*-DAP sidechain, expanding the tool set currently being used to study PG biosynthesis.

5.5 *Materials and Methods*

Materials. All peptide related reagents (resin, coupling reagent, deprotection reagent, amino acids, and cleavage reagents) were purchased from ChemImpex. Bacterial strains *M. smegmatis* WT (14468) were grown in Middlebrook 7H9 media supplemented with 0.05% Tween 80 and enriched with albumin/dextrose/catalase (ADC) and glycerol (0.2% v/v).

Flow cytometry analysis of bacterial labeling. Media containing 100 μM of each probe were prepared. Bacterial cells from an overnight culture were added to the medium (1:100 dilution) and allowed to grow overnight at 37°C with shaking at 250 rpm. The bacteria

were harvested at 6,000g and washed three times with original culture volume of 1X PBS followed by fixation with 2% formaldehyde in 1X PBS for 30 min at room temperature. The cells were washed once more to remove formaldehyde and then analyzed using an Attune NxT flow cytometer equipped with a 488 nm laser and 525/40 nm bandpass filter. The data were analyzed using the Attune NxT Software, where populations were gated and no less than 10,000 events per sample were recorded.

Muropeptide Isolation of *M. smegmatis*. M7H9 media ADC enriched containing 0.05% Tween 80 and 0.2% glycerol was aliquoted into a 96-well plate as either blank (no probe) or with 100 µM of fluorescent probe (Se-containing tripeptide) following a protocol established in the literature to miniaturize Mycobacterium muropeptide isolation.[60, 61] *M. smegmatis* bacteria were added to the medium (1:100) and allowed to grow overnight at 37°C with shaking at 250 rpm. Cells were then harvested at 2,700g for 15 min at 4°C and washed 1X in a minimal volume of 1X PBS. Pellets were resuspended in 10 mM NH_4HCO_3 with a protease inhibitor cocktail (Sigma SRE005- 1BO). This suspension was lysed using a tip sonicator (Fisher Scientific) at 60% amplitude for 60 seconds, with at least 60 seconds on ice in between. This was repeated for 5 cycles. The sonicate was digested with 10 µg/mL DNAse and RNase for 1 h at 4°C, then harvested at 2,700g for 30 min at 4°C. The pellet was resuspended in PBS with 2% SDS and incubated for 1 h at 50°C with constant stirring. This was collected using the same centrifugal parameters and the SDS process was repeated 2X. The resulting pellet was resuspended in PBS with 1% SDS and 0.1 mg/mL Proteinase K at 45°C for 1 h with stirring. The sample was then heated to 90°C for 1 h and collected as above. This step at 90°C was repeated 2X. The sample was washed 2X with PBS and 4X with dH2O. This yielded mycolic-arabinogalactan-peptidoglycan (mAGP). To remove the mycolic acid layer, samples were collected and resuspended in 0.5% KOH in MeOH and incubated at 37°C for 4 days with shaking. After 4 days, samples were collected, washed twice with MeOH and twice with diethyl ether to yield the arabinogalactan layer. To remove the arabinogalactan layer, samples were resuspended in 0.5 N H_2SO_4 at 37°C for 5 days with shaking. After 5 days, samples were collected, washed 4X with dH_2O and lyophilized. The lyophilized sacculi was resuspended in 0.5 mL of 10 mM sodium acetate pH 5 with 25 µg of muramidase

and incubated at 37°C for 16 h with shaking. Sacculi was spun down, the supernatant was filtered (10 kDa) cutoff and dried under vacuum. Dried sacculi was dissolved in HPLC-grade water and an aliquot was applied to a C18(2) column (Luna 5 µm 100Å 250 x 4.6 mm) connected to an Agilent LC-QTOF (Agilent 1260 Infinity II Prime LC with Agilent 6545B QTOF). Muropeptide samples were eluted with a 2 to 30% linear gradient of water to acetonitrile (0.5% formic acid) at 0.4 mL/min. The muropeptides were analyzed by MS using MassHunter software.

BCG Confocal Imaging. For imaging BCG: mCherry-expressing *Mycobacterium bovis* BCG Tokyo was grown in 7H9 medium at 37 C to an OD600 of 0.3 then incubated with 200 µM FL-**TriQSeLAN** for an additional 24 hrs at 37 C. Bacteria were washed 3x in PBS + 0.01% bovine serum albumin + 0.05% Tween-80 (PBSTB) then fixed with 4% formaldehyde for 2 hrs at room temperature. Samples were washed an additional 3x with PBSTB and stored at 4 C prior to imaging.

m-DAP auxotrophic growth analysis. A diaminopimelate auxotroph (strain mc21620) was grown at 30 C in 7H9 medium supplemented with L-lysine, L-methionine, and L-threonine at 40 mg/ml and D,L-homoserine at 80 µg/ml as previously described (see reference below). A primary culture was grown in the presence of 200 µg/ml DAP, then washed and resuspended at an OD600 of 0.2 in the supplemented 7H9 medium +/- DAP +/- the compounds synthesized in this manuscript at the indicated concentrations.

Ldt_{Mt2} expression and purification. Plasmid #59337 for pET21a(+) LdtMt2 was purchased from Addgene (33892 [NCBI]) and expression and purification were followed as described by the publication of the depositing lab.[62] Briefly, the protein was overexpressed in *Escherichia coli* (*E. coli*) BL21 cells grown in lysogeny broth, where protein expression was induced by 0.5 mM IPTG at 30ºC for 20 h after reaching mid-log phase. Cells were lysed in sonication buffer 50 m*M* Tris–HCl pH 7.9, 500 m*M* NaCl, 50 m*M* imidazole, 5% (v/v) glycerol, containing a protease inhibitor cocktail. The lysate was harvested at 36,000g for 1 h, the supernatant was filtered and applied to a cytiva HisTrapFF column, equilibrated with the sonication buffer and eluted with a gradient

concentration of imidazole. The protein eluted at 120-130 mM imidazole. Protein purity and MW was confirmed by SDS-PAGE (12% acrylamide, 240 V, 40 min). Sample buffer was added to 1X concentration, samples were boiled for 5 minutes, and then 15 μL were loaded into each well. A pre-stained protein ladder (ThermoFisher 26619) was loaded. The gel was imaged using a BioRad ChemiDoc XRS+ imager.

Functionalization of SPHERO Carboxy Polystyrene Particles. Sphero Carboxy Polystryene beads 3.31 um 5% w/v (Spherotech, 250 μL) were reacted with 0.05 M MES at pH 6 (250 μL), EDC (10 mg), and NH_2-Peg23-Az (BroadPharm, 2 mg) for 24 h. Beads were collected at 3,000g for 15 min. The supernatant was carefully removed, and the beads were washed in PBS. A final working suspension of 5% w/v was made for assays. Purified Alkyne-TetraLys(Ac) (see **Scheme S2**) was reacted with the beads displaying Peg23-Az once the beads were blocked with Tween 80 (0.05%) in PBS, washed, and then resuspended in PBS. To react Alk-TetraLys(Ac), beads were incubated with 1 mM $CuSO_4$, 128 μM THPTA, 1.2 mM L-Ascorbic Acid, and 30 μM Alk-TetraLys(Ac). The particles were washed as before and resuspended to a 5% w/v suspension.

Ldt_{Mt2} transpeptidation assay. Purified Ldt_{Mt2} (2 μM) was incubated with the respective fluorescent probe (**TrimCYT**, **TriSeLys**, or **TriSeLAN**) at 50 μM, 25 mM Tris pH 8, 1 mM β-mercaptoethanol (βME), and 5 μL of functionalized beads (in a final volume of 100 μL) and shook at room temperature for 5 h. The “no Ldt” sample contained 50 μM of **TriSeLAN** as the fluorescent probe. The reaction was quenched with 0.1% TFA. Beads were washed 3X by centrifugation at 6,000xg for 3 min with 10% SDS. Beads were diluted 4-fold before analysis by an Attune NxT flow cytometer as described previously. For the antibiotic assays, the same conditions were used, but no reducing agent was present. Antibiotics were prepared fresh as 10 mg/mL stock solutions in Milli-Q water before each experiment and diluted to a desired concentration. Briefly, the Ldt was incubated with each of the antibiotics (200 μM) for 15 min before addition of the remaining reagents. The reaction was quenched and washed as before and analyzed by flow cytometry. For all experiments, a minimum of 10,000 events was recorded.

5.6 *References*

1. Vollmer, W.; Blanot, D.; De Pedro, M. A., Peptidoglycan structure and architecture. *FEMS Microbiology Reviews* **2008,** *32* (2), 149-167.

2. Braun, V.; Bosch, V., Sequence of the murein-lipoprotein and the attachment site of the lipid. *Eur J Biochem* **1972,** *28* (1), 51-69.

3. Braun, V.; Wolff, H., Attachment of lipoprotein to murein (peptidoglycan) of Escherichia coli in the presence and absence of penicillin FL 1060. *J Bacteriol* **1975,** *123* (3), 888-97.

4. Ito, M.; Kim, Y. G.; Tsuji, H.; Takahashi, T.; Kiwaki, M.; Nomoto, K.; Danbara, H.; Okada, N., Transposon mutagenesis of probiotic Lactobacillus casei identifies asnH, an asparagine synthetase gene involved in its immune-activating capacity. *PLoS One* **2014,** *9* (1), e83876.

5. Pedicord, V. A.; Lockhart, A. A. K.; Rangan, K. J.; Craig, J. W.; Loschko, J.; Rogoz, A.; Hang, H. C.; Mucida, D., Exploiting a host-commensal interaction to promote intestinal barrier function and enteric pathogen tolerance. *Sci Immunol* **2016,** *1* (3).

6. Rangan, K. J.; Pedicord, V. A.; Wang, Y. C.; Kim, B.; Lu, Y.; Shaham, S.; Mucida, D.; Hang, H. C., A secreted bacterial peptidoglycan hydrolase enhances tolerance to enteric pathogens. *Science* **2016,** *353* (6306), 1434-1437.

7. Wolf, A. J.; Underhill, D. M., Peptidoglycan recognition by the innate immune system. *Nat Rev Immunol* **2018,** *18* (4), 243-254.

8. Chamaillard, M.; Hashimoto, M.; Horie, Y.; Masumoto, J.; Qiu, S.; Saab, L.; Ogura, Y.; Kawasaki, A.; Fukase, K.; Kusumoto, S.; Valvano, M. A.; Foster, S. J.; Mak, T. W.; Nuñez, G.; Inohara, N., An essential role for NOD1 in host recognition of bacterial peptidoglycan containing diaminopimelic acid. *Nat Immunol* **2003,** *4* (7), 702-7.

9. Girardin, S. E.; Travassos, L. H.; Hervé, M.; Blanot, D.; Boneca, I. G.; Philpott, D. J.; Sansonetti, P. J.; Mengin-Lecreulx, D., Peptidoglycan molecular requirements allowing detection by Nod1 and Nod2. *J Biol Chem* **2003,** *278* (43), 41702-8.

10. Vijayrajratnam, S.; Pushkaran, A. C.; Balakrishnan, A.; Vasudevan, A. K.; Biswas, R.; Mohan, C. G., Bacterial peptidoglycan with amidated meso-diaminopimelic acid

evades NOD1 recognition: an insight into NOD1 structure-recognition. *Biochem J* **2016,** *473* (24), 4573-4592.

11. Lee, M.; Hesek, D.; Shah, I. M.; Oliver, A. G.; Dworkin, J.; Mobashery, S., Synthetic peptidoglycan motifs for germination of bacterial spores. *Chembiochem* **2010,** *11* (18), 2525-9.

12. Shah, I. M.; Laaberki, M. H.; Popham, D. L.; Dworkin, J., A eukaryotic-like Ser/Thr kinase signals bacteria to exit dormancy in response to peptidoglycan fragments. *Cell* **2008,** *135* (3), 486-96.

13. Squeglia, F.; Marchetti, R.; Ruggiero, A.; Lanzetta, R.; Marasco, D.; Dworkin, J.; Petoukhov, M.; Molinaro, A.; Berisio, R.; Silipo, A., Chemical Basis of Peptidoglycan Discrimination by PrkC, a Key Kinase Involved in Bacterial Resuscitation from Dormancy. *Journal of the American Chemical Society* **2011,** *133* (51), 20676-20679.

14. Irazoki, O.; Hernandez, S. B.; Cava, F., Peptidoglycan Muropeptides: Release, Perception, and Functions as Signaling Molecules. *Front Microbiol* **2019,** *10*, 500.

15. Cava, F.; de Pedro, M. A., Peptidoglycan plasticity in bacteria: emerging variability of the murein sacculus and their associated biological functions. *Curr Opin Microbiol* **2014,** *18*, 46-53.

16. Hernández, N.; Martín, V. S., General Stereoselective Synthesis of Chemically Differentiated α-Diamino Acids: Synthesis of 2,6-Diaminopimelic and 2,7-Diaminosuberic Acids. *The Journal of Organic Chemistry* **2001,** *66* (14), 4934-4938.

17. Ross, A. C.; McKinnie, S. M. K.; Vederas, J. C., The Synthesis of Active and Stable Diaminopimelate Analogues of the Lantibiotic Peptide Lactocin S. *Journal of the American Chemical Society* **2012,** *134* (4), 2008-2011.

18. Roychowdhury, A.; Wolfert, M. A.; Boons, G. J., Synthesis and proinflammatory properties of muramyl tripeptides containing lysine and diaminopimelic acid moieties. *Chembiochem* **2005,** *6* (11), 2088-97.

19. Kawasaki, A.; Karasudani, Y.; Otsuka, Y.; Hasegawa, M.; Inohara, N.; Fujimoto, Y.; Fukase, K., Synthesis of diaminopimelic acid containing peptidoglycan fragments and tracheal cytotoxin (TCT) and investigation of their biological functions. *Chemistry* **2008,** *14* (33), 10318-30.

20. Kumar, S.; Roychowdhury, A.; Ember, B.; Wang, Q.; Guan, R.; Mariuzza, R. A.; Boons, G. J., Selective recognition of synthetic lysine and meso-diaminopimelic acid-type peptidoglycan fragments by human peptidoglycan recognition proteins I{alpha} and S. *J Biol Chem* **2005,** *280* (44), 37005-12.

21. Denoël, T.; Zervosen, A.; Gerards, T.; Lemaire, C.; Joris, B.; Blanot, D.; Luxen, A., Stereoselective synthesis of lanthionine derivatives in aqueous solution and their incorporation into the peptidoglycan of Escherichia coli. *Bioorganic & Medicinal Chemistry* **2014,** *22* (17), 4621-4628.

22. Knerr, P. J.; van der Donk, W. A., Chemical Synthesis of the Lantibiotic Lacticin 481 Reveals the Importance of Lanthionine Stereochemistry. *Journal of the American Chemical Society* **2013,** *135* (19), 7094-7097.

23. Uehara, A.; Fujimoto, Y.; Kawasaki, A.; Kusumoto, S.; Fukase, K.; Takada, H., Meso-diaminopimelic acid and meso-lanthionine, amino acids specific to bacterial peptidoglycans, activate human epithelial cells through NOD1. *J Immunol* **2006,** *177* (3), 1796-804.

24. Soni, A. S.; Lin, C. S.; Murphy, M. E. P.; Tanner, M. E., Peptides Containing meso-Oxa-Diaminopimelic Acid as Substrates for the Cell-Shape-Determining Proteases Csd6 and Pgp2. *Chembiochem* **2019,** *20* (12), 1591-1598.

25. Soni, A. S.; Vacariu, C. M.; Chen, J. Y.; Tanner, M. E., Synthesis of a meso-Oxa-Diaminopimelic Acid Containing Peptidoglycan Pentapeptide and Coupling to the GlcNAc-anhydro-MurNAc Disaccharide. *Organic Letters* **2020,** *22* (6), 2313-2317.

26. Liu, H.; Pattabiraman, V. R.; Vederas, J. C., Stereoselective syntheses of 4-oxa diaminopimelic acid and its protected derivatives via aziridine ring opening. *Org Lett* **2007,** *9* (21), 4211-4.

27. Apostolos, A. J.; Nelson, J. M.; Silva, J. R. A.; Lameira, J.; Achimovich, A. M.; Gahlmann, A.; Alves, C. N.; Pires, M. M., Facile Synthesis and Metabolic Incorporation of m-DAP Bioisosteres Into Cell Walls of Live Bacteria. *ACS Chemical Biology* **2020,** *15* (11), 2966-2975.

28. Photaki, I.; Samouilidis, I.; Caranikas, S.; Zervas, L., Lanthionine chemistry. Part 4. Synthesis of diastereoisomeric cyclolanthionyl derivatives. *Journal of the Chemical Society, Perkin Transactions 1* **1979,** (0), 2599-2605.

29. Muttenthaler, M.; Alewood, P. F., Selenopeptide chemistry. *J Pept Sci* **2008,** *14* (12), 1223-39.

30. de Araujo, A. D.; Mobli, M.; King, G. F.; Alewood, P. F., Cyclization of peptides by using selenolanthionine bridges. *Angew Chem Int Ed Engl* **2012,** *51* (41), 10298-302.

31. Bush, K., Antimicrobial agents targeting bacterial cell walls and cell membranes. *Rev Sci Tech* **2012,** *31* (1), 43-56.

32. Pidgeon, S. E.; Apostolos, A. J.; Nelson, J. M.; Shaku, M.; Rimal, B.; Islam, M. N.; Crick, D. C.; Kim, S. J.; Pavelka, M. S.; Kana, B. D.; Pires, M. M., L,D-Transpeptidase Specific Probe Reveals Spatial Activity of Peptidoglycan Cross-Linking. *ACS Chemical Biology* **2019,** *14* (10), 2185-2196.

33. Apostolos, A. J.; Pidgeon, S. E.; Pires, M. M., Remodeling of Cross-bridges Controls Peptidoglycan Cross-linking Levels in Bacterial Cell Walls. *ACS Chemical Biology* **2020,** *15* (5), 1261-1267.

34. Gautam, S.; Kim, T.; Spiegel, D. A., Chemical Probes Reveal an Extraseptal Mode of Cross-Linking in Staphylococcus aureus. *Journal of the American Chemical Society* **2015,** *137* (23), 7441-7447.

35. Gautam, S.; Kim, T.; Shoda, T.; Sen, S.; Deep, D.; Luthra, R.; Ferreira, M. T.; Pinho, M. G.; Spiegel, D. A., An Activity-Based Probe for Studying Crosslinking in Live Bacteria. *Angew Chem Int Ed Engl* **2015,** *54* (36), 10492-6.

36. Harris, K. M.; Flemer, S., Jr.; Hondal, R. J., Studies on deprotection of cysteine and selenocysteine side-chain protecting groups. *Journal of peptide science : an official publication of the European Peptide Society* **2007,** *13* (2), 81-93.

37. Petit, J. F.; Adam, A.; Wietzerbin-Falszpan, J.; Lederer, E.; Ghuysen, J. M., Chemical structure of the cell wall of Mycobacterium smegmatis. I. Isolation and partial characterization of the peptidoglycan. *Biochem Biophys Res Commun* **1969,** *35* (4), 478-85.

38. Baranowski, C.; Welsh, M. A.; Sham, L. T.; Eskandarian, H. A.; Lim, H. C.; Kieser, K. J.; Wagner, J. C.; McKinney, J. D.; Fantner, G. E.; Ioerger, T. R.; Walker, S.; Bernhardt, T. G.; Rubin, E. J.; Rego, E. H., Maturing Mycobacterium smegmatis peptidoglycan requires non-canonical crosslinks to maintain shape. *Elife* **2018,** *7*.

39. Flores, A. R.; Parsons, L. M.; Pavelka, M. S., Genetic analysis of the beta-lactamases of Mycobacterium tuberculosis and Mycobacterium smegmatis and susceptibility to beta-lactam antibiotics. *Microbiology (Reading)* **2005,** *151* (Pt 2), 521-532.

40. Maitra, A.; Munshi, T.; Healy, J.; Martin, L. T.; Vollmer, W.; Keep, N. H.; Bhakta, S., Cell wall peptidoglycan in Mycobacterium tuberculosis: An Achilles' heel for the TB-causing pathogen. *FEMS Microbiol Rev* **2019,** *43* (5), 548-575.

41. Apostolos, A. J.; Ferraro, N. J.; Dalesandro, B. E.; Pires, M. M., SaccuFlow: A High-Throughput Analysis Platform to Investigate Bacterial Cell Wall Interactions. *ACS Infect Dis* **2021,** *7* (8), 2483-2491.

42. Mahapatra, S.; Scherman, H.; Brennan Patrick, J.; Crick Dean, C., N Glycolylation of the Nucleotide Precursors of Peptidoglycan Biosynthesis of Mycobacterium spp. Is Altered by Drug Treatment. *Journal of Bacteriology* **2005,** *187* (7), 2341-2347.

43. Levengood, M. R.; van der Donk, W. A., Dehydroalanine-containing peptides: preparation from phenylselenocysteine and utility in convergent ligation strategies. *Nat Protoc* **2006,** *1* (6), 3001-10.

44. Okeley, N. M.; Zhu, Y.; van Der Donk, W. A., Facile chemoselective synthesis of dehydroalanine-containing peptides. *Org Lett* **2000,** *2* (23), 3603-6.

45. Lin, S.; He, D.; Long, T.; Zhang, S.; Meng, R.; Chen, P. R., Genetically encoded cleavable protein photo-cross-linker. *J Am Chem Soc* **2014,** *136* (34), 11860-3.

46. Silva, J. R.; Govender, T.; Maguire, G. E.; Kruger, H. G.; Lameira, J.; Roitberg, A. E.; Alves, C. N., Simulating the inhibition reaction of Mycobacterium tuberculosis L,D-transpeptidase 2 by carbapenems. *Chem Commun (Camb)* **2015,** *51* (63), 12560-2.

47. Levine, S. R.; Beatty, K. E., Investigating β-Lactam Drug Targets in Mycobacterium tuberculosis Using Chemical Probes. *ACS Infect Dis* **2021,** *7* (2), 461-470.

48. Sütterlin, L.; Edoo, Z.; Hugonnet, J. E.; Mainardi, J. L.; Arthur, M., Peptidoglycan Cross-Linking Activity of l,d-Transpeptidases from Clostridium difficile and Inactivation of These Enzymes by β-Lactams. *Antimicrob Agents Chemother* **2018,** *62* (1).

49. Zapun, A.; Philippe, J.; Abrahams, K. A.; Signor, L.; Roper, D. I.; Breukink, E.; Vernet, T., In vitro Reconstitution of Peptidoglycan Assembly from the Gram-Positive Pathogen Streptococcus pneumoniae. *ACS Chemical Biology* **2013,** *8* (12), 2688-2696.

50. Arbeloa, A.; Segal, H.; Hugonnet, J. E.; Josseaume, N.; Dubost, L.; Brouard, J. P.; Gutmann, L.; Mengin-Lecreulx, D.; Arthur, M., Role of class A penicillin-binding proteins in PBP5-mediated beta-lactam resistance in Enterococcus faecalis. *J Bacteriol* **2004,** *186* (5), 1221-8.

51. Lupoli, T. J.; Lebar, M. D.; Markovski, M.; Bernhardt, T.; Kahne, D.; Walker, S., Lipoprotein activators stimulate Escherichia coli penicillin-binding proteins by different mechanisms. *J Am Chem Soc* **2014,** *136* (1), 52-5.

52. Bertsche, U.; Breukink, E.; Kast, T.; Vollmer, W., In vitro murein peptidoglycan synthesis by dimers of the bifunctional transglycosylase-transpeptidase PBP1B from Escherichia coli. *J Biol Chem* **2005,** *280* (45), 38096-101.

53. Qiao, Y.; Srisuknimit, V.; Rubino, F.; Schaefer, K.; Ruiz, N.; Walker, S.; Kahne, D., Lipid II overproduction allows direct assay of transpeptidase inhibition by β-lactams. *Nat Chem Biol* **2017,** *13* (7), 793-798.

54. Born, P.; Breukink, E.; Vollmer, W., In vitro synthesis of cross-linked murein and its attachment to sacculi by PBP1A from Escherichia coli. *J Biol Chem* **2006,** *281* (37), 26985-93.

55. Ngadjeua, F.; Braud, E.; Saidjalolov, S.; Iannazzo, L.; Schnappinger, D.; Ehrt, S.; Hugonnet, J. E.; Mengin-Lecreulx, D.; Patin, D.; Ethève-Quelquejeu, M.; Fonvielle, M.; Arthur, M., Critical Impact of Peptidoglycan Precursor Amidation on the Activity of l,d-Transpeptidases from Enterococcus faecium and Mycobacterium tuberculosis. *Chemistry* **2018,** *24* (22), 5743-5747.

56. Hsu, Y. P.; Hall, E.; Booher, G.; Murphy, B.; Radkov, A. D.; Yablonowski, J.; Mulcahey, C.; Alvarez, L.; Cava, F.; Brun, Y. V.; Kuru, E.; VanNieuwenhze, M. S., Fluorogenic D-amino acids enable real-time monitoring of peptidoglycan biosynthesis and high-throughput transpeptidation assays. *Nat Chem* **2019,** *11* (4), 335-341.

57. Mengin-Lecreulx, D.; Blanot, D.; van Heijenoort, J., Replacement of diaminopimelic acid by cystathionine or lanthionine in the peptidoglycan of Escherichia coli. *J Bacteriol* **1994,** *176* (14), 4321-7.

58. Richaud, C.; Mengin-Lecreulx, D.; Pochet, S.; Johnson, E. J.; Cohen, G. N.; Marlière, P., Directed evolution of biosynthetic pathways. Recruitment of cysteine

thioethers for constructing the cell wall of Escherichia coli. *Journal of Biological Chemistry* **1993,** *268* (36), 26827-26835.

59. Consaul, S. A.; Wright, L. F.; Mahapatra, S.; Crick, D. C.; Pavelka, M. S., Jr., An unusual mutation results in the replacement of diaminopimelate with lanthionine in the peptidoglycan of a mutant strain of Mycobacterium smegmatis. *Journal of bacteriology* **2005,** *187* (5), 1612-1620.

60. Kühner, D.; Stahl, M.; Demircioglu, D. D.; Bertsche, U., From cells to muropeptide structures in 24 h: Peptidoglycan mapping by UPLC-MS. *Sci Rep* **2014,** *4* (1), 7494.

61. Mahapatra, S.; Crick Dean, C.; McNeil Michael, R.; Brennan Patrick, J., Unique Structural Features of the Peptidoglycan of Mycobacterium leprae. *Journal of Bacteriology* **2008,** *190* (2), 655-661.

62. Lim, D.; Strynadka, N. C., Structural basis for the beta lactam resistance of PBP2a from methicillin-resistant Staphylococcus aureus. *Nat Struct Biol* **2002,** *9* (11), 870-6.

Chapter 6 SaccuFlow- A High-throughput Analysis Platform to Investigate Bacterial Cell Wall Interactions

Adapted from: Apostolos, A. J.[#]; Ferraro, N. J.[#]; Dalesandro, B. E.; Pires, M. M., SaccuFlow: A High-Throughput Analysis Platform to Investigate Bacterial Cell Wall Interactions. *ACS Infect Dis* **2021**, *7* (8), 2483-2491.
# authors contributed equally

6.1 *Abstract*

Bacterial cell walls are formidable barriers that protect bacterial cells against external insults and oppose internal turgor pressure. While cell wall composition is variable across species, peptidoglycan is the principal component of all cell walls. Peptidoglycan is a mesh-like scaffold composed of crosslinked strands that can be heavily decorated with anchored proteins. The biosynthesis and remodeling of peptidoglycan must be tightly regulated by cells because disruption to this biomacromolecule is lethal. This essentiality is exploited by the human innate immune system in resisting colonization and by a number of clinically relevant antibiotics that target peptidoglycan biosynthesis. Evaluation of molecules or proteins that interact with peptidoglycan can be a complicated and, typically, qualitative effort. We have developed a novel assay platform (SaccuFlow) that preserves the native structure of bacterial peptidoglycan and is compatible with high-throughput flow cytometry analysis. We show that the assay is facile and versatile as demonstrated by its compatibility with sacculi from Gram-positive bacteria, Gram-negative bacteria, and mycobacteria. Finally, we highlight the utility of this assay to assess the activity of sortase A from *Staphylococcus aureus* against potential anti-virulence agents.

6.2 *Introduction*

Bacterial cell walls have many functions but none more important than acting as a protective barrier from potentially harsh external elements and attacks from host defense

mechanisms.[1, 2] Bacteria can be categorized based on the type of cell wall they possess and there are distinctive features of each that can pose a challenge, or opportunity, for the host the immune system or antibiotics.[3, 4] In the case of Gram-positive bacteria, their cell wall is composed of a thick peptidoglycan (PG) sacculus layer followed by a cytoplasmic membrane. PG is a mesh-like polymer made up of repeating disaccharide units of *N*-acetylglucosamine (GlcNAc) and *N*-acetylmuramic acid (MurNAc). Attached to each MurNAc unit is a short peptide, referred to as the stem peptide, that ranges from 3 to 5 amino acids in length. The stem pentapeptide sequence is typically L-Ala-*iso*-D-Glu-L-Lys (or *meso*-diaminopimelic acid [*m*-DAP])-D-Ala-D-Ala, although there are considerable variations in the primary sequence.[5]

Crosslinking can occur between neighboring stem peptides and the degree to which the PG is crosslinked can influence the cell wall rigidity and integrity.[2] The thick PG layer in Gram-positive bacteria is generally believed to be a permeability barrier to molecules in the extracellular space.[6-9] While most small molecules can potentially sieve through the PG, there is evidence that the PG is a formidable barrier for the permeation of larger molecules.[10-12] This feature has significant implications for molecules with intracellular and cell membrane targets; one example being the membrane attack complex (MAC), a product of the complement system that targets bacterial cell membranes. The MAC is prevented from reaching the cytoplasmic membrane of Gram-positive bacteria due in part to its inability to penetrate through the PG layer.[13, 14] Gram-positive pathogens can also alter the composition of their PG to become resistant to specific classes of antibiotics. For example, both *Staphylococcus aureus* (*S. aureus*) and *Enterococcus faecium* can alter the PG structure to resist the antibacterial actions of vancomycin.[15-17] Due to its critical role in bacterial cell survival, PG is often the target of antibiotics and components of the human immune system.[4, 18, 19] Clinically and industrially important antibacterial agents (e.g., β-lactams, teixobactin, vancomycin, bacitracin, and moenomycin) target components of the PG biosynthesis as integral parts of their mechanism of actions. Similarly, components of the human immune system (e.g., lysozyme, LysM-displaying proteins, and PG recognition proteins [PGRPs]) must reach the PG to impart their response onto the invading bacterial pathogen.

Despite the importance of characterizing interactions with the PG scaffold of bacteria, there are limited methods to investigate the specific binding of molecules to PG. More specifically, there is a clear need for a method to determine PG binding interactions that (1) retains the natural composition of native PG, (2) is applicable to all types of bacteria, (3) preserves the polymeric nature of native PG, (4) is readily attainable in high yields, and (5) is compatible with quantitative, high-throughput analysis platforms. There are several challenges with obtaining PG samples for analysis. The use of synthetic PG mimics provides some advantages such as sample homogeneity and the ability to install specific changes to the PG primary sequence. In fact, a number of important contributions to the field have been made using synthetic PG mimics.[20-24] Our own group has extensively used synthetic PG mimics in studying cell wall biosynthesis and remodeling.[25, 26] However, there are some severe drawbacks to using synthetic analogs, including the lack of commercially available building blocks for the disaccharide units and *m*-DAP. In addition, there is potential for the loss of polyvalent interactions, which are prevalent in PG-binding molecules, using monomeric PG analogs. Alternatively, PG fragments can be obtained by digesting isolated native PG (sacculi) with a hydrolase enzyme and performing chromatography.[27, 28] This last-resort method is fraught with challenges due to the difficulty in the separation of fragments, convoluted characterization of fragments (e.g., site of amidation), and low yields. Finally, the use of intact cells to study PG interactions has advantages in terms of retaining the polymeric nature and preservation of the native composition (even if variable across the PG scaffold). However, isolation of the effect of PG interaction alone in the background of surface bound proteins and other potential biomacromolecules is a major hurdle. Herein, we report a new method (SaccuFlow) that uses sacculi isolated directly from Gram-positive, Gram-negative, or mycobacterial organisms in combination with flow cytometry to assay PG binding interactions. To the best of our knowledge, flow cytometry has not yet been systematically used to evaluate isolated bacterial PG and/or its interactions with binding partners.

6.3 *Results and Discussion*

6.3.1 *Flow cytometry of sacculi from a Gram-positive organism labeled with a fluorescently modified single amino acid*

We reasoned that murein sacculus from bacteria, which is a single macromolecular scaffold made of PG, would provide a superior platform to analyze PG interactions due to its ease of isolation and proper mimicry of the PG composition and structure. Sacculi isolation steps include extensive boiling of bacterial cells in the presence of detergents and can also include protease digestion to further remove covalently linked proteins. While sacculi analysis has been implemented for decades, these studies have focused primarily on mass spectrometry analysis of digested low molecular weight PG fragments[29-31] and low-throughput qualitative analyses techniques (e.g., confocal microscopy[32] and pull-down assays[33]). We envisioned a that a higher-throughput and quantitative sacculus analysis platform could be achieved by performing the analysis using flow cytometry. Sacculi should be readily detected *via* flow cytometry because its size resembles that of the bacterial cell.[34] Significantly, sacculi preparations are routinely performed with relative ease from almost any type of bacteria with these isolation steps.

Initially, we set out to benchmark the detection of bacterial sacculi from a Gram-positive organism using a standard flow cytometer. We chose to site selectively tag the sacculi with a fluorescent handle by metabolic labeling of the PG scaffold. Our research group[35-39], and others[40-46], have previously demonstrated that co-incubation of unnatural D-amino acids, including those modified with fluorophores, metabolically label PG of live bacteria cells. More specifically, fluorescein conjugated D-Lys (**D-LysFl**) from the culture media is expected to replace the 5th position D-alanine of the PG stem peptide of *S. aureus* during the biosynthesis and remodeling of new PG (**Figure 6.1b,c**). Generally, 1-2 % of the stem peptides in the PG scaffold of *S. aureus* is labeled when cells are treated overnight with the D-amino acid label under the assay conditions.[40, 47, 48] Bacterial sacculi were isolated using standard procedures from whole cells, which were expected to yield fluorescently labeled sacculi (**Figure 6.1a**). Our results revealed that labeled sacculi formed a tight population of events that could readily be distinguished from background debris (**Figure 6.2a**). Most significantly, fluorescence levels of sacculi

from cells treated with **D-LysFl** were 17-fold higher than cells treated with the control amino acid **L-LysFl** (**Figure 6.2b**). Unlike **D-LysFl**, its enantiomer does not become incorporated as part of the bacterial PG scaffold. The same sacculi was imaged using confocal microscopy, thus confirming that the sample analyzed was primarily fluorescent sacculi (**Figure 6.2c**). A **D-LysFl** concentration dependent labeling pattern of the isolated PG was also observed (**Figure 6.2c**). Next, a series of additional experiments were performed to confirm that fluorescent **D-LysFL**, which was detected on the flow cytometer, was incorporated into *S. aureus* sacculi. Sacculi labeled with **D-LysFl** were subjected to treatment with two PG hydrolases: lysozyme and mutanolysin (**Figure 6.2d**). As expected, treatment with mutanolysin resulted in a time-dependent reduction in fluorescence levels due to the release of PG fragments. *O*-acetylation of *S. aureus* PG renders it insensitive to lysozyme digestion and, likewise, lysozyme treatment.[49] Digestion by mutanolysin was also found to be concentration dependent (**Figure 6.3**).

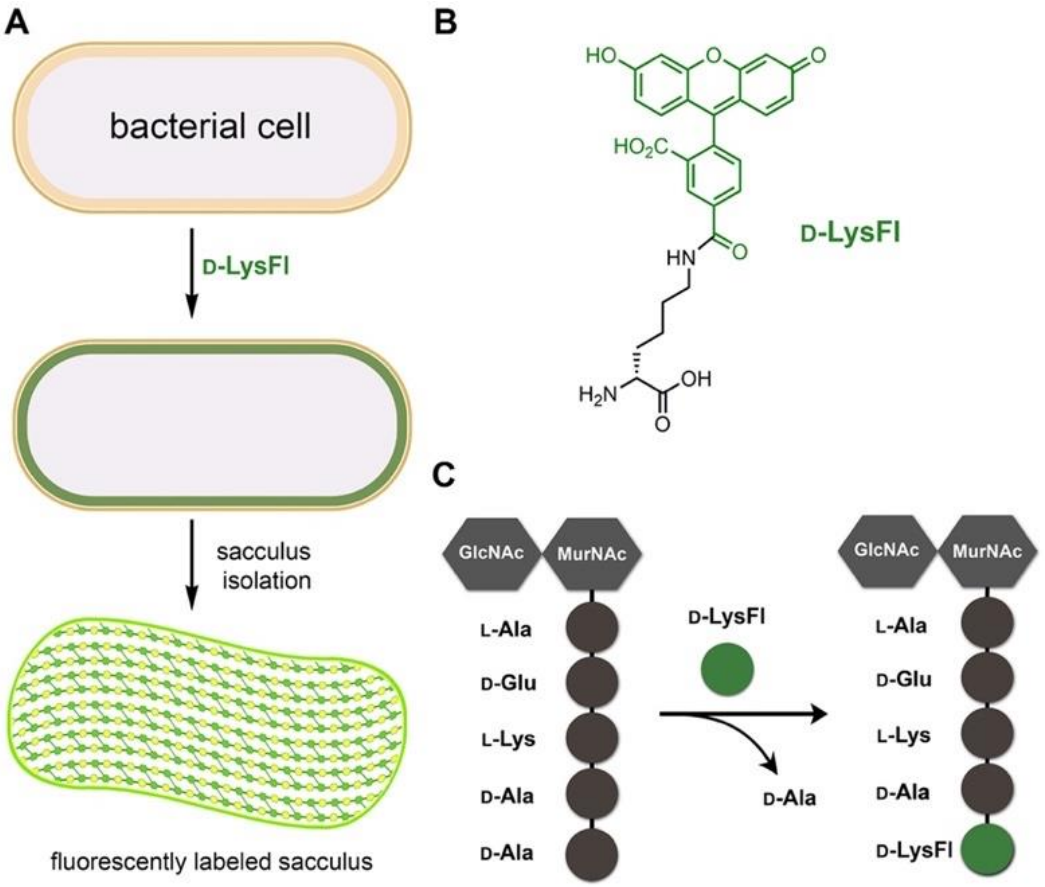

Figure 6.1 *(**A**) Assay workflow of SaccuFlow for the labeling of sacculi. (**B**) Chemical structure of **D-LysFl**. (**C**) Cartoon representation of the metabolic swapping of the terminal D-ala from the bacterial PG with the exogenously supplied **D-LysFl**.*

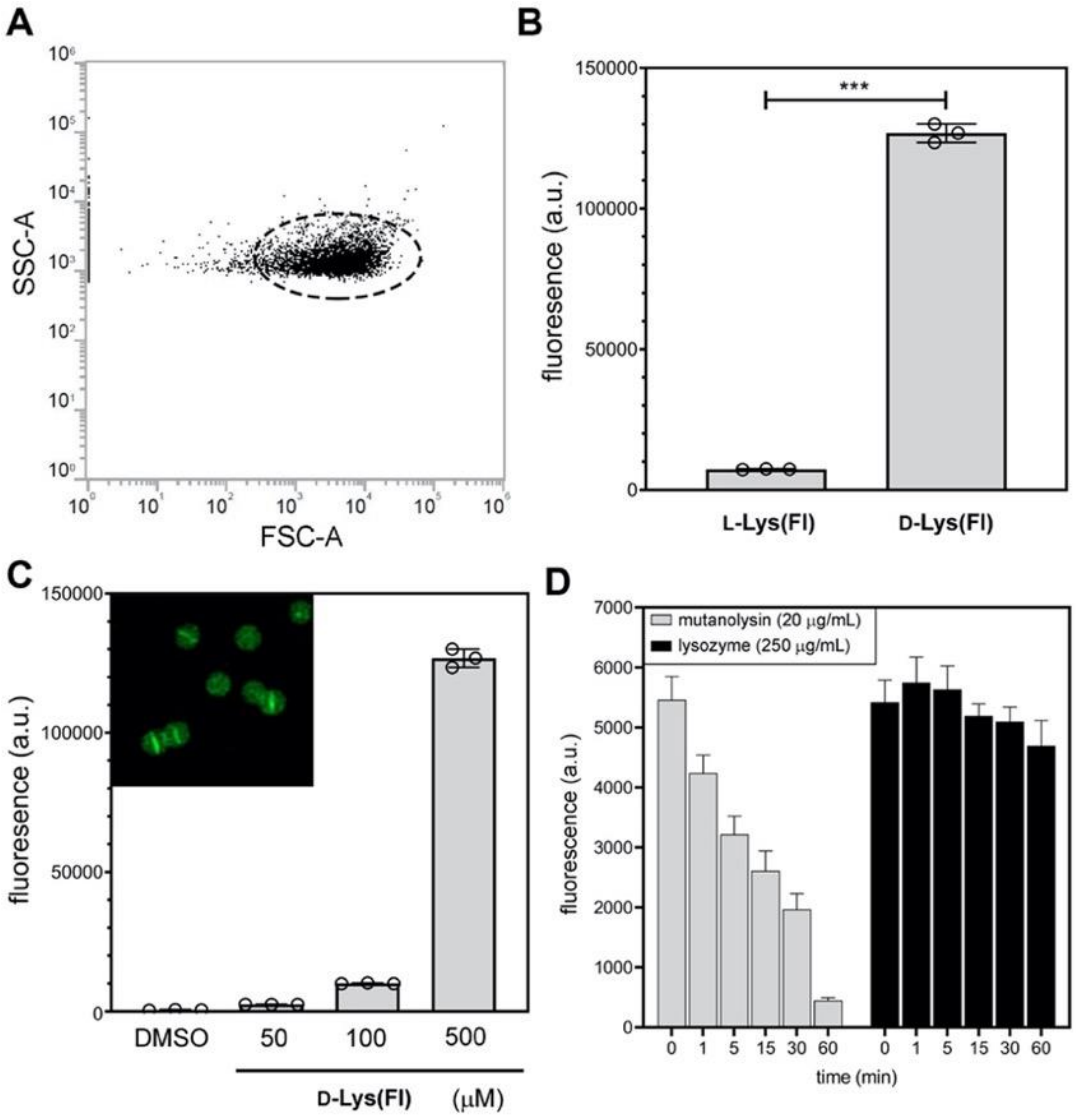

Figure 6.2 *(**A**) Side and forward scatter plot of S. aureus sacculi. (**B**) Flow cytometry analysis of sacculi isolated from S. aureus (ATCC 25923) treated overnight with 500 μM of **D-LysFl** or **L-LysFl**. (**C**) Flow cytometry analysis of sacculi isolated from S. aureus (ATCC 25923) treated overnight with varying concentrations of **D-LysFl**. Inset, Confocal microscopy of sacculi isolated from S. aureus (ATCC 25923) that was treated with 100 μM **D-LysFl** overnight (**D**) Flow cytometry analysis of sacculi isolated from S. aureus (ATCC 25923) treated overnight with 500 μM of **D-LysFl** and incubated with either mutanolysin or lysozyme. Data are represented as mean +/− SD (n = 3). P-values were determined by a two-tailed t-test (* denotes a p-value < 0.05, ** < 0.01, ***<0.001, ns = not significant).*

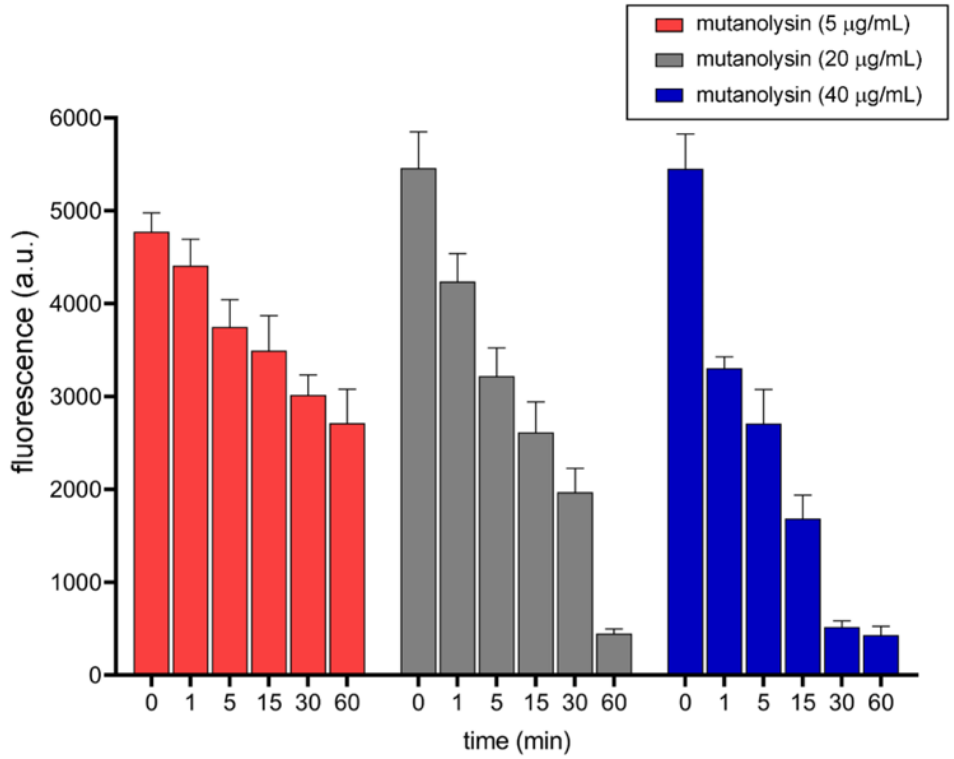

Figure 6.3 *Fluorescence read out of sacculi isolated from S. aureus (ATCC 25923) that was treated with 100 μM* ***D-LysFl*** *overnight and subjected to degradation by increasing concentrations of mutanolysin overtime.*

6.3.2 *Flow cytometry of sacculi from Gram-positive, -negative, and mycobacteria labeled with a click-chemistry compatible handle*

To show the versatility of the tagged sacculi in a flow cytometry platform, we prepared sacculi from organisms that had been co-incubated with either **D-** or **L-LysAz** (**Figure 6.4a**). We anticipated that **D-LysAz** treated cells would provide an orthogonal click handle on the PG scaffold that could be covalently linked to a variety of compounds containing the corresponding reactive moieties. Subsequent treatment with cyclooctynes should result in strain-promoted alkyne-azide cycloaddition (SPAAC) ligation with azide groups on the sacculi.[50, 51] For this assay, azide-tagged sacculi isolated from *S. aureus* were incubated with dibenzocyclooctyne (DBCO) linked to fluorescein. Our results showed

increase in of ~8-fold in sacculi fluorescence when cells were treated with **D-LysAz**, which is consistent with the successful ligation of fluorescein mediated by SPAAC (**Figure 6.4b**). Strikingly, after chemical removal of the wall teichoic acids (WTA), an increase in fluorescence was observed with the small fluorescently labeled handle (**Figure 6.4c**). WTA is an anionic polymer that is covalently anchored onto PG of some Gram-positive organisms.[52-55] It is well established that WTA can block or impede interaction of extracellular molecules with the PG scaffold. These results highlight the role that surface biopolymers play in accessibility to the PG scaffold and further demonstrates the ability to use flow cytometry to systematically assess this important feature related to bacterial cell wall biology. Similarly, to test the applicability of this method to mycobacterial and Gram-negative organisms, *Mycobacterium smegmatis* (*M. smegmatis*) and *Escherichia coli* (*E. coli*) were grown in media supplemented with either **D-** or **L-LysAz** and their sacculi were harvested following the standard procedures for each classification. The isolated PG was then treated with **Dfl0** and analyzed by flow cytometry, showing that only sacculi from cells that had been treated with **D-LysAz** labeled extensively with **Dfl0** (**Figure 6.5**). This highlights the adaptability of SaccuFlow to bacterial species of varied classifications.

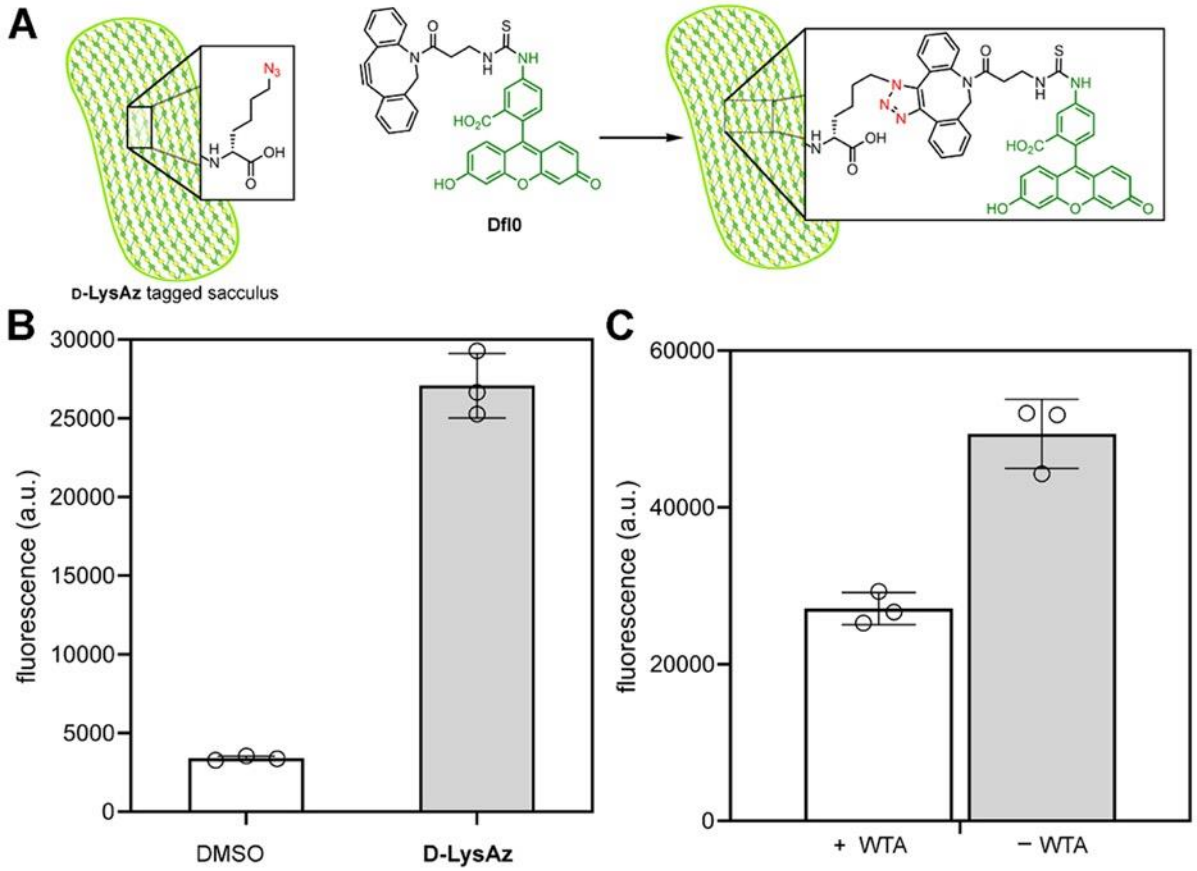

Figure 6.4 *(**A**) Chemical structures representing the SPAAC reaction between azide and a strained alkyne in DBCO. (**B**) Flow cytometry analysis of sacculi isolated from S. aureus (ATCC 25923) treated overnight with 1 mM of **D-LysAz** or DMSO. Subsequently, sacculi were incubated with 25 μM of **Dfl0**. (**C**) Flow cytometry analysis of sacculi isolated from S. aureus (ATCC 25923) treated overnight with 1 mM of **D-LysAz**. Where noted, sacculi were chemically treated to remove WTA. Subsequently, sacculi were incubated with 25 μM of **Dfl0**. Data are represented as mean +/− SD (n = 3). P-values were determined by a two-tailed t-test (* denotes a p-value < 0.05, ** < 0.01, ***<0.001, ns = not significant).*

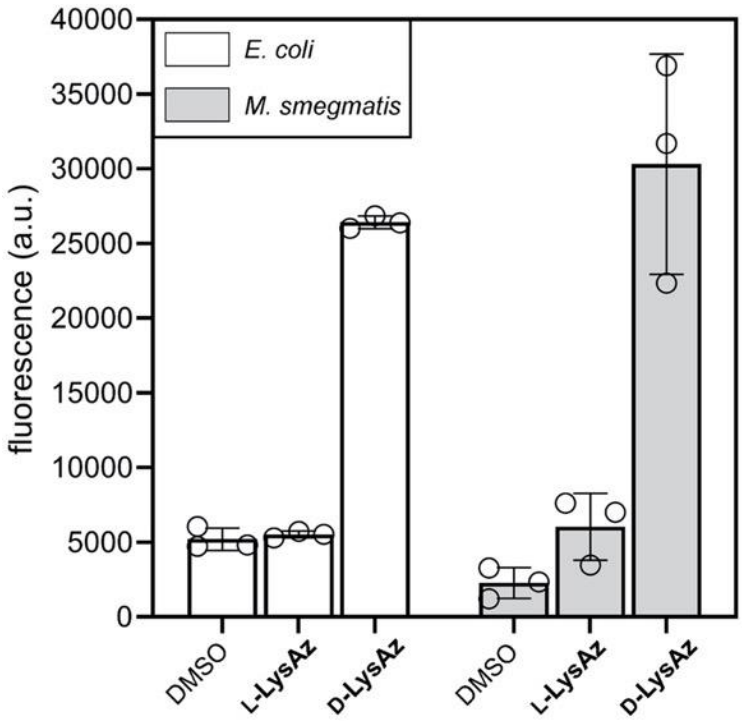

Figure 6.5 *Fluorescence read-out of sacculi isolated from E. coli BW25113 or M. smegmatis WT that was incubated with 1 mM* ***L****- or* ***D-LysAz*** *overnight, and subsequently treated with 25 μM DBCO-FITC.*

6.3.3 *Flow cytometry analysis of sacculi with antibiotics*

Having shown that SaccuFlow was operational and facile, we then set out to demonstrate that it could report on features related to PG-binding antibiotics. Vancomycin, a glycopeptide antibiotic that specifically hydrogen-binds the D-Ala-D-Ala fragment of the stem peptide, conjugated to BODIPY (**VBD**)[56] was analyzed for binding using SaccuFlow. As anticipated, *S. aureus* sacculi demonstrated ~8-fold BODIPY fluorescence over background, suggesting that vancomycin bound to isolated PG was detectable by flow cytometry (**Figure 6.6a**). To show that fluorescence levels were reflective of specific binding interactions, bacterial sacculi was treated with a synthetic analog of the PG, L-Lys-D-Ala-D-Ala. As expected, increasing concentrations of L-Lys-D-Ala-D-Ala led to decreasing fluorescence levels associated with the decrease in binding events of **VBD** to sacculi (**Figure 6.6b**). To show the versatility of this assay amongst other strains, we

isolated *Bacillus subtilis* (*B. subtilis*) sacculi from a wildtype (WT) strain and from a strain lacking *dacA* (*dacA*Δ), the gene responsible for the D-alanyl-D-alanine carboxypeptidase.[57] **VBD** would be expected to bind *dacA*Δ *B. subtilis* sacculi to a higher level in comparison to WT, as lack of the carboxypeptidase would present additional D-Ala-D-Ala binding points for **VBD**. Our results demonstrate a ~**3**-fold increase in binding of **VBD** to *dacA*Δ sacculi as compared to WT, as monitored by SaccuFlow (**Figure 6.6c**). Next, sacculi samples were isolated from an *Enterococci faecium* (*E. faecium*) strain that has a vancomycin inducible resistant phenotype based on activation of the membrane receptor VanS.[58, 59] The outcome of this activation is the intracellular removal of the terminal D-alanine in the PG precursor, which should reduce the bindings available to **VBD**. Consistent with this phenotypic switch, analysis of VRE sacculi showed that there was a significant decrease in fluorescence associated with VRE pre-treated with vancomycin (**Figure 6.6d**). Together, these results confirm that SaccuFlow can be readily adopted to monitor and quantify interactions of PG-binding molecules, which can have applicability in studying drug resistance or establish therapeutic interventions.

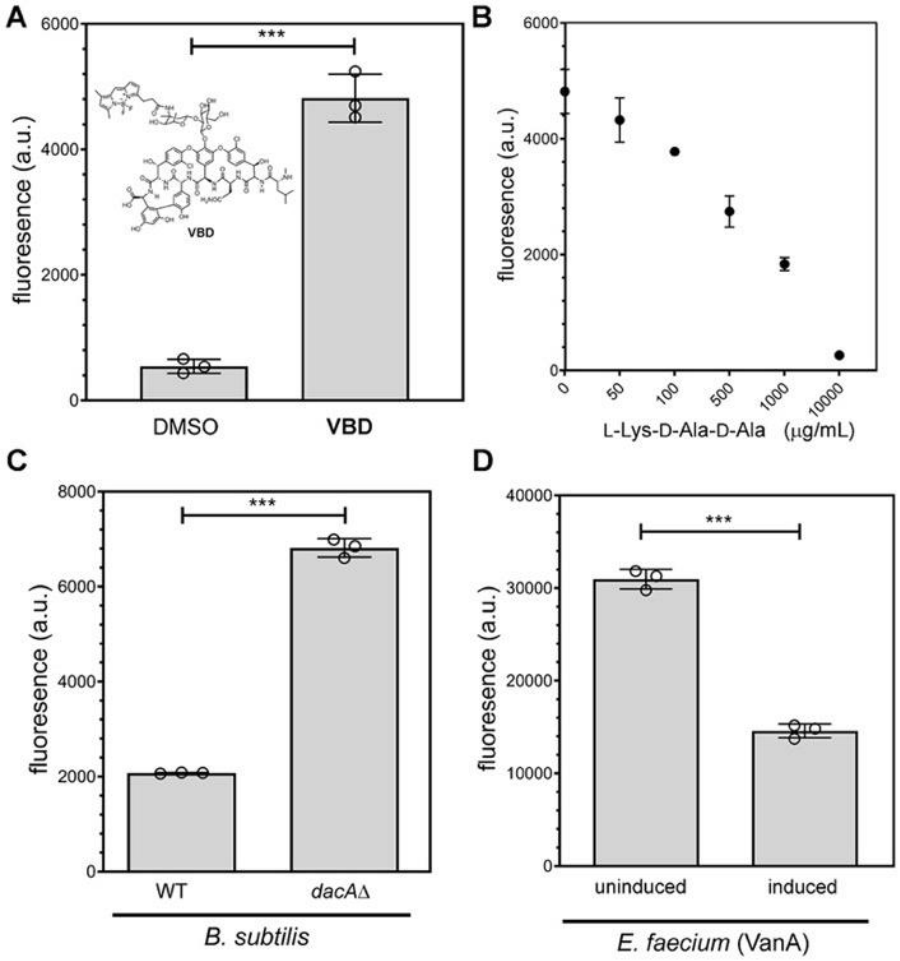

Figure 6.6 *(**A**) Flow cytometry analysis of sacculi isolated from S. aureus (ATCC 25923). Subsequently, sacculi were treated with **VBD** (2 µg/mL) or DMSO. (**B**) Flow cytometry analysis of sacculi isolated from S. aureus (ATCC 25923). Subsequently, sacculi were treated with **VBD** (2 µg/mL) and increasing concentrations of L-Lys-D-Ala-D-Ala. (**C**) Flow cytometry analysis of sacculi isolated from B. subtilis (WT and dacAΔ). Subsequently, sacculi were treated with **VBD** (4 µg/mL). (**D**) Flow cytometry analysis of sacculi isolated from E. faecium vanA (with and without pre-incubation of vancomycin). Subsequently, sacculi were treated with **VBD** (4 µg/mL). Data are represented as mean +/− SD (n = 3). P-values were determined by a two-tailed t-test (* denotes a p-value < 0.05, ** < 0.01, ***<0.001, ns = not significant).*

6.3.4 *SaccuFlow for the processing and remodeling of PG*

We tested the ability of the SaccuFlow assay to evaluate the processing and remodeling of PG. More specifically, we evaluated the possibility of tracking the activity of the enzyme sortase A from *S. aureus*. Sortase A is a transpeptidase that recognizes the sorting sequence LPXTG (where X is any amino acid) and thereby anchors proteins that contain this sequence onto the bacterial PG.[60, 61] *S. aureus* utilizes sortase A to heavily decorate the surface of the PG with proteins capable of improving host colonization and interfering with human immune response. Therefore, sortase A is considered an attractive drug target and small molecules that inhibit sortase A could prove to be promising anti-virulence agents. Prior efforts to investigate sortase A activity have generally used minimal peptide mimics of PG (e.g., penta-glycine), which may not be entirely representative of the features of the PG (or its lipid anchored precursor). For our assay, sacculi isolated from *S. aureus* were incubated with purified sortase A originating from *S. aureus* and a sorting signal substrate modified with a fluorophore. We monitored the fluorescence of the sacculi over time *via* flow cytometry and, as expected, observed an increase in fluorescence as sortase A linked the fluorescent sorting signal substrate to the isolated PG (**Figure 6.7a**). Further, sacculi treated with methanethiosulfonate (MTSET), a covalent inhibitor of sortase[62], or no sortase at all, demonstrated fluorescence that was at background levels (**Figure 6.7a**). These results provide clear demonstration that SaccuFlow can be utilized to investigate processing of PG in a quantitative manner.

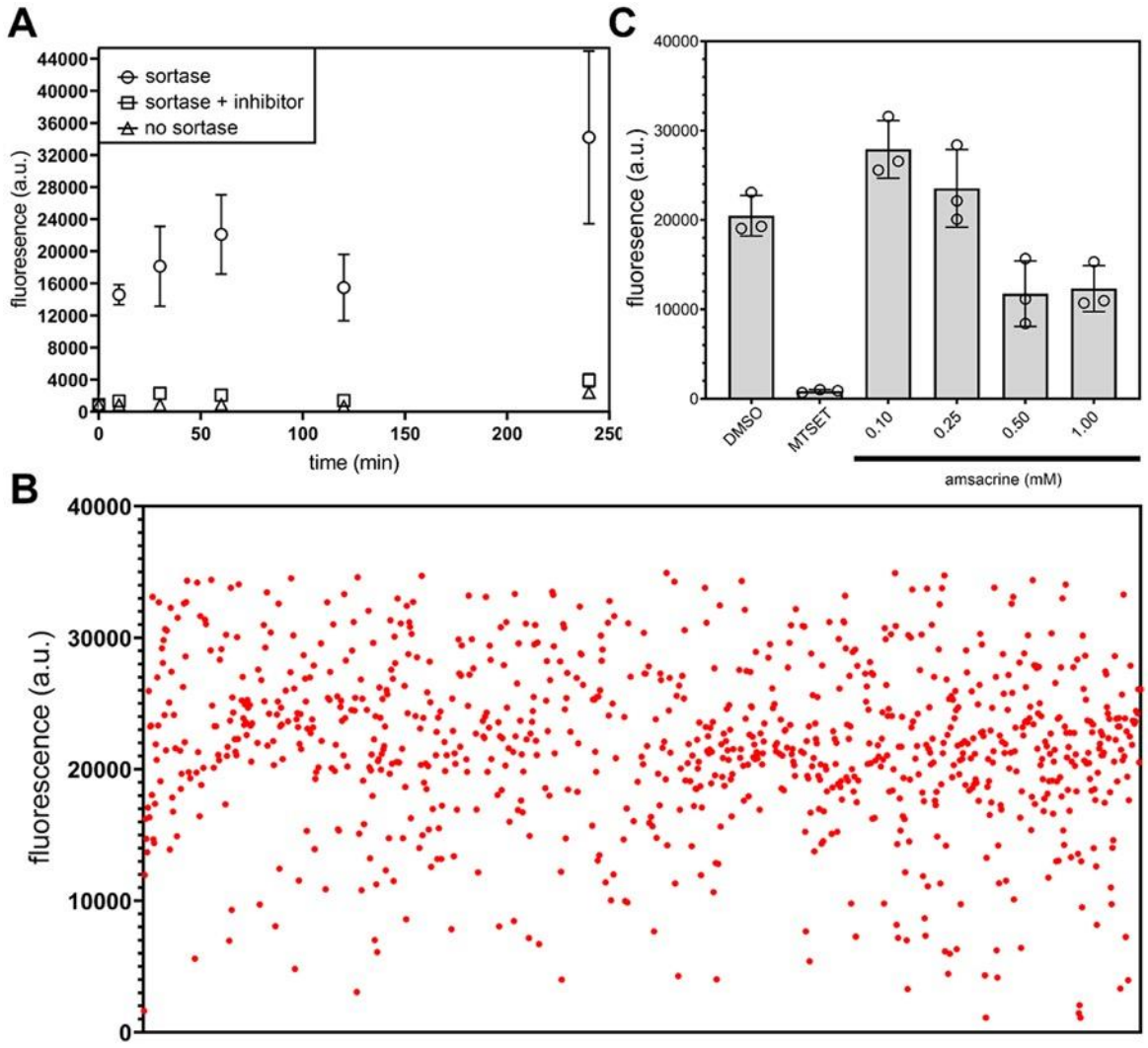

Figure 6.7 *(**A**) Time course analysis of sortase activity using sacculi from S. aureus (ATCC 25923) in the presence of the fluorescent sorting signal substrate (100 μM). Flow cytometry analysis of sacculi treated with sortase, the covalent inhibitor MTSET (1 mM), and in the absence of sortase. (**B**) Screening of LOPAC 1280 library using 384-well format. Individual dots represent members of the library in the presence of sacculi and sorting signal substrate (100 μM). The average of the untreated control was 20493 and compounds were re-evaluated with fluorescence levels. (**C**) Flow cytometry analysis of sortase activity in the presence of designated conditions. Data are represented as mean +/− SD (n = 3).*

Finally, to demonstrate the high-throughput capability of SaccuFlow, we used the established parameters of the sortase A assay to determine the ability of a library of 1,280 pharmacologically active compounds to inhibit sortase A activity (LOPAC 1280 library). Using isolated *S. aureus* sacculi, sortase A, and the fluorescently tagged sorting signal substrate, we monitored the fluorescence readout of the sacculi against individual members of the compound library. We predicted that a reduction in fluorescence would correspond to a reduction of sortase A activity. Our screening results revealed a total of 18 compounds as potential inhibitors of sortase (**Figure 6.7b**). Of interest, amsacrine, which was previously reported to inhibit Mycobacterial topoisomerases[63] as well as d-alanylation of teichoic acids in *S. aureus*[64], was identified as a potential inhibitor. We further tested the ability of amsacrine to inhibit sortase A in a titration assay, which showed a reduction in fluorescence levels in a concentration-dependent manner (**Figure 6.7c**). This pilot screen demonstrated the feasibility of SaccuFlow to be miniaturized and used in a high-throughput screen. Moreover, these results highlight the potential of SaccuFlow to assess essential enzyme operations within the PG scaffold and identify substrates or inhibitors of those enzymes of interest, paving the way to the discovery of potential therapeutics against these validated drug targets.

6.4 *Conclusion*

In conclusion, we have described the implementation of a new flow cytometry assay (SaccuFlow) that makes use of the mechanical strength and native composition of bacterial sacculi. By adopting the assay to flow cytometry, we showed that it is possible to gain quantitative information on interactions of molecules with PG. Tagging of bacterial sacculi with orthogonal epitopes led to the demonstration of the accessibility of molecules to the PG scaffold. Moreover, versatility of the assay platform was also demonstrated by analyzing sacculi from three different species of Gram-positive bacteria, one Gram-negative bacterium, and a mycobacterium. Binding studies with fluorescently labeled vancomycin showed that SaccuFlow can reveal PG interaction dynamics, including phenotypic changes due to drug resistance. Finally, enzymatic processing of PG by sortase A was performed to highlight the versatility of this assay in studying PG biology.

Given the important nature of PG binding molecules, including several clinically relevant antibiotics and components of the innate immune system, we expect that this assay platform will find wide usage across microbiology studies.

6.5 *Materials and Methods*

Materials. All peptide related reagents (resin, coupling reagent, deprotection reagent, amino acids, and cleavage reagents) were purchased from ChemImpex or BroadPharm. Bacterial strains *Staphylococcus aureus* (*S. aureus*), *Bacillus subtilis* (*B. subtilis*), *B. subtilis dacA*Δ, and *Escherichia coli* (*E. coli*) were grown in lysogeny broth, *Enterococcus faecium* (*E. faecium*) was grown in tryptic soy broth, *Mycobacterium smegmatis* (*M. smegmatis*) were grown in lysogeny broth supplemented with 0.05% Tween 80 for all experiments.

Peptidoglycan Isolation of *B. subtilis* and *B. subtilis dacΔ.* LB was supplemented with 1X kanamycin during the growth of the *B. subtilis dacA*Δ. The rest of the isolation protocol follows that of the *S. aureus* isolation protocol detailed above.

Peptidoglycan Isolation of *E. faecium.* Tryptic soy broth (TSB) was supplemented with 16 µg/mL of vancomycin in order to induce the resistance phenotype during the growth of the *E. faecium.* The rest of the isolation protocol follows that of the *S. aureus* isolation protocol detailed above.

Peptidoglycan Isolation of *E. coli.* LB (100 mL) containing 1 mM D- or L-Lys-azido, or no supplemented probe was prepared. *E. coli* BW25113 bacteria were added to the LB medium (1:100) and allowed to grow overnight at 37°C with shaking at 250 rpm. The cells were chilled on ice, then harvested at 8,000g for 10 min at 4°C. The resulting pellet was resuspended in 3 mL of 1% (w/v) NaCl, then added slowly to 6 mL of 8% SDS that was in a boiling water bath with a stir bar. Samples were boiled for 5 h, followed by incubation at room temperature with continued stirring overnight. The following morning, samples were boiled for 2 h and then pelleted at 100,000g for 10 min at 25°C. Resulting pellets

were suspended in 3 mL of 4% SDS, boiled for 2 h with stirring. Samples were collected using the same parameters and washed 5 times with sterile DI H_2O to remove all SDS. Pellets were resuspended in 1 mL of 1X PBS and 200 µg/mL of trypsin was added followed by incubation at 37°C with shaking at 115 rpm for 2 h. A second dose of trypsin was added, and samples were incubated overnight. The following morning, one-tenth volume of 10% SDS was added and samples were placed in an oil bath at 100°C for 2 h. Sacculi were collected as before, and washed 3X with sterile DI H_2O to remove residual SDS. The final pellet was lyophilized and resuspended in 400 µL of H_2O for further analysis by flow cytometry.

Peptidoglycan Isolation of *M. smegmatis.* LB (100 mL) with 0.05% Tween 80 containing 1 mM D- or L-Lys-azido, or no supplemented probe was prepared. *M. smegmatis* bacteria were added to the LB medium (1:100) and allowed to grow overnight at 37°C with shaking at 250 rpm. Cells were then harvested at 14,000g for 15 min at 4°C and washed 1X in a minimal volume of 1X PBS. Pellets were resuspended in 10 mM NH_4HCO_3 with a protease inhibitor cocktail (Sigma SRE005-1BO). This suspension was lysed using a tip sonicator (Fisher Scientific) at 60% amplitude for 60 seconds, with at least 60 seconds on ice in between. This was repeated for 5 cycles. The sonicate was digested with 10 µg/mL DNAse and RNase for 1 h at 4°C, then harvested at 27,000g for 30 min at 4°C. The pellet was resuspended in PBS with 2% SDS and incubated for 1 h at 50°C with constant stirring. This was collected using the same centrifugal parameters and the SDS process was repeated 2X. The resulting pellet was resuspended in PBS with 1% SDS and 0.1 mg/mL Proteinase K at 45°C for 1 h with stirring. The sample was then heated to 90°C for 1 h and collected as above. This step at 90°C was repeated 2X. The sample was washed 2X with PBS and 4X with dH2O. This yielded mycolic-arabinogalactan-peptidoglycan (mAGP). The final mAGP sample was lyophilized and resuspended in H_2O for further SPAAC chemistry and analysis by flow cytometry.

Sortase A Expression and Purification. The plasmid for sortase A from *S. aureus* was obtained from Addgene: pET28a-SrtAdelta59. Competent BL21 (DE3) *E. coli* were transformed with the plasmid. *E. coli* cells containing the plasmid from an overnight

culture were diluted 1:100 and grown at 37°C until the OD_{600} was 0.4-0.6. At this time, Isopropyl-β-D-thiogalactopyranoside (IPTG) was added to a concentration of 0.5 mM and the cultures were shook at 25°C for 16 h. Cells were collected at 3,000g for 30 min and resuspended in 50 mM Tris-HCl, pH 7.5, and 150 mM NaCl. Pellets were then recollected and lysed in cold lysis buffer (50 mM Tris-HCl, pH 7.5, 150 mM NaCl, 5 mM $MgCl_2$, 10 mM imidazole, 10% vol/vol glycerol, 1 mg ml^{-1} DNase and 1 mg ml^{-1} lysozyme). Cells were lysed using an ultrasonic cell sonicator and the lysate was separated from cellular debris by centrifugation at 20,000g for 30 min at 4°C. The supernatant was loaded onto a Ni-NTA agarose resin and eluted with 500 mM imidazole in buffer (50 mM Tris-HCl pH 7.5, 150 mM NaCl, and 10% vol/vol glycerol). The eluted protein was dialyzed against buffer without imidazole, aliquoted (protein concentration determined by Bradford assay), and stored at –20°C until use.

Sortase A Enzymatic Assays. Isolated *S. aureus* sacculi samples were incubated with 20 uM sortase A, 100 uM sorting signal substrate, and 1X sortase buffer (10X contains 500 mM Tris-HCl, pH 7.5, 1.5 M NaCl, 100 mM $CaCl_2$). Samples that contained the covalent inhibitor, MTSET, were run at a concentration of 1 mM. All were shook at room temperature for the given time. At each time point, 20 uL were taken out of the reaction, quenched with 0.1% TFA, and washed 3X with 100 mM Tris, 5 mM EDTA, pH 7 and freshly added 8 M urea. Samples were resuspended in a final volume of 120 uL 1X PBS and analyzed by flow cytometry as described above.

For the high-throughput scan using the LOPAC library of 1,280 small molecule compounds, the same conditions were used. However, sortase was incubated with 1 mM of the compound library and let incubate at room temperature for 20 minutes before addition of sacculi, Fl-LPMTG (sorting signal), and buffer. After the addition of the remaining reaction components, samples were shook at room temperature for 4 h before being quenched with 0.1% TFA, then washed in buffer with 8M urea as above. Samples were resuspended in a final volume of 100 uL 1X PBS and analyzed by flow cytometry as described above.

6.6 *References*

1. Vollmer, W.; Blanot, D.; De Pedro, M. A., Peptidoglycan structure and architecture. *FEMS Microbiology Reviews* **2008,** *32* (2), 149-167.
2. Silhavy, T. J.; Kahne, D.; Walker, S., The bacterial cell envelope. *Cold Spring Harb Perspect Biol* **2010,** *2* (5), a000414-a000414.
3. Royet, J.; Dziarski, R., Peptidoglycan recognition proteins: pleiotropic sensors and effectors of antimicrobial defences. *Nat Rev Microbiol* **2007,** *5* (4), 264-77.
4. Wolf, A. J.; Underhill, D. M., Peptidoglycan recognition by the innate immune system. *Nat Rev Immunol* **2018,** *18* (4), 243-254.
5. Egan, A. J. F.; Errington, J.; Vollmer, W., Regulation of peptidoglycan synthesis and remodelling. *Nat Rev Microbiol* **2020,** *18* (8), 446-460.
6. Brown, L.; Wolf, J. M.; Prados-Rosales, R.; Casadevall, A., Through the wall: extracellular vesicles in Gram-positive bacteria, mycobacteria and fungi. *Nature Reviews Microbiology* **2015,** *13* (10), 620-630.
7. O'Shea, R.; Moser, H. E., Physicochemical properties of antibacterial compounds: implications for drug discovery. *J Med Chem* **2008,** *51* (10), 2871-8.
8. Richter, M. F.; Drown, B. S.; Riley, A. P.; Garcia, A.; Shirai, T.; Svec, R. L.; Hergenrother, P. J., Predictive compound accumulation rules yield a broad-spectrum antibiotic. *Nature* **2017,** *545* (7654), 299-304.
9. Cloud-Hansen, K. A.; Peterson, S. B.; Stabb, E. V.; Goldman, W. E.; McFall-Ngai, M. J.; Handelsman, J., Breaching the great wall: peptidoglycan and microbial interactions. In *Nat Rev Microbiol*, England, 2006; Vol. 4, pp 710-6.
10. Demchick, P.; Koch, A. L., The permeability of the wall fabric of Escherichia coli and Bacillus subtilis. *J Bacteriol* **1996,** *178* (3), 768-73.
11. Dijkstra, A. J.; Keck, W., Peptidoglycan as a barrier to transenvelope transport. *J Bacteriol* **1996,** *178* (19), 5555-62.
12. Scherrer, R.; Gerhardt, P., Molecular sieving by the Bacillus megaterium cell wall and protoplast. *J Bacteriol* **1971,** *107* (3), 718-35.

13. Berends, E. T.; Dekkers, J. F.; Nijland, R.; Kuipers, A.; Soppe, J. A.; van Strijp, J. A.; Rooijakkers, S. H., Distinct localization of the complement C5b-9 complex on Gram-positive bacteria. *Cell Microbiol* **2013,** *15* (12), 1955-68.

14. Lambert, P. A., Cellular impermeability and uptake of biocides and antibiotics in Gram-positive bacteria and mycobacteria. *J Appl Microbiol* **2002,** *92 Suppl*, 46s-54s.

15. Arthur, M.; Courvalin, P., Genetics and mechanisms of glycopeptide resistance in enterococci. *Antimicrob Agents Chemother* **1993,** *37* (8), 1563-71.

16. Bugg, T. D.; Wright, G. D.; Dutka-Malen, S.; Arthur, M.; Courvalin, P.; Walsh, C. T., Molecular basis for vancomycin resistance in Enterococcus faecium BM4147: biosynthesis of a depsipeptide peptidoglycan precursor by vancomycin resistance proteins VanH and VanA. *Biochemistry* **1991,** *30* (43), 10408-15.

17. Pereira, P. M.; Filipe, S. R.; Tomasz, A.; Pinho, M. G., Fluorescence ratio imaging microscopy shows decreased access of vancomycin to cell wall synthetic sites in vancomycin-resistant Staphylococcus aureus. *Antimicrob Agents Chemother* **2007,** *51* (10), 3627-33.

18. Bush, K., Antimicrobial agents targeting bacterial cell walls and cell membranes. *Rev Sci Tech* **2012,** *31* (1), 43-56.

19. de Kruijff, B.; van Dam, V.; Breukink, E., Lipid II: a central component in bacterial cell wall synthesis and a target for antibiotics. *Prostaglandins Leukot Essent Fatty Acids* **2008,** *79* (3-5), 117-21.

20. Asong, J.; Wolfert, M. A.; Maiti, K. K.; Miller, D.; Boons, G. J., Binding and Cellular Activation Studies Reveal That Toll-like Receptor 2 Can Differentially Recognize Peptidoglycan from Gram-positive and Gram-negative Bacteria. *J Biol Chem* **2009,** *284* (13), 8643-53.

21. Fuda, C.; Hesek, D.; Lee, M.; Morio, K.; Nowak, T.; Mobashery, S., Activation for catalysis of penicillin-binding protein 2a from methicillin-resistant Staphylococcus aureus by bacterial cell wall. *J Am Chem Soc* **2005,** *127* (7), 2056-7.

22. Guan, R.; Roychowdhury, A.; Ember, B.; Kumar, S.; Boons, G. J.; Mariuzza, R. A., Structural basis for peptidoglycan binding by peptidoglycan recognition proteins. *Proc Natl Acad Sci U S A* **2004,** *101* (49), 17168-73.

23. Grimes, C. L.; Ariyananda Lde, Z.; Melnyk, J. E.; O'Shea, E. K., The innate immune protein Nod2 binds directly to MDP, a bacterial cell wall fragment. *J Am Chem Soc* **2012,** *134* (33), 13535-7.

24. Ngadjeua, F.; Braud, E.; Saidjalolov, S.; Iannazzo, L.; Schnappinger, D.; Ehrt, S.; Hugonnet, J. E.; Mengin-Lecreulx, D.; Patin, D.; Ethève-Quelquejeu, M.; Fonvielle, M.; Arthur, M., Critical Impact of Peptidoglycan Precursor Amidation on the Activity of l,d-Transpeptidases from Enterococcus faecium and Mycobacterium tuberculosis. *Chemistry* **2018,** *24* (22), 5743-5747.

25. Apostolos, A. J.; Pidgeon, S. E.; Pires, M. M., Remodeling of Cross-bridges Controls Peptidoglycan Cross-linking Levels in Bacterial Cell Walls. *ACS Chemical Biology* **2020,** *15* (5), 1261-1267.

26. Pidgeon, S. E.; Apostolos, A. J.; Nelson, J. M.; Shaku, M.; Rimal, B.; Islam, M. N.; Crick, D. C.; Kim, S. J.; Pavelka, M. S.; Kana, B. D.; Pires, M. M., L,D-Transpeptidase Specific Probe Reveals Spatial Activity of Peptidoglycan Cross-Linking. *ACS Chemical Biology* **2019,** *14* (10), 2185-2196.

27. Desmarais, S. M.; Tropini, C.; Miguel, A.; Cava, F.; Monds, R. D.; de Pedro, M. A.; Huang, K. C., High-throughput, Highly Sensitive Analyses of Bacterial Morphogenesis Using Ultra Performance Liquid Chromatography. *J Biol Chem* **2015,** *290* (52), 31090-100.

28. Mesnage, S.; Dellarole, M.; Baxter, N. J.; Rouget, J. B.; Dimitrov, J. D.; Wang, N.; Fujimoto, Y.; Hounslow, A. M.; Lacroix-Desmazes, S.; Fukase, K.; Foster, S. J.; Williamson, M. P., Molecular basis for bacterial peptidoglycan recognition by LysM domains. *Nat Commun* **2014,** *5*, 4269.

29. Desmarais, S. M.; De Pedro, M. A.; Cava, F.; Huang, K. C., Peptidoglycan at its peaks: how chromatographic analyses can reveal bacterial cell wall structure and assembly. *Mol Microbiol* **2013,** *89* (1), 1-13.

30. Lee, T. K.; Meng, K.; Shi, H.; Huang, K. C., Single-molecule imaging reveals modulation of cell wall synthesis dynamics in live bacterial cells. *Nat Commun* **2016,** *7*, 13170.

31. Sharif, S.; Singh, M.; Kim, S. J.; Schaefer, J., Staphylococcus aureus peptidoglycan tertiary structure from carbon-13 spin diffusion. *J Am Chem Soc* **2009,** *131* (20), 7023-30.

32. Yahashiri, A.; Jorgenson, M. A.; Weiss, D. S., Bacterial SPOR domains are recruited to septal peptidoglycan by binding to glycan strands that lack stem peptides. *Proc Natl Acad Sci U S A* **2015,** *112* (36), 11347-52.

33. Baik, J. E.; Jang, Y. O.; Kang, S. S.; Cho, K.; Yun, C. H.; Han, S. H., Differential profiles of gastrointestinal proteins interacting with peptidoglycans from Lactobacillus plantarum and Staphylococcus aureus. *Mol Immunol* **2015,** *65* (1), 77-85.

34. Koch, A. L., The exoskeleton of bacterial cells (the sacculus): still a highly attractive target for antibacterial agents that will last for a long time. *Crit Rev Microbiol* **2000,** *26* (1), 1-35.

35. Fura, J. M.; Kearns, D.; Pires, M. M., D-Amino Acid Probes for Penicillin Binding Protein-based Bacterial Surface Labeling. *J Biol Chem* **2015,** *290* (51), 30540-50.

36. Fura, J. M.; Pires, M. M., D-amino carboxamide-based recruitment of dinitrophenol antibodies to bacterial surfaces via peptidoglycan remodeling. *Biopolymers* **2015,** *104* (4), 351-9.

37. Pidgeon, S. E.; Fura, J. M.; Leon, W.; Birabaharan, M.; Vezenov, D.; Pires, M. M., Metabolic Profiling of Bacteria by Unnatural C-terminated D-Amino Acids. *Angew Chem Int Ed Engl* **2015,** *54* (21), 6158-62.

38. Pidgeon, S. E.; Pires, M. M., Cell Wall Remodeling of Staphylococcus aureus in Live Caenorhabditis elegans. *Bioconjugate Chemistry* **2017,** *28* (9), 2310-2315.

39. Sarkar, S.; Libby, E. A.; Pidgeon, S. E.; Dworkin, J.; Pires, M. M., In Vivo Probe of Lipid II-Interacting Proteins. *Angew Chem Int Ed Engl* **2016,** *55* (29), 8401-4.

40. Kuru, E.; Hughes, H. V.; Brown, P. J.; Hall, E.; Tekkam, S.; Cava, F.; de Pedro, M. A.; Brun, Y. V.; VanNieuwenhze, M. S., In Situ probing of newly synthesized peptidoglycan in live bacteria with fluorescent D-amino acids. *Angew Chem Int Ed Engl* **2012,** *51* (50), 12519-23.

41. Kuru, E.; Tekkam, S.; Hall, E.; Brun, Y. V.; Van Nieuwenhze, M. S., Synthesis of fluorescent D-amino acids and their use for probing peptidoglycan synthesis and bacterial growth in situ. *Nat Protoc* **2015,** *10* (1), 33-52.

42. Siegrist, M. S.; Whiteside, S.; Jewett, J. C.; Aditham, A.; Cava, F.; Bertozzi, C. R., (D)-Amino acid chemical reporters reveal peptidoglycan dynamics of an intracellular pathogen. *ACS Chem Biol* **2013,** *8* (3), 500-5.

43. Siegrist, M. S.; Swarts, B. M.; Fox, D. M.; Lim, S. A.; Bertozzi, C. R., Illumination of growth, division and secretion by metabolic labeling of the bacterial cell surface. *FEMS Microbiol Rev* **2015,** *39* (2), 184-202.

44. Lebar, M. D.; May, J. M.; Meeske, A. J.; Leiman, S. A.; Lupoli, T. J.; Tsukamoto, H.; Losick, R.; Rudner, D. Z.; Walker, S.; Kahne, D., Reconstitution of Peptidoglycan Cross-Linking Leads to Improved Fluorescent Probes of Cell Wall Synthesis. *Journal of the American Chemical Society* **2014,** *136* (31), 10874-10877.

45. Lupoli, T. J.; Tsukamoto, H.; Doud, E. H.; Wang, T.-S. A.; Walker, S.; Kahne, D., Transpeptidase-Mediated Incorporation of d-Amino Acids into Bacterial Peptidoglycan. *Journal of the American Chemical Society* **2011,** *133* (28), 10748-10751.

46. Fura, J. M.; Sabulski, M. J.; Pires, M. M., D-amino acid mediated recruitment of endogenous antibodies to bacterial surfaces. *ACS Chem Biol* **2014,** *9* (7), 1480-9.

47. Lam, H.; Oh, D.-C.; Cava, F.; Takacs Constantin, N.; Clardy, J.; de Pedro Miguel, A.; Waldor Matthew, K., D-Amino Acids Govern Stationary Phase Cell Wall Remodeling in Bacteria. *Science* **2009,** *325* (5947), 1552-1555.

48. Cava, F.; Lam, H.; de Pedro, M. A.; Waldor, M. K., Emerging knowledge of regulatory roles of D-amino acids in bacteria. *Cell Mol Life Sci* **2011,** *68* (5), 817-31.

49. Bera, A.; Herbert, S.; Jakob, A.; Vollmer, W.; Götz, F., Why are pathogenic staphylococci so lysozyme resistant? The peptidoglycan O-acetyltransferase OatA is the major determinant for lysozyme resistance of Staphylococcus aureus. *Mol Microbiol* **2005,** *55* (3), 778-87.

50. Baskin, J. M.; Prescher, J. A.; Laughlin, S. T.; Agard, N. J.; Chang, P. V.; Miller, I. A.; Lo, A.; Codelli, J. A.; Bertozzi, C. R., Copper-free click chemistry for dynamic in vivo imaging. *Proc Natl Acad Sci U S A* **2007,** *104* (43), 16793-7.

51. Jewett, J. C.; Sletten, E. M.; Bertozzi, C. R., Rapid Cu-Free Click Chemistry with Readily Synthesized Biarylazacyclooctynones. *Journal of the American Chemical Society* **2010,** *132* (11), 3688-3690.

52. Atilano, M. L.; Pereira, P. M.; Yates, J.; Reed, P.; Veiga, H.; Pinho, M. G.; Filipe, S. R., Teichoic acids are temporal and spatial regulators of peptidoglycan cross-linking in Staphylococcus aureus. *Proc Natl Acad Sci U S A* **2010,** *107* (44), 18991-6.

53. Xia, G.; Kohler, T.; Peschel, A., The wall teichoic acid and lipoteichoic acid polymers of Staphylococcus aureus. *Int J Med Microbiol* **2010,** *300* (2-3), 148-54.

54. Swoboda, J. G.; Campbell, J.; Meredith, T. C.; Walker, S., Wall teichoic acid function, biosynthesis, and inhibition. *Chembiochem* **2010,** *11* (1), 35-45.

55. Santa Maria, J. P., Jr.; Sadaka, A.; Moussa, S. H.; Brown, S.; Zhang, Y. J.; Rubin, E. J.; Gilmore, M. S.; Walker, S., Compound-gene interaction mapping reveals distinct roles for Staphylococcus aureus teichoic acids. *Proc Natl Acad Sci U S A* **2014,** *111* (34), 12510-5.

56. DeDent, A. C.; McAdow, M.; Schneewind, O., Distribution of protein A on the surface of Staphylococcus aureus. *J Bacteriol* **2007,** *189* (12), 4473-84.

57. Popham, D. L.; Gilmore, M. E.; Setlow, P., Roles of low-molecular-weight penicillin-binding proteins in Bacillus subtilis spore peptidoglycan synthesis and spore properties. *J Bacteriol* **1999,** *181* (1), 126-32.

58. Arthur, M.; Molinas, C.; Courvalin, P., The VanS-VanR two-component regulatory system controls synthesis of depsipeptide peptidoglycan precursors in Enterococcus faecium BM4147. *J Bacteriol* **1992,** *174* (8), 2582-91.

59. Koteva, K.; Hong, H. J.; Wang, X. D.; Nazi, I.; Hughes, D.; Naldrett, M. J.; Buttner, M. J.; Wright, G. D., A vancomycin photoprobe identifies the histidine kinase VanSsc as a vancomycin receptor. *Nat Chem Biol* **2010,** *6* (5), 327-9.

60. Maresso, A. W.; Schneewind, O., Sortase as a target of anti-infective therapy. *Pharmacol Rev* **2008,** *60* (1), 128-41.

61. Nelson, J. W.; Chamessian, A. G.; McEnaney, P. J.; Murelli, R. P.; Kazmierczak, B. I.; Spiegel, D. A., A biosynthetic strategy for re-engineering the Staphylococcus aureus cell wall with non-native small molecules. *ACS Chem Biol* **2010,** *5* (12), 1147-55.

62. Ton-That, H.; Schneewind, O., Anchor structure of staphylococcal surface proteins. IV. Inhibitors of the cell wall sorting reaction. *J Biol Chem* **1999,** *274* (34), 24316-20.

63. Szafran, M. J.; Kołodziej, M.; Skut, P.; Medapi, B.; Domagała, A.; Trojanowski, D.; Zakrzewska-Czerwińska, J.; Sriram, D.; Jakimowicz, D., Amsacrine Derivatives

Selectively Inhibit Mycobacterial Topoisomerase I (TopA), Impair M. smegmatis Growth and Disturb Chromosome Replication. *Front Microbiol* **2018,** *9*, 1592.

64. Pasquina, L.; Santa Maria, J. P., Jr.; McKay Wood, B.; Moussa, S. H.; Matano, L. M.; Santiago, M.; Martin, S. E.; Lee, W.; Meredith, T. C.; Walker, S., A synthetic lethal approach for compound and target identification in Staphylococcus aureus. *Nat Chem Biol* **2016,** *12* (1), 40-5.

Chapter 7 Non-invasive Fluorescence Imaging of Gut Commensal Bacteria in Mice

Apostolos, A.J., Chordia, M.D., Kolli, S., Rutkowski, M., Pires, M.M.

7.1 *Abstract*

In mammals, gut commensal microbiota interact extensively with the host and those interactions can be dysregulated in diseased states. The development of methods to monitor gut microbiota can lead to improved foundational understanding of the biological events underpinning these interactions. The current standard for non-invasive monitoring of gut bacteria entails classification by 16S rRNA sequencing from fecal samples. This method has many advantages but also has serious limitations. In recent years, several imaging techniques have been widely adopted that afford non-invasive assessment of animal subjects – most notably in cancer biology; however, these technical gains have not translated to the imaging of gut bacterial communities. Herein, we describe a method to non-invasively image commensal bacteria based on the specific metabolic labeling of bacterial cell walls to illuminate the gut bacteria of mice. This tagging strategy may enable the analysis of cell wall turnover, which has implications for bacterial cellular growth and division, in a live animal.

7.2 *Introduction*

Animal imaging is a powerful technique that is widely utilized to diagnose, measure, and track biological processes. Yet, to date, there are no existing standard techniques to image gut bacteria in live animals. There is a critical need for such methods as trillions of bacteria reside within the gastrointestinal (GI) tract of humans.[1, 2] The importance of the gut community to the host is evidenced by the wide range of pathologies linked to microbiota disruptions. These range from immune dysfunctions such as allergies and numerous autoimmune conditions to endocrine system disorders such as obesity and diabetes.[3] In the case of severe disruptions to the gut bacterial communities (e.g., colitis

caused by Clostridium difficile), it is more straight forward to establish a clear connection and causational link.[4, 5] But, more often, disruptions to gut commensals are subtle and chronic, requiring a range of techniques to adequately describe them.

The current state-of-the-art, non-invasive technique used to monitor gut bacteria is classification by 16S rRNA sequencing from fecal samples.[6] This method has advantages (relatively high convenience, compositional resolution, and prolonged analysis over time) but it also has serious limitations (time gap between collection and introduction of variable, bacterial composition of the gut may not be represented in the fecal sample, and lack of spatial resolution). Alternatively, non-invasive imaging could report on dynamic responses to potential therapeutics or other biological interventions in real-time. Surprisingly, live animal imaging of gut bacterial communities remains underdeveloped despite the growing evidence that gut bacteria play central roles in human health and disease. To directly address this technical gap, we describe a novel, non-invasive imaging modality based on the ability of bacteria to metabolically incorporate cell wall analogs that are modified with near infrared (NIR) fluorophores to illuminate gut bacteria in live mice (**Figure 7.1**).

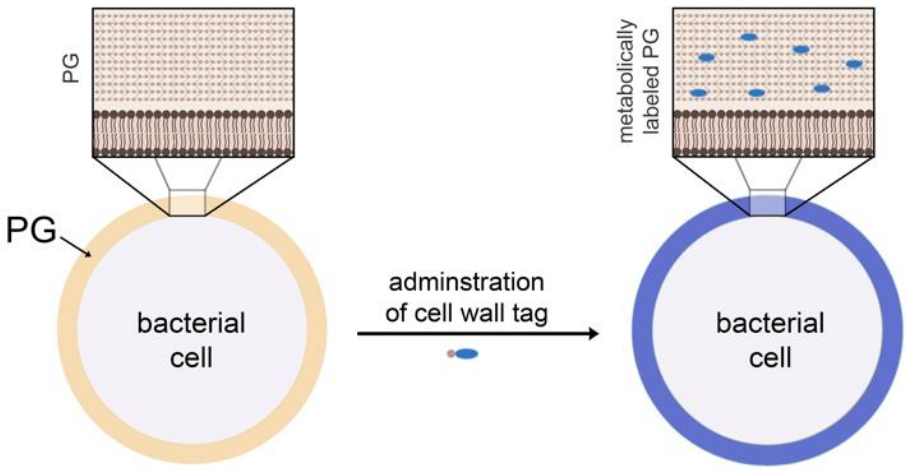

Figure 7.1 *Schematic representation of the installation of fluorescent tags within the cell wall of bacteria.*

Nearly all bacteria, including those residing in the gut of humans, are protected by a shield-like structure called the bacterial cell wall.[7, 8] The unique chemical composition of the bacterial cell wall makes it an ideal target for designing imaging agents with high specificity, as compared to mammalian cells, because humans do not have an equivalent biomacromolecule. A principal component of the cell wall is peptidoglycan (PG), a polymer composed of repetitive disaccharide units (*N*-acetylglucosamine and *N*-acetylmuramic acid) with short peptides (called stem peptides) linked to the *N*-acetylmuramic acid (**Figure 7.2A**). One of the unique structural characteristics of PG is the inclusion of D-amino acids in the stem peptide.[7, 9] Additionally, it has been found that bacteria grown in culture can swap exogenous D-amino acids from the medium into their expanding PG scaffold during cellular growth *via* surface bound transpeptidases (**Figure 7.2A**).[10-20]

We posited that gut bacteria imaging can be achieved by oral administration of D-amino acid surface tags to enable the selective installation of NIR fluorophores. In 2017, Kasper et al. (and since others[21-23]) used a D-amino acid conjugated to a visible range fluorophore to label gut bacteria of mice. These seminal results demonstrated that gut bacteria can also be remodeled with single D-amino acid probes; however, these visible-range fluorophores cannot be used to image live animals.[24] Also in 2017, our laboratory independently demonstrated *in vivo* labeling of bacteria in the gut of *Caenorhabditis elegans* (*C. elegans*)[25] using a 2-step strategy mediated by an inverse electron demand Diels-Alder (IED-DA) reaction.[11, 26, 27] IED-DA reactants include *trans*-cyclooctene (TCO) and tetrazine moieties, which rapidly react to form a stable covalent bond (**Figure 7.2B**).[28] Critically, the biocompatibility of the tetrazine/TCO handles is highlighted by the first successful completion of a human clinical trial in which doxorubicin-TCO was periodically administered to selectively release drugs from a tetrazine-modified polymer implanted within tumor masses.[29] Herein, we showed that tetrazine-displaying D-amino acids tagged the surface of bacteria in *C. elegans* and after treatment with a *trans*-cyclooctene (TCO)-linked Cy5 fluorophore, bacterial cells were selectively labeled with the fluorophore.

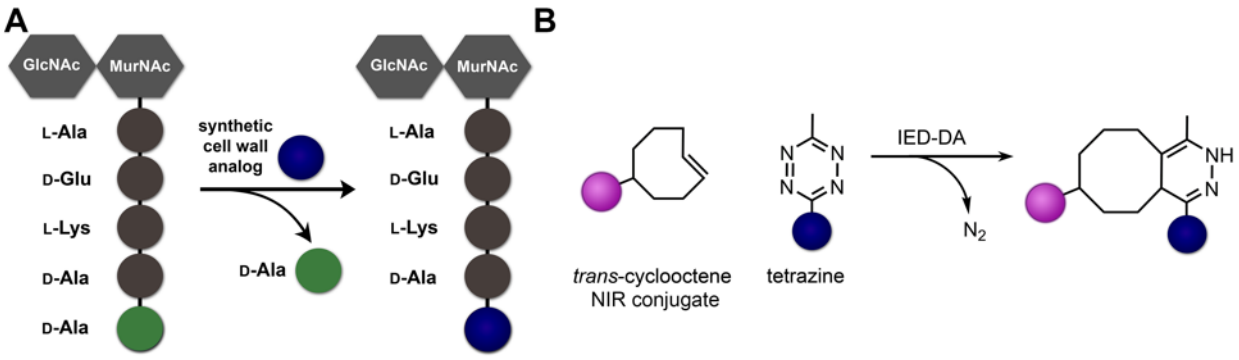

Figure 7.2 *(A) Schematic representation of an example of a PG building block in which an exogenous D-amino acid can be exchanged with D-alanine within the PG of live bacteria. (B) Representation of the two reactants and the product of IED-DA reactions.*

7.3 *Results and Discussion*

7.3.1 *In vitro and In vivo Two-Step Labeling with PheZ and TCO-Cy7.5*

Herein, we initially attempted to adopt our earlier findings with *C. elegans*. To this end, we utilized the combination of a tetrazine-modified D-amino acid (**D-PheZ**) and a TCO-linked fluorophore (**Figure 7.3A**). Surface tagging conditions were first analyzed *in vitro* by incubation with the metabolic tag followed by labeling with the reactive fluorophore, which should result in fluorescently modified PG (**Figure 7.3B**). However, when transitioning to *in vivo* studies, a key feature to consider when developing a dosing and imaging schedule is the kinetics of PG biosynthesis and remodeling of gut bacteria. These features are tightly tied to bacterial cell growth, which requires new PG material to be assembled to support *de novo* cellular replication. Recent efforts have started to provide estimates into the doubling rate of gut bacteria in mice.[30, 31] However, these tools have limitations in that they primarily measure relative growth rates and they require the use of non-native genetically modified organisms. As such, the open questions regarding the rate of gut bacteria PG turn-over in situ are yet to be fully elucidated. In the context of our assay, if there is considerably rapid PG biosynthesis (consistent with fast bacterial replication), the expectation would be that the PG probe would be readily incorporated

into the cell wall, as typically observed in a nutrient-rich culture with rapidly dividing bacterial species. To mimic fast-growth kinetics, *Lactobacillus casei* (*L. casei*) were diluted (1:100) and grown through log-phase (**Figure 7.3C**). As expected, and similar to our previous results using other bacterial species, cellular fluorescence levels were high after treatment with TCO-linked Cy5. Cells treated with **L-PheZ** did not show an increase in fluorescence after treatment with TCO-Cy5 as anticipated, for the D-enantiomer of non-canonical amino acids has been shown to be preferentially incorporated in the PG.[10] Conversely, there is the possibility that the majority of bacterial cells in the gut are in a slower-replicating state. To model this metabolic state, **D-PheZ** was added to stationary phase *L. casei* and fluorescence levels were monitored over time (**Figure 7.3D**). A clear increase in cellular fluorescence was observed despite limited cellular growth. It is likely that PG remodeling, rather than PG biosynthesis, would account for this increase in metabolic tagging.

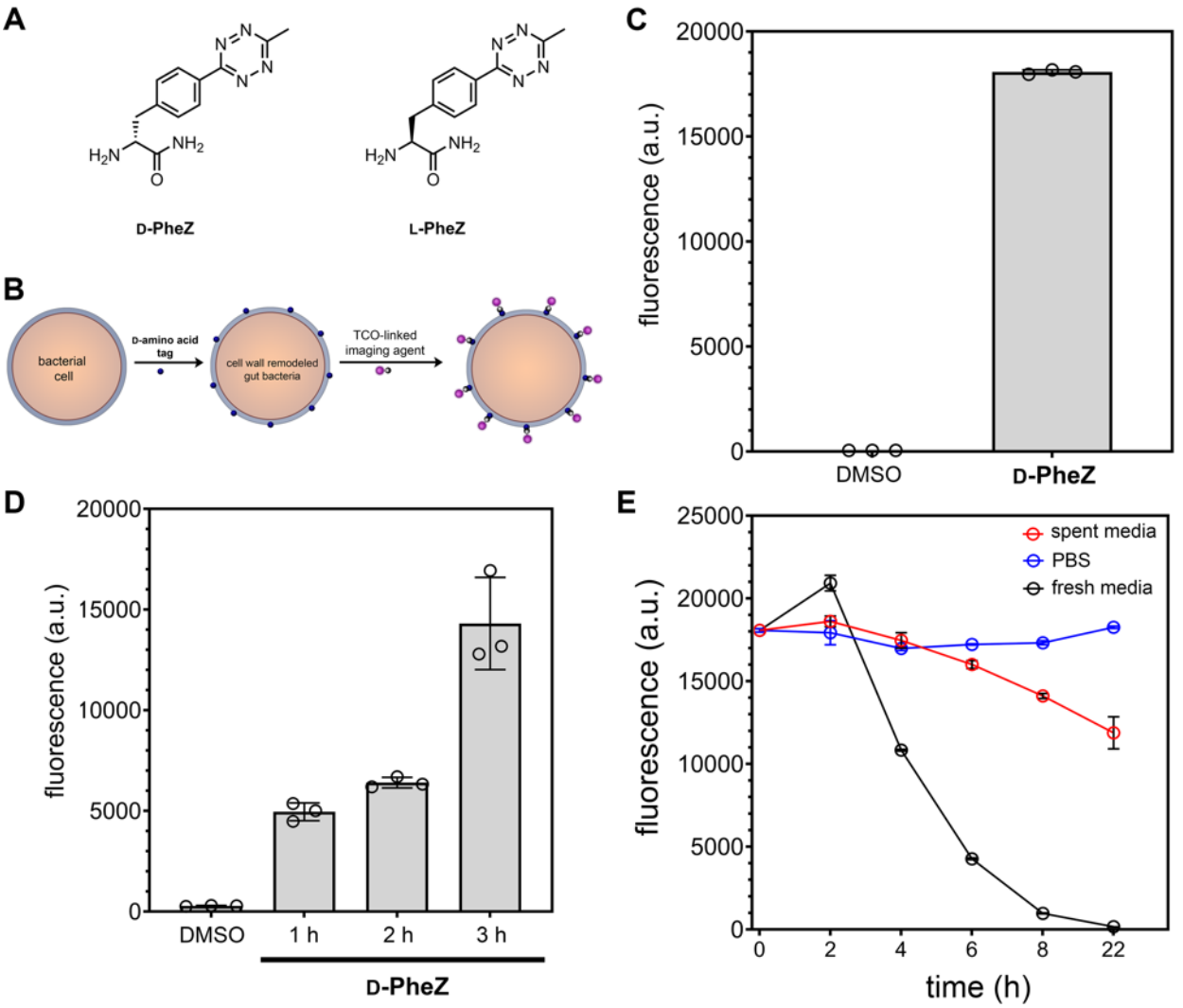

Figure 7.3 *(A) Chemical structures of D-PheZ and L-PheZ. (B) Schematic representation of the steps leading to surface tagging of bacterial cells following metabolic incorporation of D-amino acids. (C) Flow cytometry analysis of L. casei grown overnight with 25 μM TCO-Cy5. (**D**) Flow cytometry analysis of L. casei grown to stationary phase and then treated with 25 μM **D-PheZ**, followed by TCO-Cy5 at different time points. (**E**). Flow cytometry analysis of L. casei treated overnight with 100 μM of **D-PheZ**. Subsequently, cells were incubated with 50 μM of TCO-Cy5 and then resuspended in the conditions noted. Data are represented as mean +/- SD (n = 3). P-values were determined by a two-tailed t-test (* denotes a p-value < 0.05, ** < 0.01, ***<0.001, ns = not significant).*

Additionally, the kinetics of loss of the metabolic tag needed to be considered. To model this, *L. casei* was labeled with the combination of **D-PheZ** and TCO-Cy5 from an overnight culture. Cells were washed, the supernatant was removed and replaced with either PBS or media isolated from *L. casei* during stationary growth (spent media). A third condition involved the back-dilution of cells into fresh media. From these results, it is evident that fresh media stimulates a rapid loss of surface tagging, supposedly due to faster cellular growth and PG remodeling kinetics, whereas media promoting slower kinetics demonstrated considerably less of a decrease in cellular fluorescence. (**Figure 3E**). Therefore, we anticipate that loss of cellular tagging could be a proxy for the kinetics of cellular growth and remodeling. While Cy5 can be used to image bacteria in the transparent *C. elegans*, we chose an NIR fluorophore (Cy7.5) to image gut commensal bacteria in mice. *In vitro* labeling of bacteria was performed to establish the suitability of TCO-Cy7.5 in PG tagging. Three species of bacteria were chosen: *Lactobacillus casei* (*L. casei*), *Enterococcus faecalis* (*E. faecalis*), and *Lactobacillus plantarum* (*L. plantarum*). These organisms have previously been found in the gut of humans.[32] Cells were individually subjected to the 2-step surface tagging scheme and analyzed by flow cytometry (**Figure 7.4**). High levels of cellular fluorescence were observed across the three species of bacteria. Background cellular fluorescence levels were low and, similarly, treatment with the dye alone (TCO-Cy7.5) led to minimal cellular fluorescence.

These confirmatory results led us to test a similar bacteria labeling scheme in live mice. For these experiments, mice were first orally gavaged **D-PheZ**, followed by a 2-hour chase period, then administered TCO-Cy7.5. Mice were imaged *via* IVIS 2 hours following the gavaging with the dye (**Figure 7.5**). A measurable difference in fluorescence was observed in mice treated with the **D-PheZ** relative to the stereocontrol **L-PheZ**, a finding that is suggestive of cell wall labeling of gut commensals. Interestingly, it was observed that the labeling half-live was short as evidenced by the decrease in fluorescence signal by 4 and 22 hours after the final dosing period. Together, these results establish that D-amino acids can potentially be applied to illuminate the gut commensal community of live animals.

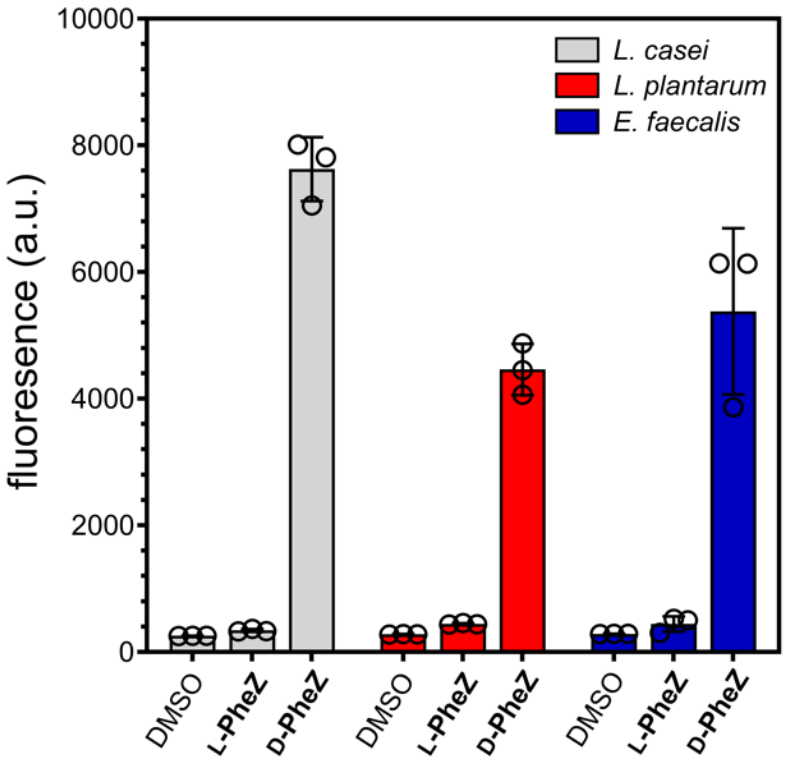

Figure 7.4 *In vitro labeling of L.casei (gray), L. plantarum (red), and E. faecalis (blue) with L- or D-PheZ, followed by click with TCO-Cy7.5.*

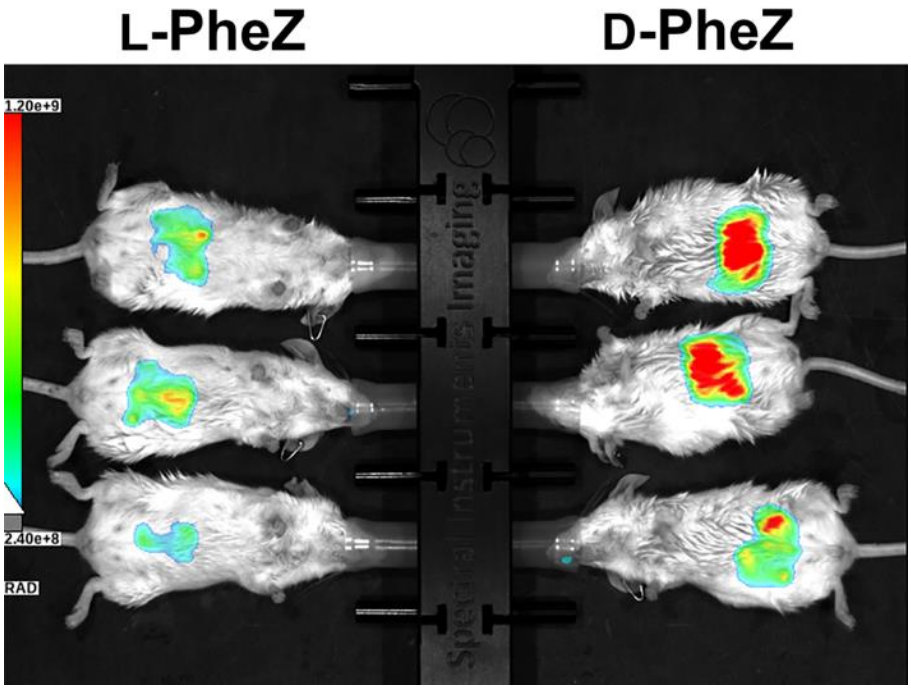

Figure 7.5 *IVIS imaging of female mice orally gavaged with D-PheZ or L-PheZ (5 mM in 200 µL of PBS) twice (1 hour apart). After 4 hours, mice were orally administered TCO-Cy7.5 (1 mM in 100 µL of PBS). Imaging was performed 2 hours after dye administration.*

7.3.2 *In vitro and In vivo One-Step Labeling with D-Tet*

Encouraged by the results of single D-amino acid gut labeling, and as an alternative strategy, we sought to image gut bacteria by using a one-step method in which the fluorophore is connected directly to the metabolic tag, thus reducing some of the potential confounding variables that could be associated with the 2-step IED-DA strategy. One option would be to directly conjugate the fluorophore onto the sidechain of a single D-amino acid (e.g., D-lysine). However, we hypothesized that large sidechains would significantly impede PG incorporation. This hypothesis was premised on our previous systematic study using a library of D-amino acid variants in which the fluorophore was held constant but the chemical structure of the sidechain varied in physical characteristics (size, length, flexibility, charge).[27] Because NIR fluorophores are typically large (and often

highly charged to compensate for the hydrophobicity of the elongated conjugate system), we had anticipated that modification of a NIR fluorophore onto the D-amino acid sidechain would greatly reduce PG incorporation. Instead, we envisioned that gavaging of a synthetic stem peptide analog conjugated to a NIR fluorophore would circumvent this challenge (**Figure 7.6A**). We[33-35], and others[36-38], have shown that treatment of bacterial cells with stem peptide analogs result in their incorporation the PG by PG-related transpeptidases. More specifically, our laboratory has found that the *N*-terminus of a tetra- or penta- stem peptide analog demonstrates much greater tolerability to large chemical modifications, presumably due to a greater separation from the recognition elements of the transpeptidase active site.

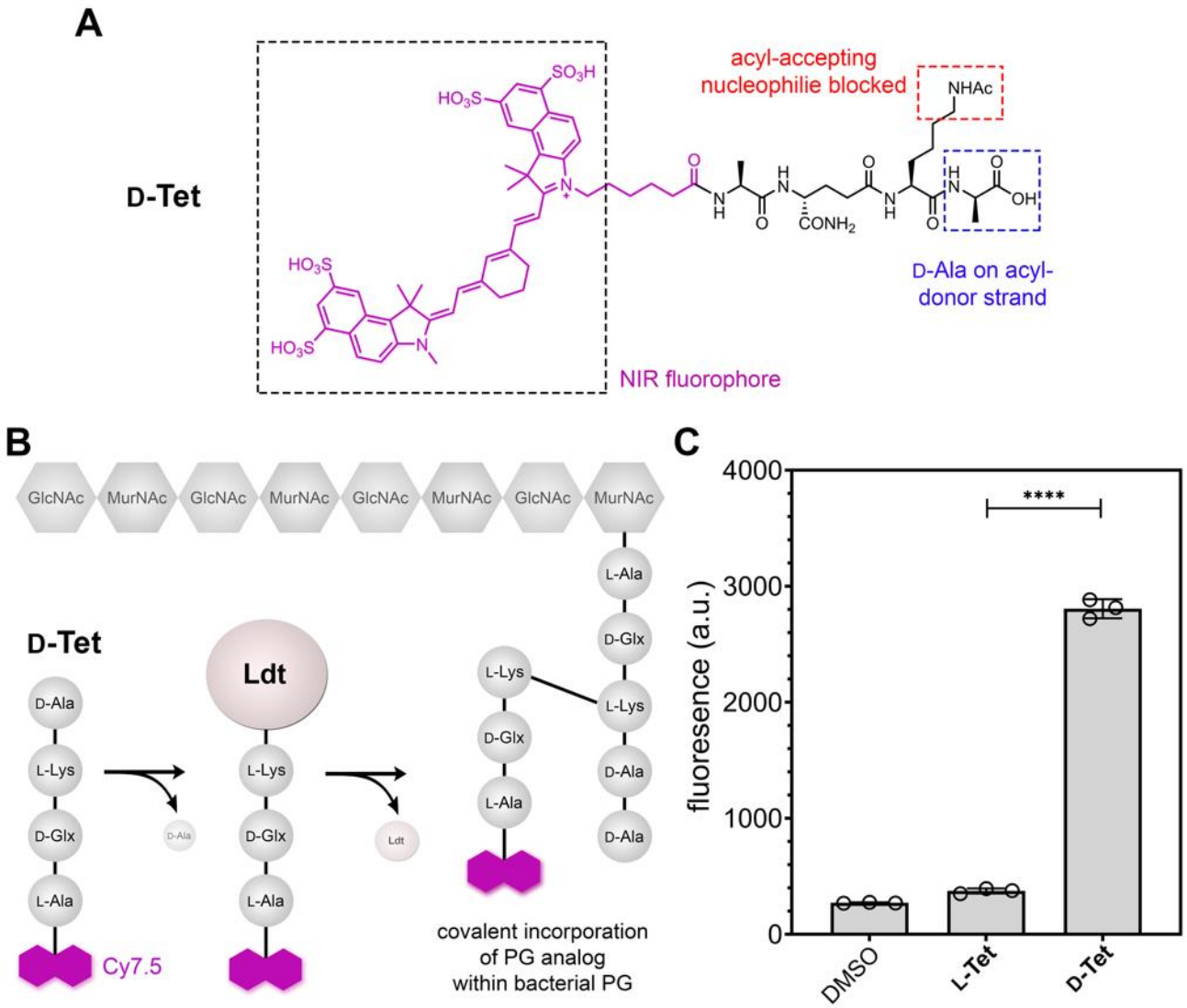

Figure 7.6 *(A) Chemical structure of D-Tet and description of the three primary design features. (B) Schematic representation of the mode of incorporation of D-Tet within existing PG in live bacteria. The tetrapeptide is expected to be processed by transpeptidases by the removal of the terminal D-Ala, which yields a thioester intermediate in the active site of Ldts. Subsequent capture by a nearby nucleophile leads to the formation of a stable covalent bond between the PG and the imaging probe. (**C**) L. casei treated overnight with 100 μM of L- or D-Tet and subsequently analyzed by flow cytometry. Data are represented as mean +/- SD (n = 3). P-values were determined by a two-tailed t-test (* denotes a p-value < 0.05, ** < 0.01, ***<0.001, ns = not significant).*

Synthetic stem peptide analogs get incorporated within the growing PG scaffold of bacteria via crosslinking by transpeptidases into the scaffold. We previously showed that the use of a tetrapeptide guides the incorporation towards one class of crosslinking transpeptidases, namely L,D-transpeptidases (Ldts).[41] In the case of a tetrapeptide analog that harbors a lysine in the third position, the tag could potentially act as an acyl-donor strand (by removal of the terminal 4th position D-alanine) or as an acyl-acceptor strand (by nucleophilic attack within the 3rd position ε-amino group on lysine). As before, incorporation of the tetrapeptide tag (**D-Tet**) was first assessed *in vitro* (**Figure 7.6C**). As expected, bacterial cells treated with **D-Tet** displayed notably higher cellular fluorescence relative to untreated cells and cells treated with the diastereomer **L-Tet,** in which the stereochemistry of the *C*-terminal alanine is inversed.

With these results, our next target was to evaluate the tetra-peptide probes *in vivo*. Mice were orally gavaged either **D-Tet** or **L-Tet** and imaged periodically afterwards using standard IVIS (**Figure 7.7**). As expected, in early time points there was minimal difference between the two treatment groups, of which is reflective of the time for the tagging reagents to passage through the GI tract. After this chase period, there was a measurable difference in the fluorescence levels of mice administered the cell wall tags, which suggests that **D-Tet** can selectively tag and report on the presence of gut bacteria in live mice.

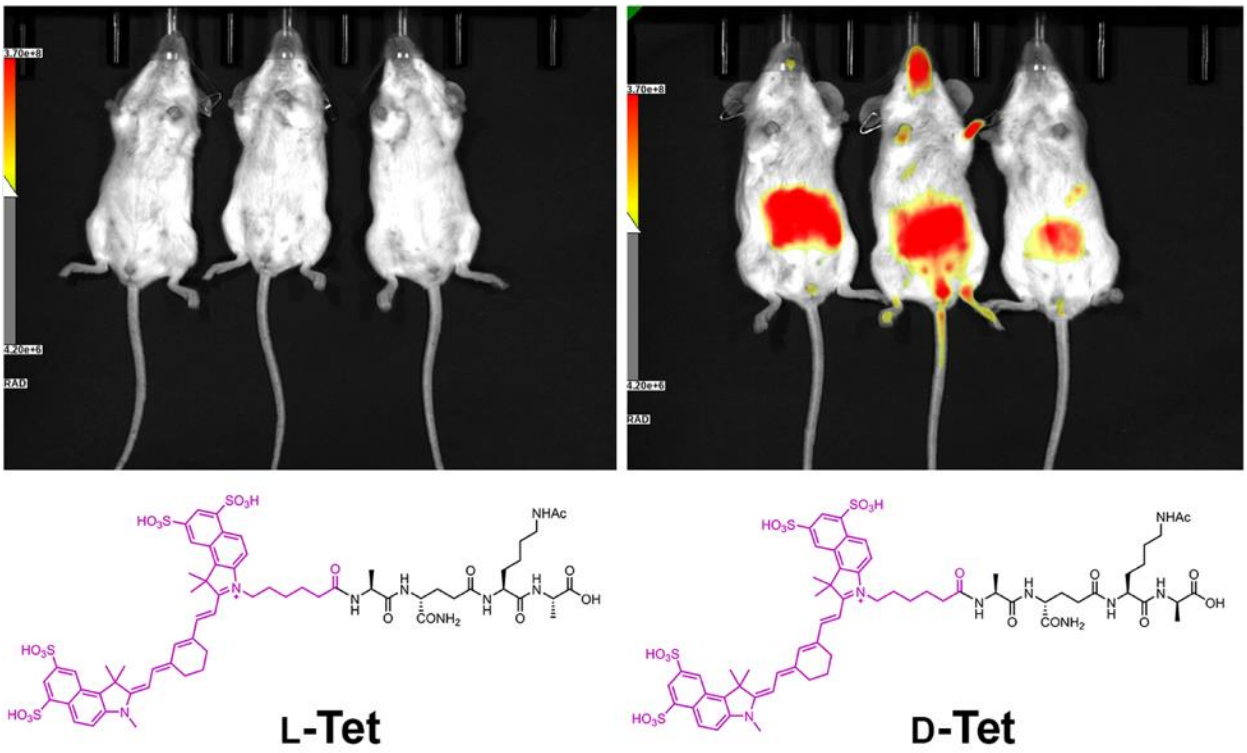

Figure 7.7 *IVIS imaging of female mice orally gavaged 2x, 1 h apart, with a tetrapeptide tag (1 mM in 100 µL of PBS) containing a terminal L-Ala (**L-Tet**), expected not to incorporate in the bacterial PG (left) and with a tetrapeptide tag containing a terminal D-Ala (**D-Tet**), expected to incorporate in the cell walls of bacteria in the mouse gut (right). Mice were imaged 22 hours after the final administration.*

7.4 *Conclusion*

In conclusion, we have demonstrated that cell wall probes can provide a potential route to the non-invasive imaging of gut commensal bacteria in mice. To this end, animals were administered synthetic analogs of PG (either single D-amino acids or tetrapeptide stem mimetics) to induce their metabolic incorporation into the PG scaffold. Single amino acid labeling was based on biorthogonal installation of a NIR fluorophore while the tetrapeptide was directly linked to the NIR fluorophore. Overall, there was discernable differences observed in both routes of tagging; however, the tetrapeptide labeling showed a stronger contrast between the metabolic tag and a stereocontrol. Interestingly, there was a relatively short half-life of the PG label, which may indicate that the cell walls of gut

commensals undergo considerable levels of PG remodeling. In the future, we plan to optimize the labeling conditions to gain greater insight into the dynamics related to cell wall biology in gut bacteria of live mice in response to various stressors (antibiotics, bacteriophage, and probiotics).

7.5 *Materials and Methods*

Materials. All peptide related reagents (resin, coupling reagent, deprotection reagent, amino acids, and cleavage reagents) were purchased from ChemImpex. Sulfo-Cy7.5-NHS was purchase from Lumiprobe. TCO-Amine was purchased from Click Chemistry Tools. Nickel (II) trifluoromethanesulfonate, anhydrous hydrazine, and sodium nitrite were purchased from Sigma Aldrich. Bacterial strains *L. casei* and *L. plantarum* were grown in lactobacillus MRS broth for *in vitro* studies. *E. faecium* 29212 was grown in Brain Heart Infusion (BHI) broth for *in vitro* studies.

In vitro **flow cytometry analysis of bacterial labeling with single amino acid probes.** Media containing 25, 50, or 100 µM of each single amino acid were prepared. Bacterial cells from an overnight culture were added to the medium (1:100 dilution) and allowed to grow overnight at 37°C with shaking at 250 rpm. The bacteria were harvested at 6,000g and washed three times with original culture volume of 1X PBS followed by fixation with 2% formaldehyde in 1X PBS for 30 min at room temperature. The cells were washed once more to remove formaldehyde and then resuspended in 50 µM of Cy5-TCO (Click Chemistry Tools) for 30 min at room temperature with shaking. Cells were washed three times with 1X PBS before analysis with an AttuneNxT (Thermo Fisher) flow cytometer equipped with a 638 nm laser and 670/14 nm bandpass filter. The data were analyzed using the AttuneNxT Software, where populations were gated and no less than 10,000 events per sample were recorded.

In vitro **flow cytometry analysis of bacterial labeling with tetrapeptide probes.** Media containing 100 µM of each probe were prepared. Bacterial cells from an overnight culture were added to the medium (1:100 dilution) and allowed to grow overnight at 37°C with

shaking at 250 rpm. The bacteria were harvested at 6,000g and washed three times with original culture volume of 1X PBS followed by fixation with 2% formaldehyde in 1X PBS for 30 min at room temperature. The cells were washed once more to remove formaldehyde and then analyzed using a Cytoflex S (Beckmann Coulter) flow cytometer equipped with an 808 nm laser and 840/20 nm bandpass filter. The data were analyzed using the CytExpert Software, where populations were gated and no less than 10,000 events per sample were recorded.

***In vivo* gut labeling and imaging of mice with single amino acid probes (two step)**. Female BALB/c mice (age 15-16 weeks) were orally gavaged twice with 200 µL of 5 mM of **D-Tet-NH$_2$** single amino acid, one hour apart. Four hours later, mice were orally gavaged with 100 µL of 1 mM Sulfo-Cy7.5-TCO. Images of live mice were taken at selected time points after the final gavage. To image, mice were anesthetized with vaporized isoflurane (covetrus) by use of an anesthetic machine following protocols implemented by the University of Virginia and Animal Care & Use Committee (ACUC). Images were taken using Spectral Instruments Lago X bioluminescence, fluorescence, and X-ray scanner with the fluorescence excitation set to 745 nm and the emission set to 810 nm. Images were processed using the Spectral Imaging software.

***In vivo* gut labeling and imaging of mice with single amino acid probes (two step).** Female BALB/c mice (age 15-16 weeks) were orally gavaged twice with 200 µL of 5 mM of **D-Tet-NH$_2$** or **D-Tet-OH**, one hour apart. A group of mice was not gavaged with any amino acid probe. Four hours later, mice were orally gavaged with 100 µL of 1 mM Sulfo-Cy7.5-TCO. Images of live mice were taken at selected time points after the final gavage. To image, mice were anesthetized and imaged with the parameters previously described.

***In vivo* gut labeling and imaging of mice with tetrapeptide probes (one step)**. Female BALB/c mice (age 15-16 weeks) were orally gavaged with 100 µL of 1 mM of each probe twice, one hour apart. Images of live mice were taken at selected time points starting two hours after the final gavage. To image, mice were anesthetized and imaged with the parameters previously described.

7.6 *References*

1. Sender, R.; Fuchs, S.; Milo, R., Revised Estimates for the Number of Human and Bacteria Cells in the Body. *PLoS Biol* **2016,** *14* (8), e1002533.

2. Fan, Y.; Pedersen, O., Gut microbiota in human metabolic health and disease. *Nat Rev Microbiol* **2021,** *19* (1), 55-71.

3. Shreiner, A. B.; Kao, J. Y.; Young, V. B., The gut microbiome in health and in disease. *Curr Opin Gastroenterol* **2015,** *31* (1), 69-75.

4. Bäumler, A. J.; Sperandio, V., Interactions between the microbiota and pathogenic bacteria in the gut. *Nature* **2016,** *535* (7610), 85-93.

5. Theriot, C. M.; Koenigsknecht, M. J.; Carlson, P. E., Jr.; Hatton, G. E.; Nelson, A. M.; Li, B.; Huffnagle, G. B.; J, Z. L.; Young, V. B., Antibiotic-induced shifts in the mouse gut microbiome and metabolome increase susceptibility to Clostridium difficile infection. *Nat Commun* **2014,** *5*, 3114.

6. Gill, S. R.; Pop, M.; Deboy, R. T.; Eckburg, P. B.; Turnbaugh, P. J.; Samuel, B. S.; Gordon, J. I.; Relman, D. A.; Fraser-Liggett, C. M.; Nelson, K. E., Metagenomic analysis of the human distal gut microbiome. *Science* **2006,** *312* (5778), 1355-9.

7. Vollmer, W.; Blanot, D.; De Pedro, M. A., Peptidoglycan structure and architecture. *FEMS Microbiology Reviews* **2008,** *32* (2), 149-167.

8. Typas, A.; Banzhaf, M.; Gross, C. A.; Vollmer, W., From the regulation of peptidoglycan synthesis to bacterial growth and morphology. *Nat Rev Microbiol* **2011,** *10* (2), 123-136.

9. Silhavy, T. J.; Kahne, D.; Walker, S., The bacterial cell envelope. *Cold Spring Harb Perspect Biol* **2010,** *2* (5), a000414-a000414.

10. Kuru, E.; Hughes, H. V.; Brown, P. J.; Hall, E.; Tekkam, S.; Cava, F.; de Pedro, M. A.; Brun, Y. V.; VanNieuwenhze, M. S., In Situ probing of newly synthesized peptidoglycan in live bacteria with fluorescent D-amino acids. *Angew Chem Int Ed Engl* **2012,** *51* (50), 12519-23.

11. Siegrist, M. S.; Whiteside, S.; Jewett, J. C.; Aditham, A.; Cava, F.; Bertozzi, C. R., d-Amino Acid Chemical Reporters Reveal Peptidoglycan Dynamics of an Intracellular Pathogen. *ACS Chemical Biology* **2013,** *8* (3), 500-505.

12. Bisson-Filho, A. W.; Hsu, Y.-P.; Squyres, G. R.; Kuru, E.; Wu, F.; Jukes, C.; Sun, Y.; Dekker, C.; Holden, S.; VanNieuwenhze, M. S.; Brun, Y. V.; Garner, E. C., Treadmilling by FtsZ filaments drives peptidoglycan synthesis and bacterial cell division. *Science (New York, N.Y.)* **2017,** *355* (6326), 739-743.

13. Pilhofer, M.; Aistleitner, K.; Biboy, J.; Gray, J.; Kuru, E.; Hall, E.; Brun, Y. V.; VanNieuwenhze, M. S.; Vollmer, W.; Horn, M.; Jensen, G. J., Discovery of chlamydial peptidoglycan reveals bacteria with murein sacculi but without FtsZ. *Nature communications* **2013,** *4*, 2856-2856.

14. Fleurie, A.; Lesterlin, C.; Manuse, S.; Zhao, C.; Cluzel, C.; Lavergne, J. P.; Franz-Wachtel, M.; Macek, B.; Combet, C.; Kuru, E.; VanNieuwenhze, M. S.; Brun, Y. V.; Sherratt, D.; Grangeasse, C., MapZ marks the division sites and positions FtsZ rings in Streptococcus pneumoniae. *Nature* **2014,** *516* (7530), 259-262.

15. Liechti, G. W.; Kuru, E.; Hall, E.; Kalinda, A.; Brun, Y. V.; VanNieuwenhze, M.; Maurelli, A. T., A new metabolic cell-wall labelling method reveals peptidoglycan in Chlamydia trachomatis. *Nature* **2014,** *506* (7489), 507-510.

16. Faure, L. M.; Fiche, J. B.; Espinosa, L.; Ducret, A.; Anantharaman, V.; Luciano, J.; Lhospice, S.; Islam, S. T.; Tréguier, J.; Sotes, M.; Kuru, E.; Van Nieuwenhze, M. S.; Brun, Y. V.; Théodoly, O.; Aravind, L.; Nollmann, M.; Mignot, T., The mechanism of force transmission at bacterial focal adhesion complexes. *Nature* **2016,** *539* (7630), 530-535.

17. Qiao, Y.; Lebar, M. D.; Schirner, K.; Schaefer, K.; Tsukamoto, H.; Kahne, D.; Walker, S., Detection of Lipid-Linked Peptidoglycan Precursors by Exploiting an Unexpected Transpeptidase Reaction. *Journal of the American Chemical Society* **2014,** *136* (42), 14678-14681.

18. Lebar, M. D.; May, J. M.; Meeske, A. J.; Leiman, S. A.; Lupoli, T. J.; Tsukamoto, H.; Losick, R.; Rudner, D. Z.; Walker, S.; Kahne, D., Reconstitution of Peptidoglycan Cross-Linking Leads to Improved Fluorescent Probes of Cell Wall Synthesis. *Journal of the American Chemical Society* **2014,** *136* (31), 10874-10877.

19. Shieh, P.; Siegrist, M. S.; Cullen, A. J.; Bertozzi, C. R., Imaging bacterial peptidoglycan with near-infrared fluorogenic azide probes. *Proceedings of the National Academy of Sciences* **2014,** *111* (15), 5456.

20. Ngo, J. T.; Adams, S. R.; Deerinck, T. J.; Boassa, D.; Rodriguez-Rivera, F.; Palida, S. F.; Bertozzi, C. R.; Ellisman, M. H.; Tsien, R. Y., Click-EM for imaging metabolically tagged nonprotein biomolecules. *Nat Chem Biol* **2016,** *12* (6), 459-65.

21. Wang, W.; Lin, L.; Du, Y.; Song, Y.; Peng, X.; Chen, X.; Yang, C. J., Assessing the viability of transplanted gut microbiota by sequential tagging with D-amino acid-based metabolic probes. *Nature Communications* **2019,** *10* (1), 1317.

22. Lin, L.; Song, J.; Du, Y.; Wu, Q.; Gao, J.; Song, Y.; Yang, C.; Wang, W., Quantification of Bacterial Metabolic Activities in the Gut by d-Amino Acid-Based In Vivo Labeling. *Angew Chem Int Ed Engl* **2020,** *59* (29), 11923-11926.

23. Wang, W.; Yang, Q.; Du, Y.; Zhou, X.; Du, X.; Wu, Q.; Lin, L.; Song, Y.; Li, F.; Yang, C.; Tan, W., Metabolic Labeling of Peptidoglycan with NIR-II Dye Enables In Vivo Imaging of Gut Microbiota. *Angew Chem Int Ed Engl* **2020,** *59* (7), 2628-2633.

24. Hudak, J. E.; Alvarez, D.; Skelly, A.; von Andrian, U. H.; Kasper, D. L., Illuminating vital surface molecules of symbionts in health and disease. *Nat Microbiol* **2017,** *2*, 17099-17099.

25. Pidgeon, S. E.; Pires, M. M., Cell Wall Remodeling of Staphylococcus aureus in Live Caenorhabditis elegans. *Bioconjugate Chemistry* **2017,** *28* (9), 2310-2315.

26. Fura, J. M.; Sabulski, M. J.; Pires, M. M., D-amino acid mediated recruitment of endogenous antibodies to bacterial surfaces. *ACS Chem Biol* **2014,** *9* (7), 1480-9.

27. Fura, J. M.; Kearns, D.; Pires, M. M., D-Amino Acid Probes for Penicillin Binding Protein-based Bacterial Surface Labeling. *J Biol Chem* **2015,** *290* (51), 30540-50.

28. Blackman, M. L.; Royzen, M.; Fox, J. M., Tetrazine ligation: fast bioconjugation based on inverse-electron-demand Diels-Alder reactivity. *J Am Chem Soc* **2008,** *130* (41), 13518-9.

29. Wu, K.; Yee, N. A.; Srinivasan, S.; Mahmoodi, A.; Zakharian, M.; Mejia Oneto, J. M.; Royzen, M., Click activated protodrugs against cancer increase the therapeutic potential of chemotherapy through local capture and activation. *Chem Sci* **2021,** *12* (4), 1259-1271.

30. Korem, T.; Zeevi, D.; Suez, J.; Weinberger, A.; Avnit-Sagi, T.; Pompan-Lotan, M.; Matot, E.; Jona, G.; Harmelin, A.; Cohen, N.; Sirota-Madi, A.; Thaiss, C. A.; Pevsner-Fischer, M.; Sorek, R.; Xavier, R.; Elinav, E.; Segal, E., Growth dynamics of

gut microbiota in health and disease inferred from single metagenomic samples. *Science* **2015,** *349* (6252), 1101-1106.

31. Myhrvold, C.; Kotula, J. W.; Hicks, W. M.; Conway, N. J.; Silver, P. A., A distributed cell division counter reveals growth dynamics in the gut microbiota. *Nat Commun* **2015,** *6*, 10039.

32. Structure, function and diversity of the healthy human microbiome. *Nature* **2012,** *486* (7402), 207-14.

33. Pidgeon, S. E.; Apostolos, A. J.; Nelson, J. M.; Shaku, M.; Rimal, B.; Islam, M. N.; Crick, D. C.; Kim, S. J.; Pavelka, M. S.; Kana, B. D.; Pires, M. M., L,D-Transpeptidase Specific Probe Reveals Spatial Activity of Peptidoglycan Cross-Linking. *ACS Chemical Biology* **2019,** *14* (10), 2185-2196.

34. Dalesandro, B. E.; Pires, M. M., Induction of Endogenous Antibody Recruitment to the Surface of the Pathogen Enterococcus faecium. *ACS Infect Dis* **2021,** *7* (5), 1116-1125.

35. Apostolos, A. J.; Pidgeon, S. E.; Pires, M. M., Remodeling of Cross-bridges Controls Peptidoglycan Cross-linking Levels in Bacterial Cell Walls. *ACS Chemical Biology* **2020,** *15* (5), 1261-1267.

36. Ngadjeua, F.; Braud, E.; Saidjalolov, S.; Iannazzo, L.; Schnappinger, D.; Ehrt, S.; Hugonnet, J. E.; Mengin-Lecreulx, D.; Patin, D.; Ethève-Quelquejeu, M.; Fonvielle, M.; Arthur, M., Critical Impact of Peptidoglycan Precursor Amidation on the Activity of l,d-Transpeptidases from Enterococcus faecium and Mycobacterium tuberculosis. *Chemistry* **2018,** *24* (22), 5743-5747.

37. Gautam, S.; Kim, T.; Shoda, T.; Sen, S.; Deep, D.; Luthra, R.; Ferreira, M. T.; Pinho, M. G.; Spiegel, D. A., An Activity-Based Probe for Studying Crosslinking in Live Bacteria. *Angew Chem Int Ed Engl* **2015,** *54* (36), 10492-6.

38. Lin, H.; Lin, L.; Du, Y.; Gao, J.; Yang, C.; Wang, W., Biodistributions of l,d-Transpeptidases in Gut Microbiota Revealed by In Vivo Labeling with Peptidoglycan Analogs. *ACS Chem Biol* **2021,** *16* (7), 1164-1171.

Summary and Future Outlook

The work in this thesis highlights probes that were designed, synthesized, and used to interrogate TP enzyme preferences in live bacterial cells. Chapter 3 described studies that demonstrated the need for the modified lysine crossbridge to tune the PG crosslinking machinery. This was demonstrated in three distinct types of bacterial species, reinforcing the idea that the acyl acceptor modification is required for crosslinking. Based on the probes designed and developed in this work, we described (in Chapters 4 and 5) a similar panel of probes to assay acyl acceptor ability in *m*-DAP containing organisms. Fundamental studies of *m*-DAP containing organisms had been hampered by the lack of facile synthesis routes to obtain *m*-DAP building blocks or other derivatives. We reported on a strategy that made use of the simple and widely available Fmoc-protected L-Cys to build *m*-CYT, which recapitulated key structural features of *m*-DAP. We were able to label live bacterial cells with strictly acyl acceptor probes (tripeptide stem peptide mimics) which showed that TPs accepted *m*-CYT in place of m-DAP. Similarly, we designed a selenolanthionine *m*-DAP mimic within a tripeptide mimetic probe which permitted the use of slightly acidic conditions to generate selenolanthionine from L-selenocysteine and β-Cl-D-Ala to prevent racemization that typically occurs at basic pH with lanthionine synthesis. This probe was tolerated by endogenous PG crosslinking machinery in live cells, as investigated by the use of flow cytometry and confocal microscopy. Importantly, the *m*-SeLAN tripeptide probe specifically suggests proper *m*-DAP mimicry, as it acted as an acyl-acceptor in the PG crosslinking step. We envision that both building blocks (*m*-CYT and *m*-SeLAN) can provide an alternate synthetic route for various *m*-DAP bioisosteres that would allow for further study of *m*-DAP containing organisms. Hopefully these probes can be adapted by others in the field for a more comprehensive study of organisms that contain *m*-DAP in their PG to elucidate their TP machinery preferences to develop a better understanding of potential enzymatic substrates or inhibitors.

To develop an assay platform that allows for the study of interactions between molecules with PG, we described “SaccuFlow” in Chapter 6. This platform makes use of the mechanical strength and native composition of bacterial sacculi to assay

interactions with flow cytometry, which provides a high-throughput methodology. We tagged bacterial sacculi with orthogonal epitopes which led to the demonstration of the accessibility of molecules to the PG scaffold. The versatility of this method was demonstrated by assaying Gram-negative, -positive and mycobacterial species. We used vancomycin to show PG interaction dynamics, and sortase A to demonstrate enzymatic processing PG and to explore potential inhibitors of sortase A using a LOPAC library. This assay platform can be utilized in microbiology studies in the future to assay PG interactions. It would be of interest to adapt this platform to organisms not discussed in our work, as well as to investigate further PG-protein interactions (such as LysM, pattern recognition receptor (PRR) proteins, TP enzymatic processing, and/or a platform to study β-lactam inhibition of specific TPs).

Lastly, we investigated a way to non-invasively image the gut microbiome of a live animal by use of either a single D-amino acid or a NIR-modified stem peptide mimetic probe. This work demonstrated that cell wall probes can provide a potential route to the non-invasive imaging of gut commensal bacteria in mice. Overall, we observed discernable differences in both routes of tagging over the negative control, indicating that the probes described may report on the presence of gut bacteria in a live animal model. In the future, it would be ideal to optimize the labeling conditions to gain greater insight into the dynamics related to cell wall biology in gut bacteria of live mice in response to various stressors. For instance, differences in the read-out of the probe after the introduction of antibiotics or probiotics to the animal could be easily studied by the non-invasive imaging method. Additionally, it would be of interest to gain insight on native gut bacterial PG remodeling and turnover, as not much is currently known regarding this topic.

Together, the work described details the development of chemical reporters to study the substrate preferences of bacterial cell wall enzymes, to report on PG interactions, and to study native gut commensals in live animals.

Appendix

*Note: All chromatograms for HPLC analysis were observed at 220 nm.

A.3 *Synthesis and Characterization of Compounds in Chapter 3*

Scheme S1. Synthesis of TriQK.

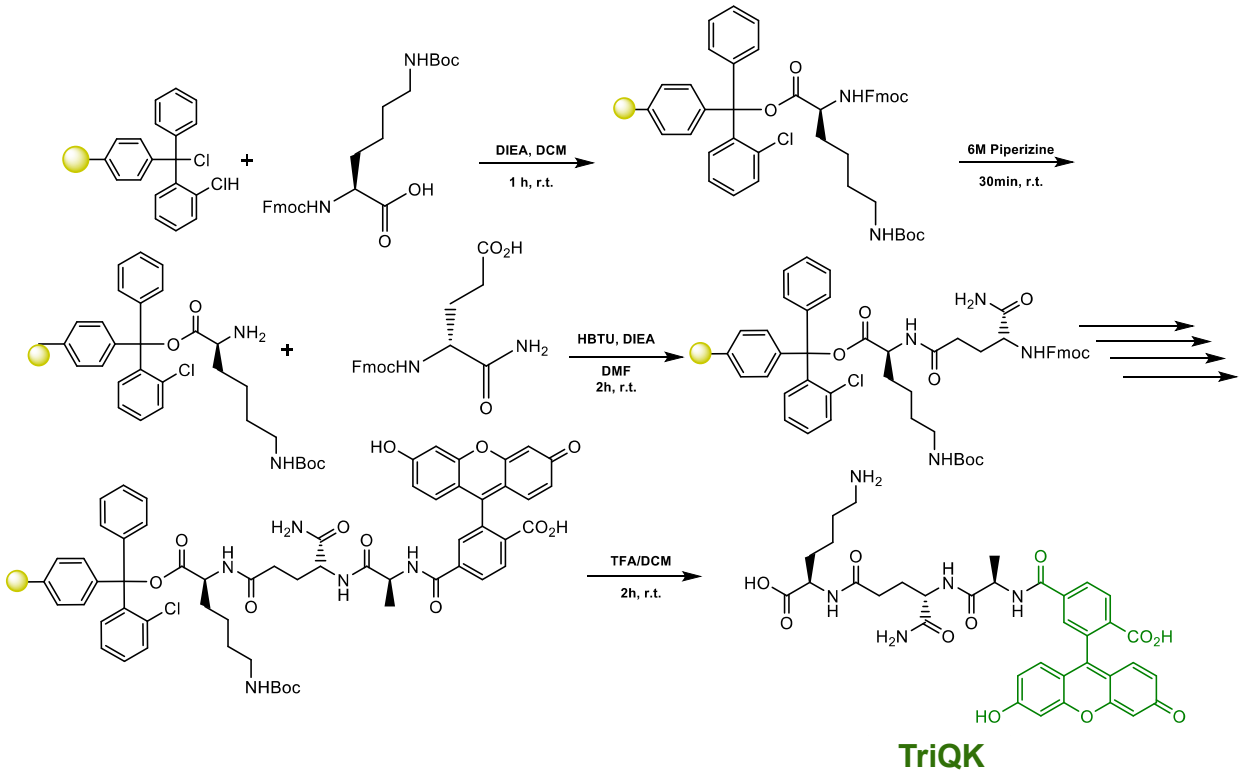

A 25 mL peptide synthesis vessel charged with 2-Chlorotrityl chloride resin (500mg, 0.55mmol) was added Fmoc-L-Lysine(Boc)-OH (1.1 eq, 283 mg, 0.605 mmol) and DIEA (3 eq, 0.286 mL, 1.65 mmol) in dry DCM (15 mL). The resin was agitated for 1 h at ambient temperature and washed with MeOH and DCM (3 x 15 mL each). The Fmoc protecting group was removed with 6 M piperazine/100 mM HOBt in DMF (15 ml) for 30 min at ambient temperature, then washed as before. Fmoc-D-glutamic acid α-amide (3 eq, 607 mg, 1.65 mmol), HBTU (3 eq, 625 mg, 1.65 mmol), and DIEA (6 eq, 0.574 mL, 3.30 mmol) in DMF (15 mL) were added to the reaction flask and agitated for 2 h at ambient temperature. The Fmoc deprotection and coupling procedure was repeated as before using the same equivalencies with Fmoc-L-Alanine-OH. The Fmoc group of L-alanine was deprotected and resin coupled with 5(6)-carboxyfluorescein (2 eq, 413 mg, 1.1

mmol), HBTU (2 eq, 416 mg, 1.1 mmol) and DIEA (6 eq, 0.574 mL, 3.30 mmol) in DMF (15 mL) shaking overnight. The resin was washed as before and added to a solution of TFA/DCM (2:1, 20 mL) with agitation for 2 h at ambient temperature. The resin was filtered and resulting solution concentrated *in vacuo*. The residue was trituated with cold diethyl ether and purified using reverse phase HPLC using H_2O/MeOH to yield **TriQK**. The sample was analyzed for purity using a Shimadzu LC 2020 with a Phenomenex Luna 5µ C18(2) 100Å (30 x 2.00 mm) column; gradient elution with H_2O/CH_3CN.

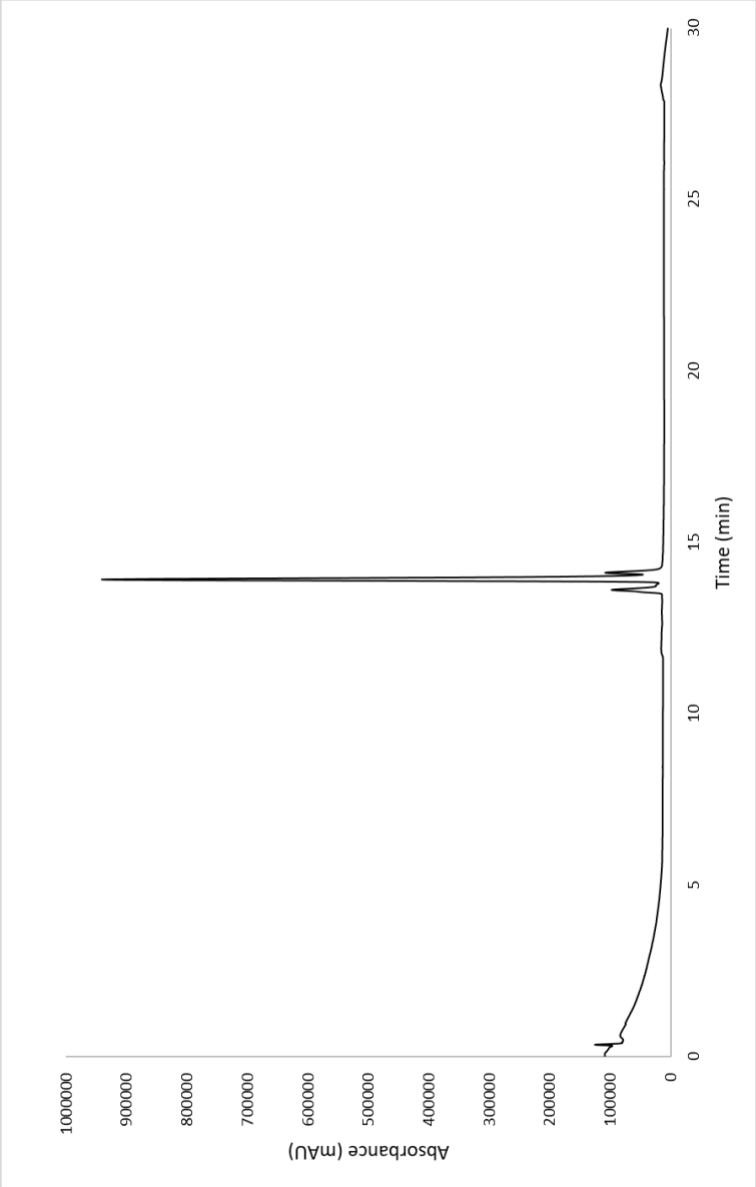

ESI-MS calculated: 703.2490, found: 703.2498

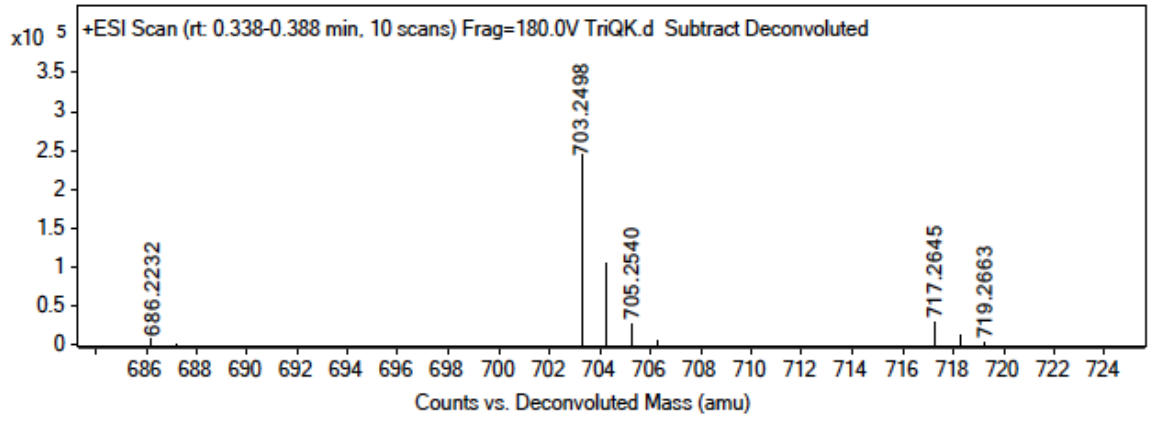

Scheme S2. Synthesis of TriQN.

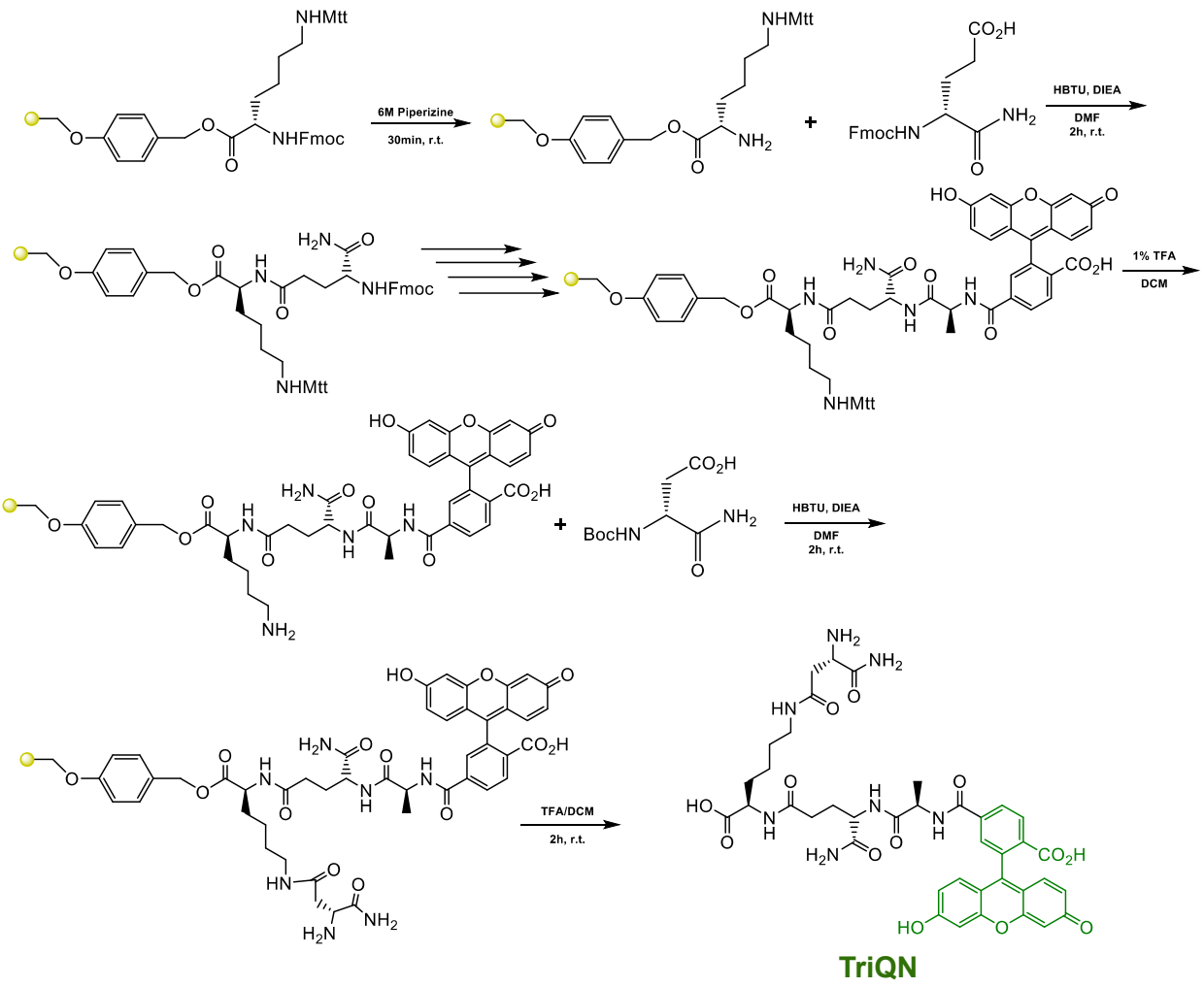

To a 25 mL peptide synthesis vessel charged with Fmoc-Lysine(Mtt)-Wang resin (1.0 g, 0.55mmol). The Fmoc protecting group was removed with 6 M piperazine/100 mM HOBt in DMF (15 ml) for 30 min at ambient temperature, then washed with washed with MeOH and DCM (3 x 15 mL each). Fmoc-D-glutamic acid α-amide (3 eq, 607 mg, 1.65 mmol), HBTU (3 eq, 625 mg, 1.65 mmol), and DIEA (6 eq, 0.574 mL, 3.30 mmol) in DMF (15 mL) were added to the reaction flask and agitated for 2 h at ambient temperature and washed as before. The Fmoc deprotection and coupling procedure was repeated as before using the same equivalencies with Fmoc-L-Alanine-OH. The Fmoc group of L-alanine was deprotected and resin coupled with 5(6)-carboxyfluorescein (2 eq, 413 mg, 1.1 mmol), HBTU (2 eq, 416 mg, 1.1 mmol) and DIEA (6 eq, 0.574 mL, 3.30 mmol) in DMF (15 mL) shaking overnight. The Mtt protecting group was removed by the addition of 1% TFA, 2.5% TIPS, in 10 mL DCM for 15 min, washed and repeated 3 more

times. Boc-D-aspartic acid α-amide (3 eq, 382 mg, 1.65 mmol), HBTU (3 eq, 625 mg, 1.65 mmol), and DIEA (6 eq, 0.574 mL, 3.30 mmol) in DMF (15 mL) were added to the reaction flask and agitated for 2 h at ambient temperature and washed as before. A solution of TFA/DCM (2:1, 20 mL) was added to the resin with agitation for 2 h at ambient temperature. The resin was filtered and resulting solution concentrated *in vacuo*. The residue was trituated with cold diethyl ether and purified using reverse phase HPLC using H_2O/MeOH to yield **TriQN**. The sample was analyzed for purity using a Shimadzu LC 2020 with a Phenomenex Luna 5µ C18(2) 100Å (30 x 2.00 mm) column; gradient elution with H_2O/CH_3CN.

Absorbance (mAU)
140000
120000
100000
80000
60000
40000
20000
0
0
5
10
15
20
25
Time (min)

ESI-MS calculated: 817.2919, found: 817.2942

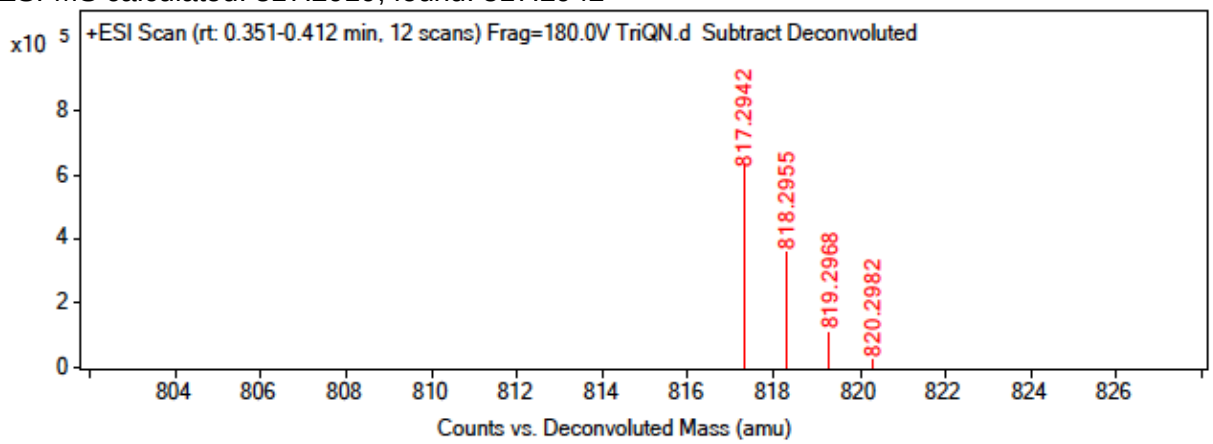

Scheme S3. Synthesis of TriQD.

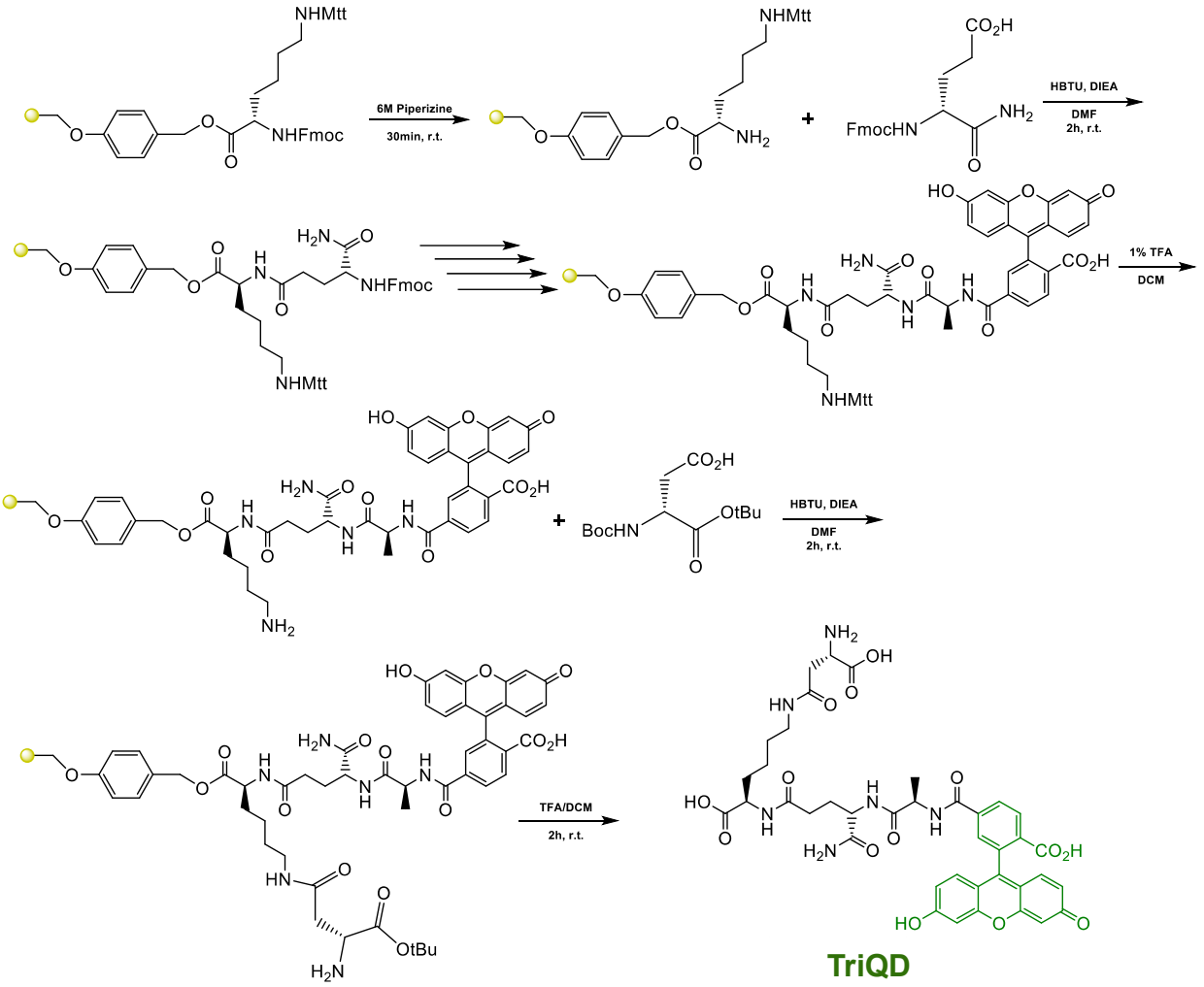

To a 25 mL peptide synthesis vessel charged with Fmoc-Lysine(Mtt)-Wang resin (1.0 g, 0.55mmol). The Fmoc protecting group was removed with 6 M piperazine/100 mM HOBt in DMF (15 ml) for 30 min at ambient temperature, then washed with washed with MeOH and DCM (3 x 15 mL each). Fmoc-D-glutamic acid α-amide (3 eq, 607 mg, 1.65 mmol), HBTU (3 eq, 625 mg, 1.65 mmol), and DIEA (6 eq, 0.574 mL, 3.30 mmol) in DMF (15 mL) were added to the reaction flask and agitated for 2 h at ambient temperature and washed as before. The Fmoc deprotection and coupling procedure was repeated as before using the same equivalencies with Fmoc-L-Alanine-OH. The Fmoc group of L-alanine was deprotected and resin coupled with 5(6)-carboxyfluorescein (2 eq, 413 mg, 1.1 mmol), HBTU (2 eq, 416 mg, 1.1 mmol) and DIEA (6 eq, 0.574 mL, 3.30 mmol) in DMF (15 mL) shaking overnight. The Mtt protecting group was removed

by the addition of 1% TFA, 2.5% TIPS, in 10 mL DCM for 15 min, washed and repeated 3 more times. Boc-D-aspartic acid α-*tert*-butyl ester (3 eq, 476 mg, 1.65 mmol), HBTU (3 eq, 625 mg, 1.65 mmol), and DIEA (6 eq, 0.574 mL, 3.30 mmol) in DMF (15 mL) were added to the reaction flask and agitated for 2 h at ambient temperature and washed as before. A solution of TFA/DCM (2:1, 20 mL) was added to the resin with agitation for 2 h at ambient temperature. The resin was filtered and resulting solution concentrated *in vacuo*. The residue was trituated with cold diethyl ether and purified using reverse phase HPLC using H_2O/MeOH to yield **TriQD**. The sample was analyzed for purity using a Shimadzu LC 2020 with a Phenomenex Luna 5µ C18(2) 100Å (30 x 2.00 mm) column; gradient elution with H_2O/CH_3CN.

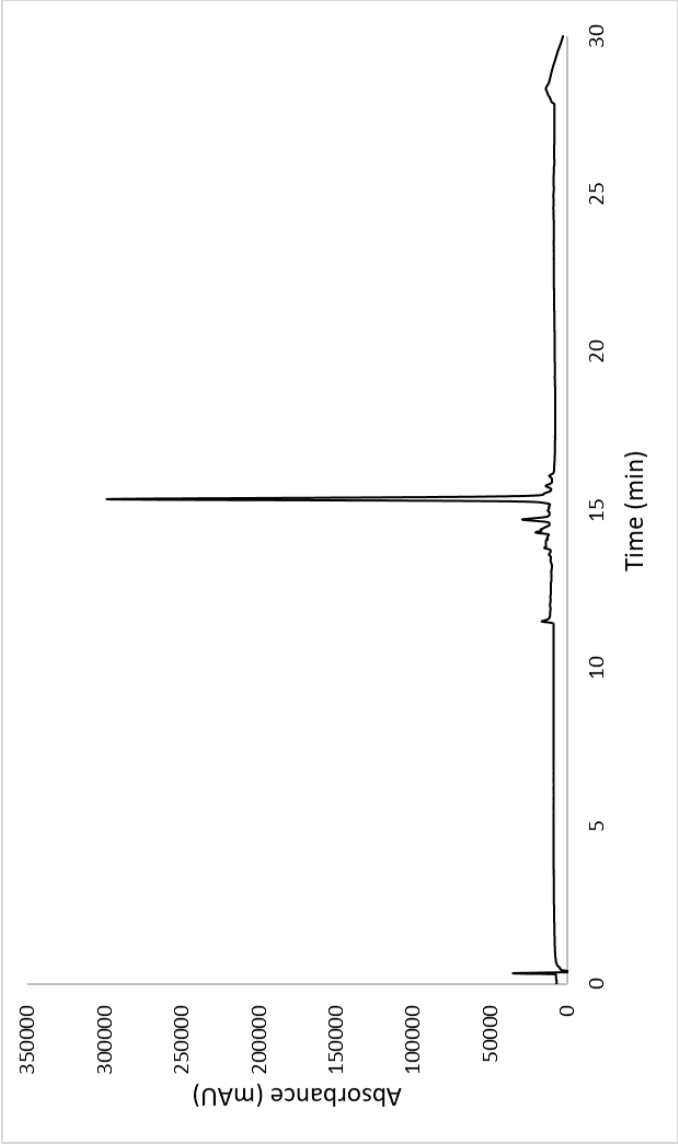

ESI-MS calculated: 818.2759, found: 818.2758

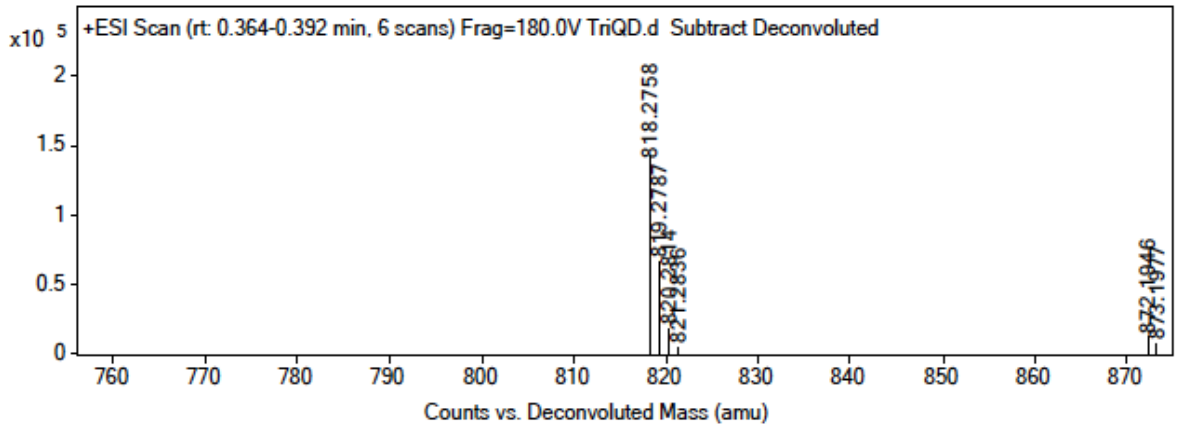

Scheme S4. Synthesis of TriEN.

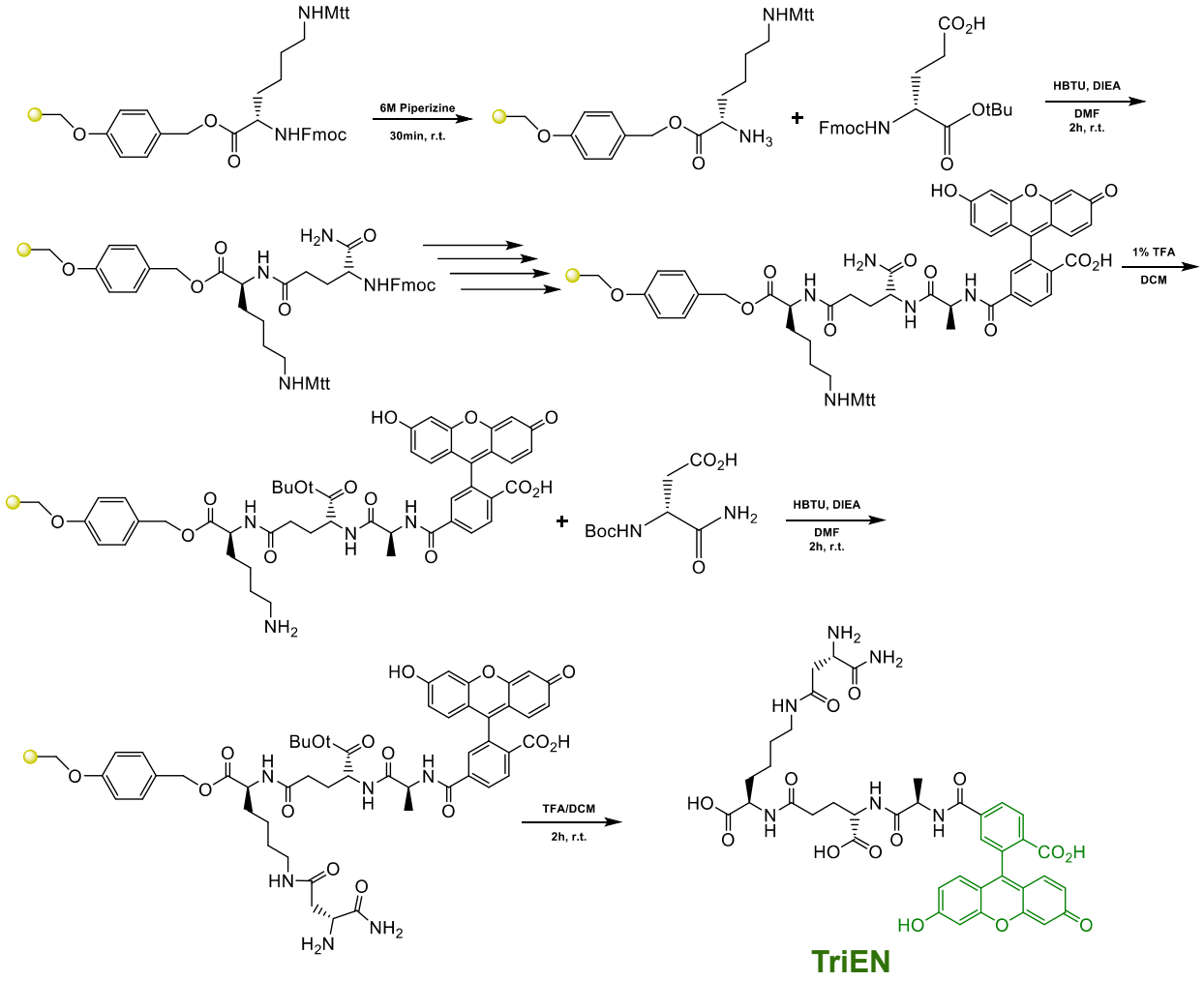

To a 25 mL peptide synthesis vessel charged with Fmoc-Lysine(Mtt)-Wang resin (1.0 g, 0.55mmol). The Fmoc protecting group was removed with 6 M piperazine/100 mM HOBt in DMF (15 ml) for 30 min at ambient temperature, then washed with washed with MeOH and DCM (3 x 15 mL each). Fmoc-D-glutamic acid-a-*tert*-butyl ester (3 eq, 701 mg, 1.65 mmol), HBTU (3 eq, 625 mg, 1.65 mmol), and DIEA (6 eq, 0.574 mL, 3.30 mmol) in DMF (15 mL) were added to the reaction flask and agitated for 2 h at ambient temperature and washed as before. The Fmoc deprotection and coupling procedure was repeated as before using the same equivalencies with Fmoc-L-Alanine-OH. The Fmoc group of L-alanine was deprotected and resin coupled with 5(6)-carboxyfluorescein (2 eq, 413 mg, 1.1 mmol), HBTU (2 eq, 416 mg, 1.1 mmol) and DIEA (6 eq, 0.574 mL, 3.30 mmol) in DMF (15 mL) shaking overnight. The Mtt protecting group was removed by the addition of 1% TFA, 2.5% TIPS, in 10 mL DCM for 15 min, washed and repeated 3 more times. Boc-D-aspartic acid α-amide (3 eq, 382 mg, 1.65 mmol), HBTU (3 eq, 625 mg, 1.65 mmol),

and DIEA (6 eq, 0.574 mL, 3.30 mmol) in DMF (15 mL) were added to the reaction flask and agitated for 2 h at ambient temperature and washed as before. A solution of TFA/DCM (2:1, 20 mL) was added to the resin with agitation for 2 h at ambient temperature. The resin was filtered and resulting solution concentrated *in vacuo*. The residue was trituated with cold diethyl ether and purified using reverse phase HPLC using H_2O/MeOH to yield **TriEN**. The sample was analyzed for purity using a Shimadzu LC 2020 with a Phenomenex Luna 5µ C18(2) 100Å (30 x 2.00 mm) column; gradient elution with H_2O/CH_3CN.

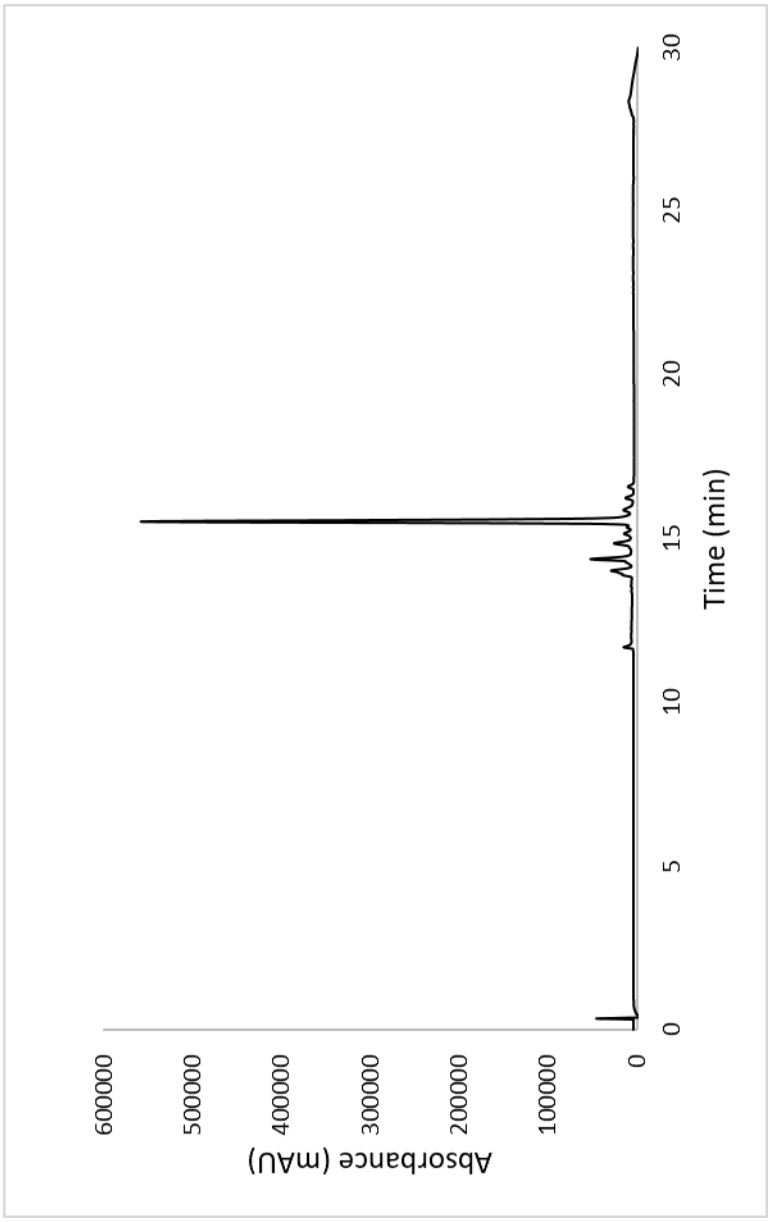

ESI-MS calculated: 818.2759, found: 818.2749

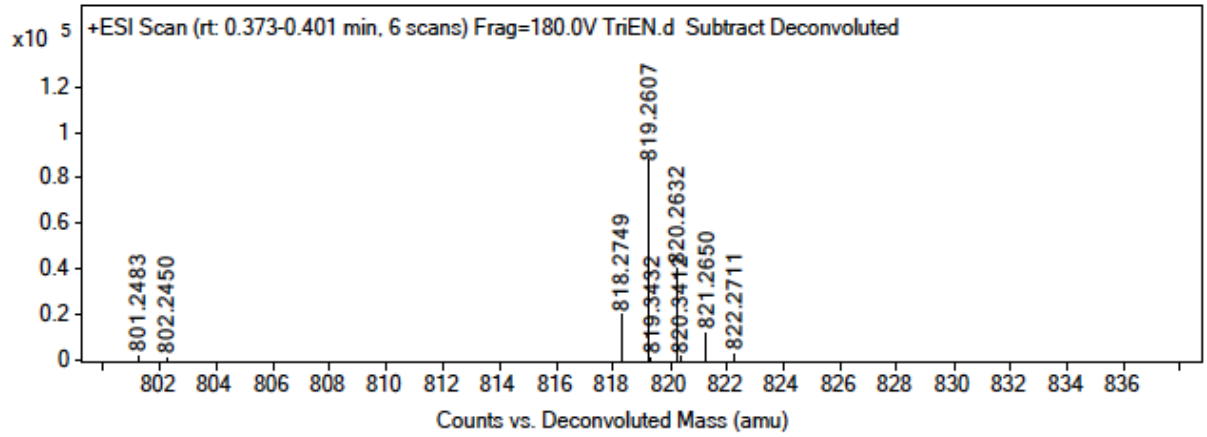

Scheme S5. Synthesis of TriQAA.

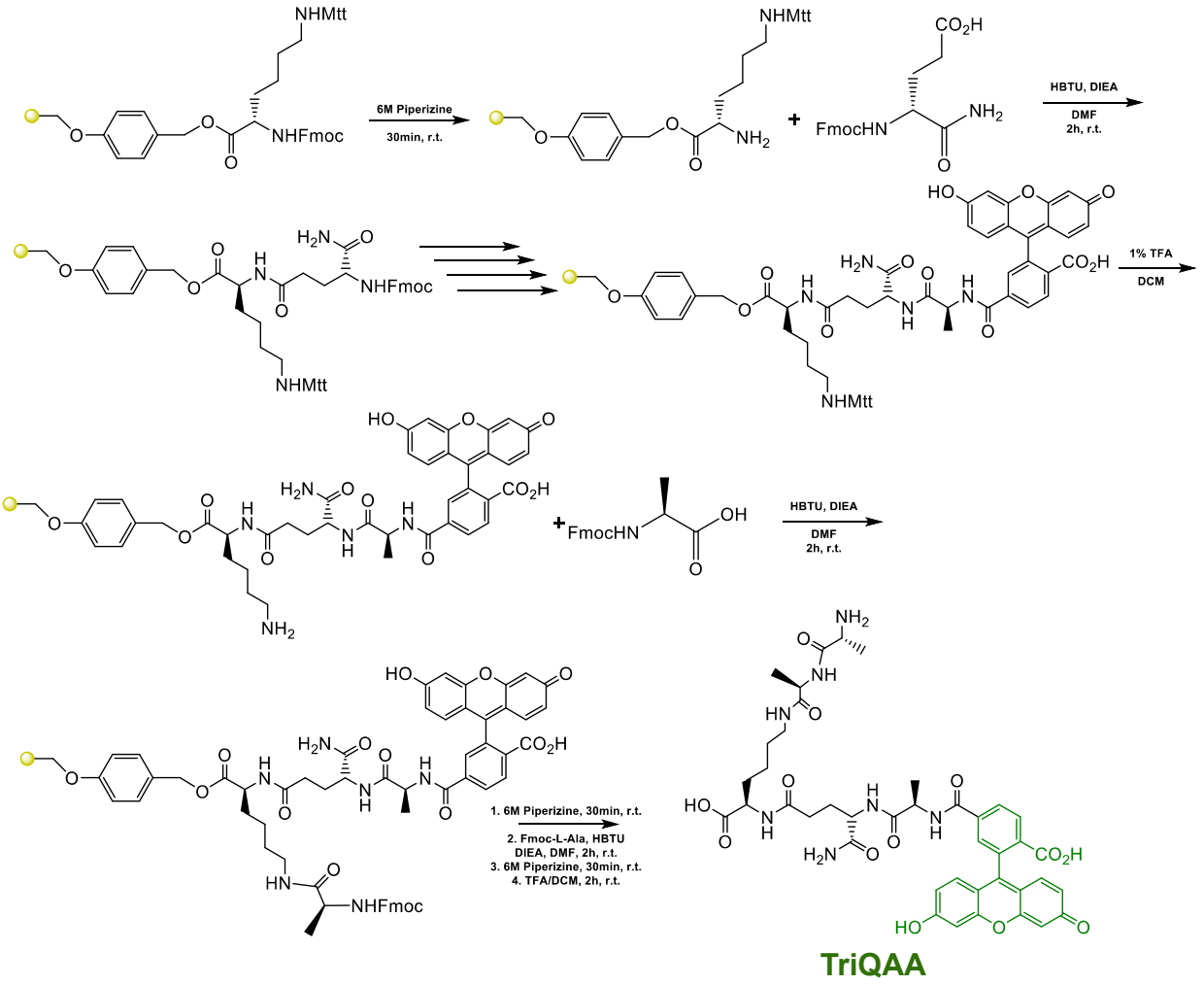

To a 25 mL peptide synthesis vessel charged with Fmoc-Lysine(Mtt)-Wang resin (1.0 g, 0.55mmol). The Fmoc protecting group was removed with 6 M piperazine/100 mM HOBt in DMF (15 ml) for 30 min at ambient temperature, then washed with washed with MeOH and DCM (3 x 15 mL each). Fmoc-D-glutamic acid α-amide (3 eq, 607 mg, 1.65 mmol), HBTU (3 eq, 625 mg, 1.65 mmol), and DIEA (6 eq, 0.574 mL, 3.30 mmol) in DMF (15 mL) were added to the reaction flask and agitated for 2 h at ambient temperature and washed as before. The Fmoc deprotection and coupling procedure was repeated as before using the same equivalencies with Fmoc-L-Alanine-OH. The Fmoc group of L-alanine was deprotected and resin coupled with 5(6)-carboxyfluorescein (2 eq, 413 mg, 1.1 mmol), HBTU (2 eq, 416 mg, 1.1 mmol) and DIEA (6 eq, 0.574 mL, 3.30 mmol) in DMF (15 mL) shaking overnight. The Mtt protecting group was removed by the addition of 1% TFA, 2.5% TIPS, in 10 mL DCM for 15 min, washed and repeated 3 more

times. Fmoc-L-alanine (3 eq, 513 mg, 1.65 mmol), HBTU (3 eq, 625 mg, 1.65 mmol), and DIEA (6 eq, 0.574 mL, 3.30 mmol) in DMF (15 mL) were added to the reaction flask and agitated for 2 h at ambient temperature and washed as before. The Fmoc group of L-alanine was deprotected and washed as before. Fmoc-L-alanine (3 eq, 513 mg, 1.65 mmol), HBTU (3 eq, 625 mg, 1.65 mmol), and DIEA (6 eq, 0.574 mL, 3.30 mmol) in DMF (15 mL) were added to the reaction flask and agitated for 2 h at ambient temperature and washed as before. The Fmoc protecting group was removed and a solution of TFA/DCM (2:1, 20 mL) was added to the resin with agitation for 2 h at ambient temperature. The resin was filtered and resulting solution concentrated *in vacuo*. The residue was trituated with cold diethyl ether and purified using reverse phase HPLC using H_2O/MeOH to yield **TriQAA**. The sample was analyzed for purity using a Shimadzu LC 2020 with a Phenomenex Luna 5µ C18(2) 100Å (30 x 2.00 mm) column; gradient elution with H_2O/CH_3CN.

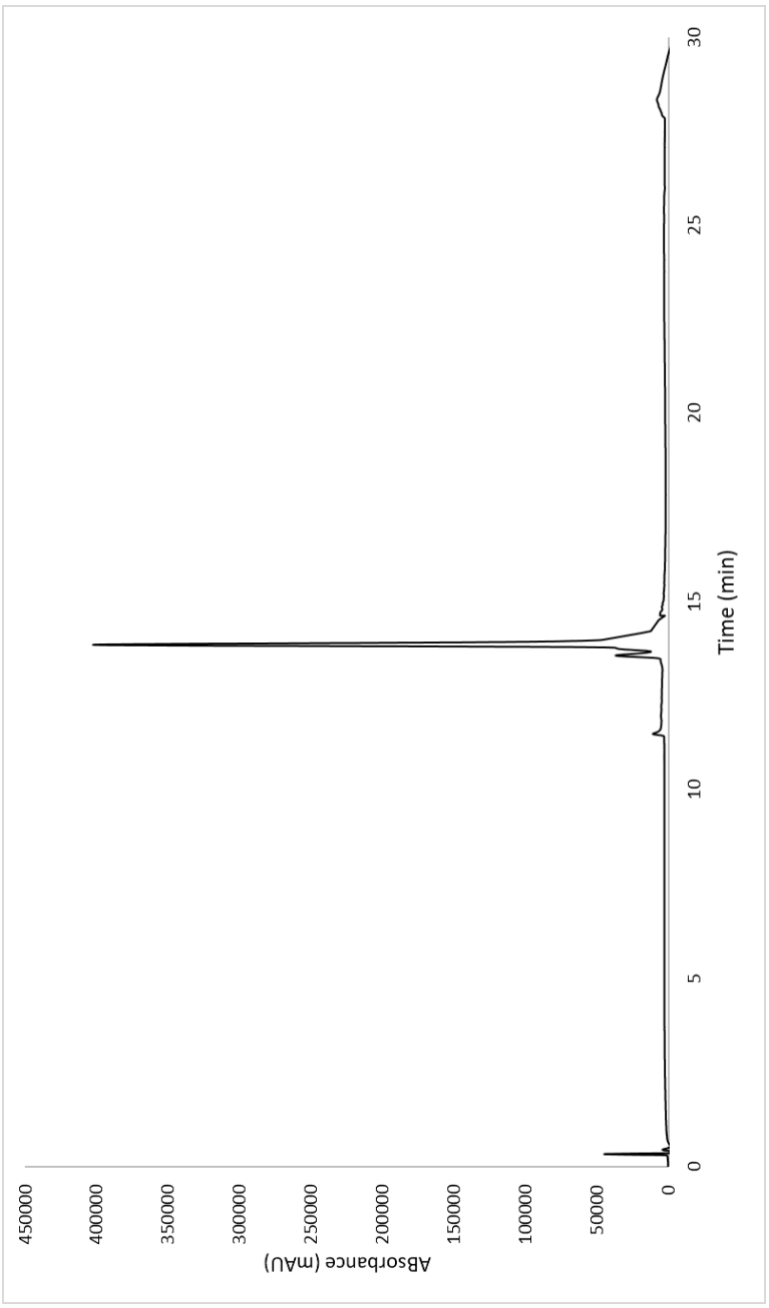
450000
400000
350000
300000
250000
200000
150000
100000
50000
0
Absorbance (mAU)
0
5
10
15
20
25
30
Time (min)

ESI-MS calculated: 845.3232, found: 845.3227

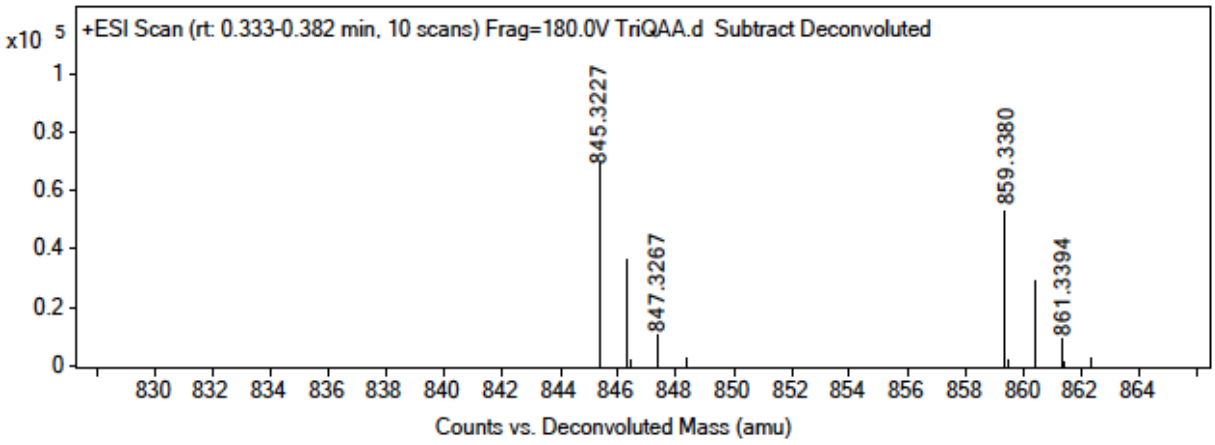

Scheme S6. Synthesis of TriEAA.

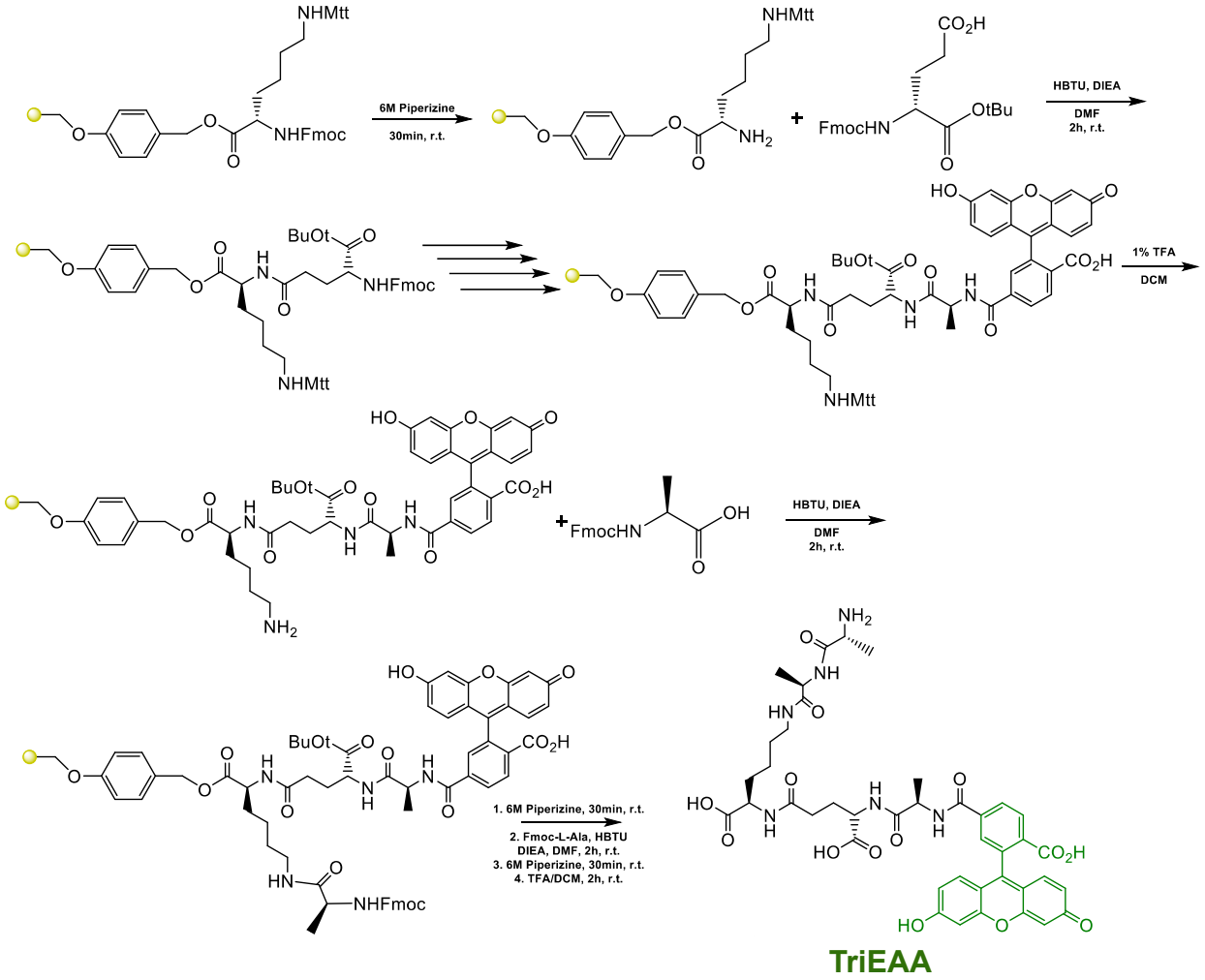

To a 25 mL peptide synthesis vessel charged with Fmoc-Lysine(Mtt)-Wang resin (1.0 g, 0.55mmol). The Fmoc protecting group was removed with 6 M piperazine/100 mM HOBt in DMF (15 ml) for 30 min at ambient temperature, then washed with washed with MeOH and DCM (3 x 15 mL each). Fmoc-D-glutamic acid-a-*tert*-butyl ester (3 eq, 701 mg, 1.65 mmol), HBTU (3 eq, 625 mg, 1.65 mmol), and DIEA (6 eq, 0.574 mL, 3.30 mmol) in DMF (15 mL) were added to the reaction flask and agitated for 2 h at ambient temperature and washed as before. The Fmoc deprotection and coupling procedure was repeated as before using the same equivalencies with Fmoc-L-Alanine-OH. The Fmoc group of L-alanine was deprotected and resin coupled with 5(6)-carboxyfluorescein (2 eq, 413 mg, 1.1 mmol), HBTU (2 eq, 416 mg, 1.1 mmol) and DIEA (6 eq, 0.574 mL, 3.30 mmol) in DMF (15 mL) shaking overnight. The Mtt protecting group was removed by the addition of 1% TFA, 2.5% TIPS, in 10 mL DCM for 15 min, washed and repeated 3 more times. Fmoc-L-alanine (3 eq, 513 mg, 1.65 mmol), HBTU (3 eq, 625 mg, 1.65 mmol), and DIEA

(6 eq, 0.574 mL, 3.30 mmol) in DMF (15 mL) were added to the reaction flask and agitated for 2 h at ambient temperature and washed as before. The Fmoc group of L-alanine was deprotected and washed as before. Fmoc-L-alanine (3 eq, 513 mg, 1.65 mmol), HBTU (3 eq, 625 mg, 1.65 mmol), and DIEA (6 eq, 0.574 mL, 3.30 mmol) in DMF (15 mL) were added to the reaction flask and agitated for 2 h at ambient temperature and washed as before. The Fmoc protecting group was removed and a solution of TFA/DCM (2:1, 20 mL) was added to the resin with agitation for 2 h at ambient temperature. The resin was filtered and resulting solution concentrated *in vacuo*. The residue was trituated with cold diethyl ether and purified using reverse phase HPLC using H_2O/MeOH to yield **TriEAA**. The sample was analyzed for purity using a Shimadzu LC 2020 with a Phenomenex Luna 5µ C18(2) 100Å (30 x 2.00 mm) column; gradient elution with H_2O/CH_3CN.

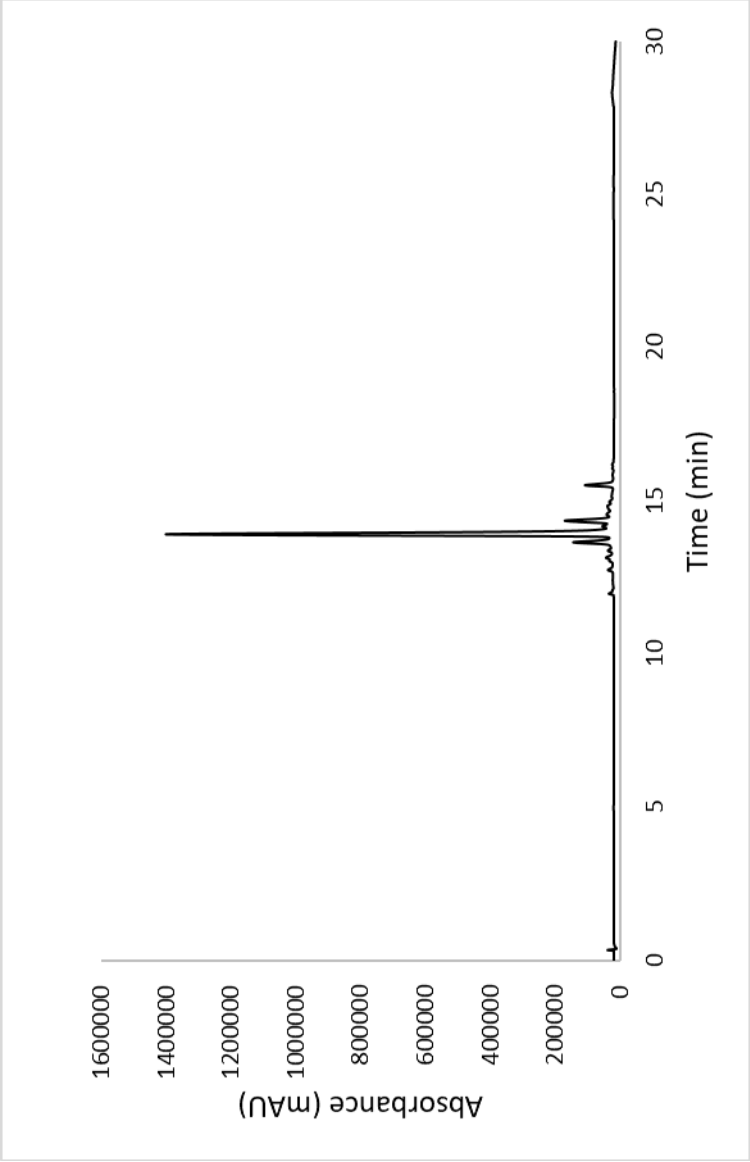

ESI-MS calculated: 846.3072, found: 846.3072

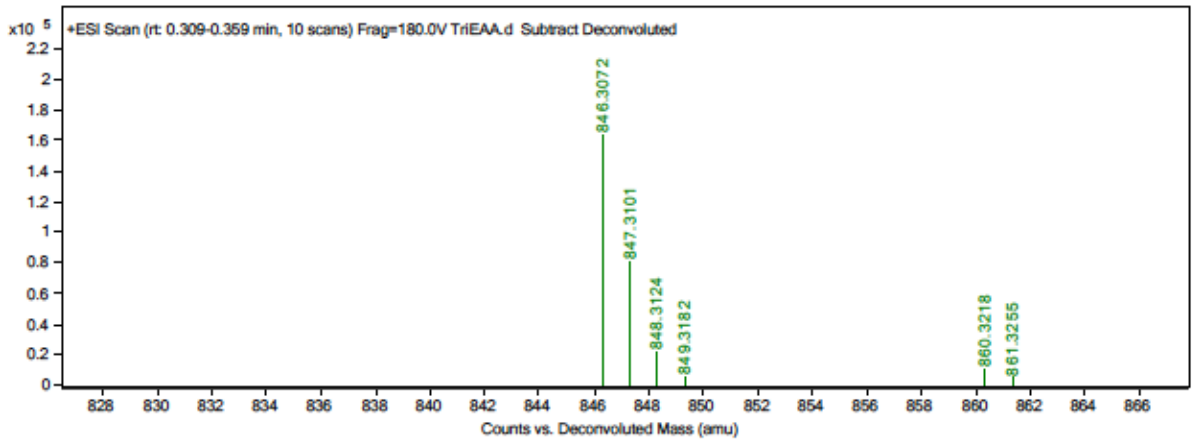

Scheme S7. Synthesis of TriQaa.

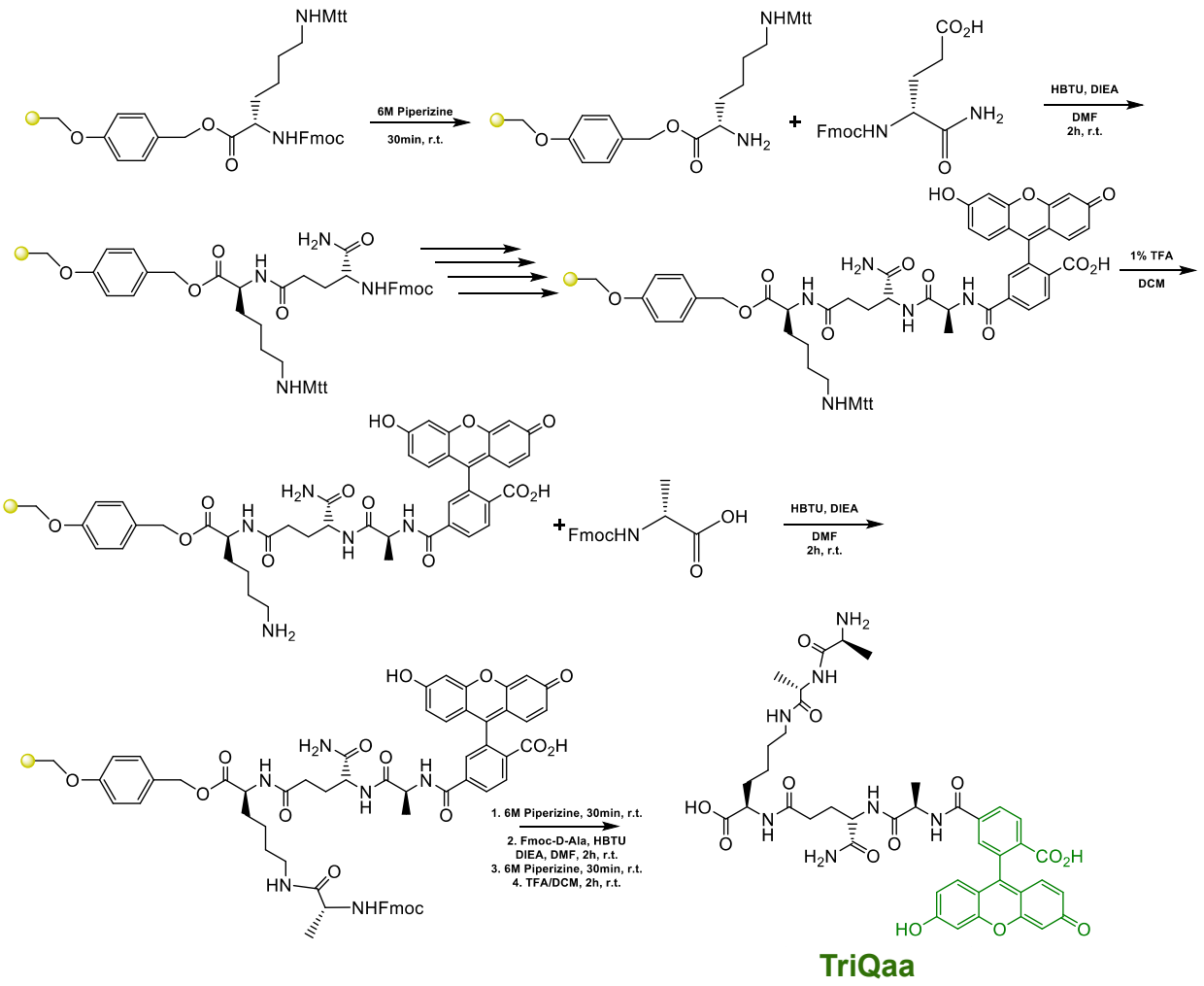

To a 25 mL peptide synthesis vessel charged with Fmoc-Lysine(Mtt)-Wang resin (1.0 g, 0.55mmol). The Fmoc protecting group was removed with 6 M piperazine/100 mM HOBt in DMF (15 ml) for 30 min at ambient temperature, then washed with washed with MeOH and DCM (3 x 15 mL each). Fmoc-D-glutamic acid α-amide (3 eq, 607 mg, 1.65 mmol), HBTU (3 eq, 625 mg, 1.65 mmol), and DIEA (6 eq, 0.574 mL, 3.30 mmol) in DMF (15 mL) were added to the reaction flask and agitated for 2 h at ambient temperature and washed as before. The Fmoc deprotection and coupling procedure was repeated as before using the same equivalencies with Fmoc-L-Alanine-OH. The Fmoc group of L-alanine was deprotected and resin coupled with 5(6)-carboxyfluorescein (2 eq, 413 mg, 1.1 mmol), HBTU (2 eq, 416 mg, 1.1 mmol) and DIEA (6 eq, 0.574 mL, 3.30 mmol) in DMF (15 mL) shaking overnight. The Mtt protecting group was removed by the addition of 1% TFA, 2.5% TIPS, in 10 mL DCM for 15 min, washed and repeated 3 more times. Fmoc-D-alanine (3 eq, 513 mg, 1.65 mmol), HBTU (3 eq, 625 mg, 1.65 mmol), and DIEA

(6 eq, 0.574 mL, 3.30 mmol) in DMF (15 mL) were added to the reaction flask and agitated for 2 h at ambient temperature and washed as before. The Fmoc group of D-alanine was deprotected and washed as before. Fmoc-D-alanine (3 eq, 513 mg, 1.65 mmol), HBTU (3 eq, 625 mg, 1.65 mmol), and DIEA (6 eq, 0.574 mL, 3.30 mmol) in DMF (15 mL) were added to the reaction flask and agitated for 2 h at ambient temperature and washed as before. The Fmoc protecting group was removed and a solution of TFA/DCM (2:1, 20 mL) was added to the resin with agitation for 2 h at ambient temperature. The resin was filtered and resulting solution concentrated *in vacuo*. The residue was trituated with cold diethyl ether and purified using reverse phase HPLC using H_2O/MeOH to yield **TriQaa**. The sample was analyzed for purity using a Shimadzu LC 2020 with a Phenomenex Luna 5µ C18(2) 100Å (30 x 2.00 mm) column; gradient elution with H_2O/CH_3CN.

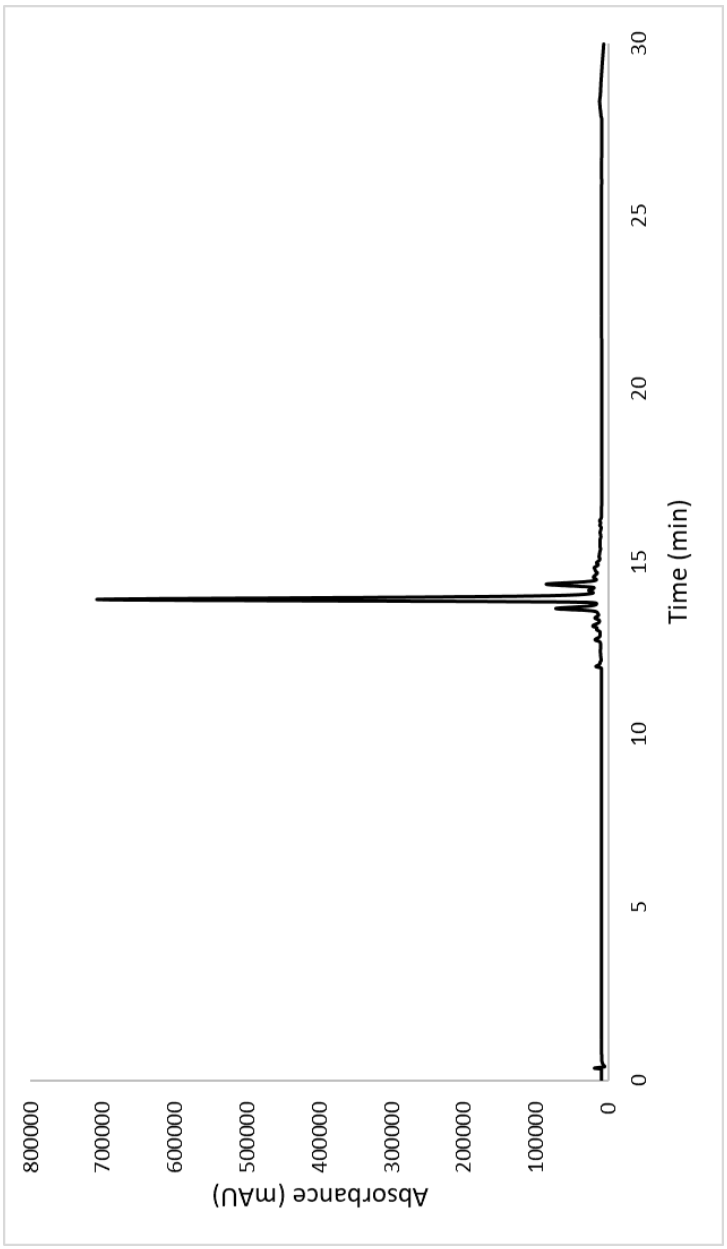
Absorbance (mAU)
800000
700000
600000
500000
400000
300000
200000
100000
0
0
5
10
15
20
25
30
Time (min)

ESI-MS calculated: 845.3232, found: 845.3234

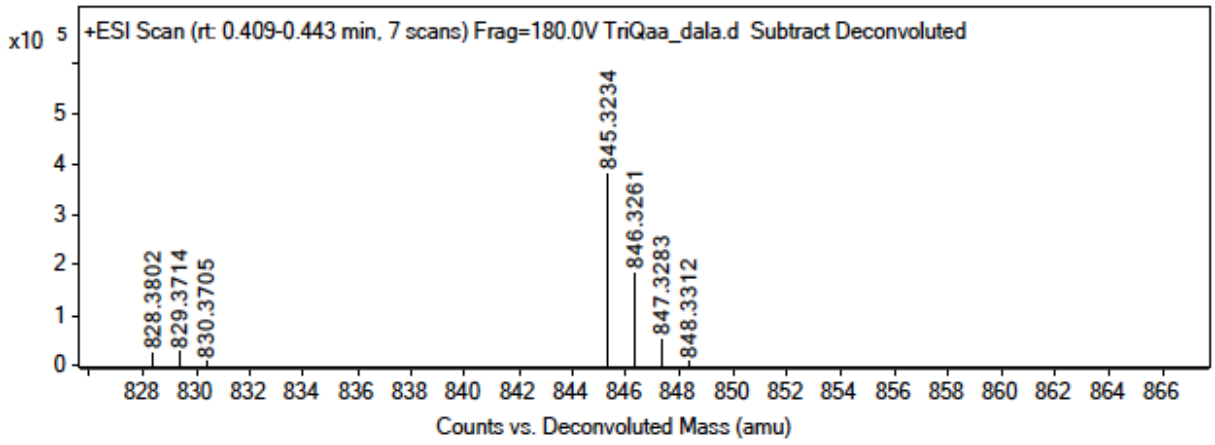

Scheme S8. Synthesis of TriQAAac.

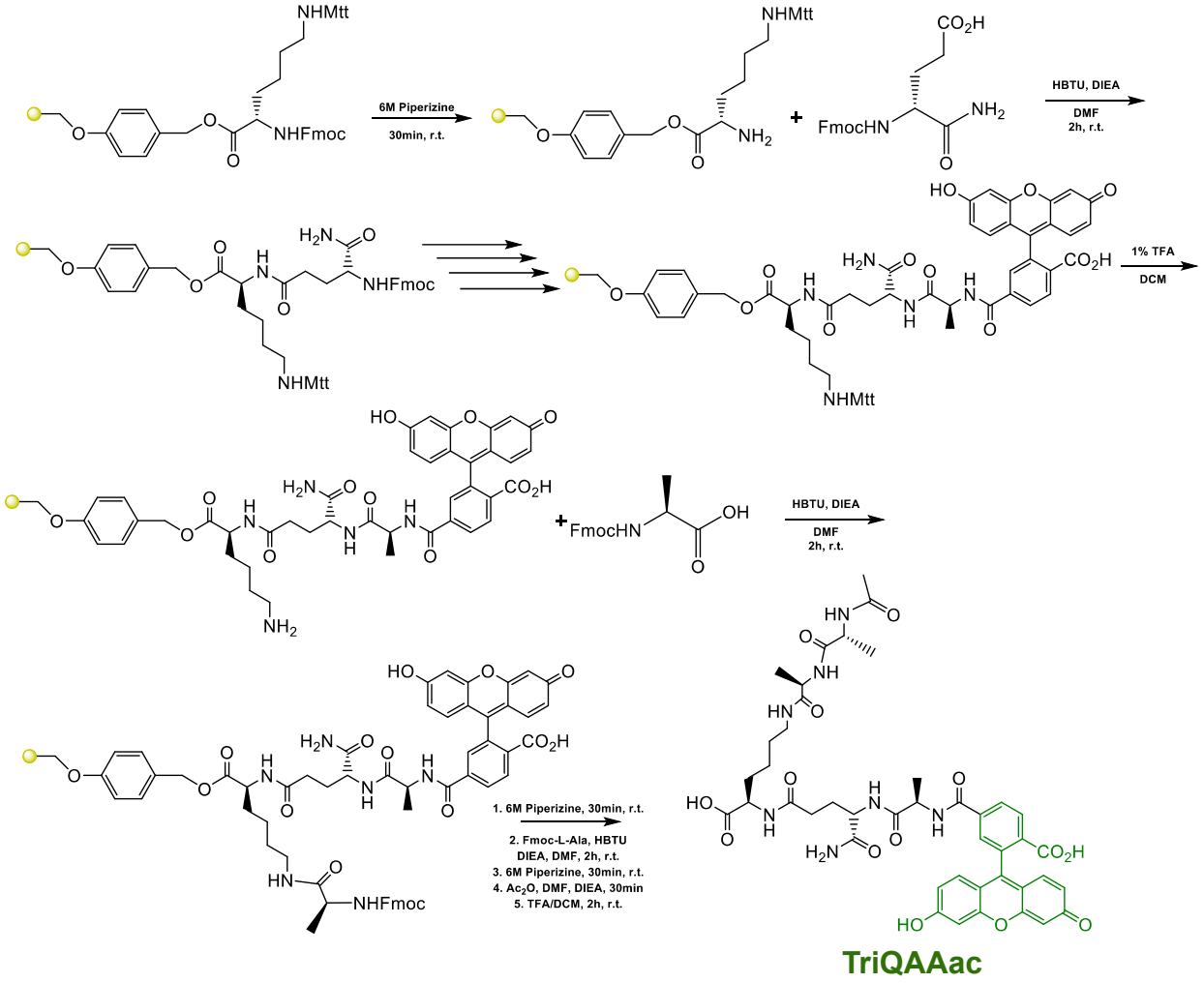

To a 25 mL peptide synthesis vessel charged with Fmoc-Lysine(Mtt)-Wang resin (1.0 g, 0.55mmol). The Fmoc protecting group was removed with 6 M piperazine/100 mM HOBt in DMF (15 ml) for 30 min at ambient temperature, then washed with washed with MeOH and DCM (3 x 15 mL each). Fmoc-D-glutamic acid α-amide (3 eq, 607 mg, 1.65 mmol), HBTU (3 eq, 625 mg, 1.65 mmol), and DIEA (6 eq, 0.574 mL, 3.30 mmol) in DMF (15 mL) were added to the reaction flask and agitated for 2 h at ambient temperature and washed as before. The Fmoc deprotection and coupling procedure was repeated as before using the same equivalencies with Fmoc-L-Alanine-OH. The Fmoc group of L-alanine was deprotected and resin coupled with 5(6)-carboxyfluorescein (2 eq, 413 mg, 1.1 mmol), HBTU (2 eq, 416 mg, 1.1 mmol) and DIEA (6 eq, 0.574 mL, 3.30 mmol) in DMF (15 mL) shaking overnight. The Mtt protecting group was removed by the addition of 1% TFA, 2.5% TIPS, in 10 mL DCM for 15 min, washed and repeated 3 more times. Fmoc-L-alanine (3 eq, 513 mg, 1.65 mmol), HBTU (3 eq, 625 mg, 1.65 mmol), and DIEA (6 eq, 0.574 mL, 3.30 mmol) in DMF (15 mL) were added to the reaction flask and agitated for 2

h at ambient temperature and washed as before. The Fmoc group of L-alanine was deprotected and washed as before. Fmoc-L-alanine (3 eq, 513 mg, 1.65 mmol), HBTU (3 eq, 625 mg, 1.65 mmol), and DIEA (6 eq, 0.574 mL, 3.30 mmol) in DMF (15 mL) were added to the reaction flask and agitated for 2 h at ambient temperature and washed as before. The Fmoc protecting group was removed and a solution of acetic anhydride (5 eq, 0.260 mL) and DIEA (10 eq, 0.956 mL) in DMF was added and resin shaken for 30 min at ambient temperature. The resin was washed and added to a solution of TFA/DCM (2:1, 20 mL) with agitation for 2 h at ambient temperature. The resin was filtered and resulting solution concentrated *in vacuo*. The residue was trituated with cold diethyl ether and purified using reverse phase HPLC using H_2O/MeOH to yield **TriQAAac.** The sample was analyzed for purity using a Shimadzu LC 2020 with a Phenomenex Luna 5µ C18(2) 100Å (30 x 2.00 mm) column; gradient elution with H_2O/CH_3CN**.**

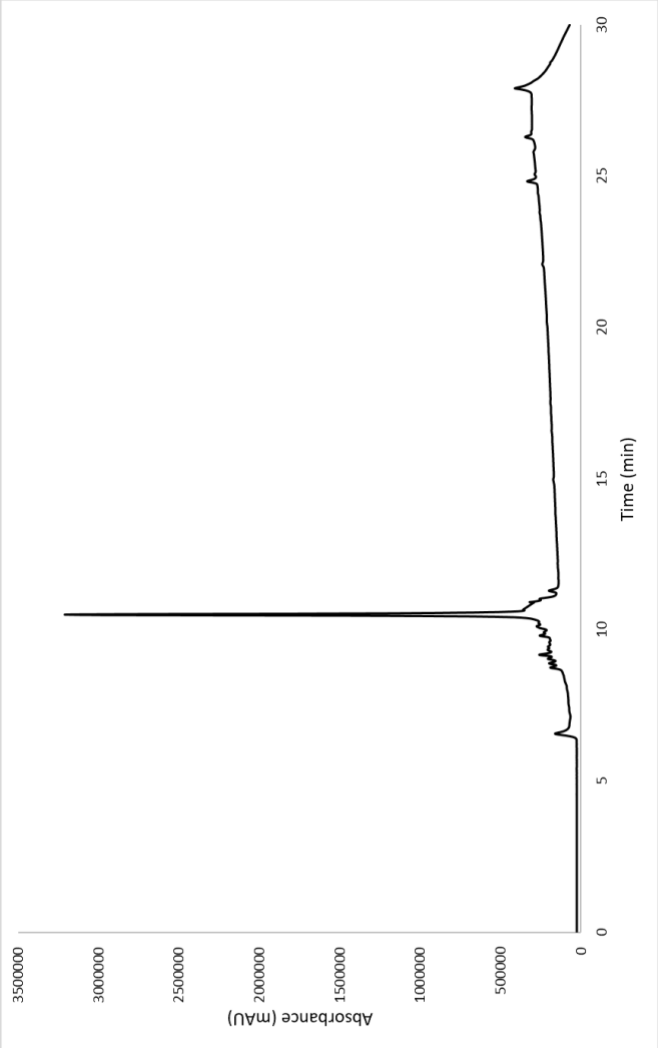

ESI-MS calculated: 887.3337, found: 887.3337

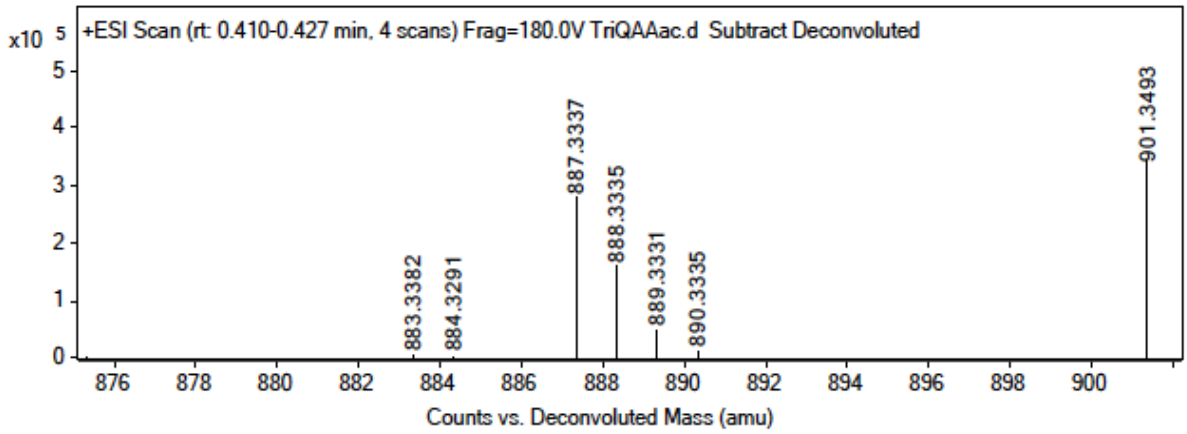

Scheme S9. Synthesis of TriQG1.

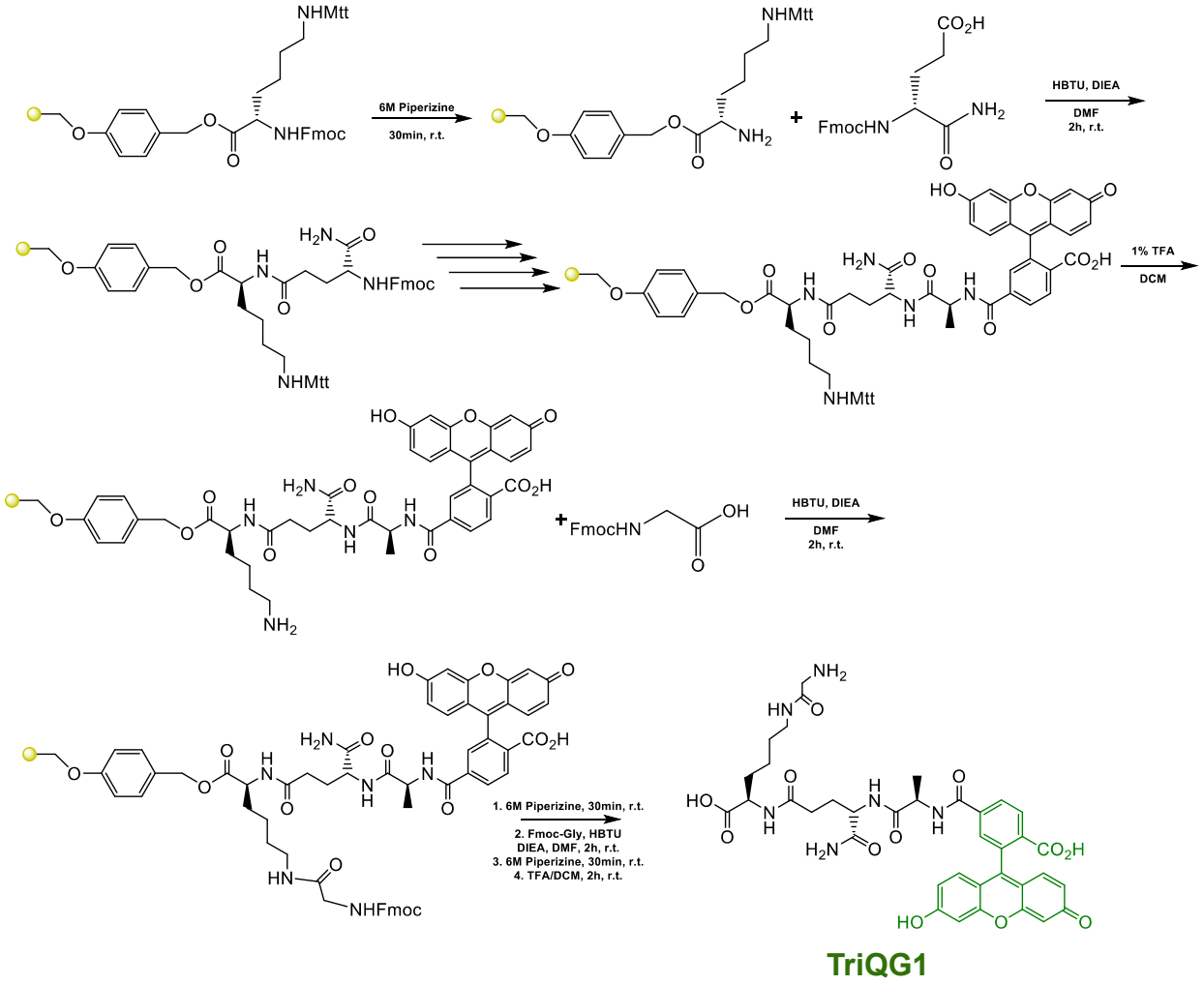

To a 25 mL peptide synthesis vessel charged with Fmoc-Lysine(Mtt)-Wang resin (1.0 g, 0.55mmol). The Fmoc protecting group was removed with 6 M piperazine/100 mM HOBt in DMF (15 ml) for 30 min at ambient temperature, then washed with washed with MeOH and DCM (3 x 15 mL each). Fmoc-D-glutamic acid α-amide (3 eq, 607 mg, 1.65 mmol), HBTU (3 eq, 625 mg, 1.65 mmol), and DIEA (6 eq, 0.574 mL, 3.30 mmol) in DMF (15 mL) were added to the reaction flask and agitated for 2 h at ambient temperature and washed as before. The Fmoc deprotection and coupling procedure was repeated as before using the same equivalencies with Fmoc-L-Alanine-OH. The Fmoc group of L-alanine was deprotected and resin coupled with 5(6)-carboxyfluorescein (2 eq, 413 mg, 1.1 mmol), HBTU (2 eq, 416 mg, 1.1 mmol) and DIEA (6 eq, 0.574 mL, 3.30 mmol) in DMF (15 mL) shaking overnight. The Mtt protecting group was removed by the addition of 1% TFA, 2.5% TIPS, in 10 mL DCM for 15 min, washed and repeated 3 more times. Fmoc-glycine (3 eq, 513 mg, 1.65 mmol), HBTU (3 eq, 625 mg, 1.65 mmol), and DIEA (6 eq, 0.574 mL, 3.30 mmol) in DMF (15 mL) were added to the reaction flask and agitated for 2 h

at ambient temperature and washed as before. The Fmoc group of glycine was deprotected, resin washed, and a solution of TFA/DCM (2:1, 20 mL) was added with agitation for 2 h at ambient temperature. The resin was filtered and resulting solution concentrated *in vacuo*. The residue was trituated with cold diethyl ether and purified using reverse phase HPLC using H_2O/MeOH to yield **TriQG1**. The sample was analyzed for purity using a Shimadzu LC 2020 with a Phenomenex Luna 5µ C18(2) 100Å (30 x 2.00 mm) column; gradient elution with H_2O/CH_3CN.

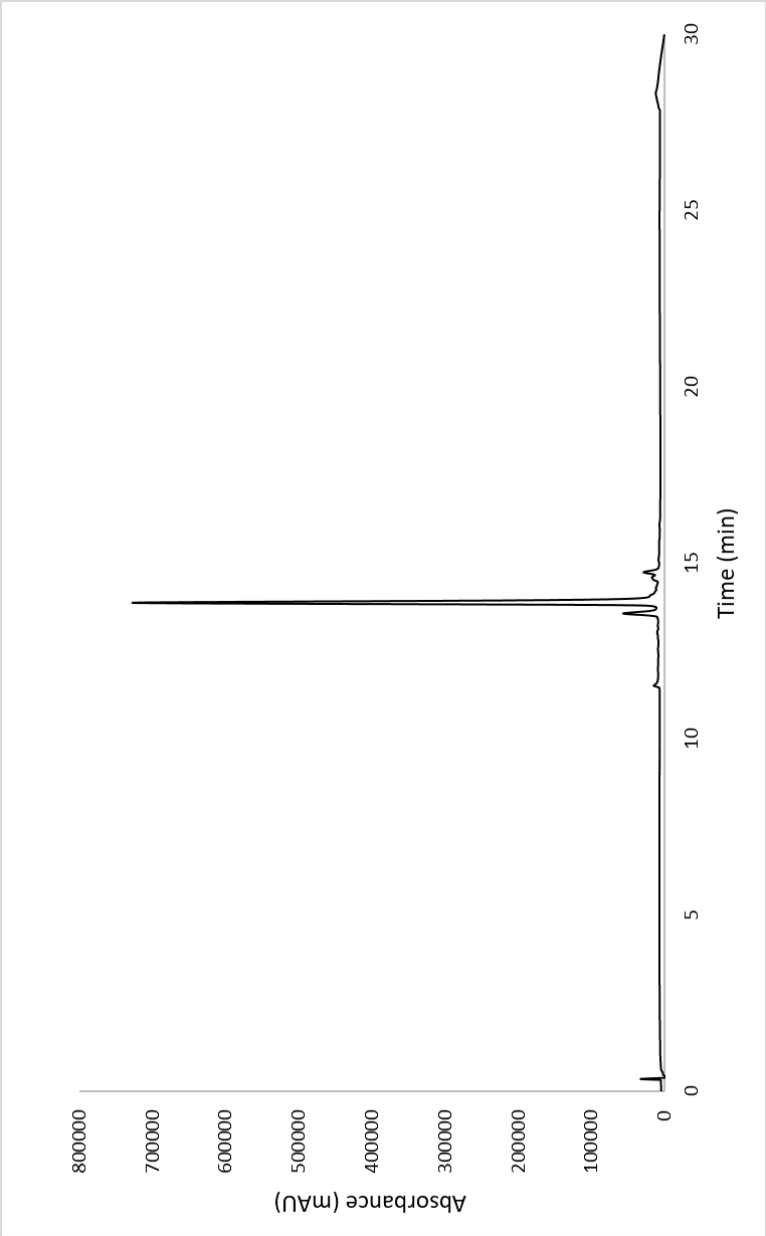

ESI-MS calculated: 760.2704, found: 760.2740

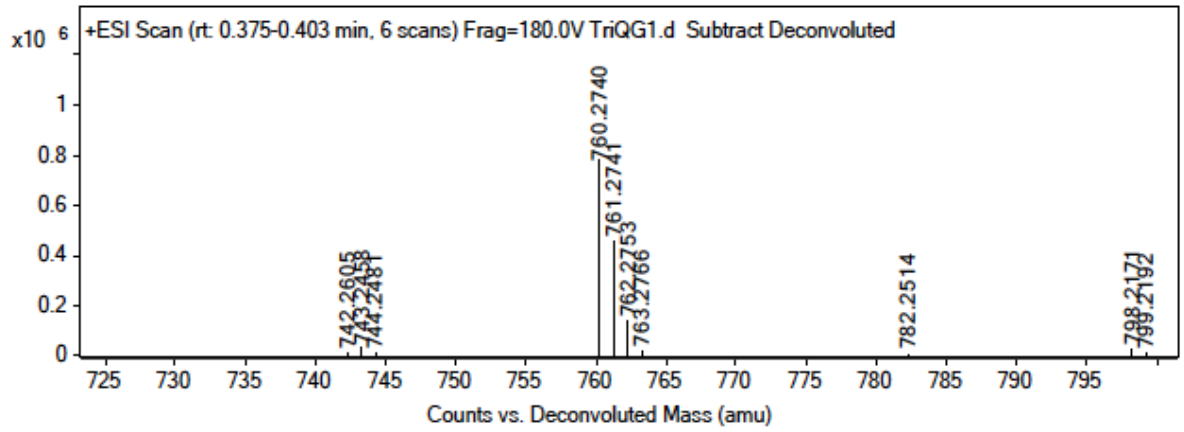

Scheme S10. Synthesis of TriQG2.

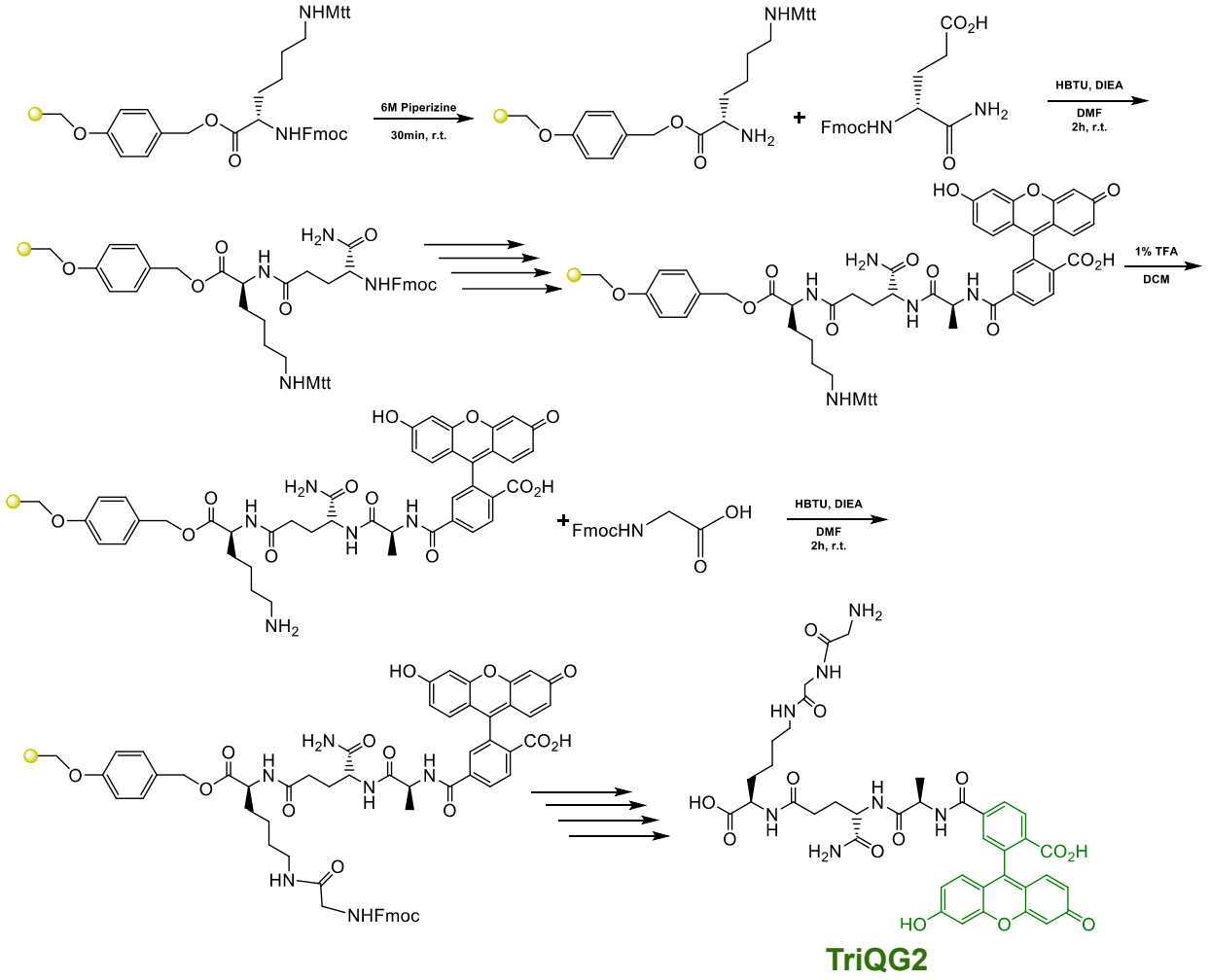

To a 25 mL peptide synthesis vessel charged with Fmoc-Lysine(Mtt)-Wang resin (1.0 g, 0.55mmol). The Fmoc protecting group was removed with 6 M piperazine/100 mM HOBt in DMF (15 ml) for 30 min at ambient temperature, then washed with washed with MeOH and DCM (3 x 15 mL each). Fmoc-D-glutamic acid α-amide (3 eq, 607 mg, 1.65 mmol), HBTU (3 eq, 625 mg, 1.65 mmol), and DIEA (6 eq, 0.574 mL, 3.30 mmol) in DMF (15 mL) were added to the reaction flask and agitated for 2 h at ambient temperature and washed as before. The Fmoc deprotection and coupling procedure was repeated as before using the same equivalencies with Fmoc-L-Alanine-OH. The Fmoc group of L-alanine was deprotected and resin coupled with 5(6)-carboxyfluorescein (2 eq, 413 mg, 1.1 mmol), HBTU (2 eq, 416 mg, 1.1 mmol) and DIEA (6 eq, 0.574 mL, 3.30 mmol) in DMF (15 mL) shaking overnight. The Mtt protecting group was removed by the addition of 1% TFA, 2.5% TIPS, in 10 mL DCM for 15 min, washed and repeated 3 more times. Fmoc-glycine (3 eq, 513 mg, 1.65 mmol), HBTU (3 eq, 625 mg, 1.65 mmol), and DIEA (6

eq, 0.574 mL, 3.30 mmol) in DMF (15 mL) were added to the reaction flask and agitated for 2 h at ambient temperature and washed as before. The Fmoc group of glycine was deprotected, resin washed, and the Fmoc-glycine procedure was repeated once more. After Fmoc deprotection, a solution of TFA/DCM (2:1, 20 mL) was added to the resin with agitation for 2 h at ambient temperature. The resin was filtered and resulting solution concentrated *in vacuo*. The residue was trituated with cold diethyl ether and purified using reverse phase HPLC using H_2O/MeOH to yield **TriQG2**. The sample was analyzed for purity using a Shimadzu LC 2020 with a Phenomenex Luna 5µ C18(2) 100Å (30 x 2.00 mm) column; gradient elution with H_2O/CH_3CN.

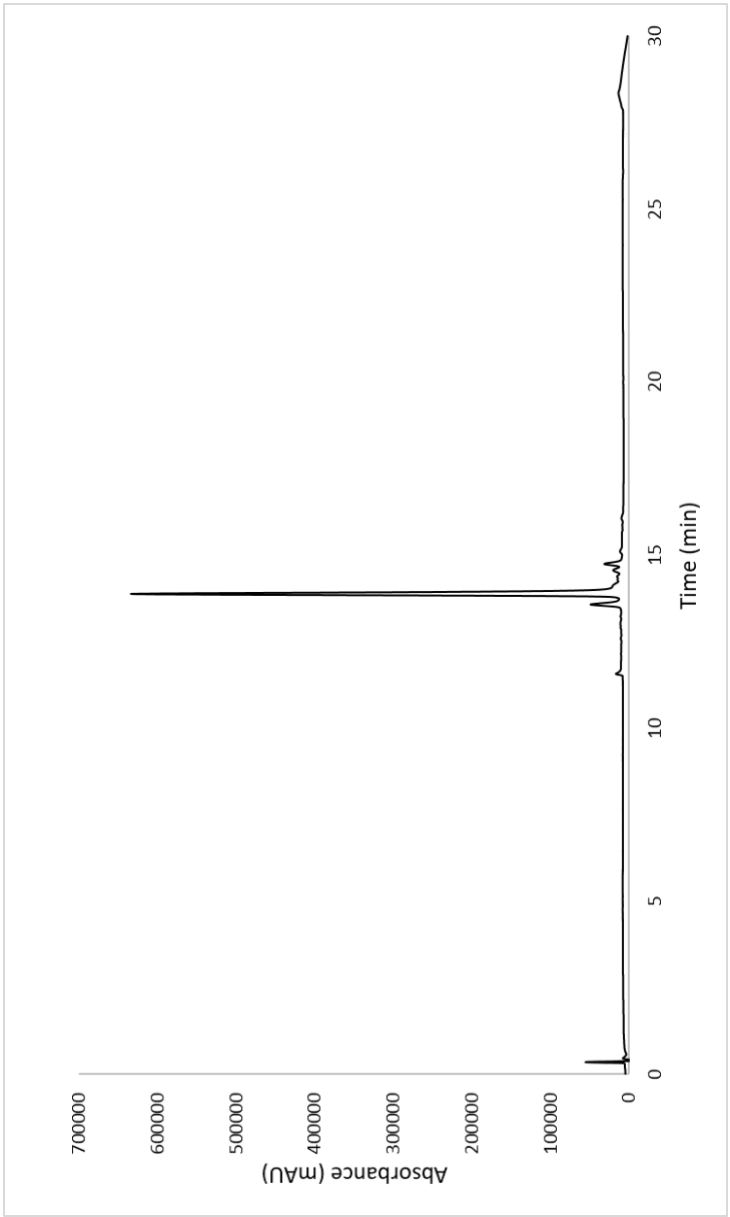

ESI-MS calculated: 817.2919, found: 817.2925

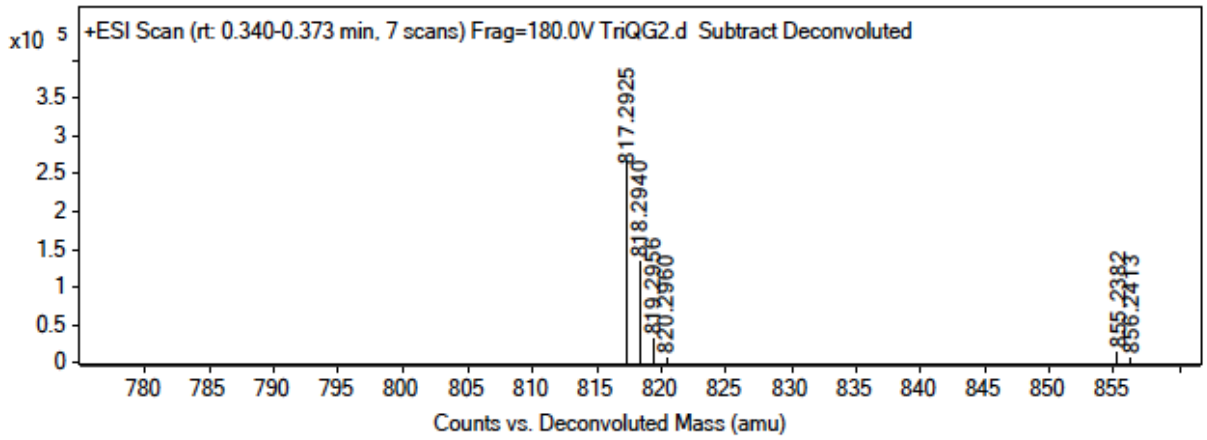

Scheme S11. Synthesis of TriQG3.

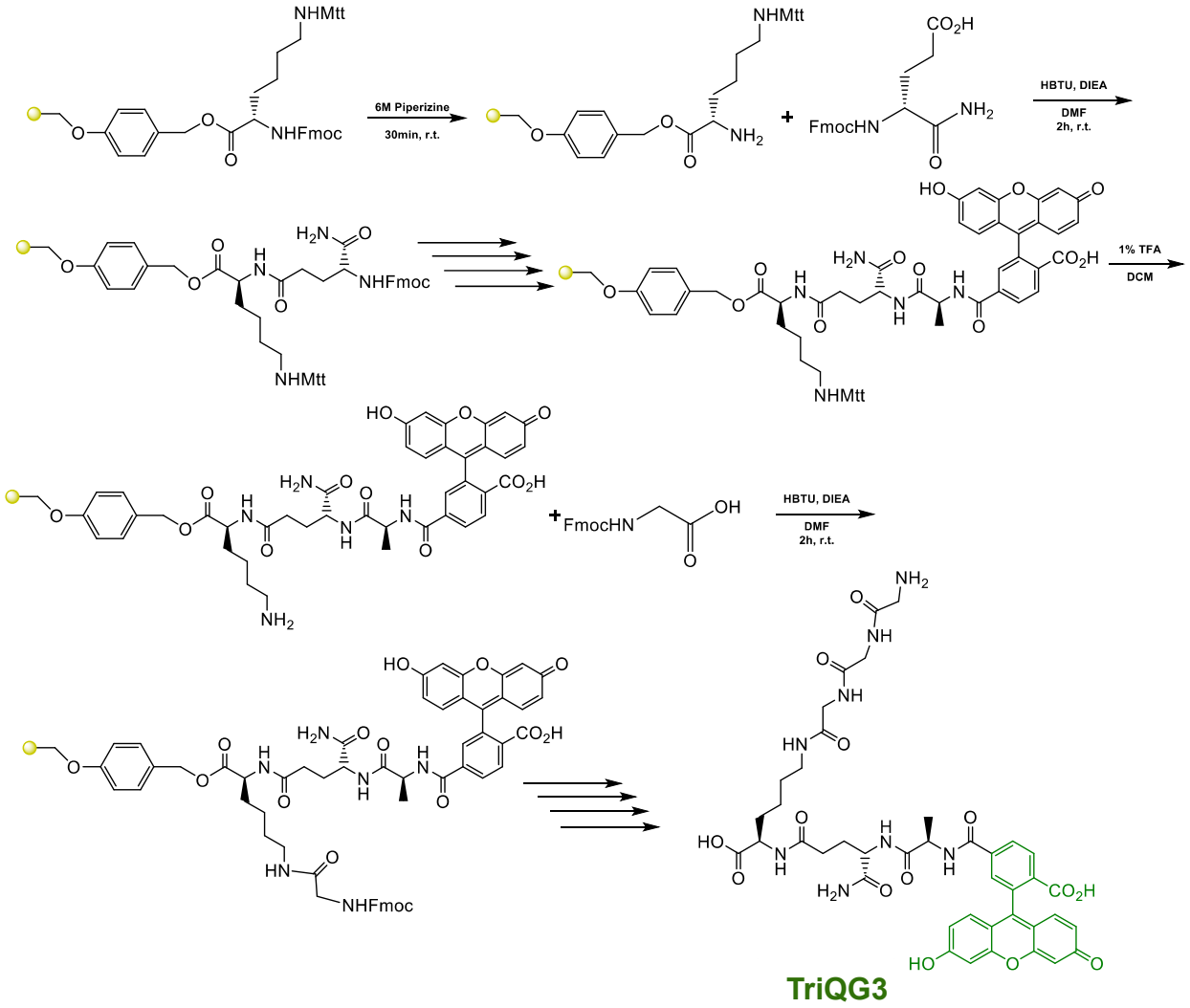

To a 25 mL peptide synthesis vessel charged with Fmoc-Lysine(Mtt)-Wang resin (1.0 g, 0.55mmol). The Fmoc protecting group was removed with 6 M piperazine/100 mM HOBt in DMF (15 ml) for 30 min at ambient temperature, then washed with washed with MeOH and DCM (3 x 15 mL each). Fmoc-D-glutamic acid α-amide (3 eq, 607 mg, 1.65 mmol), HBTU (3 eq, 625 mg, 1.65 mmol), and DIEA (6 eq, 0.574 mL, 3.30 mmol) in DMF (15 mL) were added to the reaction flask and agitated for 2 h at ambient temperature and washed as before. The Fmoc deprotection and coupling procedure was repeated as before using the same equivalencies with Fmoc-L-Alanine-OH. The Fmoc group of L-alanine was deprotected and resin coupled with 5(6)-carboxyfluorescein (2 eq, 413 mg, 1.1 mmol), HBTU (2 eq, 416 mg, 1.1 mmol) and DIEA (6 eq, 0.574 mL, 3.30 mmol) in DMF (15 mL) shaking overnight. The Mtt protecting group was removed by the addition of 1% TFA, 2.5% TIPS, in 10 mL DCM for 15 min, washed and repeated 3 more times. Fmoc-glycine (3 eq, 513 mg, 1.65 mmol), HBTU (3 eq, 625 mg, 1.65 mmol), and DIEA (6

eq, 0.574 mL, 3.30 mmol) in DMF (15 mL) were added to the reaction flask and agitated for 2 h at ambient temperature and washed as before. The Fmoc group of glycine was deprotected, resin washed, and the Fmoc-glycine procedure was repeated twice more. After Fmoc deprotection, a solution of TFA/DCM (2:1, 20 mL) was added to the resin with agitation for 2 h at ambient temperature. The resin was filtered and resulting solution concentrated *in vacuo*. The residue was trituated with cold diethyl ether and purified using reverse phase HPLC using H_2O/MeOH to yield **TriQG3**. The sample was analyzed for purity using a Shimadzu LC 2020 with a Phenomenex Luna 5µ C18(2) 100Å (30 x 2.00 mm) column; gradient elution with H_2O/CH_3CN.

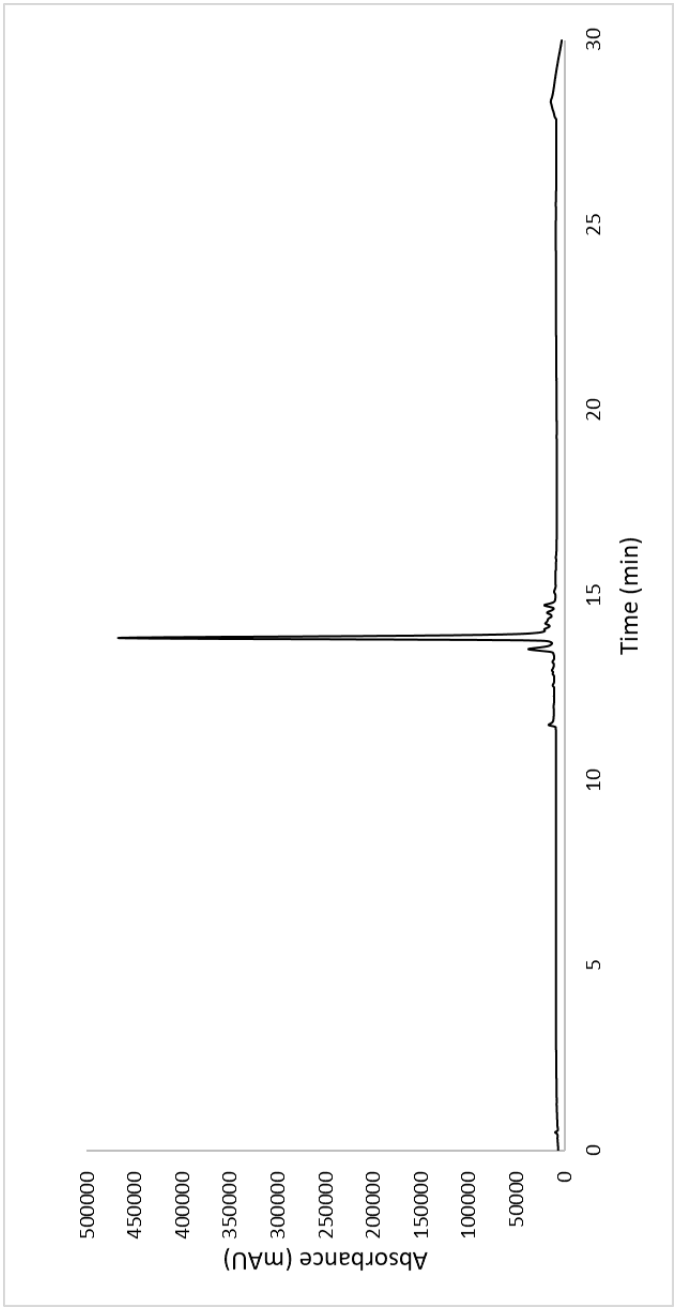

ESI-MS calculated: 874.3133, found: 874.3133

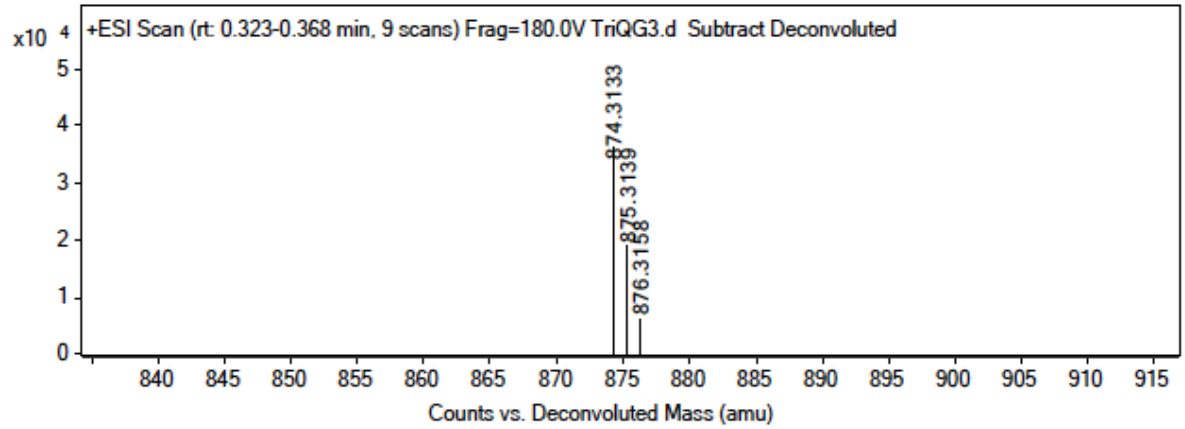

Scheme S12. Synthesis of TriQG4.

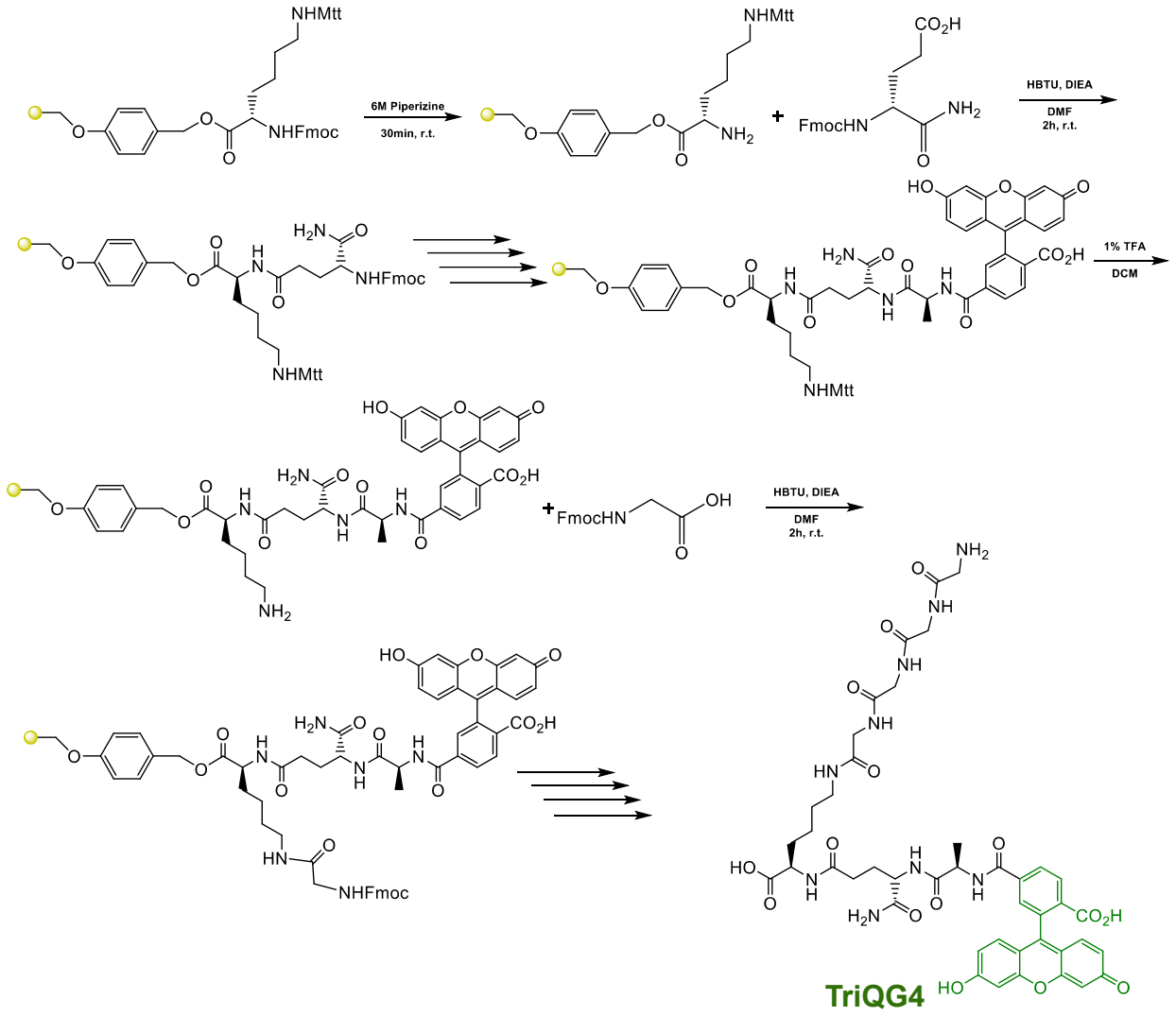

To a 25 mL peptide synthesis vessel charged with Fmoc-Lysine(Mtt)-Wang resin (1.0 g, 0.55mmol). The Fmoc protecting group was removed with 6 M piperazine/100 mM HOBt in DMF (15 ml) for 30 min at ambient temperature, then washed with washed with MeOH and DCM (3 x 15 mL each). Fmoc-D-glutamic acid α-amide (3 eq, 607 mg, 1.65 mmol), HBTU (3 eq, 625 mg, 1.65 mmol), and DIEA (6 eq, 0.574 mL, 3.30 mmol) in DMF (15 mL) were added to the reaction flask and agitated for 2 h at ambient temperature and washed as before. The Fmoc deprotection and coupling procedure was repeated as before using the same equivalencies with Fmoc-L-Alanine-OH. The Fmoc group of L-alanine was deprotected and resin coupled with 5(6)-carboxyfluorescein (2 eq, 413 mg, 1.1 mmol), HBTU (2 eq, 416 mg, 1.1 mmol) and DIEA (6 eq, 0.574 mL, 3.30 mmol) in DMF (15 mL) shaking overnight. The Mtt protecting group was removed by the addition of 1% TFA, 2.5% TIPS, in 10 mL DCM for 15 min, washed and repeated 3 more

times. Fmoc-glycine (3 eq, 513 mg, 1.65 mmol), HBTU (3 eq, 625 mg, 1.65 mmol), and DIEA (6 eq, 0.574 mL, 3.30 mmol) in DMF (15 mL) were added to the reaction flask and agitated for 2 h at ambient temperature and washed as before. The Fmoc group of glycine was deprotected, resin washed, and the Fmoc-glycine procedure was repeated three more times. After Fmoc deprotection, a solution of TFA/DCM (2:1, 20 mL) was added to the resin with agitation for 2 h at ambient temperature. The resin was filtered and resulting solution concentrated *in vacuo*. The residue was trituated with cold diethyl ether and purified using reverse phase HPLC using H_2O/MeOH to yield **TriQG4**. The sample was analyzed for purity using a Shimadzu LC 2020 with a Phenomenex Luna 5µ C18(2) 100Å (30 x 2.00 mm) column; gradient elution with H_2O/CH_3CN.

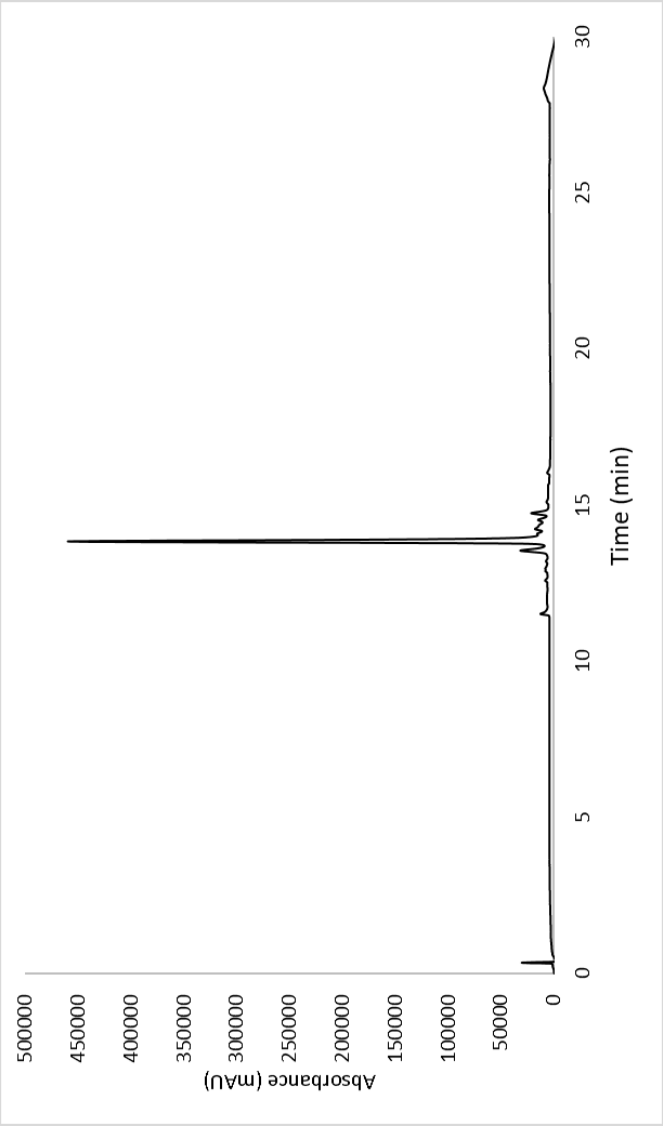

ESI-MS calculated: 931.3348, found 931.3359:

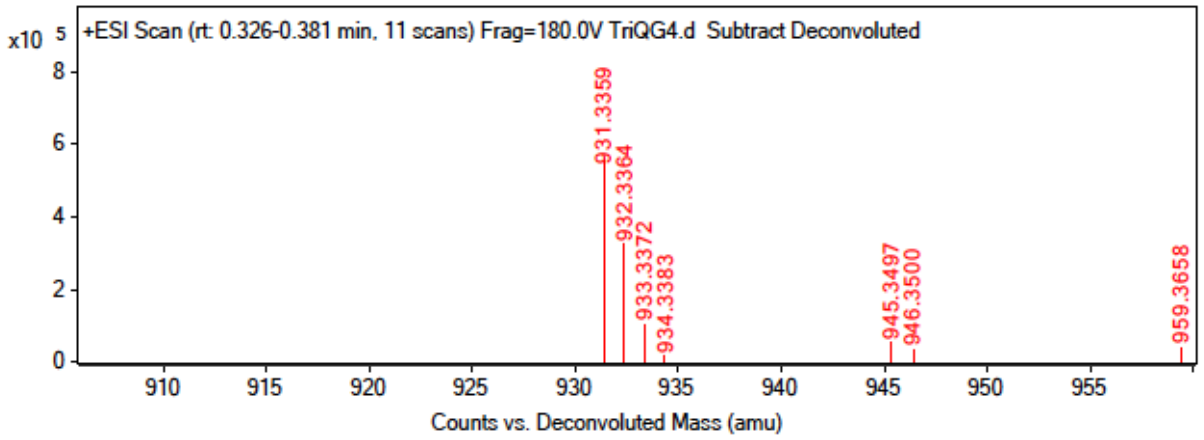

Scheme S13. Synthesis of TriQG5.

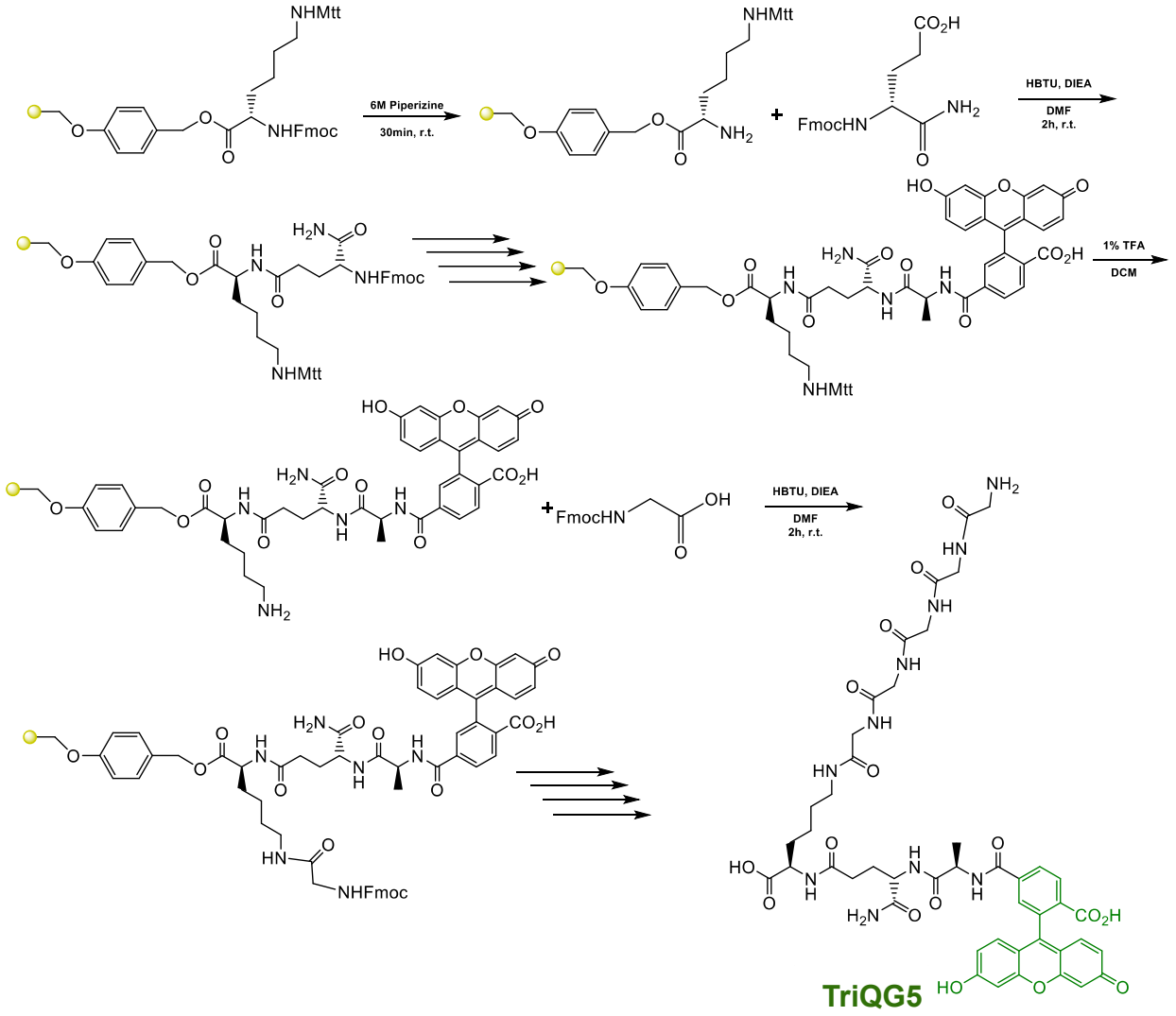

To a 25 mL peptide synthesis vessel charged with Fmoc-Lysine(Mtt)-Wang resin (1.0 g, 0.55mmol). The Fmoc protecting group was removed with 6 M piperazine/100 mM HOBt in DMF (15 ml) for 30 min at ambient temperature, then washed with washed with MeOH and DCM (3 x 15 mL each). Fmoc-D-glutamic acid α-amide (3 eq, 607 mg, 1.65 mmol), HBTU (3 eq, 625 mg, 1.65 mmol), and DIEA (6 eq, 0.574 mL, 3.30 mmol) in DMF (15 mL) were added to the reaction flask and agitated for 2 h at ambient temperature and washed as before. The Fmoc deprotection and coupling procedure was repeated as before using the same equivalencies with Fmoc-L-Alanine-OH. The Fmoc group of L-alanine was deprotected and resin coupled with 5(6)-carboxyfluorescein (2 eq, 413 mg, 1.1 mmol), HBTU (2 eq, 416 mg, 1.1 mmol) and DIEA (6 eq, 0.574 mL, 3.30 mmol) in DMF (15 mL) shaking overnight. The Mtt protecting group was removed by the addition of 1% TFA, 2.5% TIPS, in 10 mL DCM for 15 min, washed and repeated 3 more

times. Fmoc-glycine (3 eq, 513 mg, 1.65 mmol), HBTU (3 eq, 625 mg, 1.65 mmol), and DIEA (6 eq, 0.574 mL, 3.30 mmol) in DMF (15 mL) were added to the reaction flask and agitated for 2 h at ambient temperature and washed as before. The Fmoc group of glycine was deprotected, resin washed, and the Fmoc-glycine procedure was repeated four more times. After Fmoc deprotection, a solution of TFA/DCM (2:1, 20 mL) was added to the resin with agitation for 2 h at ambient temperature. The resin was filtered and resulting solution concentrated *in vacuo*. The residue was trituated with cold diethyl ether and purified using reverse phase HPLC using H_2O/MeOH to yield **TriQG5**. The sample was analyzed for purity using a Shimadzu LC 2020 with a Phenomenex Luna 5µ C18(2) 100Å (30 x 2.00 mm) column; gradient elution with H_2O/CH_3CN.

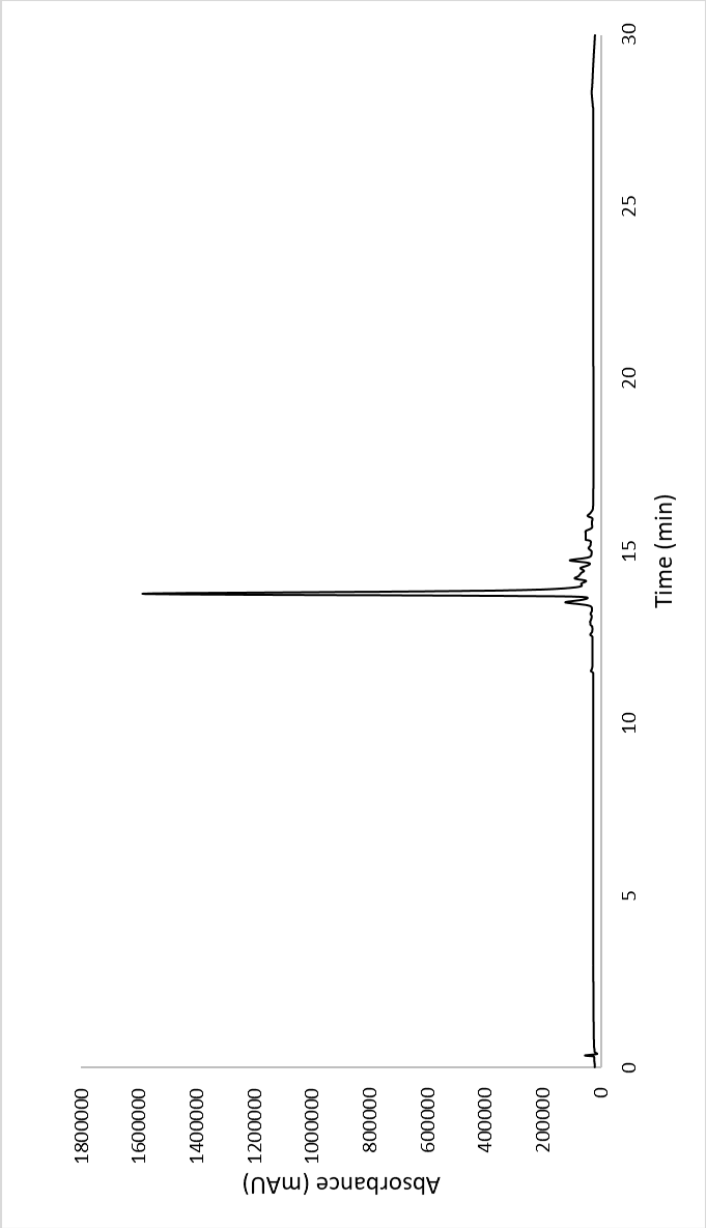

ESI-MS calculated: 988.3563, found: 988.3560

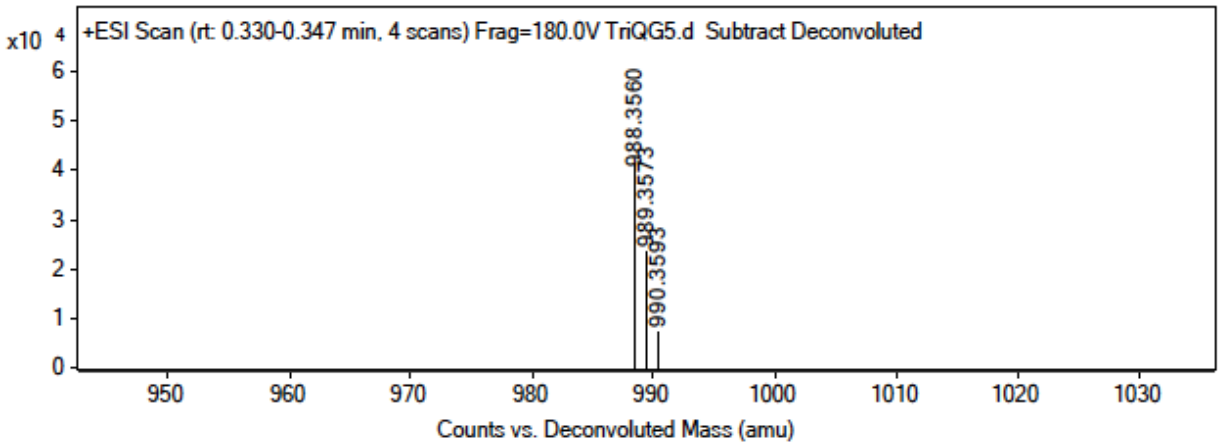

Scheme S14. Synthesis of TriQG6.

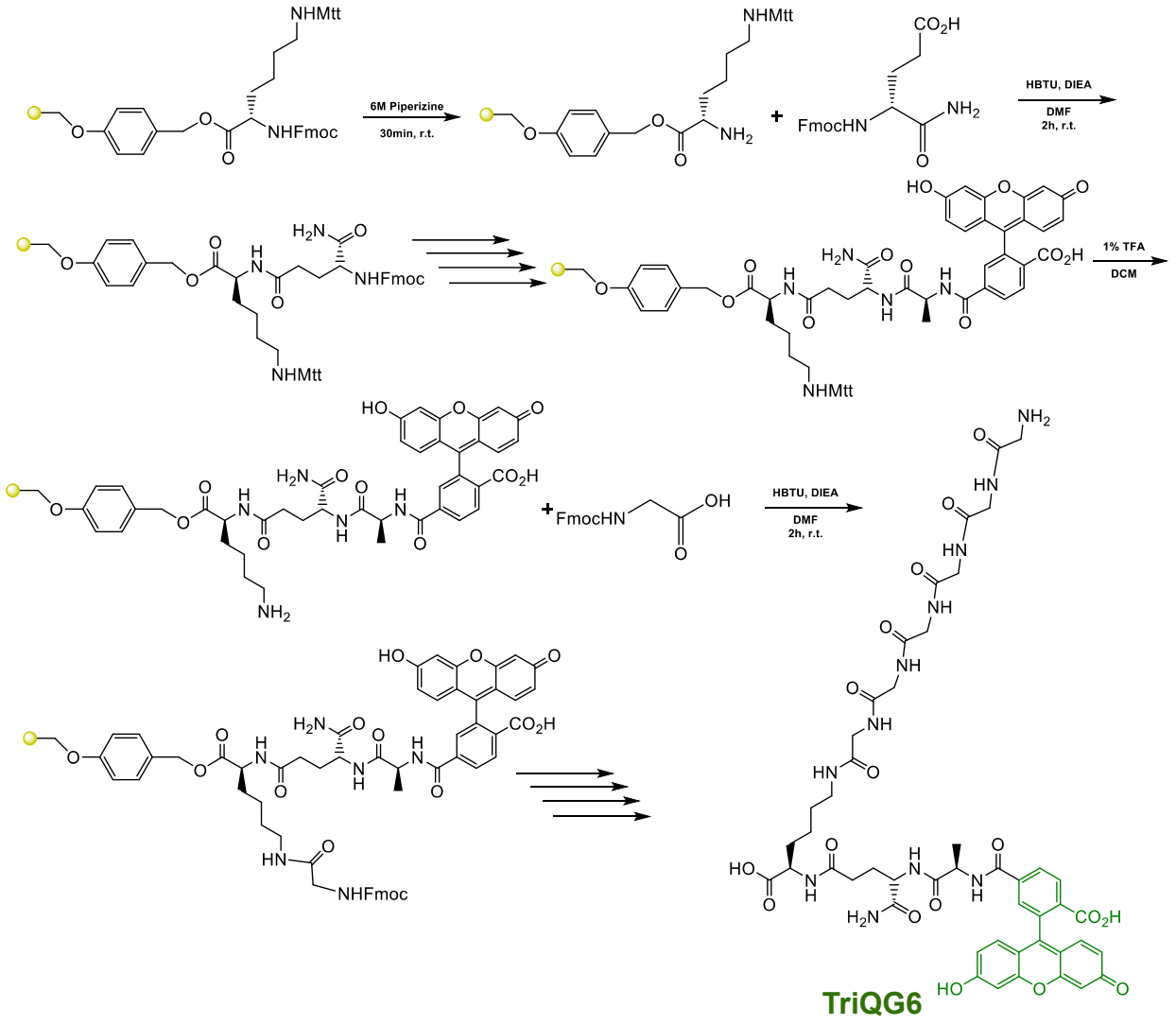

To a 25 mL peptide synthesis vessel charged with Fmoc-Lysine(Mtt)-Wang resin (1.0 g, 0.55mmol). The Fmoc protecting group was removed with 6 M piperazine/100 mM HOBt in DMF (15 ml) for 30 min at ambient temperature, then washed with washed with MeOH and DCM (3 x 15 mL each). Fmoc-D-glutamic acid α-amide (3 eq, 607 mg, 1.65 mmol), HBTU (3 eq, 625 mg, 1.65 mmol), and DIEA (6 eq, 0.574 mL, 3.30 mmol) in DMF (15 mL) were added to the reaction flask and agitated for 2 h at ambient temperature and washed as before. The Fmoc deprotection and coupling procedure was repeated as before using the same equivalencies with Fmoc-L-Alanine-OH. The Fmoc group of L-alanine was deprotected and resin coupled with 5(6)-carboxyfluorescein (2 eq, 413 mg, 1.1 mmol), HBTU (2 eq, 416 mg, 1.1 mmol) and DIEA (6 eq, 0.574 mL, 3.30 mmol) in DMF (15 mL) shaking overnight. The Mtt protecting group was removed by the addition of 1% TFA, 2.5% TIPS, in 10 mL DCM for 15 min, washed and repeated 3 more

times. Fmoc-glycine (3 eq, 513 mg, 1.65 mmol), HBTU (3 eq, 625 mg, 1.65 mmol), and DIEA (6 eq, 0.574 mL, 3.30 mmol) in DMF (15 mL) were added to the reaction flask and agitated for 2 h at ambient temperature and washed as before. The Fmoc group of glycine was deprotected, resin washed, and the Fmoc-glycine procedure was repeated five more times. After Fmoc deprotection, a solution of TFA/DCM (2:1, 20 mL) was added to the resin with agitation for 2 h at ambient temperature. The resin was filtered and resulting solution concentrated *in vacuo*. The residue was trituated with cold diethyl ether and purified using reverse phase HPLC using H_2O/MeOH to yield **TriQG6**. The sample was analyzed for purity using a Shimadzu LC 2020 with a Phenomenex Luna 5µ C18(2) 100Å (30 x 2.00 mm) column; gradient elution with H_2O/CH_3CN.

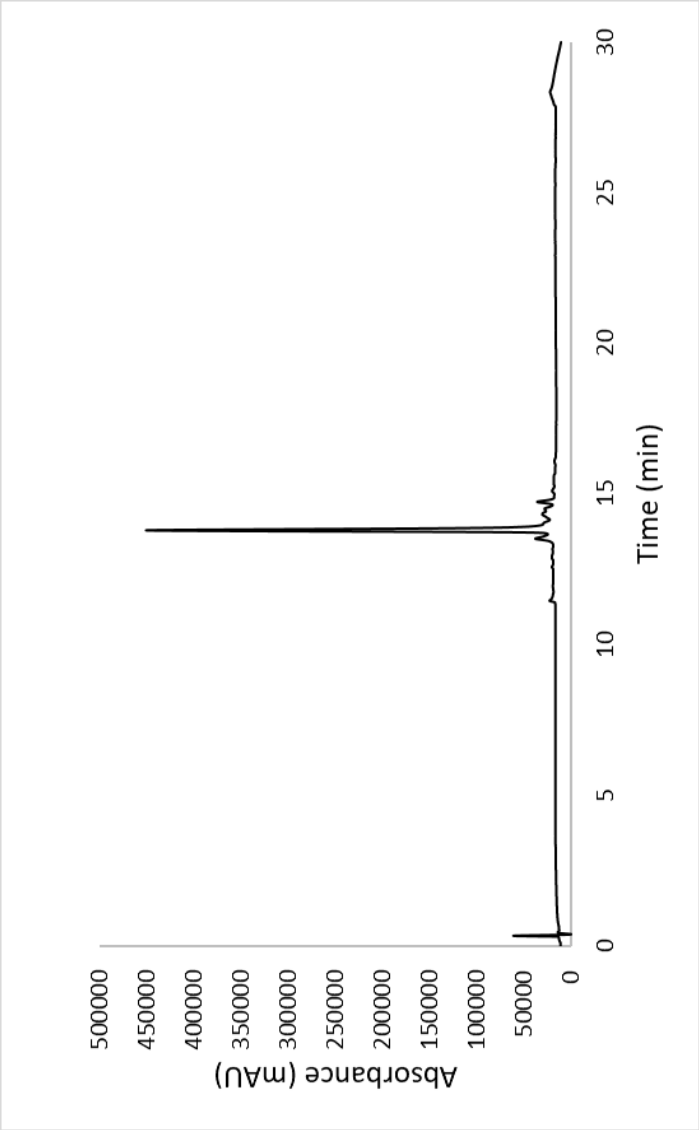

ESI-MS calculated: 1045.3777, found: 1045.3783

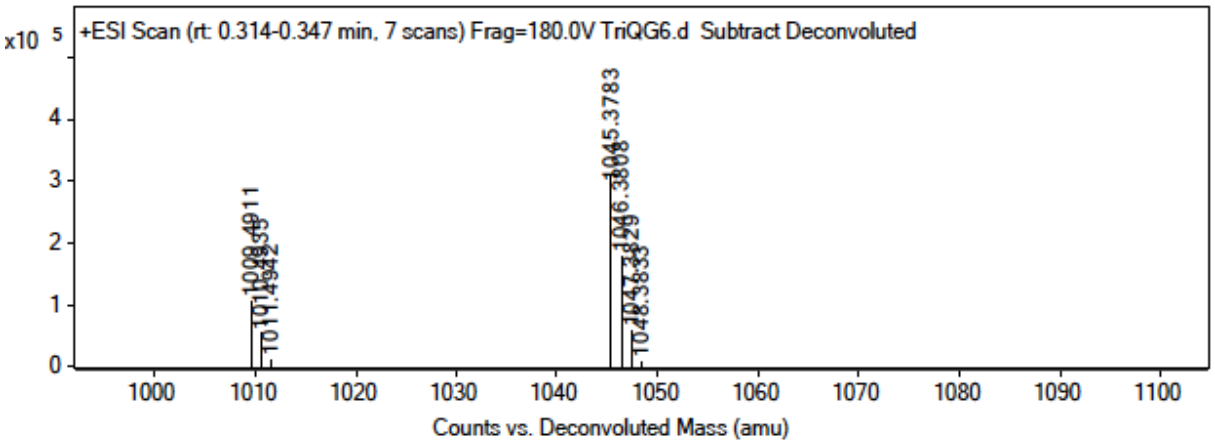

Scheme S15. Synthesis of Coumarin-Tri(Asn).

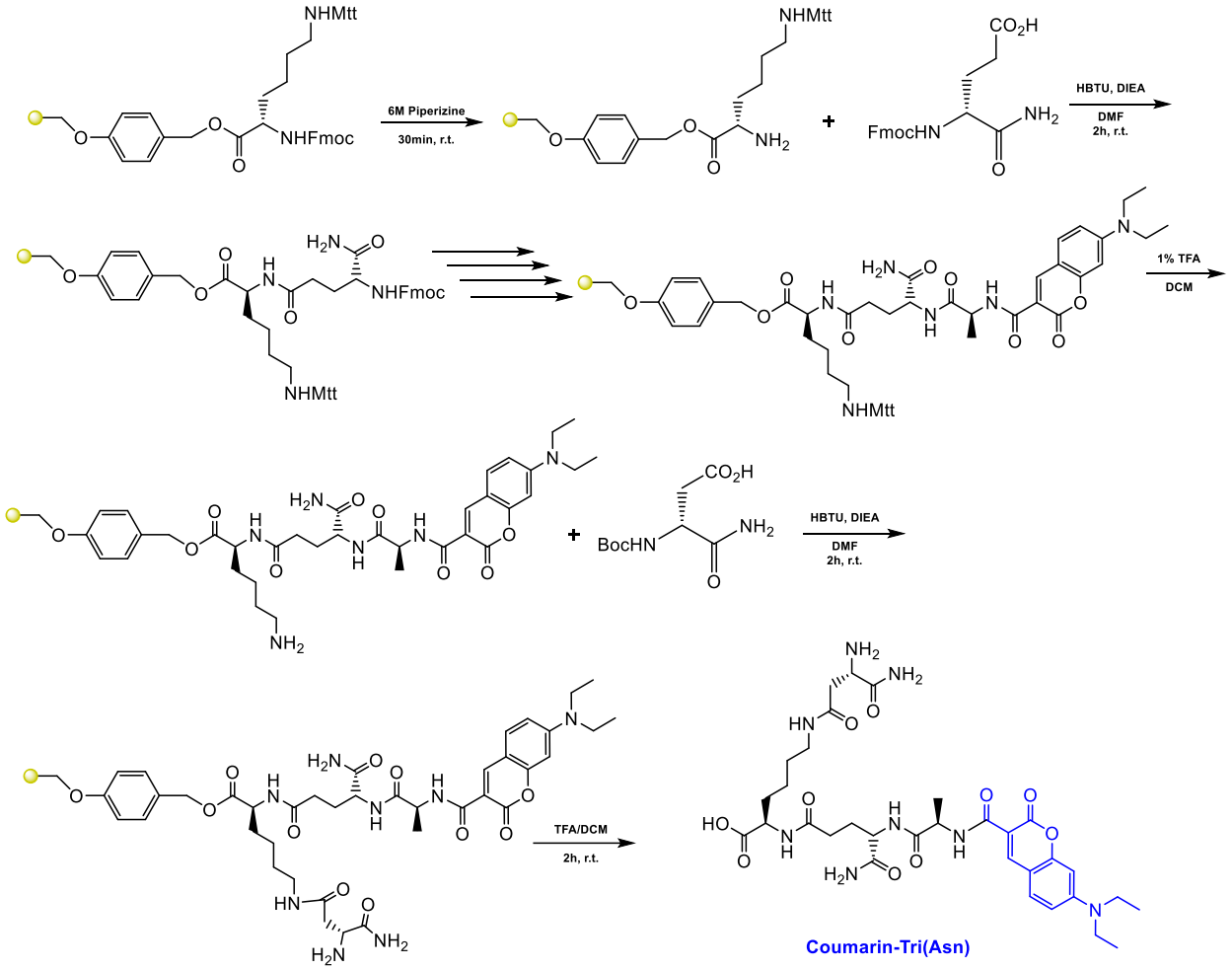

To a 25 mL peptide synthesis vessel charged with Fmoc-Lysine(Mtt)-Wang resin (1.0 g, 0.55mmol). The Fmoc protecting group was removed with 6 M piperazine/100 mM HOBt in DMF (15 ml) for 30 min at ambient temperature, then washed with washed with MeOH and DCM (3 x 15 mL each). Fmoc-D-glutamic acid α-amide (3 eq, 607 mg, 1.65 mmol), HBTU (3 eq, 625 mg, 1.65 mmol), and DIEA (6 eq, 0.574 mL, 3.30 mmol) in DMF (15 mL) were added to the reaction flask and agitated for 2 h at ambient temperature and washed as before. The Fmoc deprotection and coupling procedure was repeated as before using the same equivalencies with Fmoc-L-Alanine-OH. The Fmoc group of L-alanine was deprotected and resin coupled with 7-(Diethylamino)-2-oxo-2H-chromene-3-carboxylic acid (2 eq, 287 mg, 1.1 mmol), HBTU (2 eq, 416 mg, 1.1 mmol) and DIEA (6 eq, 0.574 mL, 3.30 mmol) in DMF (15 mL) shaking overnight. The Mtt protecting group was removed by the addition of 1% TFA, 2.5% TIPS, in 10 mL DCM for 15 min, washed and repeated 3 more times. Boc-D-aspartic acid α-amide (3 eq, 382 mg, 1.65 mmol), HBTU (3 eq, 625 mg, 1.65 mmol), and DIEA (6 eq, 0.574 mL, 3.30 mmol) in DMF (15 mL) were

added to the reaction flask and agitated for 2 h at ambient temperature and washed as before. A solution of TFA/DCM (2:1, 20 mL) was added to the resin with agitation for 2 h at ambient temperature. The resin was filtered and resulting solution concentrated *in vacuo*. The residue was trituated with cold diethyl ether and purified using reverse phase HPLC using H_2O/MeOH to yield **Coumarin-Tri(Asn)**. The sample was analyzed for purity using a Shimadzu LC 2020 with a Phenomenex Luna 5µ C18(2) 100Å (30 x 2.00 mm) column; gradient elution with H_2O/CH_3CN.

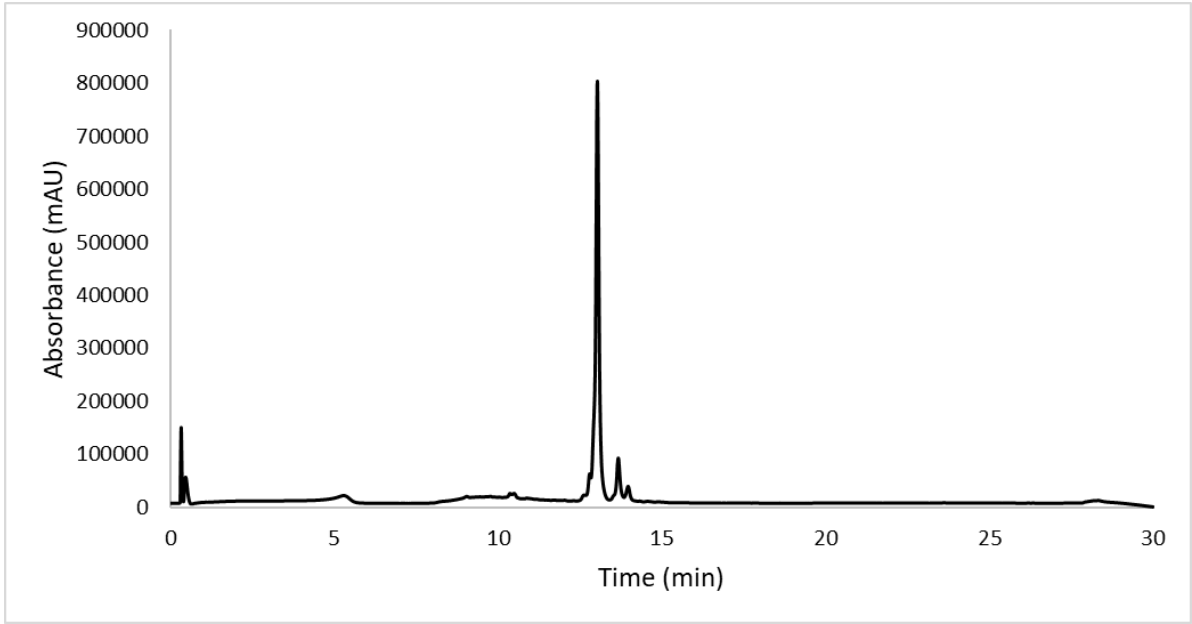
900000
800000
700000
600000
500000
400000
300000
200000
100000
0
Absorbance (mAU)
0
5
10
15
20
25
30
Time (min)

ESI-MS calculated: 702.3337, found: 702.3327

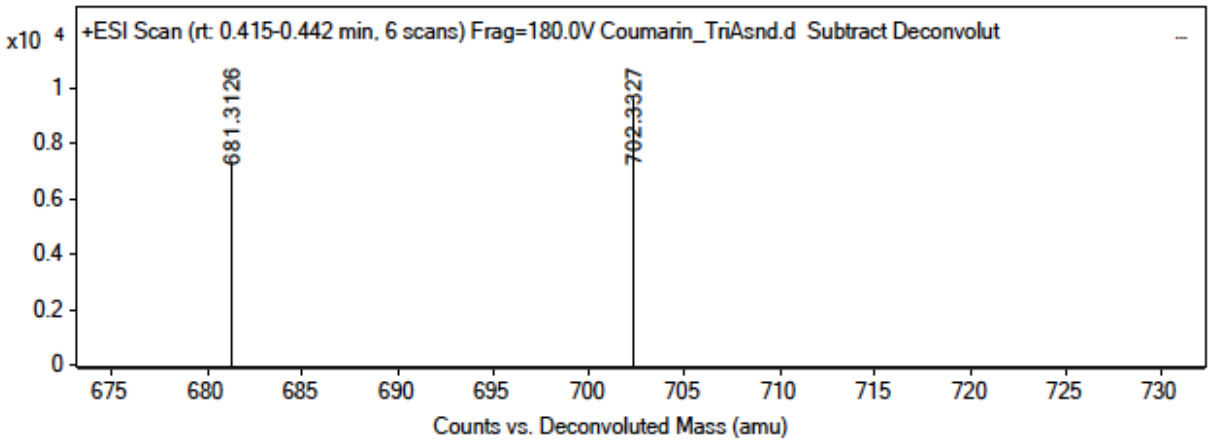

Scheme S16. Synthesis of Rh-TetraQK(Ac).

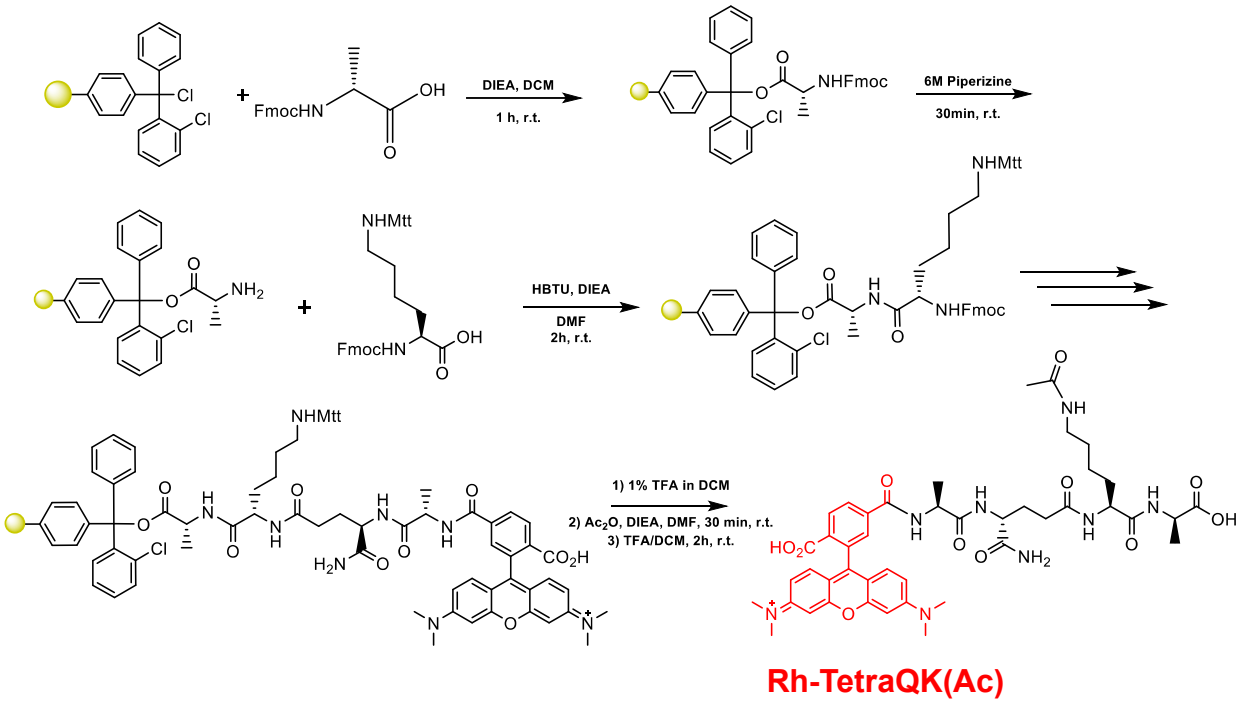

To a 25 mL peptide synthesis vessel charged with Fmoc-D-Alanine Wang resin (950 mg, 0.55 mmol). The Fmoc protecting group was removed with 6 M piperazine/100 mM HOBt in DMF (15 ml) for 30 min at ambient temperature, then washed with MeOH and DCM (3 x 15 mL each). Fmoc-L-Lys(Mtt)-OH (3 eq, 1.02 g, 1.65 mmol), HBTU (3 eq, 625 mg, 1.65 mmol), and DIEA (6 eq, 0.574 mL, 3.30 mmol) in DMF (15 mL) was added to the reaction flask and agitated for 2 h at ambient temperature. The Fmoc deprotection and coupling procedure was repeated as before using the same equivalencies with Fmoc-D-glutamic acid α-amide and Fmoc-L-alanine. The Fmoc group of L-alanine was deprotected and resin coupled with 5(6)-carboxytetramethylrhodamine (2 eq, 473 mg, 1.1 mmol), HBTU (2 eq, 416 mg, 1.1 mmol) and DIEA (6 eq, 0.574 mL, 3.30 mmol) in DMF (15 mL) shaking overnight. The resin was washed as before and added to a solution of 1% TFA / 5% TIPS in DCM and shaken for 10 min and washed. The step was repeated five times for removal of the Mtt group. Acetic anhydride (5 eq, 0.260 mL) and DIEA (10 eq, 0.956 mL) in DMF was added and resin shaken for 30 min at ambient temperature. The resin was washed and added to a solution of TFA/DCM (2:1, 20 mL) with agitation for 2 h at ambient temperature. The resin was filtered and resulting solution concentrated *in vacuo*. The residue was trituated with cold diethyl ether and purified using reverse phase HPLC using H_2O/MeOH**.** The sample was analyzed for purity using a Shimadzu LC 2020 with a

Phenomenex Luna 5µ C18(2) 100Å (30 x 2.00 mm) column; gradient elution with H_2O/CH_3CN.

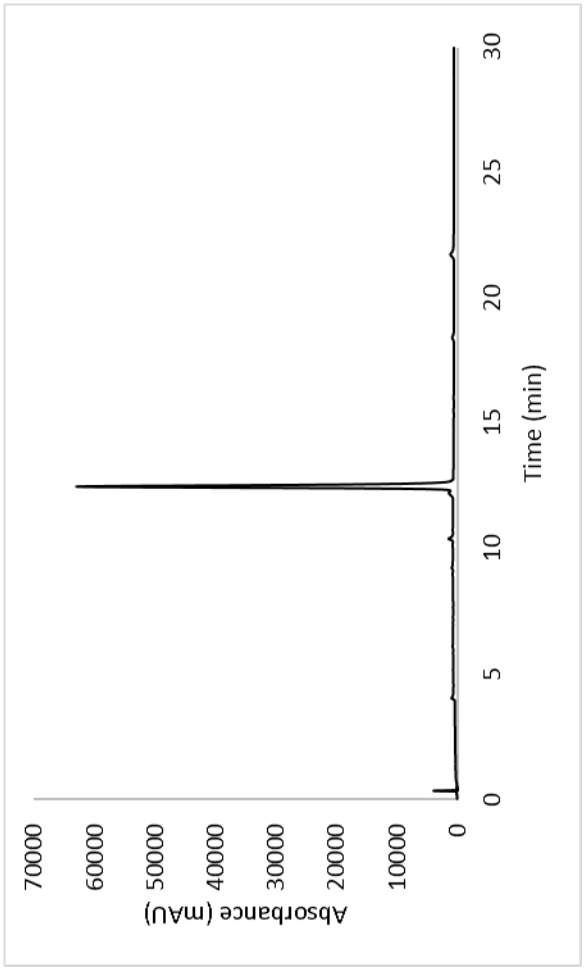

ESI-MS calculated: 870.3912, found: 870.3903

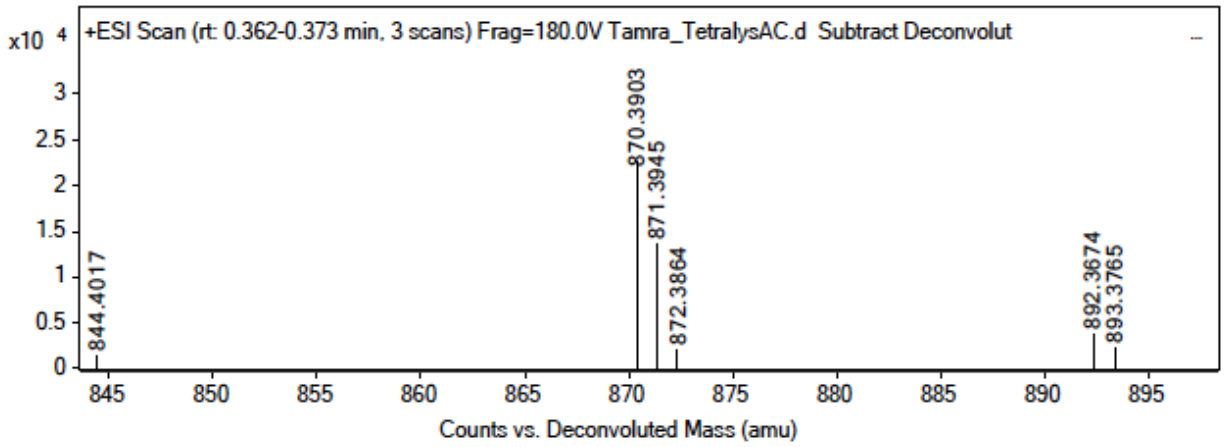

A.4 *Synthesis and Characterization of Compounds in Chapter 4*

Scheme S1. Synthesis of Tri_{Q}Cysteine

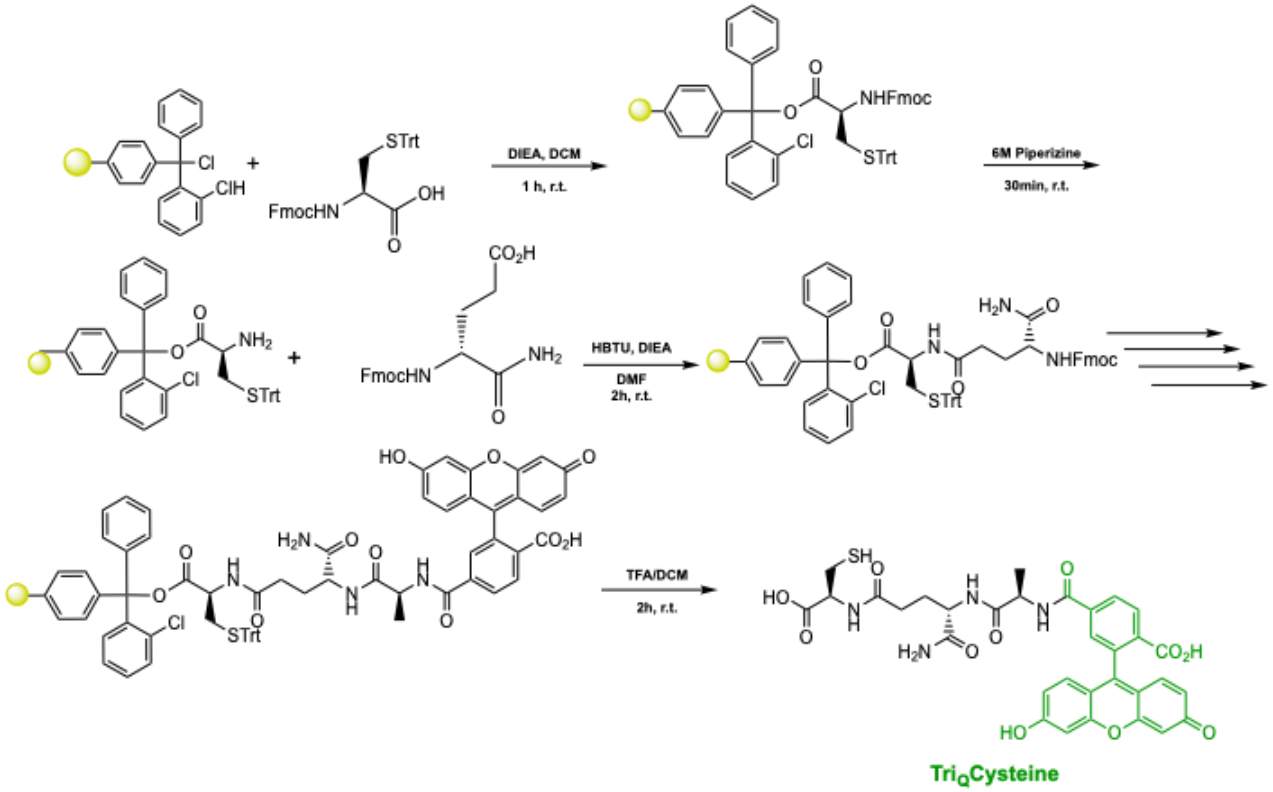

Fmoc-L-Cysteine(Trt)-OH (1.1 eq, 354 mg, 0.605 mmol) was added to a 25 mL peptide synthesis vessel charged with 2-Chlorotrityl chloride resin (500 mg, 0.55 mmol) and DIEA (4 eq, 0.422 mL, 2.20 mmol) in dry DCM (5 mL). The resin was agitated for 1 h at ambient temperature and washed with MeOH and DCM (3 x 15 mL each). The Fmoc protecting group was removed with 6 M piperazine/100 mM HOBt in DMF (15 ml) for 30 min at ambient temperature, then washed as before. Fmoc-D-glutamic acid α-amide (3 eq, 607 mg, 1.65 mmol), HBTU (3 eq, 625 mg, 1.65 mmol), and DIEA (6 eq, 0.574 mL, 3.30 mmol) in DMF (10 mL) were added to the reaction flask and agitated for 2 h at ambient temperature. The Fmoc deprotection and coupling procedure was repeated as before using the same equivalencies with Fmoc-L-Alanine-OH. The Fmoc group of L-alanine was deprotected and coupled with 5(6)-carboxyfluorescein (2 eq, 413 mg, 1.1 mmol), HBTU (2 eq, 416 mg, 1.10 mmol) and DIEA (6 eq, 0.574 mL, 3.30 mmol) in DMF (10 mL) shaking overnight. The resin was washed as before and added to a solution of TFA/H_2O/TIPS (95%, 2.5%, 2.5%, 20 mL) with agitation for 2 h at ambient temperature. The resin was

filtered and resulting solution concentrated *in vacuo*. The residue was trituated with cold diethyl ether.

Reaction: Tri$_Q$*m*CYT

Crude **Tri$_Q$Cysteine** was dissolved in Ammonium Bicarbonate (1M, pH 9) and flowed with N_2 gas. D-Cystine (ChemImpex, 02872) (5 eq, 220 mg, 2.75 mmol) was dissolved in 0.1 M NaOH, pH 8, sonicated and vacuum pumped to remove air, and added to **Tri$_Q$Cysteine** with mixing for 2 h sealed from air. The resulting solution was concentrated *in vacuo* and purified using Reversed-Phase HPLC with H_2O/MeOH to yield **Tri$_Q$*m*CYT**. The sample was analyzed for purity using an Agilent 1200 HPLC with a Phenomenex Luna 5µ C4 300Å (250 x 2.00 mm) column; gradient elution with H_2O/CH_3CN.

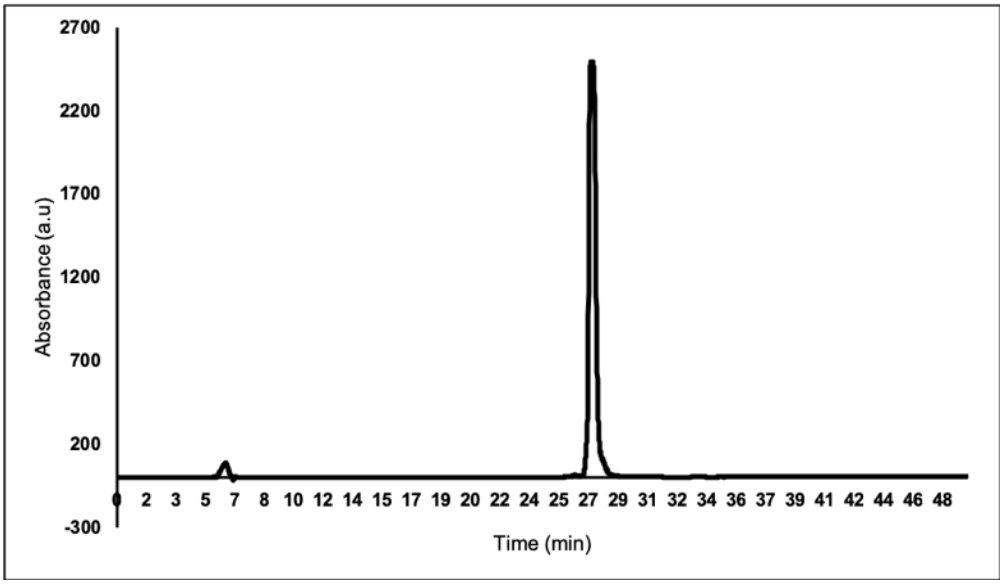

ESI-MS calculated [M + H$^+$]: 798.1746, found: 798.1739

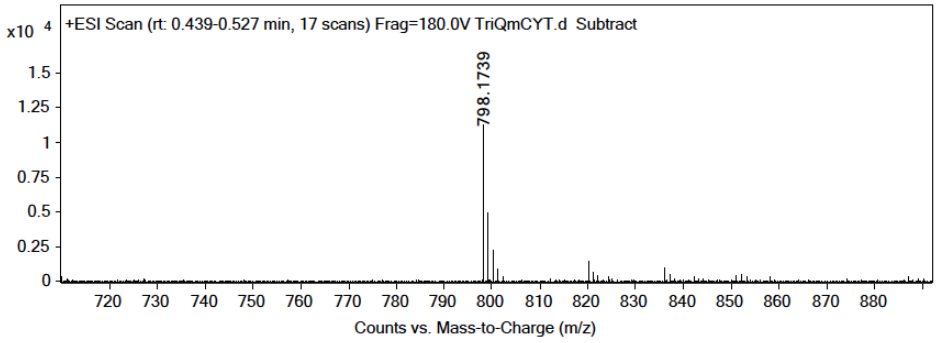

Reaction: Tri$_Q$Cystamine

Crude **Tri$_Q$Cysteine** was dissolved in Ammonium Bicarbonate (1M, pH 9) and flowed with N_2 gas. Cystamine dihydrochloride (TCI, C0875) (10 eq, 756 mg, 5.5 mmol) was dissolved in 0.1 M NaOH, pH 8, sonicated and vacuum pumped to remove air, and added to **Tri$_Q$Cysteine** with mixing for 2 h sealed from air. The resulting solution was concentrated *in vacuo* and purified using Reversed-Phase HPLC with H_2O/MeOH to yield **Tri$_Q$Cystamine**. The sample was analyzed for purity using an Agilent 1200 HPLC with a Phenomenex Luna 5µ C4 300Å (250 x 2.00 mm) column; gradient elution with H_2O/CH_3CN.

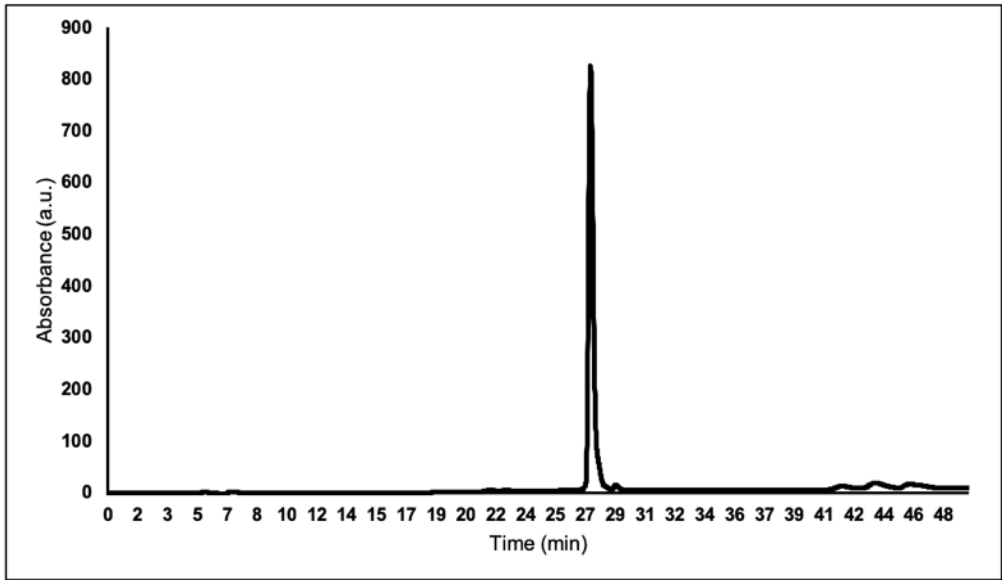

ESI-MS calculated [M + H$^+$]: 754.1847, found: 754.1844

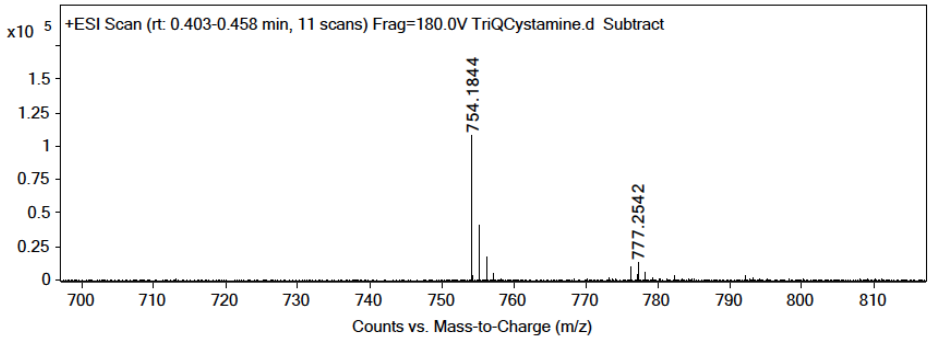

Scheme S2. Synthesis of D-Cys(NH_2)

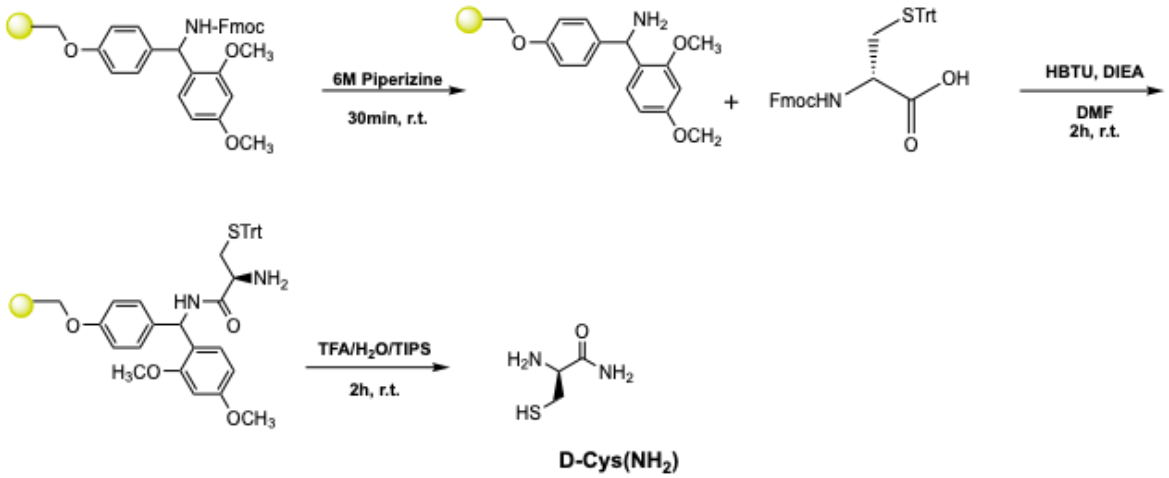

D-Cys(NH_2)

A 50 mL peptide synthesis vessel charged with rink amide resin (3.00g, 0.45 mmol) was deprotected for 30 min at ambient temperature, washed as before, and loaded with Fmoc-D-Cysteine(Trt) (3 eq, 2.37 g, 1.35 mmol), HBTU (3 eq, 1.54 g, 1.35 mmol), and DIEA (6 eq, 1.41 mL, 2.70 mmol) in DMF (30 mL) for 2 h with agitation at ambient temperature. The Fmoc protecting group was removed, washed as before, and the resin was added to a solution of TFA/H_2O/TIPS (95%, 2.5%, 2.5%, 20 mL) with agitation for 2 h at ambient temperature. The resin was filtered and resulting solution concentrated *in vacuo*.

Reaction: Tri_Q*m*CYT_{NH2}.

Crude **Tri_QCysteine** was added to the concentrated **D-Cys(NH_2)**. Both were dissolved in Ammonium Bicarbonate (1M, pH 9) and 0.1 M NaOH, pH 8 with a small amount of DMSO to aid in oxidation. The reaction was left open to air with stirring for 2 h. The resulting solution was concentrated *in vacuo* and purified using Reversed-Phase HPLC with H_2O/MeOH to yield **Tri_Q*m*CYT_{NH2}**. The sample was analyzed for purity using an Agilent 1200 HPLC with a Phenomenex Luna 5µ C4 300Å (250 x 2.00 mm) column; gradient elution with H_2O/CH_3CN.

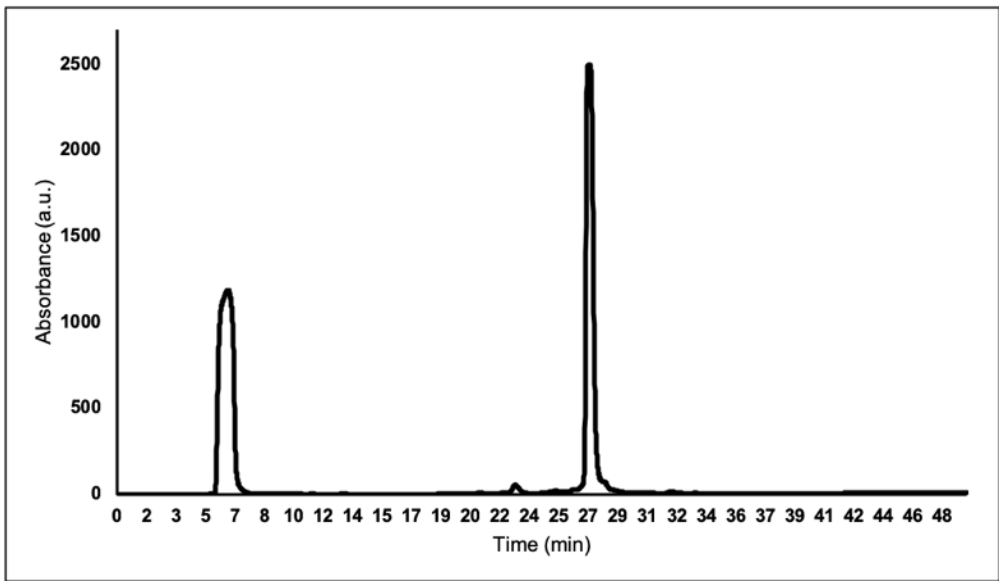

ESI-MS calculated [M + H^+]: 797.1906, found: 797.1907

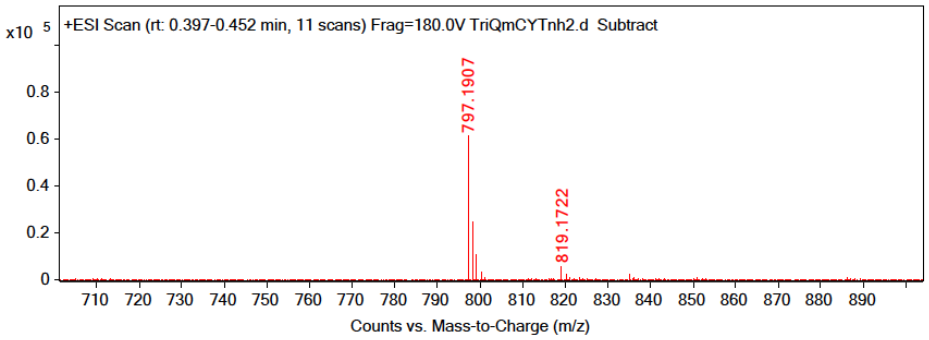

Scheme S3. Synthesis of Tri$_E$Cysteine

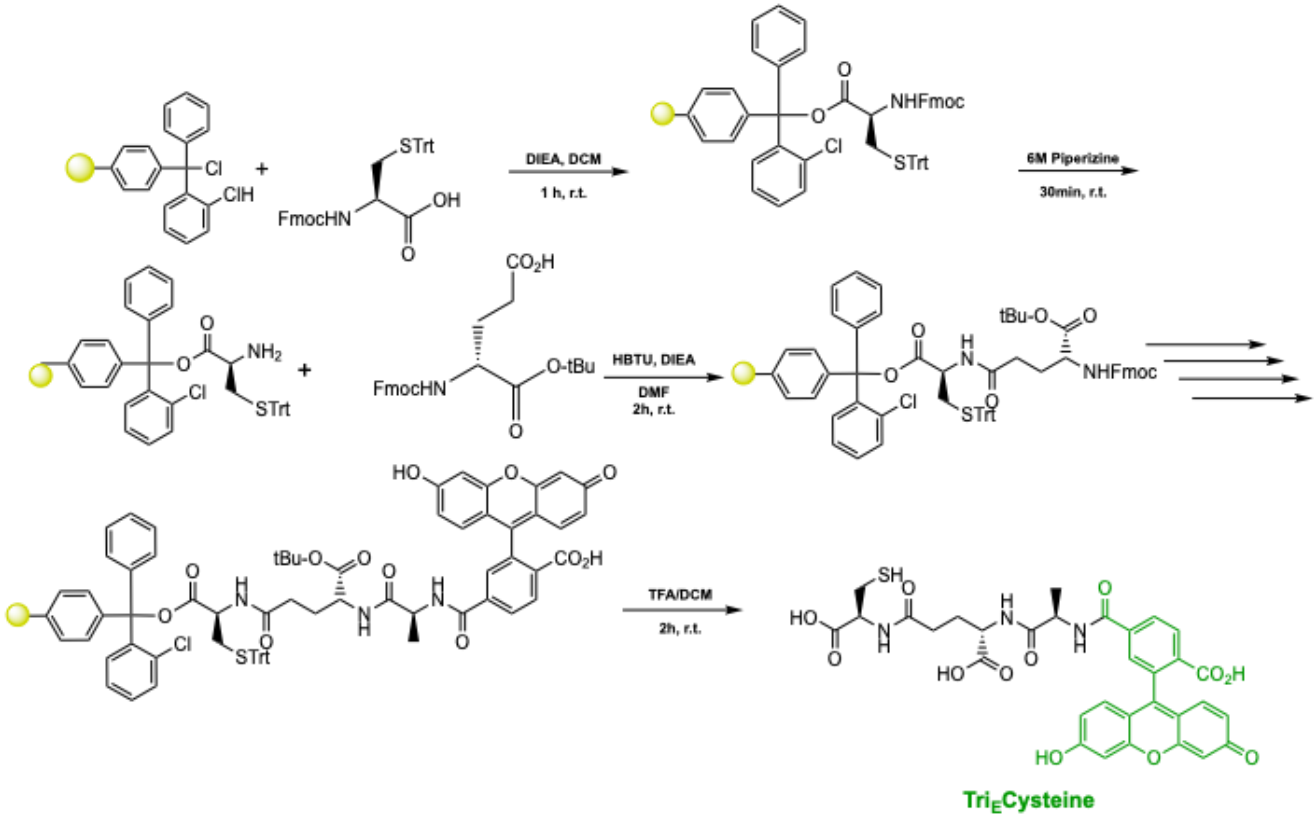

Fmoc-L-Cysteine(Trt)-OH (1.1 eq, 354 mg, 0.605 mmol) was added to a 25 mL peptide synthesis vessel charged with 2-Chlorotrityl chloride resin (500 mg, 0.55 mmol) and DIEA (4 eq, 0.422 mL, 2.20 mmol) in dry DCM (5 mL). The resin was agitated for 1 h at ambient temperature and washed with MeOH and DCM (3 x 15 mL each). The Fmoc protecting group was removed with 6 M piperazine/100 mM HOBt in DMF (15 ml) for 30 min at ambient temperature, then washed as before. Fmoc-D-glutamic acid α-*tert* butyl ester (3 eq, 701 mg, 1.65 mmol), HBTU (3 eq, 625 mg, 1.65 mmol), and DIEA (6 eq, 0.574 mL, 3.30 mmol) in DMF (10 mL) were added to the reaction flask and agitated for 2 h at ambient temperature. The Fmoc deprotection and coupling procedure was repeated as before using the same equivalencies with Fmoc-L-Alanine-OH. The Fmoc group of L-alanine was deprotected and coupled with 5(6)-carboxyfluorescein (2 eq, 413 mg, 1.1 mmol), HBTU (2 eq, 416 mg, 1.10 mmol) and DIEA (6 eq, 0.574 mL, 3.30 mmol) in DMF (10 mL) shaking overnight. The resin was washed as before and added to a solution of TFA/H_2O/TIPS (95%, 2.5%, 2.5%, 20 mL) with agitation for 2 h at ambient temperature. The resin was

filtered and resulting solution concentrated *in vacuo*. The residue was trituated with cold diethyl ether.

Reaction: Tri$_E$*m*CYT

Crude **Tri$_E$Cysteine** was dissolved in Ammonium Bicarbonate (1M, pH 9) and flowed with N_2 gas. D-Cystine (ChemImpex, 02872) (5 eq, 220 mg, 2.75 mmol) was dissolved in 0.1 M NaOH, pH 8, sonicated and vacuum pumped to remove air, and added to **Tri$_E$Cysteine** with mixing for 2 h sealed from air. The resulting solution was concentrated *in vacuo* and purified using Reversed-Phase HPLC with H_2O/MeOH to yield **Tri$_E$*m*CYT**. The sample was analyzed for purity using an Agilent 1200 HPLC with a Phenomenex Luna 5µ C4 300Å (250 x 2.00 mm) column; gradient elution with H_2O/CH_3CN.

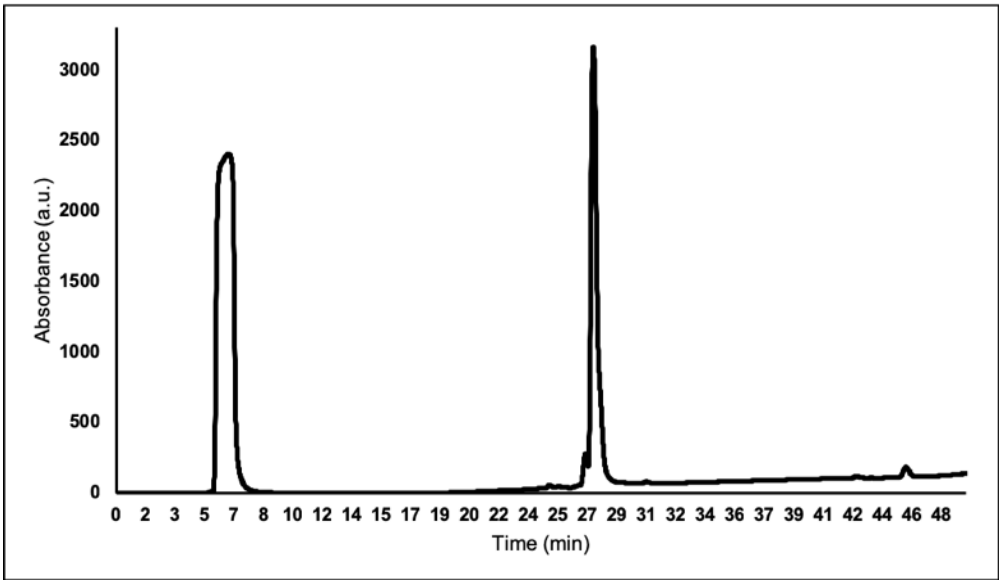

ESI-MS calculated [M + H$^+$]: 799.1586, found: 799.1577

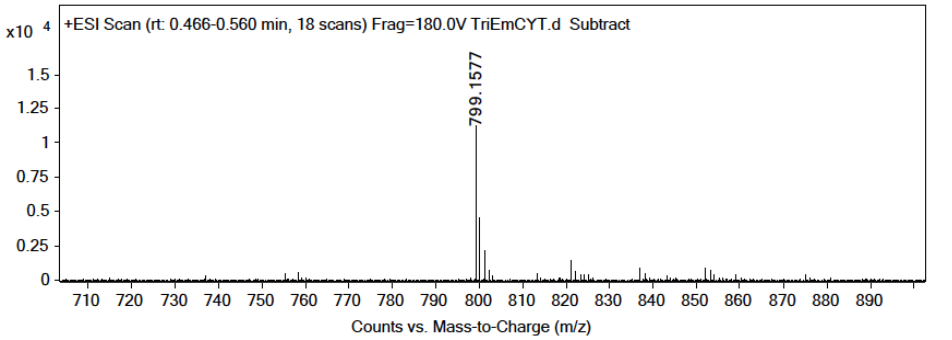

Reaction: Tri$_E$*m*CYT$_{NH2}$

Crude **Tri$_E$Cysteine** was added to the concentrated **D-Cys(NH$_2$)**. Both were dissolved in Ammonium Bicarbonate (1M, pH 9) and 0.1 M NaOH, pH 8 with a small amount of DMSO to aid in oxidation. The reaction was left open to air with stirring for 2 h. The resulting solution was concentrated *in vacuo* and purified using Reversed-Phase HPLC with H_2O/MeOH to yield **Tri$_E$*m*CYT$_{NH2}$**. The sample was analyzed for purity using an Agilent 1200 HPLC with a Phenomenex Luna 5µ C4 300Å (250 x 2.00 mm) column; gradient elution with H_2O/CH_3CN.

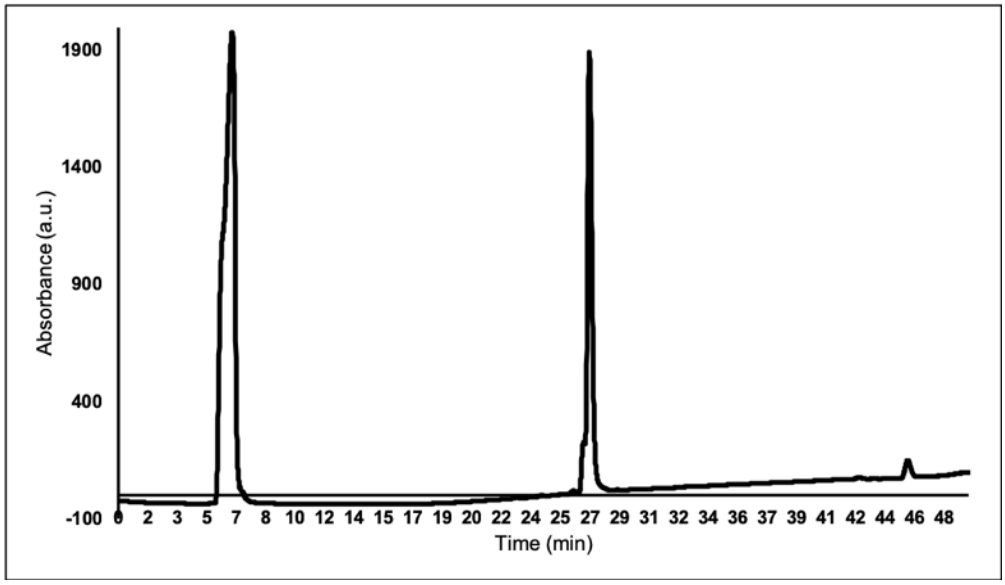

ESI-MS calculated [M + H$^+$]: 798.1746, found: 798.1741

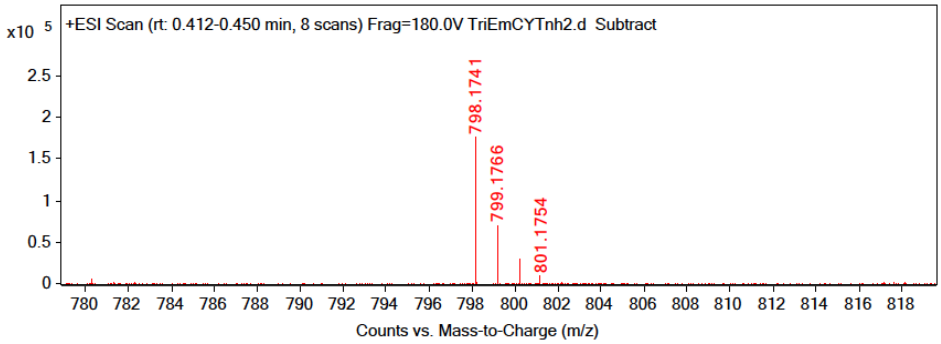

Scheme S4. Synthesis of Tri_QLLys

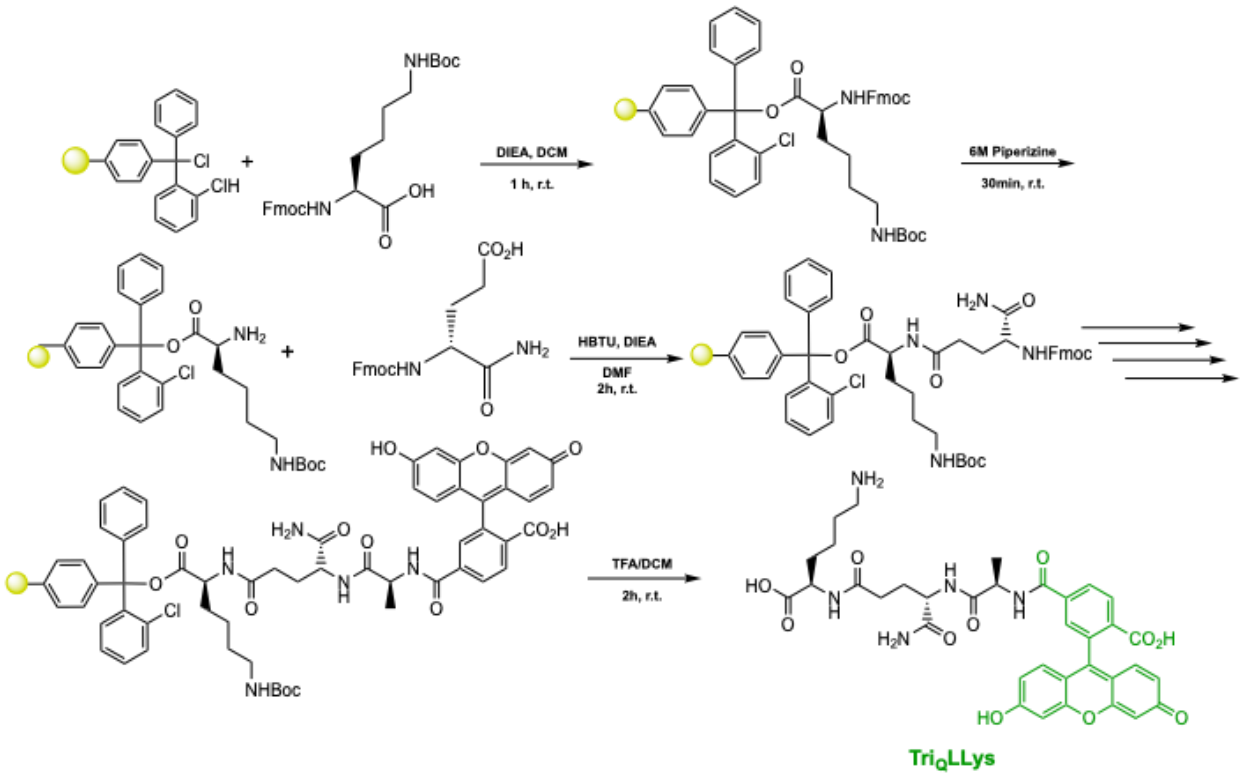

Fmoc-L-Lysine(Boc)-OH (1.1 eq, 283 mg, 0.605 mmol) was added to a 25 mL peptide synthesis vessel charged with 2-Chlorotrityl chloride resin (500 mg, 0.55 mmol) and DIEA (4 eq, 0.422 mL, 2.20 mmol) in dry DCM (5 mL). The resin was agitated for 1 h at ambient temperature and washed with MeOH and DCM (3 x 15 mL each). The Fmoc protecting group was removed with 6 M piperazine/100 mM HOBt in DMF (15 ml) for 30 min at ambient temperature, then washed as before. Fmoc-D-glutamic acid α-amide (3 eq, 607 mg, 1.65 mmol), HBTU (3 eq, 625 mg, 1.65 mmol), and DIEA (6 eq, 0.574 mL, 3.30 mmol) in DMF (10 mL) were added to the reaction flask and agitated for 2 h at ambient temperature. The Fmoc deprotection and coupling procedure was repeated as before using the same equivalencies with Fmoc-L-Alanine-OH. The Fmoc group of L-alanine was deprotected and coupled with 5(6)-carboxyfluorescein (2 eq, 413 mg, 1.1 mmol), HBTU (2 eq, 416 mg, 1.10 mmol) and DIEA (6 eq, 0.574 mL, 3.30 mmol) in DMF (10 mL) shaking overnight. The resin was washed as before and added to a solution of TFA/H_2O/TIPS (95%, 2.5%, 2.5%, 20 mL) with agitation for 2 h at ambient temperature. The resin was filtered and resulting solution concentrated *in vacuo*. The residue was trituated with cold diethyl ether and purified using reverse phase HPLC using H_2O/MeOH to yield **Tri_QLLys**.

The sample was analyzed for purity using an Agilent 1200 HPLC with a Phenomenex Luna 5µ C4 300Å (250 x 2.00 mm) column; gradient elution with H_2O/CH_3CN.

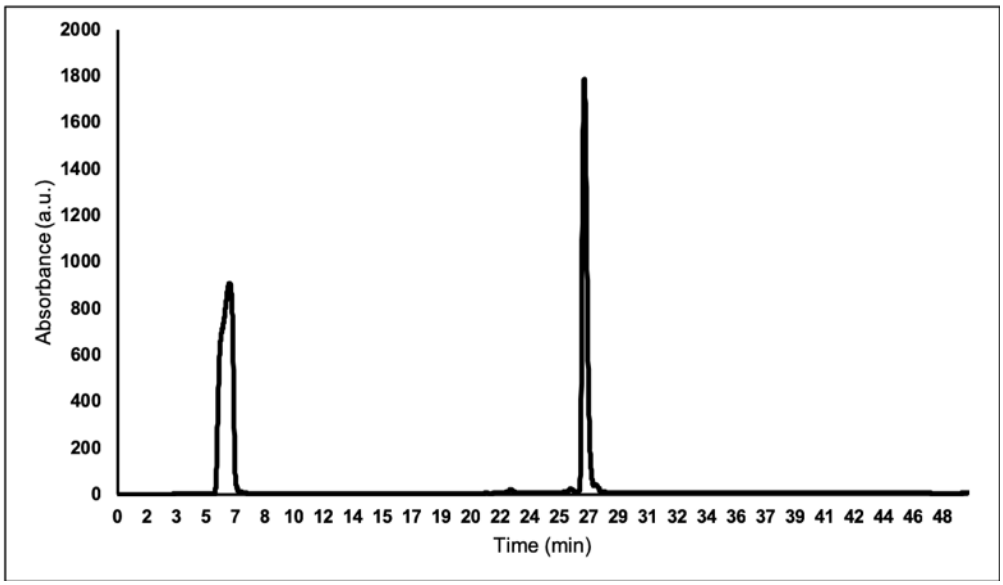

ESI-MS calculated [M + H^+]: 704.2563, found: 704.2706

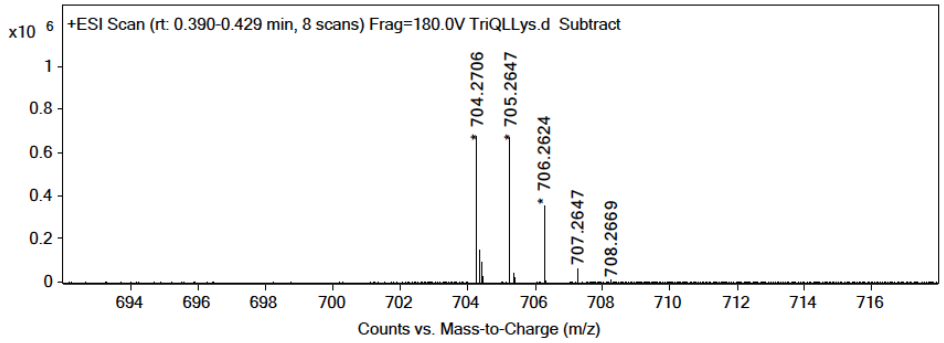

Scheme S5. Synthesis of Tetra$_Q$LLys

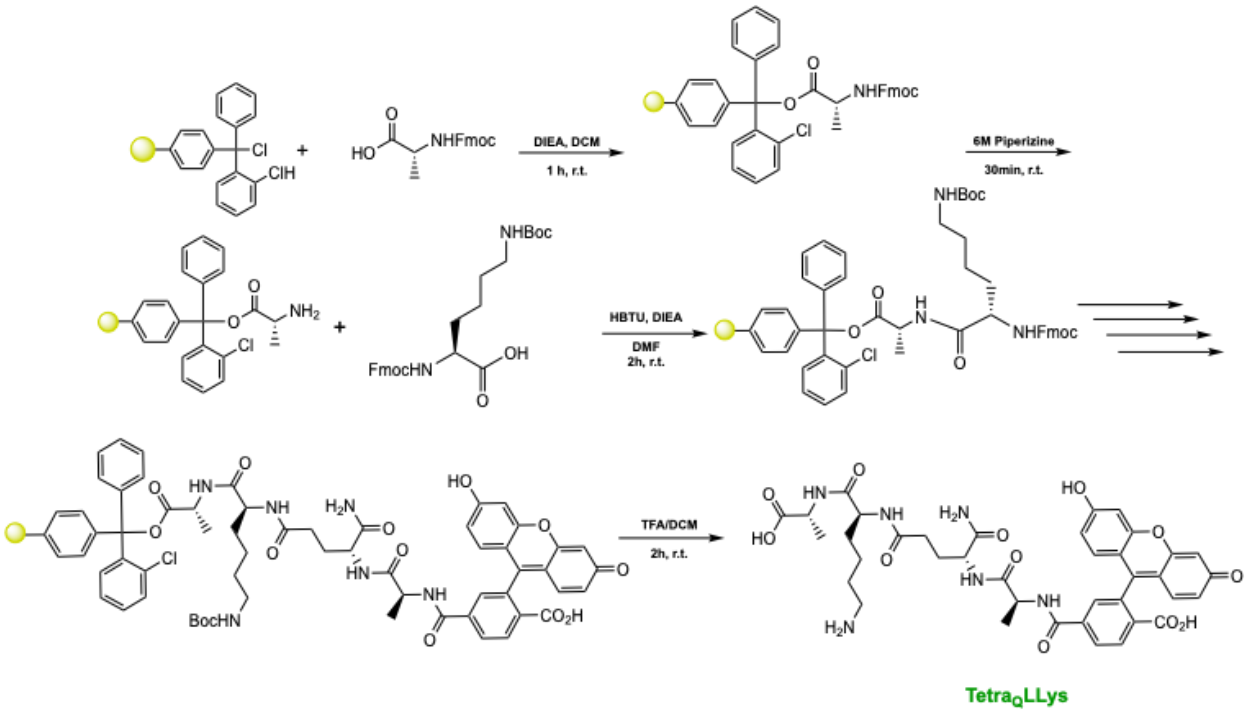

Fmoc-D-Alanine-OH (1.1 eq, 188 mg, 0.605 mmol) was added to a 25 mL peptide synthesis vessel charged with 2-Chlorotrityl chloride resin (500 mg, 0.55 mmol) and DIEA (4 eq, 0.422 mL, 2.20 mmol) in dry DCM (5 mL). The resin was agitated for 1 h at ambient temperature and washed with MeOH and DCM (3 x 15 mL each). The Fmoc protecting group was removed with 6 M piperazine/100 mM HOBt in DMF (15 ml) for 30 min at ambient temperature, then washed as before. Fmoc-L-Lys(Boc)-OH (3 eq, 773 mg, 1.65 mmol), HBTU (3 eq, 625 mg, 1.65 mmol), and DIEA (6 eq, 0.574 mL, 3.30 mmol) in DMF (15 mL) were added to the reaction flask and agitated for 2 h at ambient temperature. The Fmoc deprotection and coupling procedure was repeated as before using the same equivalencies with Fmoc-D-glutamic acid α-amide and Fmoc-L-Alanine-OH. The Fmoc group of L-alanine was deprotected and coupled with 5(6)-carboxyfluorescein (2 eq, 413 mg, 1.1 mmol), HBTU (2 eq, 416 mg, 1.10 mmol) and DIEA (6 eq, 0.574 mL, 3.30 mmol) in DMF (10 mL) shaking overnight. The resin was washed as before and added to a solution of TFA/H_2O/TIPS (95%, 2.5%, 2.5%, 20 mL) with agitation for 2 h at ambient temperature. The resin was filtered and resulting solution concentrated *in vacuo*. The residue was trituated with cold diethyl ether and purified using reverse phase HPLC using H_2O/MeOH to yield **Tetra$_Q$LLys**. The sample was analyzed for purity using a Waters 1525 HPLC with a Phenomenex Luna 5µ C8(2) 100Å (250 x 4.6 mm) column; gradient elution with H_2O/CH_3CN.

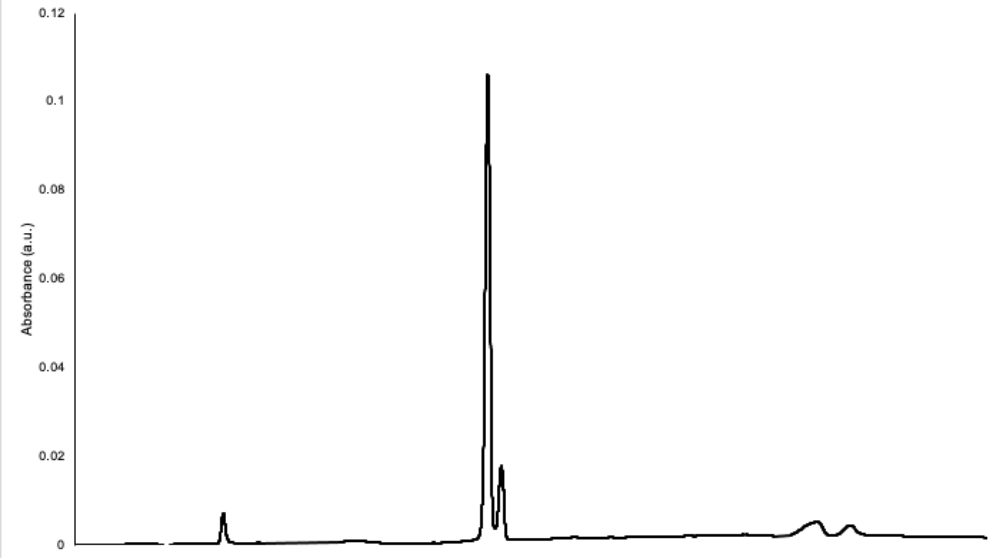

ESI-MS calculated [M + H^+]: 775.2933, found: 775.2927

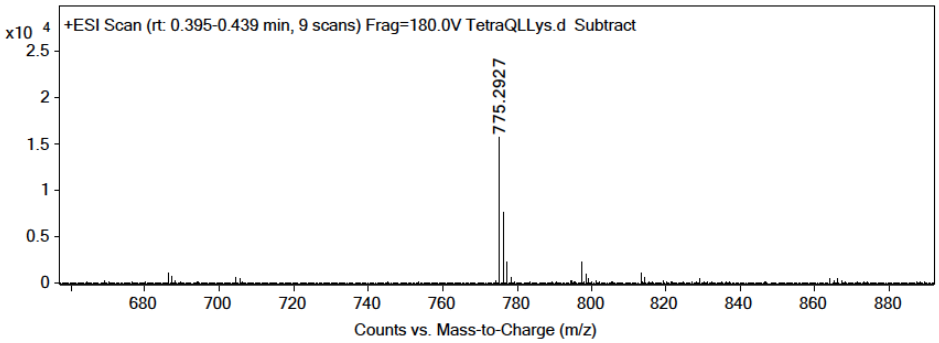

Scheme S6. Synthesis of Tetra$_Q$Cysteine

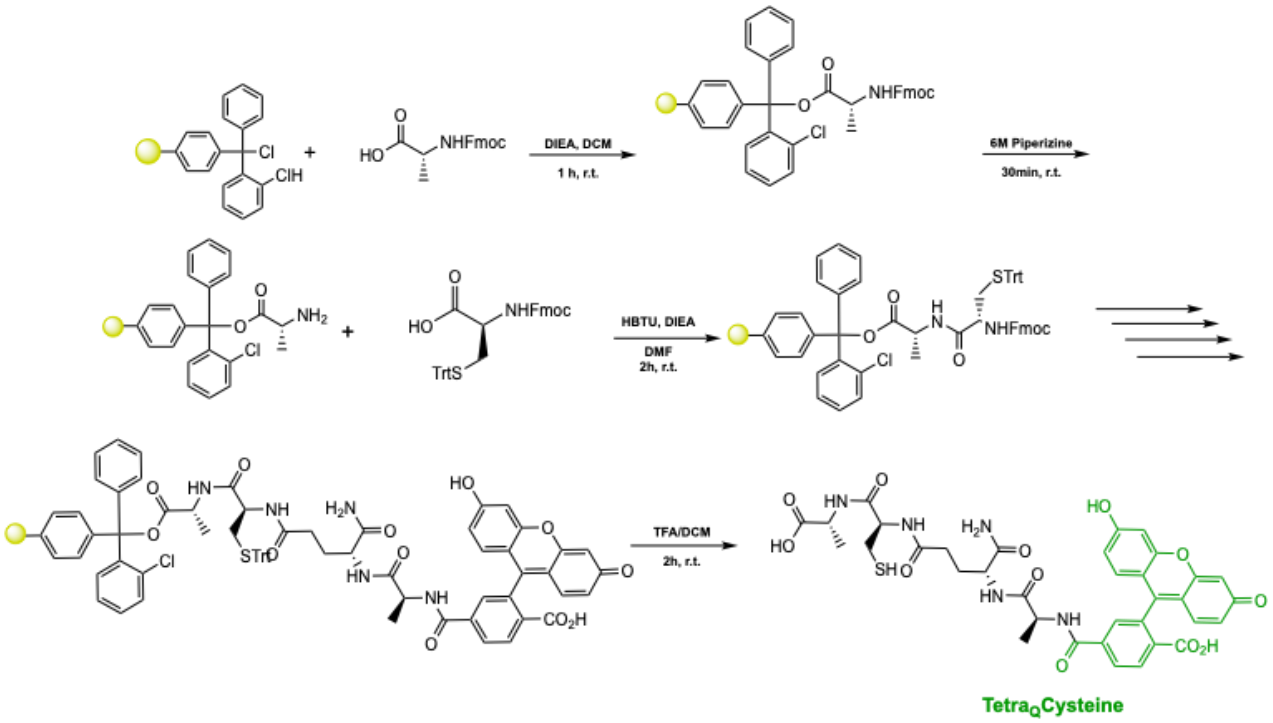

Fmoc-D-Alanine-OH (1.1 eq, 188 mg, 0.605 mmol) was added to a 25 mL peptide synthesis vessel charged with 2-Chlorotrityl chloride resin (500 mg, 0.55 mmol) and DIEA (4 eq, 0.422 mL, 2.20 mmol) in dry DCM (5 mL). The resin was agitated for 1 h at ambient temperature and washed with MeOH and DCM (3 x 15 mL each). The Fmoc protecting group was removed with 6 M piperazine/100 mM HOBt in DMF (15 ml) for 30 min at ambient temperature, then washed as before. Fmoc-L-Cysteine(Trt)-OH (3 eq, 967 mg, 1.65 mmol), HBTU (3 eq, 625 mg, 1.65 mmol), and DIEA (6 eq, 0.574 mL, 3.30 mmol) in DMF (10 mL) were added to the reaction flask and agitated for 2 h at ambient temperature. The Fmoc deprotection and coupling procedure was repeated as before using the same equivalencies with Fmoc-D-glutamic acid α-*tert* butyl ester and Fmoc-L-Alanine-OH. The Fmoc group of L-alanine was deprotected and coupled with 5(6)-carboxyfluorescein (2 eq, 413 mg, 1.1 mmol), HBTU (2 eq, 416 mg, 1.10 mmol) and DIEA (6 eq, 0.574 mL, 3.30 mmol) in DMF (10 mL) shaking overnight. The resin was washed as before and added to a solution of TFA/H_2O/TIPS (95%, 2.5%, 2.5%, 20 mL) with agitation for 2 h at ambient temperature. The resin was filtered and resulting solution concentrated *in vacuo*. The residue was trituated with cold diethyl ether.

Reaction: Tetra$_Q$*m*CYT

Crude **Tetra$_Q$Cysteine** was dissolved in Ammonium Bicarbonate (1M, pH 9) and flowed with N_2 gas. D-Cystine (ChemImpex, 02872) (5 eq, 220 mg, 2.75 mmol) was dissolved in 0.1 M NaOH, pH 8, sonicated and vacuum pumped to remove air, and added to **Tetra$_Q$Cysteine** with mixing for 2 h sealed from air. The resulting solution was concentrated *in vacuo* and purified using Reversed-Phase HPLC with H_2O/MeOH to yield **Tetra$_Q$*m*CYT**. The sample was analyzed for purity using a Waters 1525 HPLC with a Phenomenex Luna 5µ C8(2) 100Å (250 x 4.6 mm) column; gradient elution with H_2O/CH_3CN.

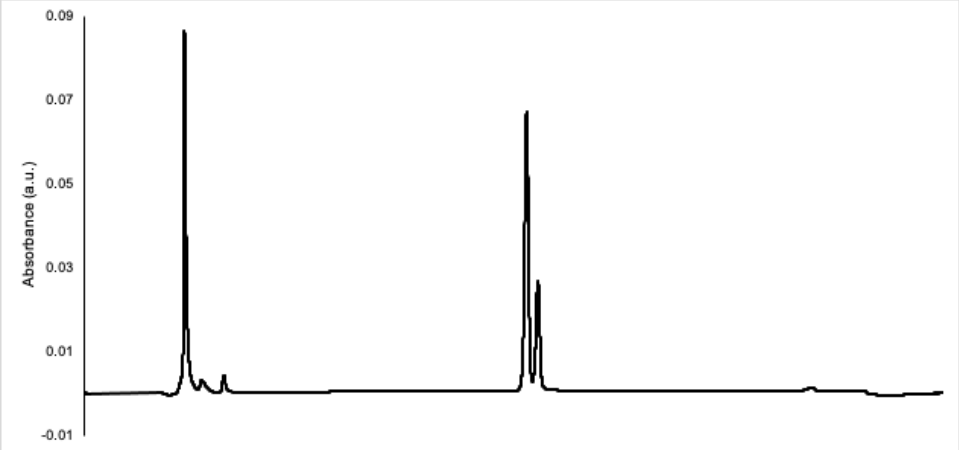

ESI-MS calculated [M + H^+]: 869.2117, found: 869.2112

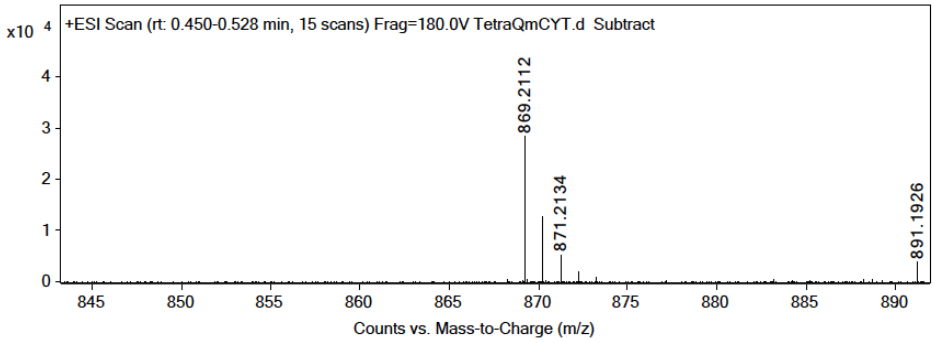

Scheme S7. Synthesis of Penta$_Q$LLys

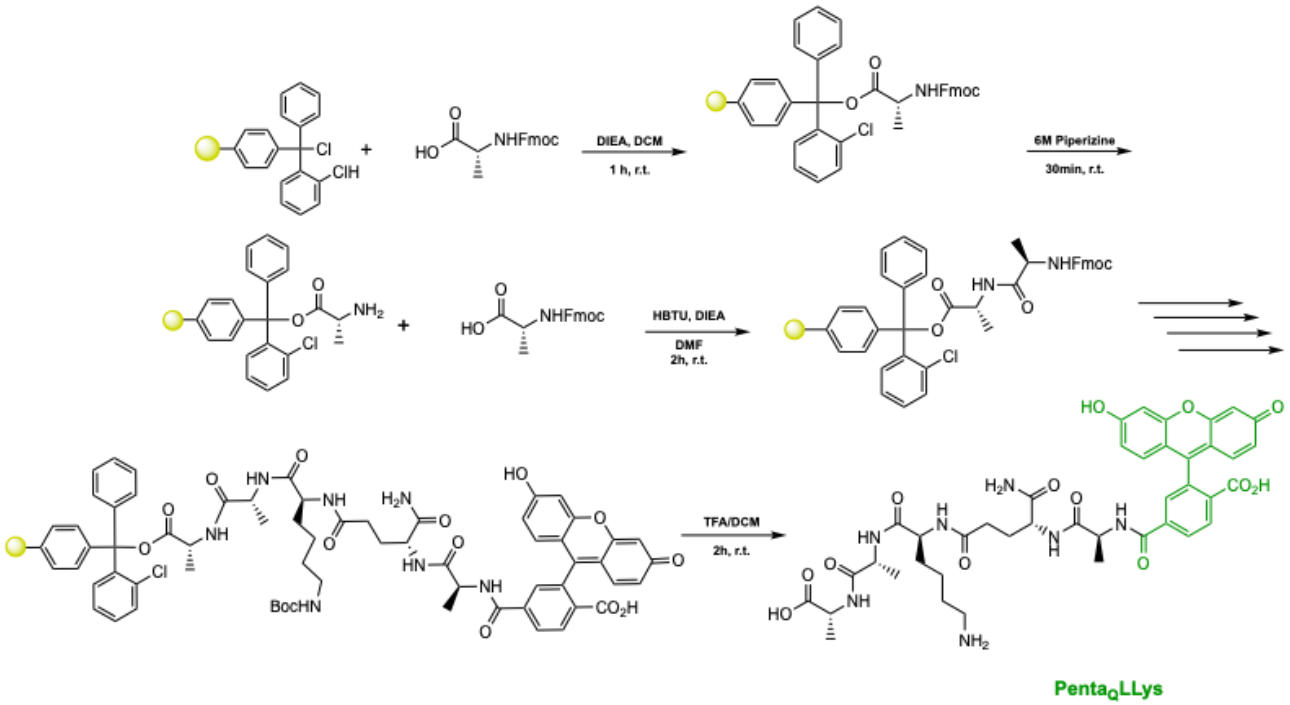

Fmoc-D-Alanine-OH (1.1 eq, 188 mg, 0.605 mmol) was added to a 25 mL peptide synthesis vessel charged with 2-Chlorotrityl chloride resin (500 mg, 0.55 mmol) and DIEA (4 eq, 0.422 mL, 2.20 mmol) in dry DCM (5 mL). The resin was agitated for 1 h at ambient temperature and washed with MeOH and DCM (3 x 15 mL each). The Fmoc protecting group was removed with 6 M piperazine/100 mM HOBt in DMF (15 ml) for 30 min at ambient temperature, then washed as before. Fmoc-D-alanine-OH (3 eq, 513 mg, 1.65 mmol), HBTU (3 eq, 625 mg, 1.65 mmol), and DIEA (6 eq, 0.574 mL, 3.30 mmol) in DMF (15 mL) were added to the reaction flask and agitated for 2 h at ambient temperature. The Fmoc deprotection and coupling procedure was repeated as before using the same equivalencies with Fmoc-L-Lys(Boc)-OH, Fmoc-D-glutamic acid α-amide and Fmoc-L-Alanine-OH. The Fmoc group of L-alanine was deprotected and coupled with 5(6)-carboxyfluorescein (2 eq, 413 mg, 1.1 mmol), HBTU (2 eq, 416 mg, 1.10 mmol) and DIEA (6 eq, 0.574 mL, 3.30 mmol) in DMF (10 mL) shaking overnight. The resin was washed as before and added to a solution of TFA/H_2O/TIPS (95%, 2.5%, 2.5%, 20 mL) with agitation for 2 h at ambient temperature. The resin was filtered and resulting solution concentrated *in vacuo*. The residue was trituated with cold diethyl ether and purified using reverse phase HPLC using H_2O/MeOH to yield **Penta$_Q$LLys**. The sample was analyzed

for purity using a Waters 1525 HPLC with a Phenomenex Luna 5µ C8(2) 100Å (250 x 4.6 mm) column; gradient elution with H_2O/CH_3CN.

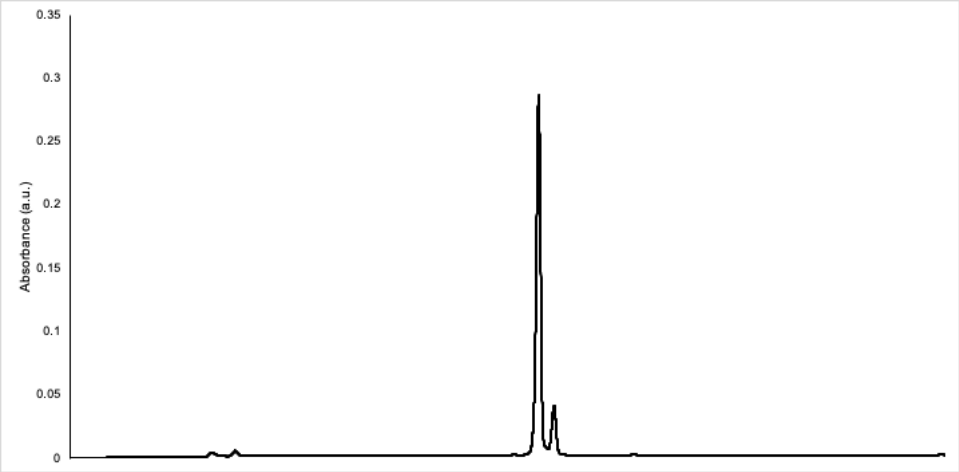

ESI-MS calculated [M + H^+]: 846.3305, found: 846.3296

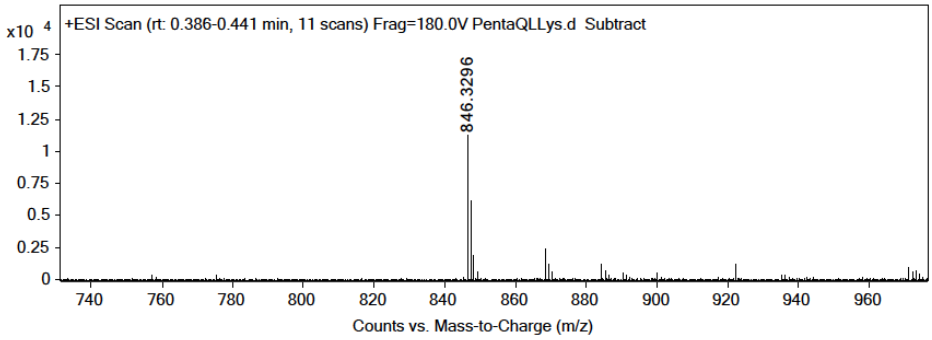

Scheme S8. Synthesis of Penta$_Q$Cysteine

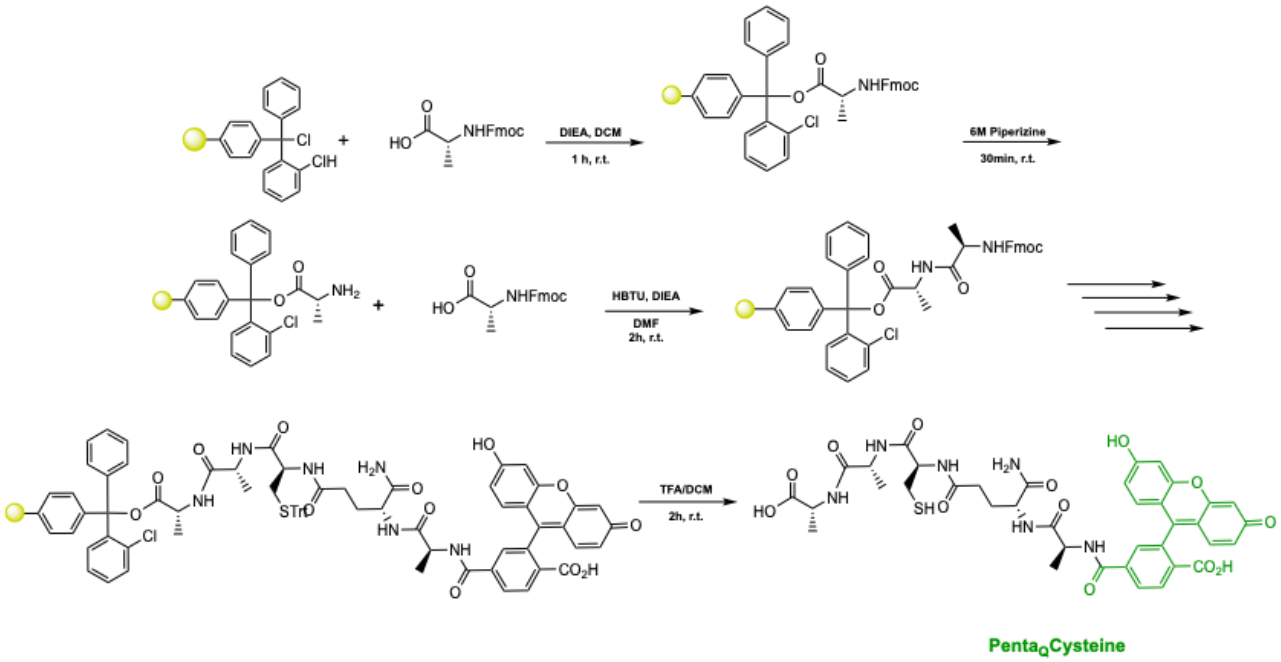

Fmoc-D-Alanine-OH (1.1 eq, 188 mg, 0.605 mmol) was added to a 25 mL peptide synthesis vessel charged with 2-Chlorotrityl chloride resin (500 mg, 0.55 mmol) and DIEA (4 eq, 0.422 mL, 2.20 mmol) in dry DCM (5 mL). The resin was agitated for 1 h at ambient temperature and washed with MeOH and DCM (3 x 15 mL each). The Fmoc protecting group was removed with 6 M piperazine/100 mM HOBt in DMF (15 ml) for 30 min at ambient temperature, then washed as before. Fmoc-D-Alanine-OH (3 eq, 514 mg, 1.65 mmol), HBTU (3 eq, 625 mg, 1.65 mmol), and DIEA (6 eq, 0.574 mL, 3.30 mmol) in DMF (10 mL) were added to the reaction flask and agitated for 2 h at ambient temperature. The Fmoc deprotection and coupling procedure was repeated as before using the same equivalencies with Fmoc-L-Cysteine(Trt)-OH, Fmoc-D-glutamic acid α-*tert* butyl ester, and Fmoc-L-Alanine-OH. The Fmoc group of L-alanine was deprotected and coupled with 5(6)-carboxyfluorescein (2 eq, 413 mg, 1.1 mmol), HBTU (2 eq, 416 mg, 1.10 mmol) and DIEA (6 eq, 0.574 mL, 3.30 mmol) in DMF (10 mL) shaking overnight. The resin was washed as before and added to a solution of TFA/H_2O/TIPS (95%, 2.5%, 2.5%, 20 mL) with agitation for 2 h at ambient temperature. The resin was filtered and resulting solution concentrated *in vacuo*. The residue was trituated with cold diethyl ether.

Reaction: Penta$_Q$*m*CYT

Crude **Penta$_Q$Cysteine** was dissolved in Ammonium Bicarbonate (1M, pH 9) and flowed with N_2 gas. D-Cystine (ChemImpex, 02872) (5 eq, 220 mg, 2.75 mmol) was dissolved in

0.1 M NaOH, pH 8, sonicated and vacuum pumped to remove air, and added to **Penta$_Q$Cysteine** with mixing for 2 h sealed from air. The resulting solution was concentrated *in vacuo* and purified using Reversed-Phase HPLC with H_2O/MeOH to yield **Penta$_Q$*m*CYT**. The sample was analyzed for purity using a Shimadzu LC 2020 with a Phenomenex Luna 5µ C4 300Å (250 x 2.00 mm) column; gradient elution with H_2O/CH_3CN.

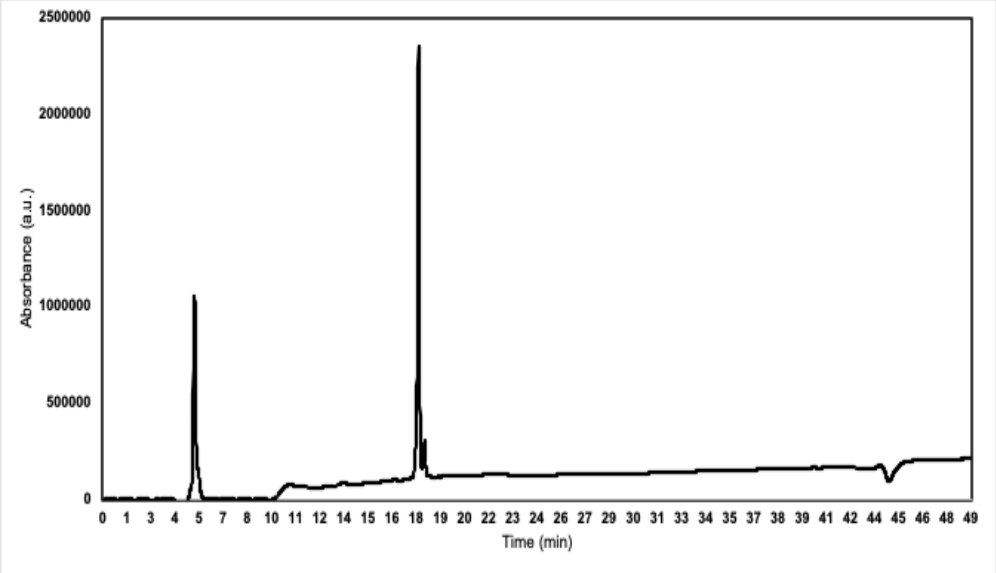

ESI-MS calculated [M + H^+]: 940.2488, found: 940.2487

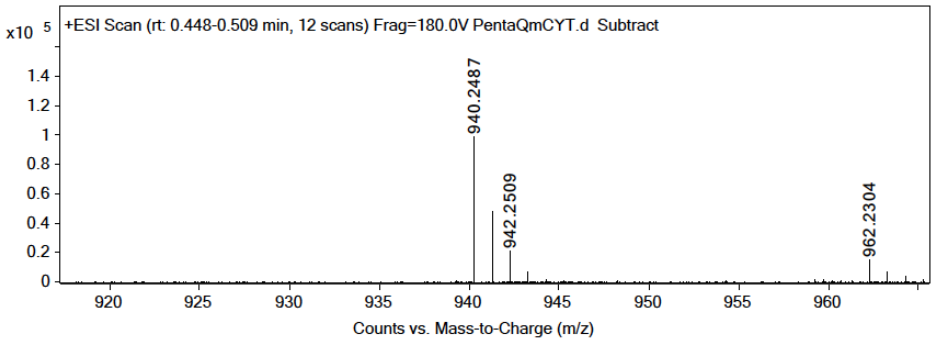

Scheme S9. Synthesis of TAMRA-Tri$_Q$Cysteine

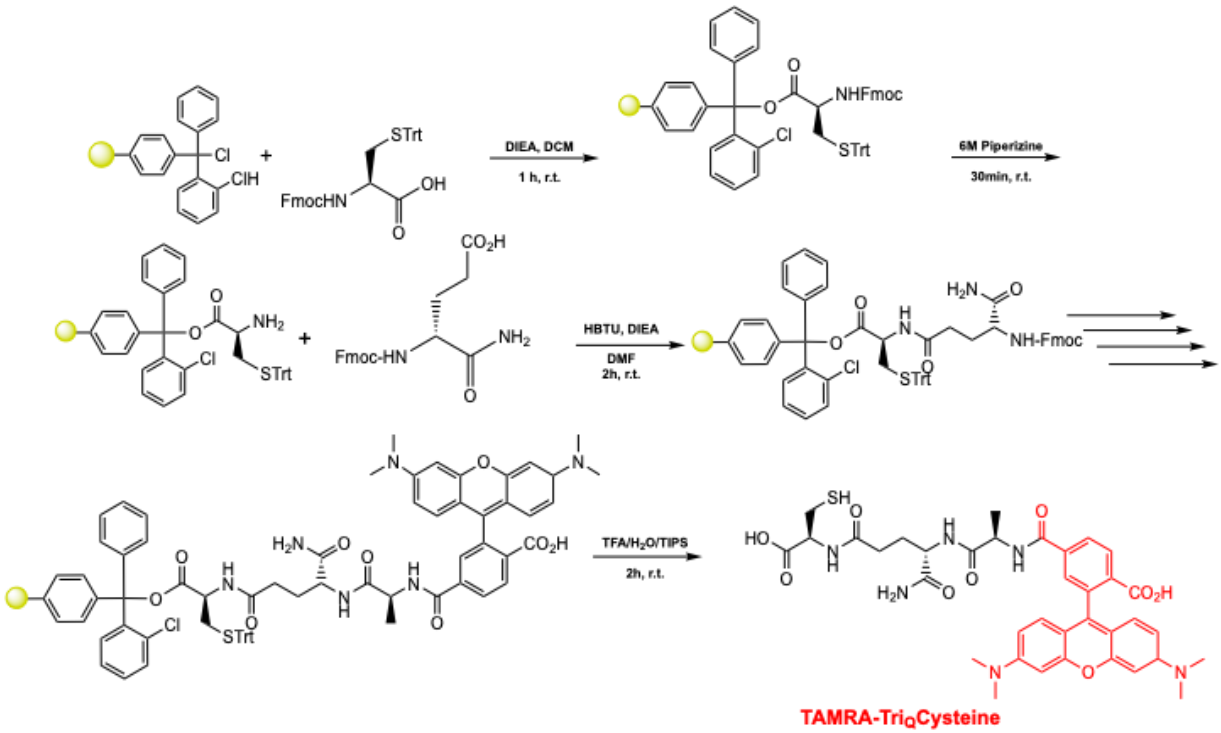

Fmoc-L-Cysteine(Trt)-OH (1.1 eq, 354 mg, 0.605 mmol) was added to a 25 mL peptide synthesis vessel charged with 2-Chlorotrityl chloride resin (500 mg, 0.55 mmol) and DIEA (4 eq, 0.422 mL, 2.20 mmol) in dry DCM (5 mL). The resin was agitated for 1 h at ambient temperature and washed with MeOH and DCM (3 x 15 mL each). The Fmoc protecting group was removed with 6 M piperazine/100 mM HOBt in DMF (15 ml) for 30 min at ambient temperature, then washed as before. Fmoc-D-glutamic acid α-amide (3 eq, 607 mg, 1.65 mmol), HBTU (3 eq, 625 mg, 1.65 mmol), and DIEA (6 eq, 0.574 mL, 3.30 mmol) in DMF (10 mL) were added to the reaction flask and agitated for 2 h at ambient temperature. The Fmoc deprotection and coupling procedure was repeated as before using the same equivalencies with Fmoc-L-Alanine-OH. The Fmoc group of L-alanine was deprotected and coupled with 5(6)-carboxytetramethylrhoadmine (2 eq, 474 mg, 1.1 mmol), HBTU (2 eq, 416 mg, 1.10 mmol) and DIEA (6 eq, 0.574 mL, 3.30 mmol) in DMF (10 mL) shaking overnight. The resin was washed as before and added to a solution of TFA/H_2O/TIPS (95%, 2.5%, 2.5%, 20 mL) with agitation for 2 h at ambient temperature. The resin was filtered and resulting solution concentrated *in vacuo*. The residue was trituated with cold diethyl ether.

Reaction: TAMRA-Tri$_Q$*m*CYT

Crude **TAMRA-Tri$_Q$Cysteine** was dissolved in Ammonium Bicarbonate (1M, pH 9) and flowed with N_2 gas. D-Cystine (ChemImpex, 02872) (5 eq, 220 mg, 2.75 mmol) was dissolved in 0.1 M NaOH, pH 8, sonicated and vacuum pumped to remove air, and added to **TAMRA-Tri$_Q$Cysteine** with mixing for 2 h sealed from air. The resulting solution was concentrated *in vacuo* and purified using Reversed-Phase HPLC with H_2O/MeOH to yield **TAMRA-Tri$_Q$*m*CYT**. The sample was analyzed for purity using an Agilent 1200 HPLC with a Phenomenex Luna 5µ C4 300Å (250 x 2.00 mm) column; gradient elution with H_2O/CH_3CN.

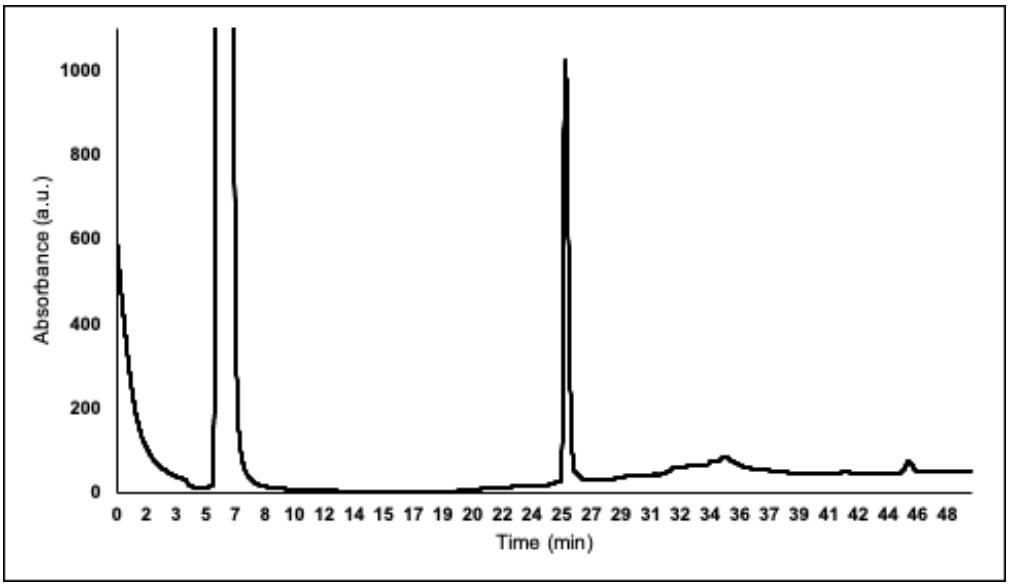

ESI-MS calculated [M + H^+]: 852.2691, found: 852.2684

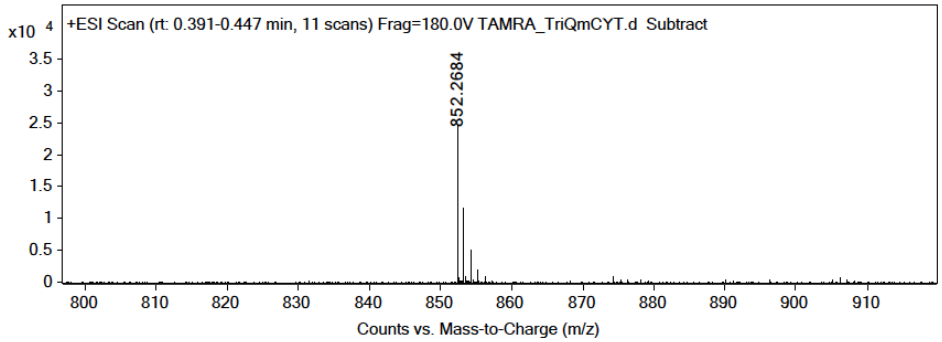

Reaction: TAMRA-Tri$_Q$*m*CYT$_{NH2}$

Crude **TAMRA-Tri$_Q$Cysteine** was added to concentrated **D-Cys(NH_2)**. Both were dissolved in Ammonium Bicarbonate (1M, pH 9) and 0.1 M NaOH, pH 8 with a small amount of DMSO to aid in oxidation. The reaction was left open to air with stirring for 2 h. The resulting solution was concentrated *in vacuo* and purified using Reversed-Phase

HPLC with H_2O/MeOH to yield **TAMRA-Tri$_Q$*m*CYT$_{NH2}$**. The sample was analyzed for purity using an Agilent 1200 HPLC with a Phenomenex Luna 5µ C4 300Å (250 x 2.00 mm) column; gradient elution with H_2O/CH_3CN.

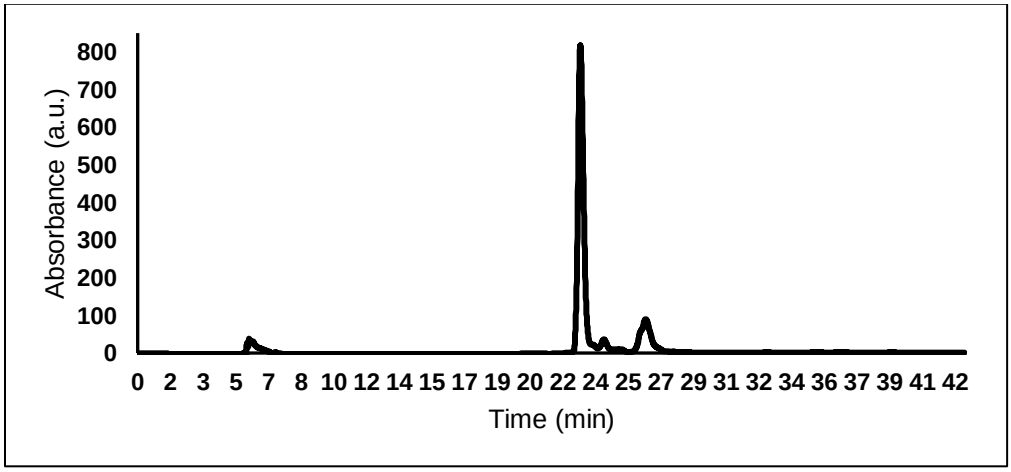

ESI-MS calculated [M + H^+]: 851.2851, found: 851.2847

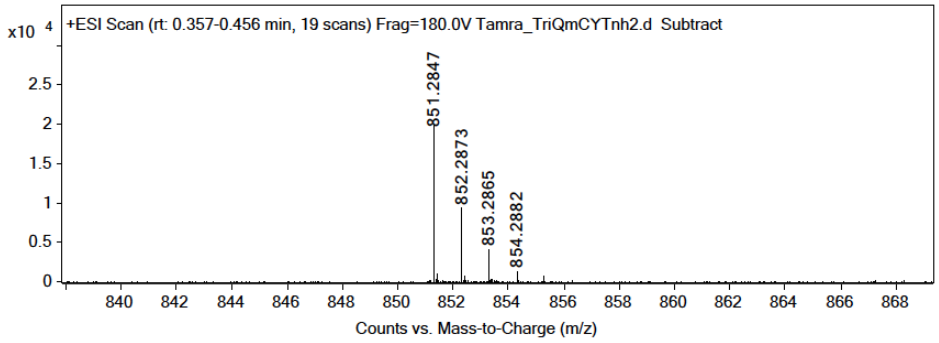

Scheme S10. Synthesis of Tri_REVERSO

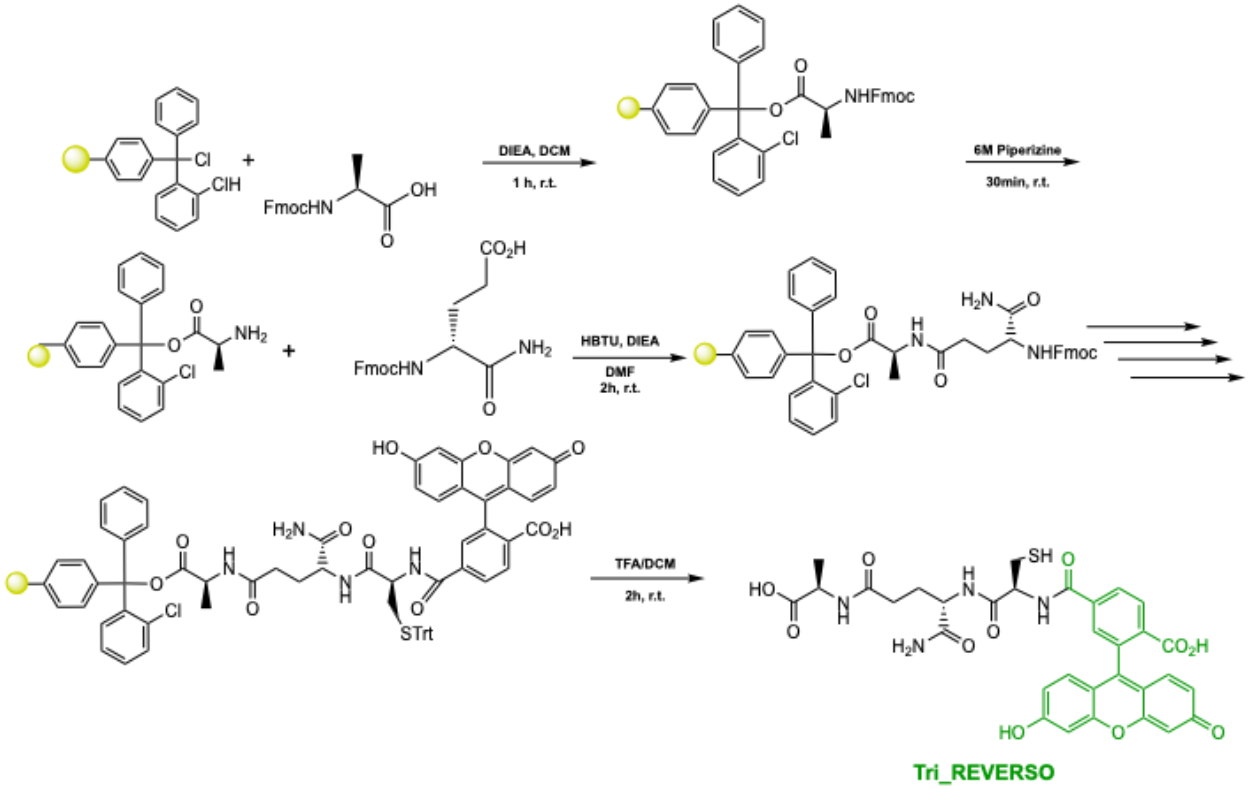

Fmoc-L-Alanine-OH (1.1 eq, 188 mg, 0.605 mmol) was added to a 25 mL peptide synthesis vessel charged with 2-Chlorotrityl chloride resin (500 mg, 0.55 mmol) and DIEA (4 eq, 0.422 mL, 2.20 mmol) in dry DCM (5 mL). The resin was agitated for 1 h at ambient temperature and washed with MeOH and DCM (3 x 15 mL each). The Fmoc protecting group was removed with 6 M piperazine/100 mM HOBt in DMF (15 ml) for 30 min at ambient temperature, then washed as before. Fmoc-D-glutamic acid α-amide (3 eq, 607 mg, 1.65 mmol), HBTU (3 eq, 625 mg, 1.65 mmol), and DIEA (6 eq, 0.574 mL, 3.30 mmol) in DMF (10 mL) were added to the reaction flask and agitated for 2 h at ambient temperature. The Fmoc deprotection and coupling procedure was repeated as before using the same equivalencies with Fmoc-L-Cysteine(Trt)-OH. The Fmoc group of L-cysteine was deprotected and coupled with 5(6)-carboxyfluorescein (2 eq, 413 mg, 1.1 mmol), HBTU (2 eq, 416 mg, 1.10 mmol) and DIEA (6 eq, 0.574 mL, 3.30 mmol) in DMF (10 mL) shaking overnight. The resin was washed as before and added to a solution of TFA/H_2O/TIPS (95%, 2.5%, 2.5%, 20 mL) with agitation for 2 h at ambient temperature. The resin was filtered and resulting solution concentrated *in vacuo*. The residue was trituated with cold diethyl ether.

Reaction: Tri_REVERSO_CYT

Crude **Tri_REVERSO** was dissolved in Ammonium Bicarbonate (1M, pH 9) and flowed with N_2 gas. D-Cystine (ChemImpex, 02872) (5 eq, 220 mg, 2.75 mmol) was dissolved in 0.1 M NaOH, pH 8, sonicated and vacuum pumped to remove air, and added to **Tri_REVERSO** with mixing for 2 h sealed from air. The resulting solution was concentrated *in vacuo* and purified using Reversed-Phase HPLC with H_2O/MeOH to yield **Tri_REVERSO_CYT**. The sample was analyzed for purity using a Waters 1525 HPLC with a Phenomenex Luna 5µ C8(2) 100Å (250 x 4.6 mm) column; gradient elution with H_2O/CH_3CN.

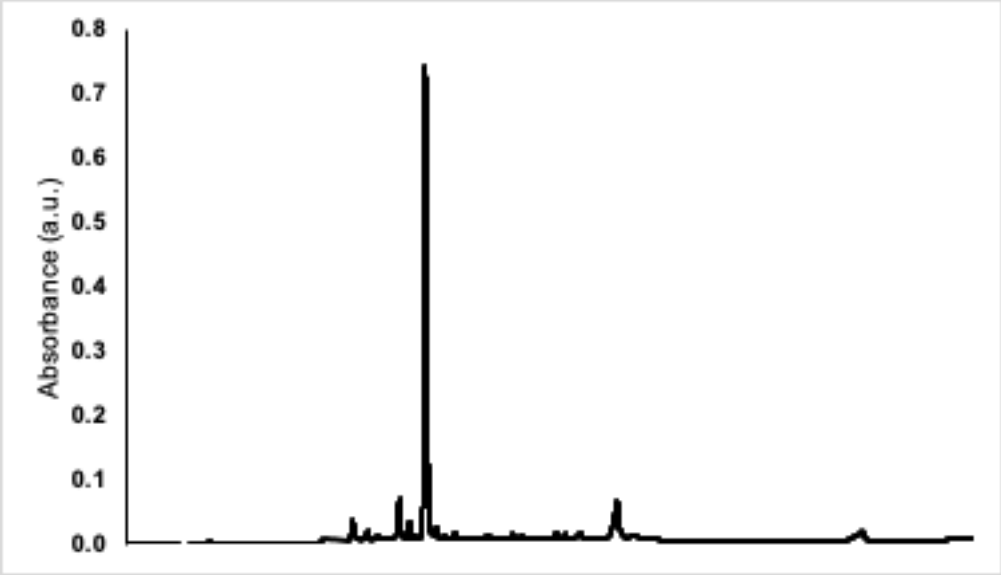

ESI-MS calculated [M + H^+]: 798.1746, found: 798.1737

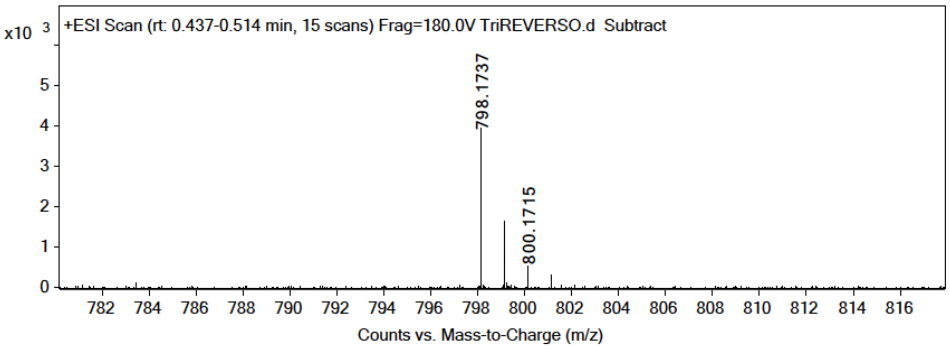

A.5 Synthesis and Characterization of Compounds in Chapter 5

Scheme S1. Synthesis of TriSe(Mob).

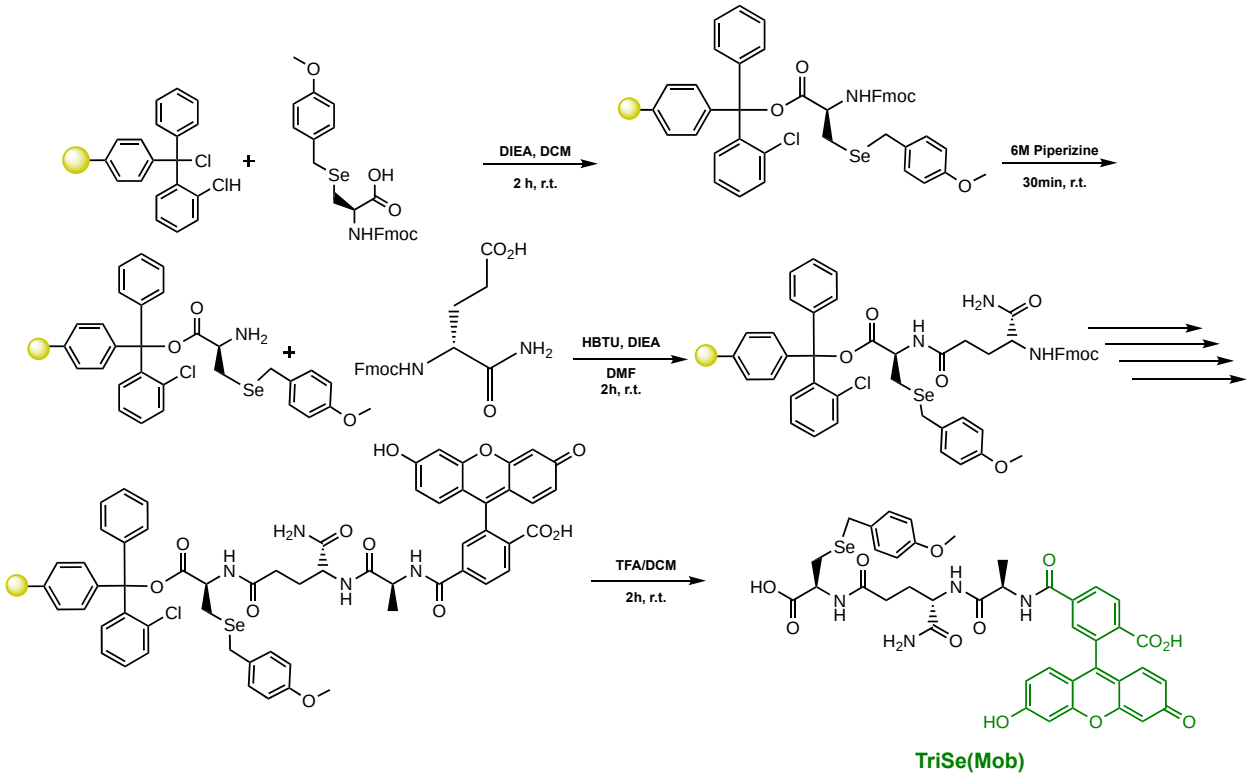

Fmoc-L-Sec(Mob) (1.1 eq, 154 mg, 0.303 mmol) was added to a 25 mL peptide synthesis vessel charged with 2-chlorotrityl chloride resin (250 mg, 0.275 mmol) and DIEA (4 eq, 0.191 mL, 1.10 mmol) in dry DCM (5 mL). The resin was agitated for 2 h at ambient temperature and washed with MeOH and DCM (3 x 15 mL each). The Fmoc protecting group was removed with 6 M piperazine/100 mM HOBt in DMF (15 ml) for 30 min at ambient temperature, then washed as before. Fmoc-D-glutamic acid α-amide (3 eq, 304 mg, 0.825 mmol), HBTU (3 eq, 314 mg, 0.825 mmol), and DIEA (6 eq, 0.287 mL, 1.65 mmol) in DMF (10 mL) were added to the reaction flask and agitated for 2 h at ambient temperature. The Fmoc deprotection and coupling procedure was repeated as before using the same equivalencies with Fmoc-L-Alanine-OH. The Fmoc group of L-alanine was deprotected and coupled with 5(6)-carboxyfluorescein (2 eq, 207 mg, 0.55 mmol), HBTU (2 eq, 209 mg, 0.55 mmol) and DIEA (4 eq, 0.191 mL, 1.10 mmol) in DMF (10 mL) shaking overnight. The resin was washed as before and added to a solution of TFA/H_2O/TIPS (95%, 2.5%, 2.5%, 20 mL) with agitation for 2 h at ambient temperature. The resin was

filtered, and the resulting solution was concentrated *in vacuo* and trituated with cold diethyl ether, leaving the Mob protecting group intact.

R1. Reaction to obtain TriSeLAN.

The crude peptide from Scheme S1 (**TriSe(Mob)**) was treated with TFA:thioanisole (9.75 : 0.25, v/v) and 1.3 equivalents of 2,2′-dithiobis(5-nitropyridine) (DTNP) for 1 h at room temperature to *in situ* swap out the Mob group for TNP. This intermediated was then allowed to react with β-chloro-D-Ala in 0.1 M phosphate buffer pH 6 and isopropanol (7:3, v/v) containing 40 equivalents of dithiothreitol (DTT). This reaction proceeded for 24 h at 37 ºC, was quenched with 5% TFA, and isopropanol was removed *in vacuo*. The final product was then purified using RP-HPLC with H_2O/MeOH and analyzed for purity using a Waters 1525 pump and 2489 detector equipped with a Phenomenex Luna 5µ C8(2) 100Å (250 x 4.60 mm) column; gradient elution with H_2O/CH_3CN.

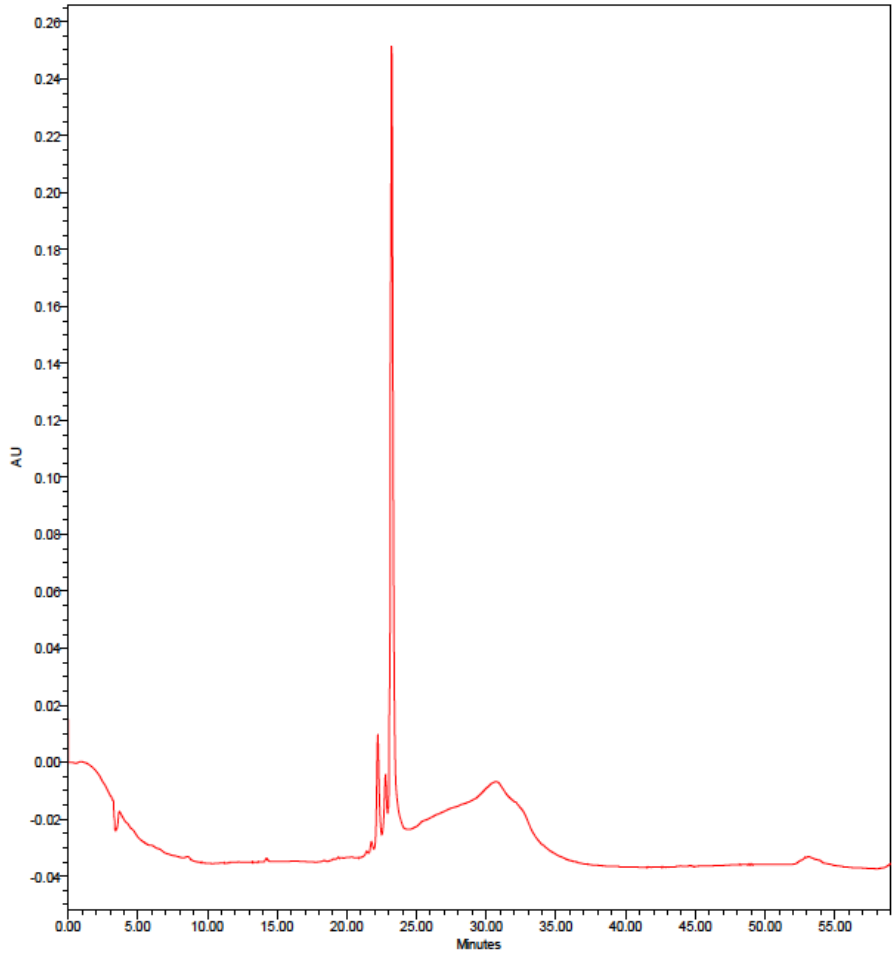

ESI-MS calculated [M + H^+]: 814.1470, found: 814.1439

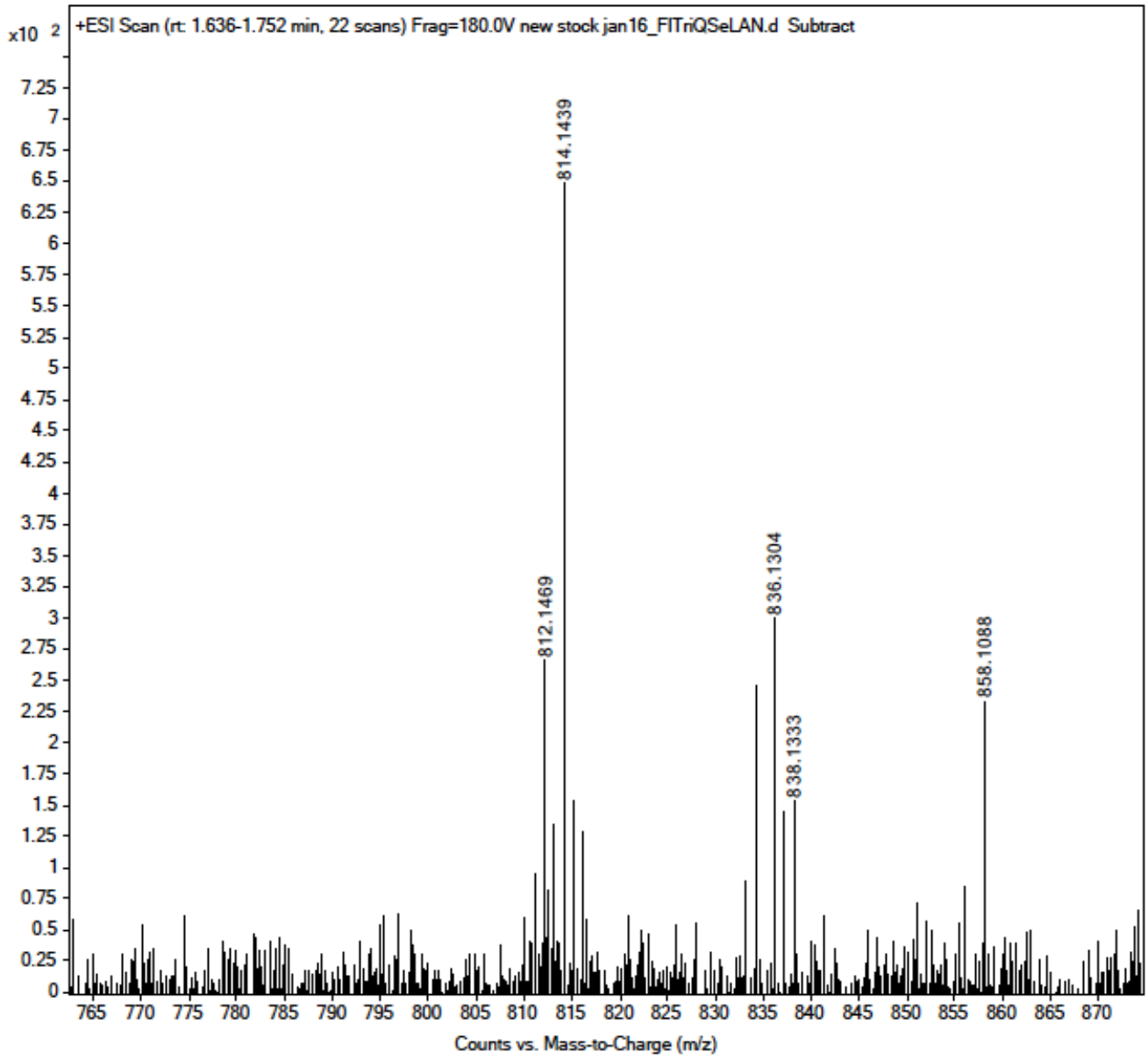

R2. Reaction to obtain TriSeLys.

The crude peptide from Scheme S1 (**TriSe(Mob)**) was treated with TFA:thioanisole (9.75 : 0.25, v/v) and 1.3 equivalents of 2,2′-dithiobis(5-nitropyridine) (DTNP) for 1 h at room temperature to *in situ* swap out the Mob group for TNP. This intermediated was then allowed to react with 2-chloro-ethylamine in 0.1 M phosphate buffer pH 6 and isopropanol (7:3, v/v) containing 40 equivalents of dithiothreitol (DTT). This reaction proceeded for 24 h at 37 ºC, was quenched with 5% TFA, and isopropanol was removed *in vacuo*. The final product was then purified using RP-HPLC with H_2O/MeOH and analyzed for purity using a Waters 1525 pump and 2489 detector equipped with a Phenomenex Luna 5µ C8(2) 100Å (250 x 4.60 mm) column; gradient elution with H_2O/CH_3CN.

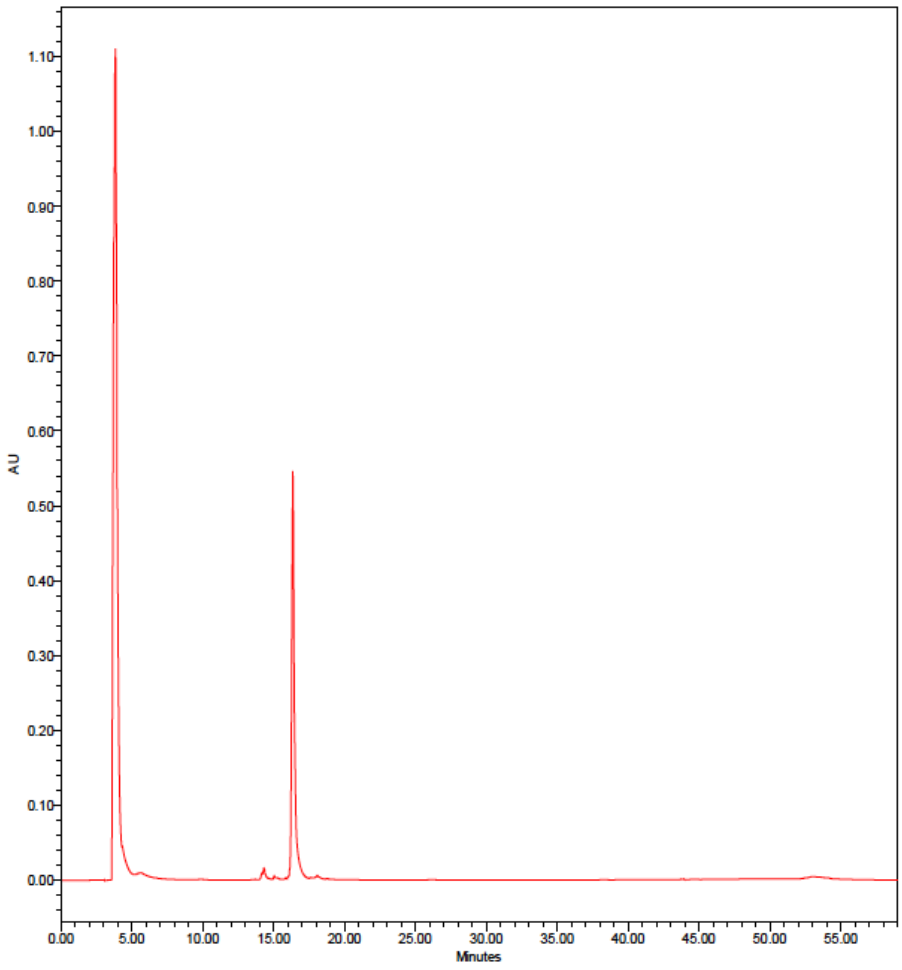

ESI-MS calculated [M + H^+]: 770.1571, found: 770.1561

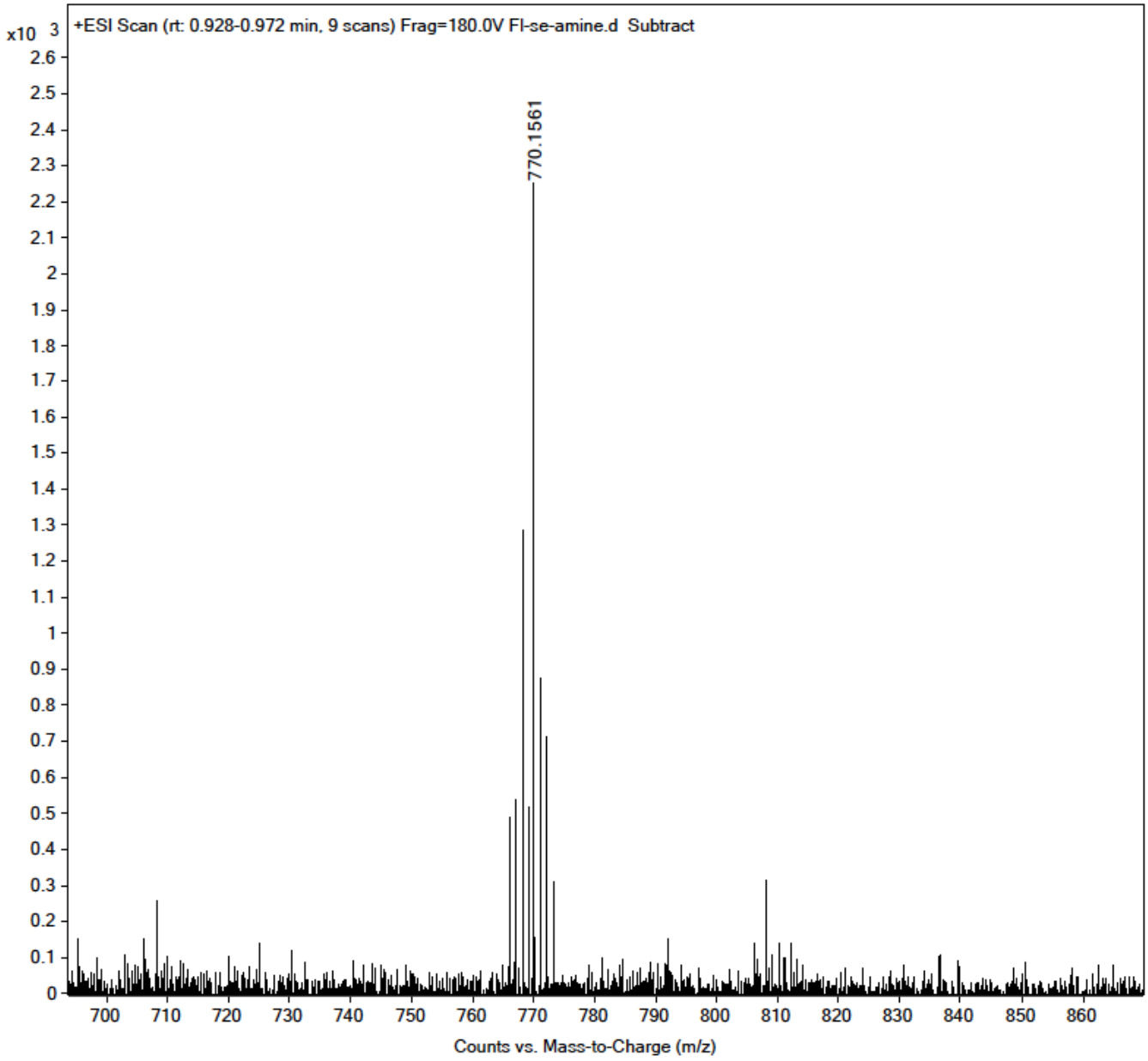

R3. Reaction to obtain Single AA SeLAN.

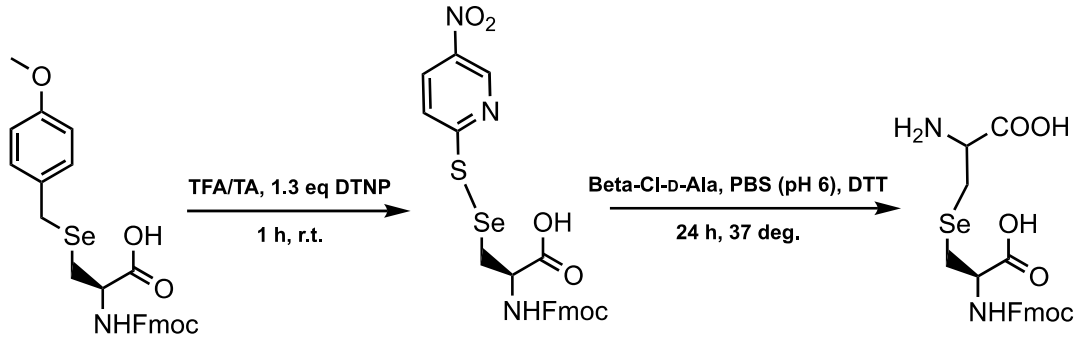

Fmoc-L-Sec(Mob) (50 mg) was treated with TFA:thioanisole (9.75 : 0.25, v/v) and 1.3 equivalents of 2,2′-dithiobis(5-nitropyridine) (DTNP) for 1 h at room temperature to *in situ* swap out the Mob group for TNP. The resulting solution was concentrated *in vacuo*, dissolved in H_2O and lyophilized. Resulting solid Fmoc-L-Sec-TNP was reacted with β-chloro-D-Ala in 0.1 M phosphate buffer pH 6 and isopropanol (7:3, v/v) containing 40 equivalents of dithiothreitol (DTT). This reaction proceeded for 24 h at 37 ºC, was quenched with 5% TFA, and isopropanol was removed *in vacuo*. The final product (Fmoc-SeLAN) was then purified using RP-HPLC with H_2O/MeOH. Piperazine (100 mg, 1.2 mmol) was coupled to 2-chlorotrityl chloride resin (150 mg, 0.165 mmol) for 1 h at ambient temperature with anhydrous DCM (5 mL) and DIEA (4 eq, 0.574 mL, 3.3 mmol). The resin was washed with 1% DIEA in MeOH (50 mL) and transferred to a round bottom flask with a stir bar, where the concentrated HPLC fractions were added and stirred for 30 m at room temperature to remove Fmoc. The resin was filtered and the resulting liquid was concentrated *in vacuo*.

Fmoc-SeLAN

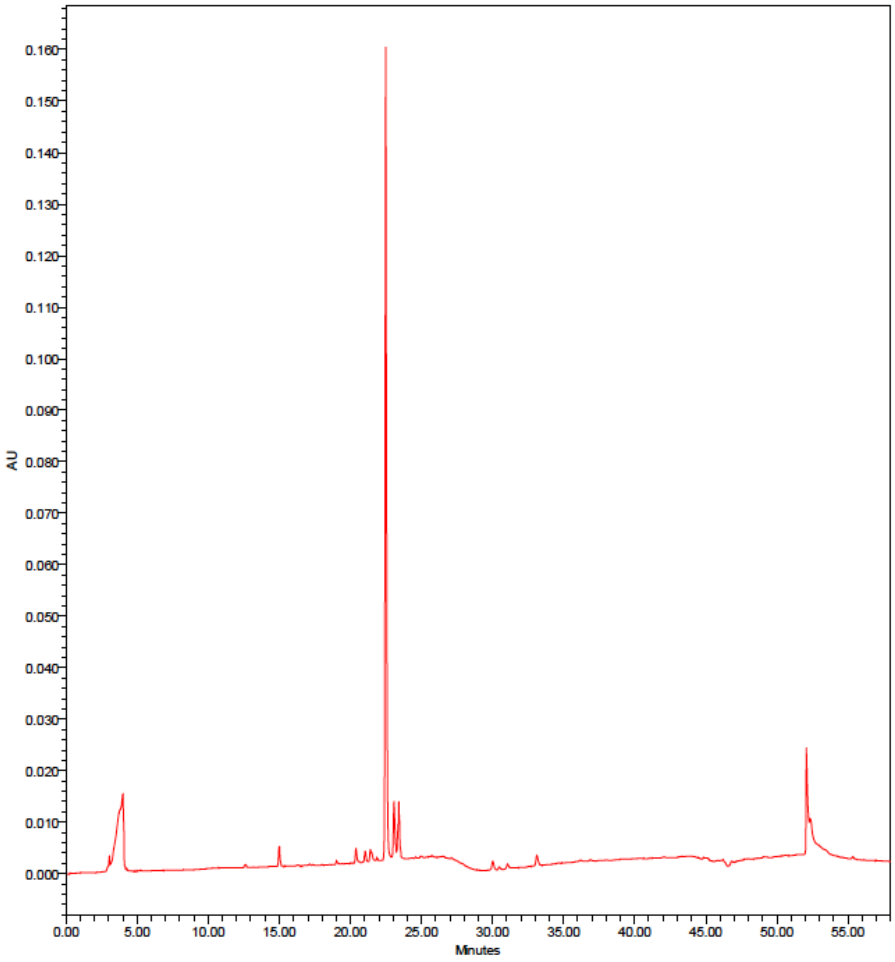
AU
0.160
0.150
0.140
0.130
0.120
0.110
0.100
0.090
0.080
0.070
0.060
0.050
0.040
0.030
0.020
0.010
0.000
0.00
5.00
10.00
15.00
20.00
25.00
30.00
35.00
40.00
45.00
50.00
55.00
Minutes

ESI-MS calculated [M + H^+]: 479.0716, found: 479.0706

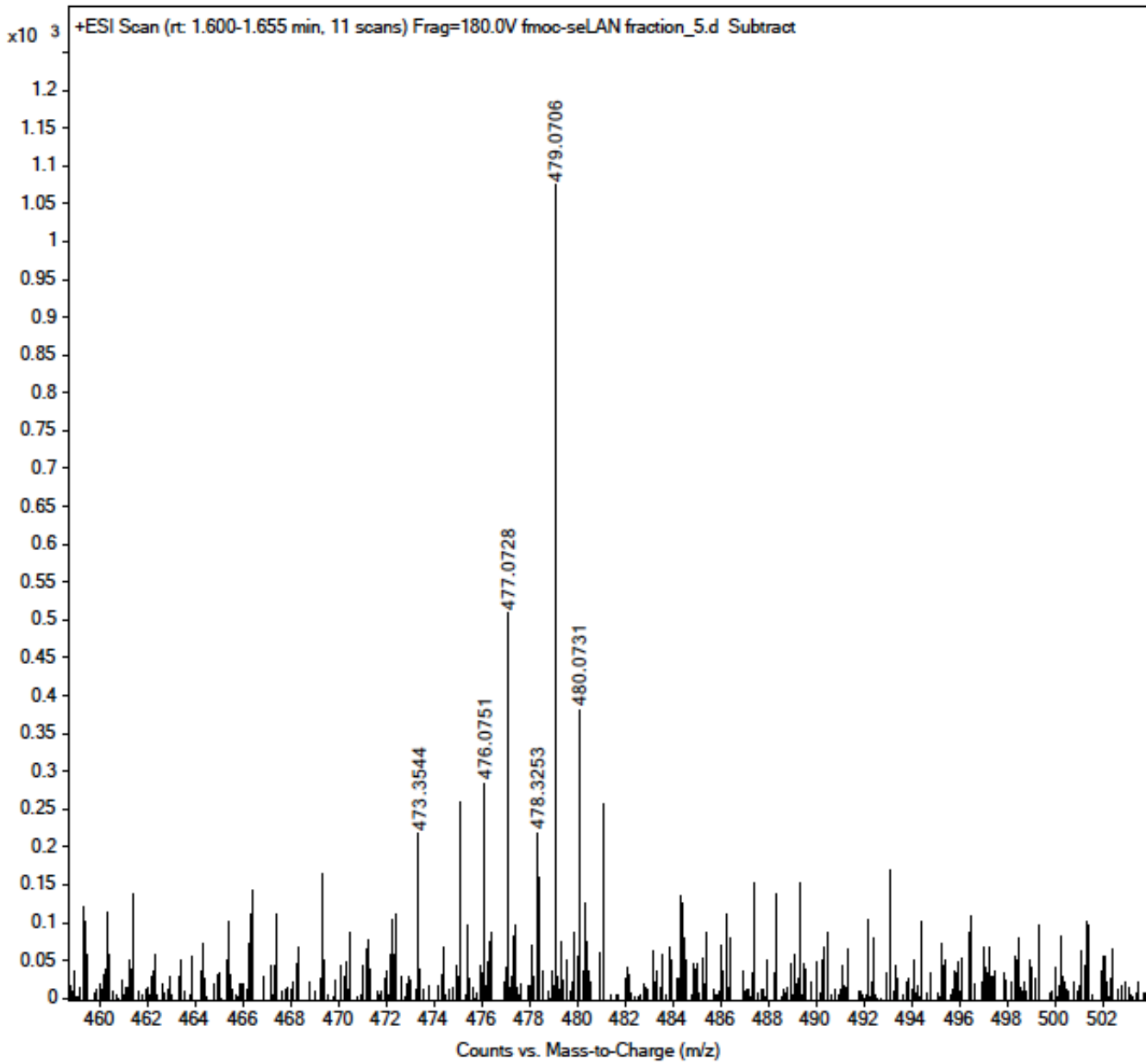

SeLAN ESI-MS calculated [M + H^+]: 257.0035, found: 256.9601

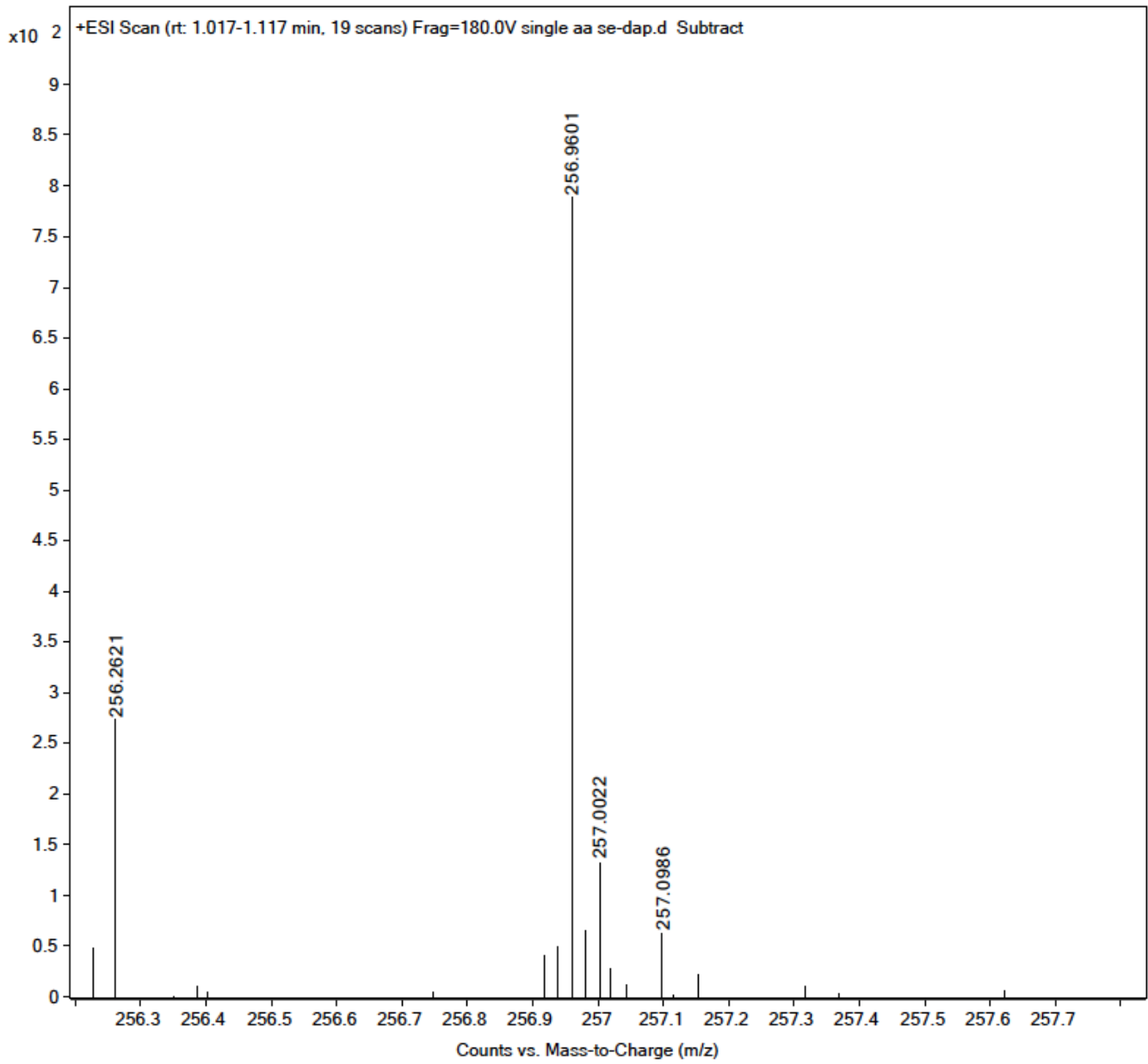

Scheme S2. Synthesis of Alk-TetraLys(Ac)

Fmoc-D-Ala-OH (1.1 eq, 188 mg, 0.605 mmol) was added to a 25 mL peptide synthesis vessel charged with 2-chlorotrityl chloride resin (500 mg, 0.55 mmol) and DIEA (4 eq, 0.382 mL, 2.20 mmol) in dry DCM (5 mL). The resin was agitated for 1 h at ambient temperature and washed with MeOH and DCM (3 x 15 mL each). The Fmoc protecting group was removed with 20% piperidine in DMF (15 ml) for 30 min at ambient temperature, then washed as before. Fmoc-L-Lys(Ac)-OH (3 eq, 677 mg, 1.65 mmol), HBTU (3 eq, 625 mg, 1.65 mmol), and DIEA (6 eq, 0.574 mL, 3.30 mmol) in DMF (10 mL) were added to the reaction flask and agitated for 2 h at ambient temperature. The Fmoc deprotection and coupling procedure was repeated as before using the same equivalencies with Fmoc-D-glutamic acid α-amide (3 eq, 608 mg, 1.65 mmol) and then with Fmoc-L-Alanine-OH (3 eq, 514 mg, 1.65 mmol). The Fmoc group at the *N*-terminus was removed and 4-pentynoic acid (3 eq, 162 mg, 1.65 mmol) was coupled with HBTU and DIEA. The resin was washed as before, and the peptide was cleaved from resin with a solution of TFA/H_2O/TIPS (95%, 2.5%, 2.5%, 20 mL) with agitation for 2 h at ambient temperature. The resin was filtered and resulting solution concentrated *in vacuo*. The residue was triturated with cold diethyl ether, concentrated *in vacuo*, and purified by RP-HPLC.

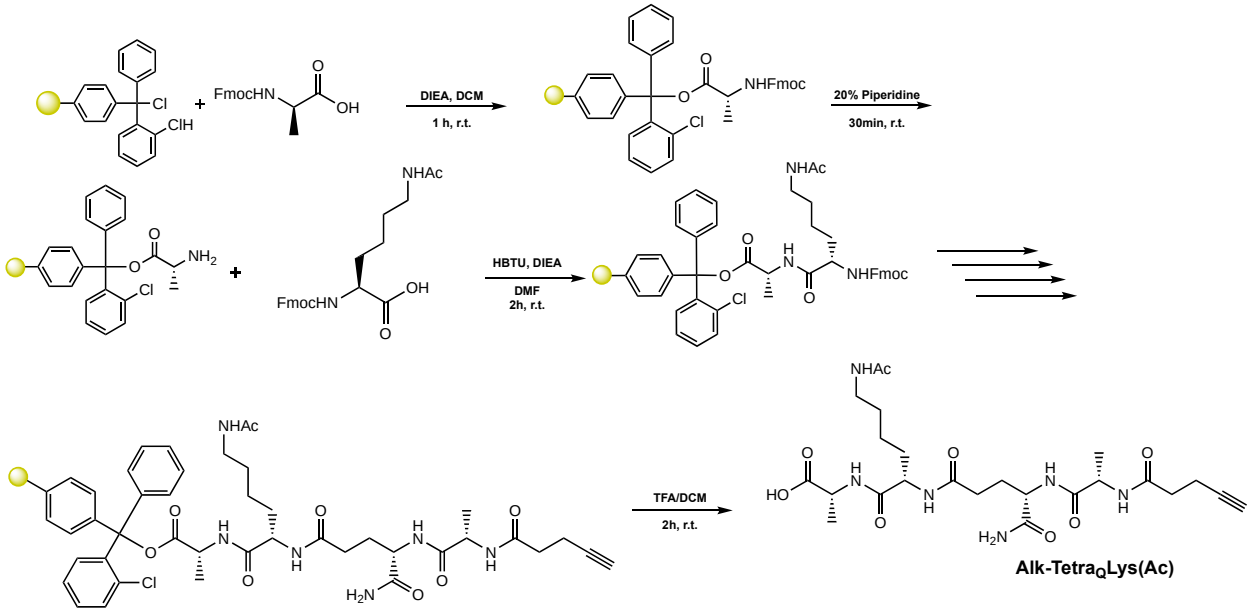

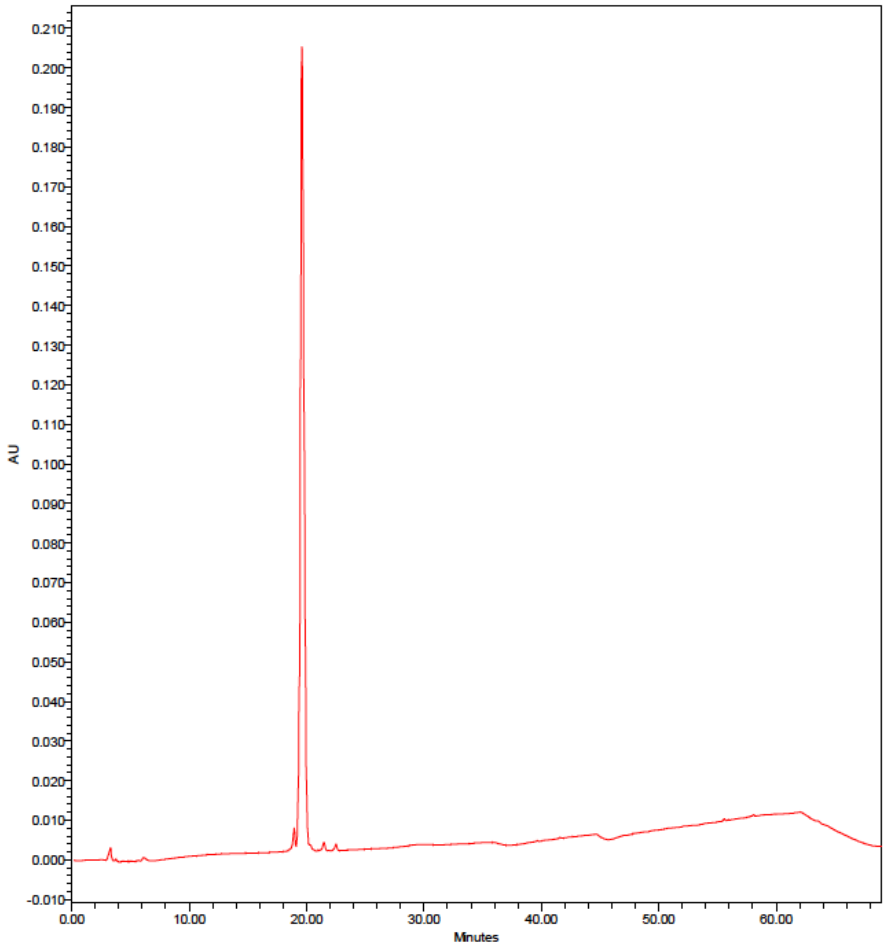
AU
0.210
0.200
0.190
0.180
0.170
0.160
0.150
0.140
0.130
0.120
0.110
0.100
0.090
0.080
0.070
0.060
0.050
0.040
0.030
0.020
0.010
0.000
-0.010
0.00
10.00
20.00
30.00
40.00
50.00
60.00
Minutes

ESI-MS calculated [M + H^+]: 539.2821, found: 539.2818

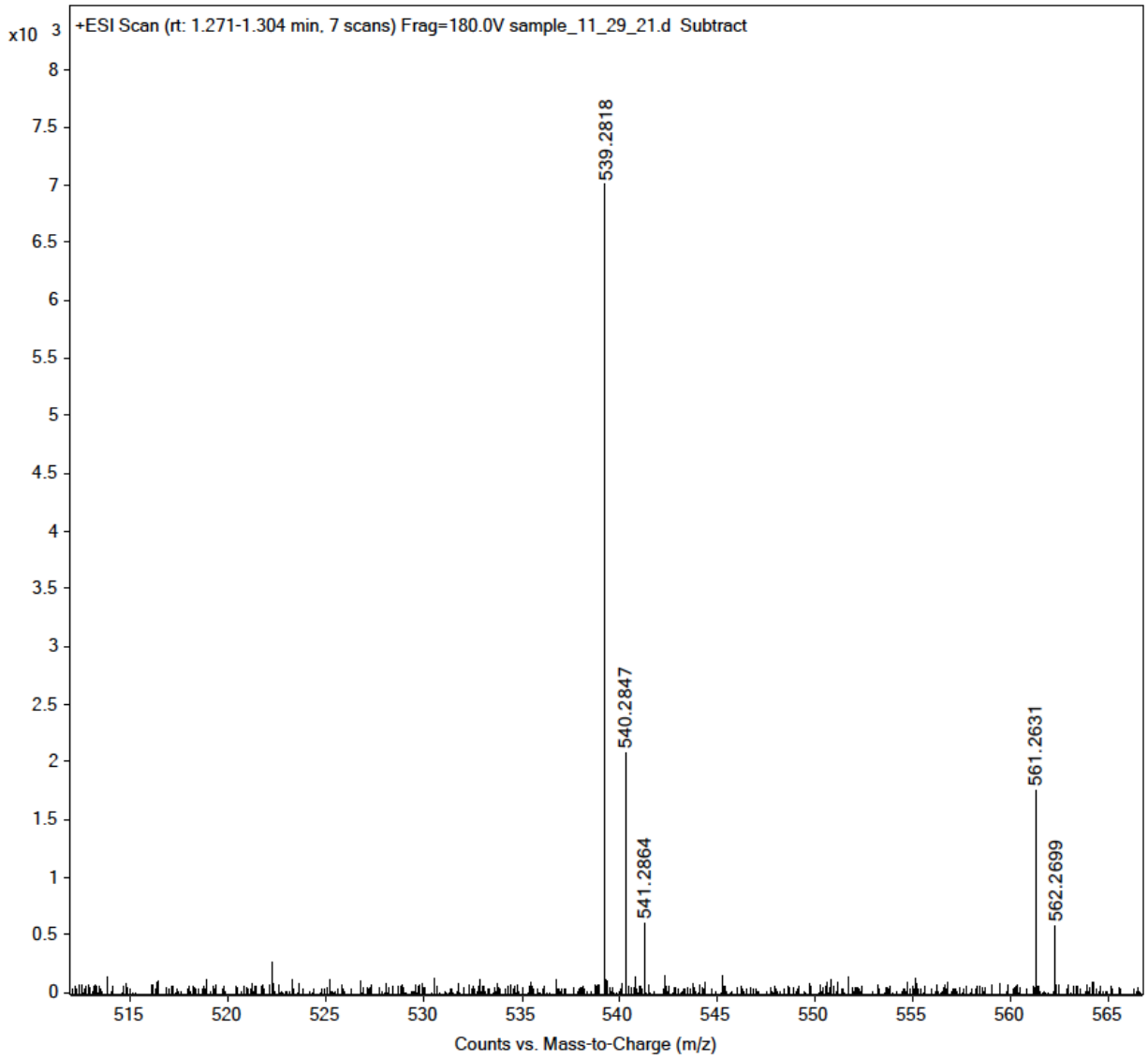

A.6 *Synthesis and Characterization of Compounds in Chapter 6*

Scheme S1. Synthesis of D-LysFl (shown) and L-LysFl

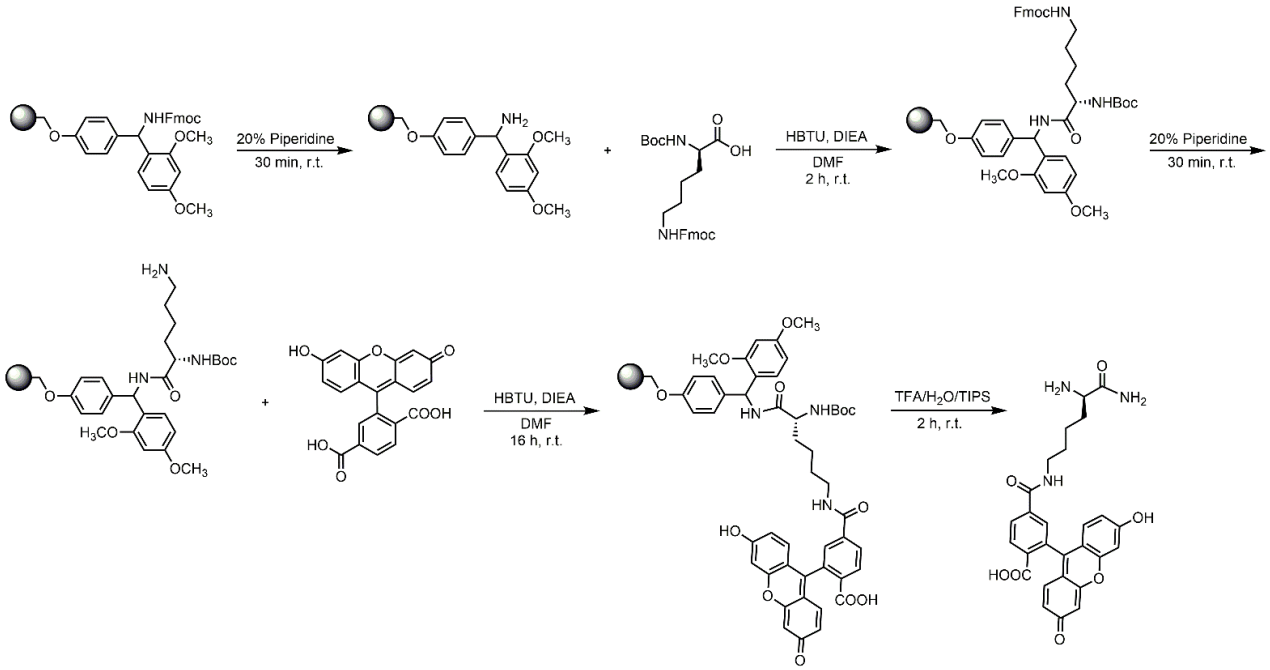

A 25 mL peptide synthesis vessel charged with rink amide resin (250 mg, 0.11 mmol) underwent the Fmoc removal procedure and was washed as described above. Boc-D-Lysine(Fmoc)-OH (5 eq, 257 mg, 0.55 mmol), HBTU (4.9 eq, 204 mg, 0.53 mmol), and DIEA (10 eq, 0.191 mL, 1.10 mmol) in DMF (15 mL) were added to the reaction vessel and agitated for 2 h at ambient temperature. After 2 h the resin was washed as previously stated and the Fmoc protecting group removal was also performed as described above followed by washing. The resin was coupled with 5,6-carboxyfluorescein (2 eq, 82 mg, 0.22 mmol), HBTU (1.9 eq, 79 mg, 0.20 mmol), and DIEA (4 eq, 0.076 mL, 0.44 mmol) in DMF (15 mL) and agitated for 16h at ambient temperature. The resin was washed as previously described and then added to a solution of TFA/H_2O/TIPS (95%, 2.5%, 2.5%, 20 mL) with agitation for 2 h at ambient temperature. The resin was filtered and the resulting solution was concentrated *in vacuo*. The residue was trituated with cold diethyl ether. The sample was analyzed for purity using a Waters 1525 Binary HPLC Pump using a Phenomenex Luna 5u C8(2) 100A (250 x 4.60 mm) column; gradient elution with H_2O/CH_3CN.

D-LysFl

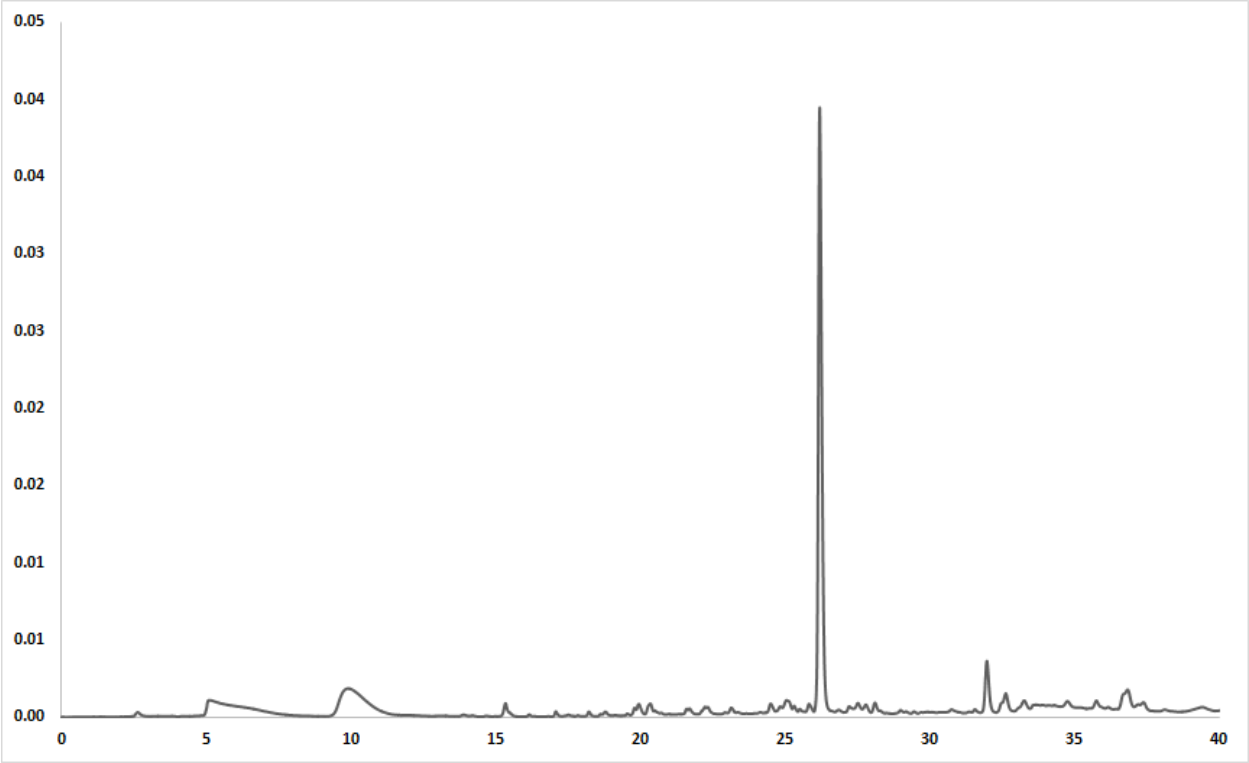

ESI-MS calculated $[M + H]^+$: 504.1765, found: 504.1765

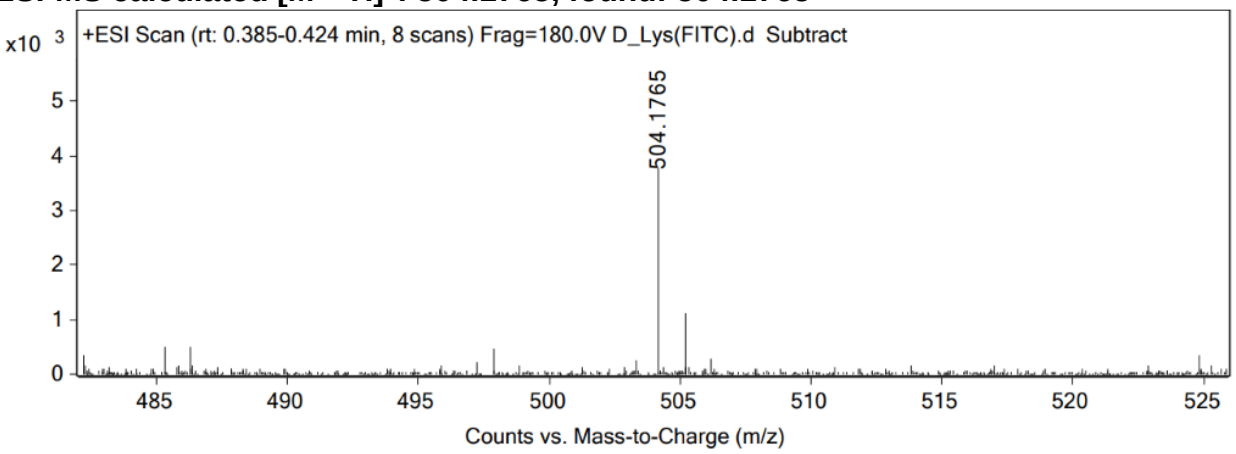

L-LysFl

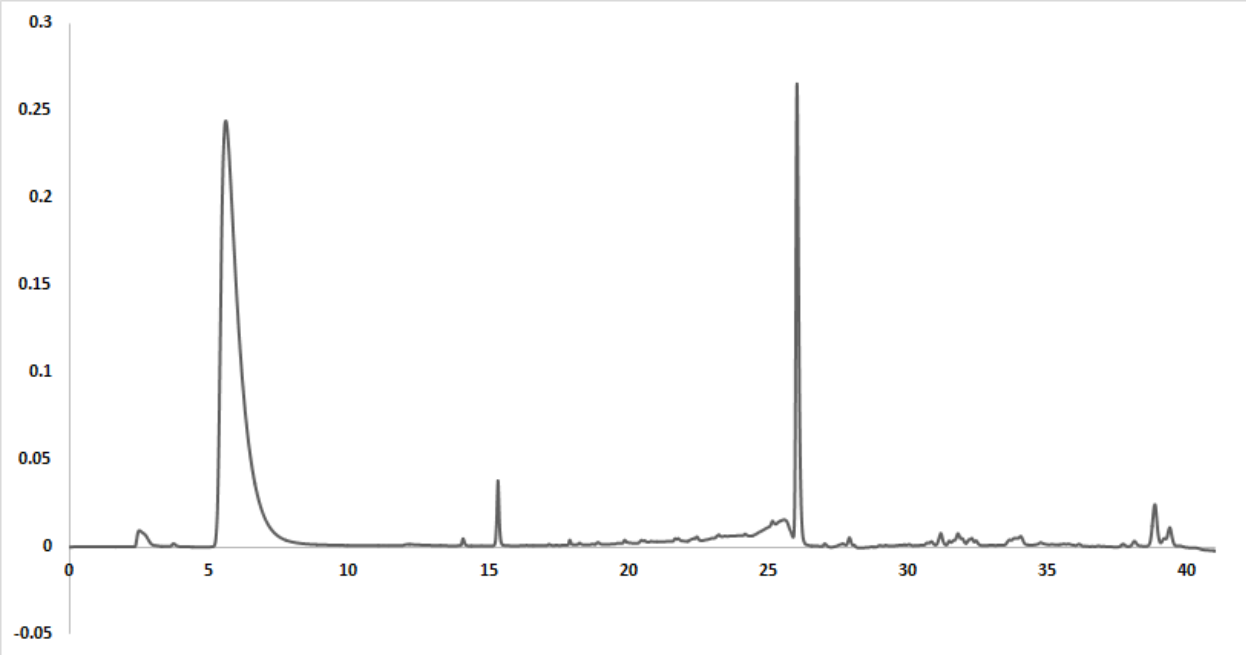

ESI-MS calculated $[M + H]^+$: 504.1765, found: 504.1767

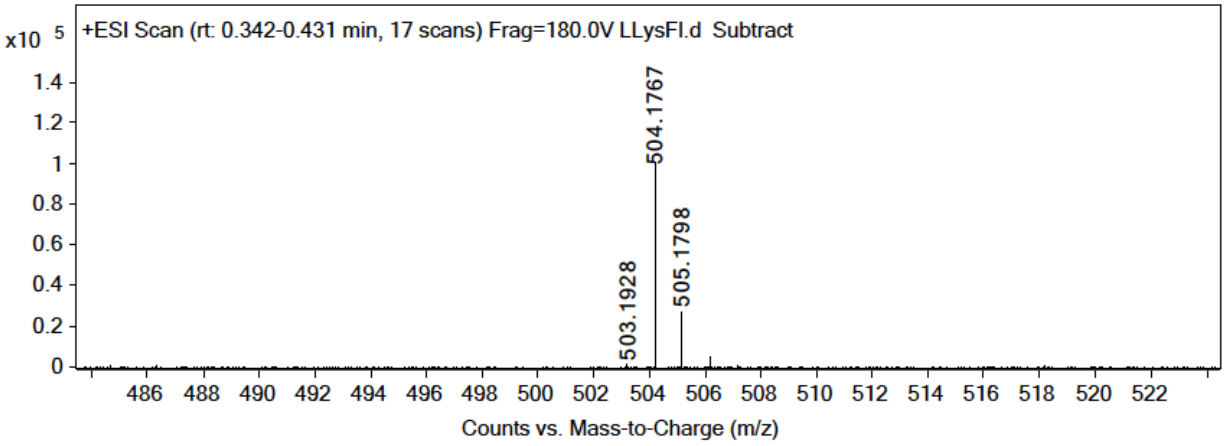

Scheme S2. Synthesis of DBCO-peg$_9$-Fl

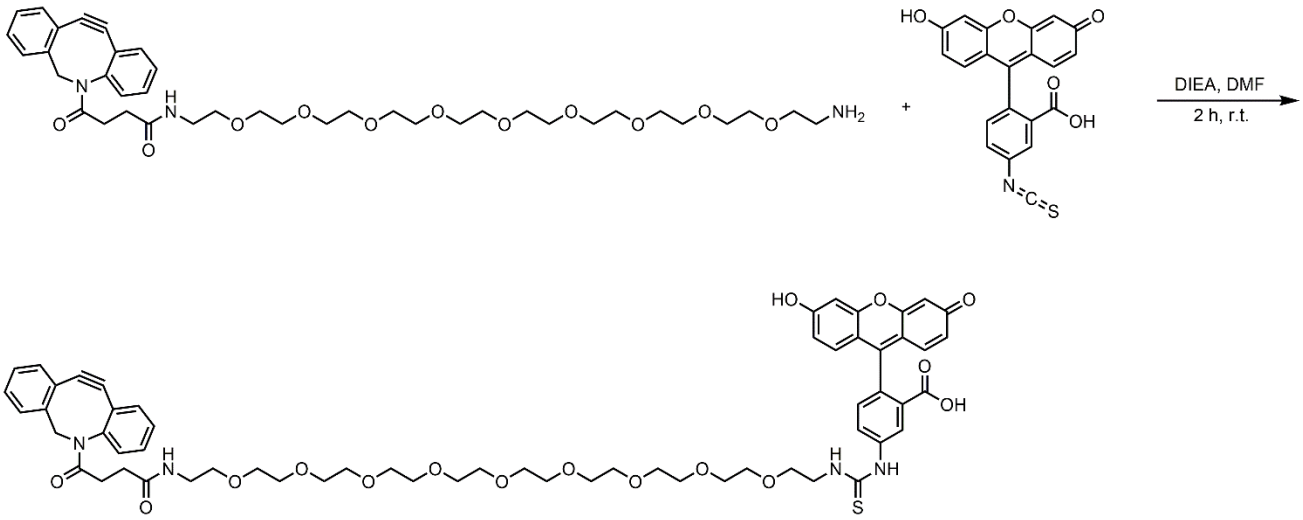

DBCO-PEG$_9$-amine was added to fluorescein isothiocyanate isomer I (2 eq) and DIEA (2 eq) in DMF and allowed to react at ambient temperature for 2 h. The reaction mix was purified using reverse phase HPLC using H_2O/MeOH. The sample was analyzed for purity using a Waters 1525 Binary HPLC Pump using a Phenomenex Luna 5u C8(2) 100A (250 x 4.60 mm) column; gradient elution with H_2O/CH_3CN (DMSO signal has been subtracted).

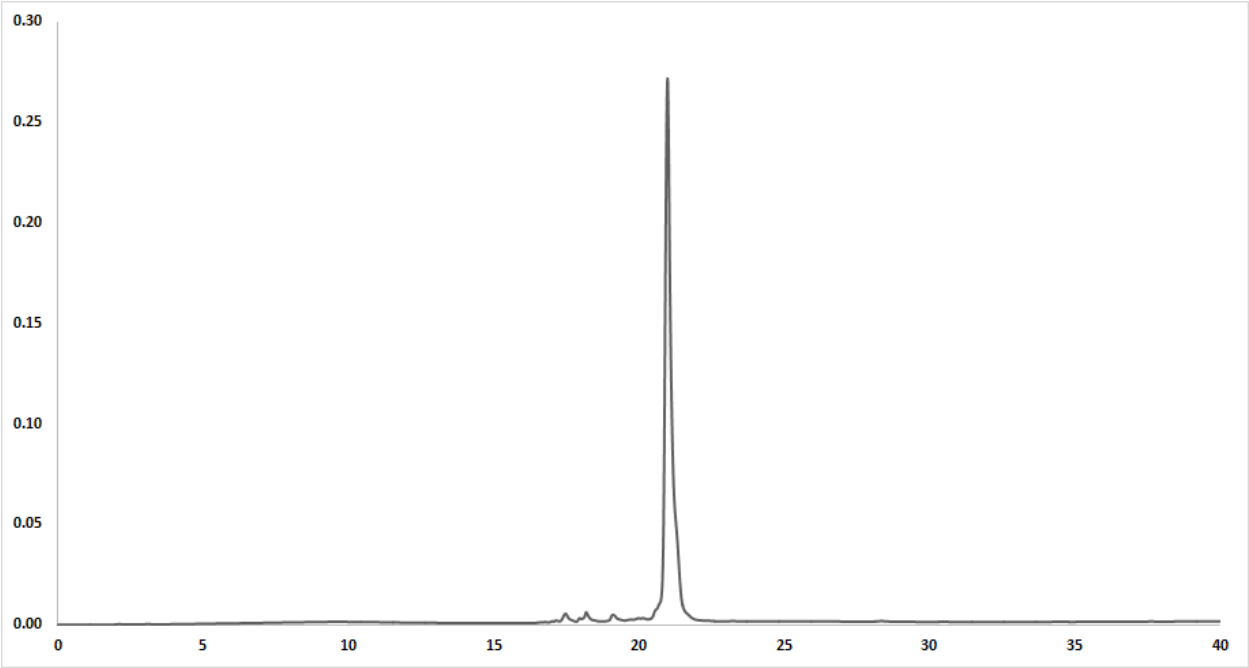

ESI-MS calculated $[M + H]^+$: 1133.4423, found: 1133.4428

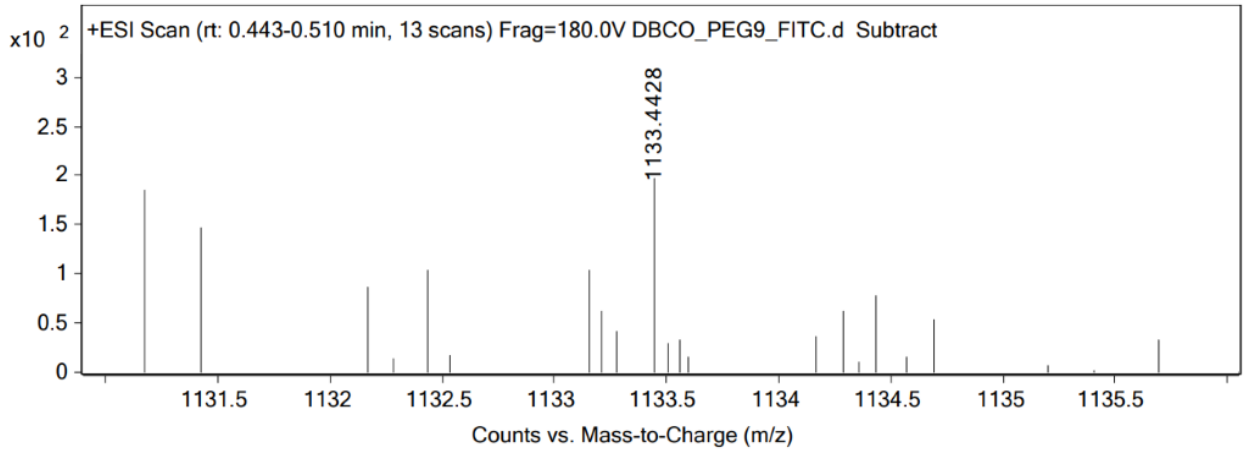

Scheme S3. Synthesis of Fl-LPMTG

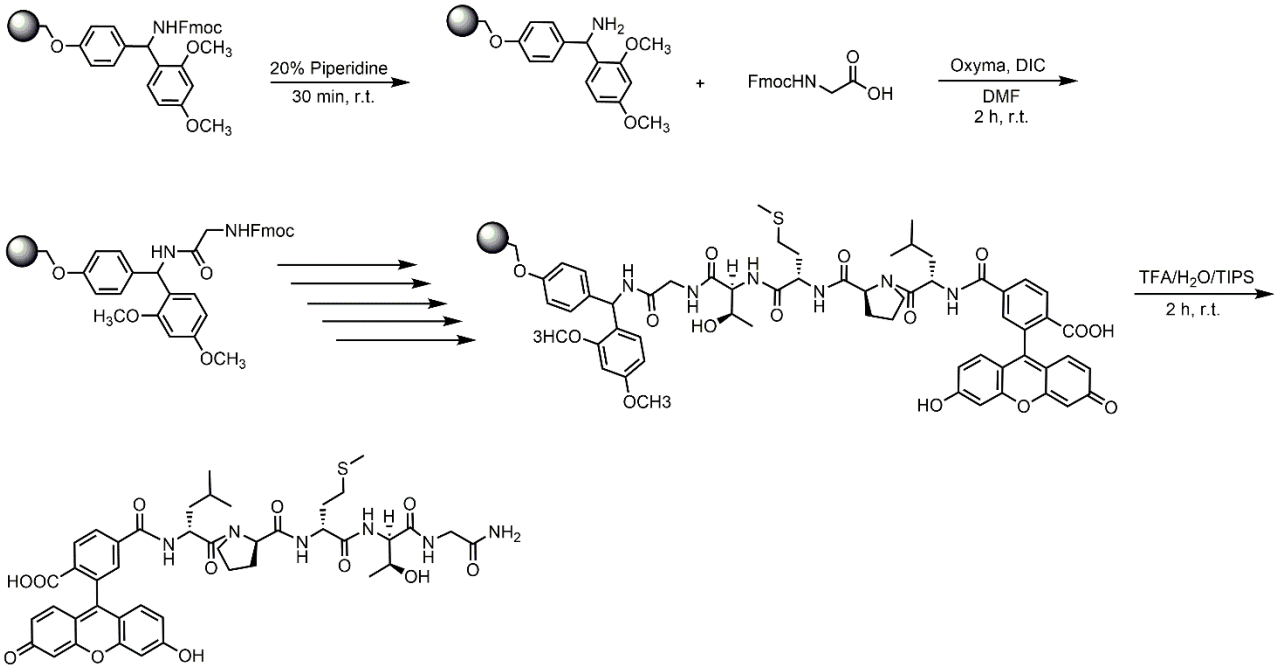

A 25 mL synthetic vessel was charged with 500 mg (0.27 mmol) of Fmoc-Rink amide resin. The Fmoc protecting group was removed with a 20% piperidine in DMF solution (15 mL) for 30 minutes at ambient temperature, then washed with MeOH and DCM (3 x 15 mL each). Fmoc-glycine-OH (3 eq, 240 mg, 0.810 mmol), Oxyma (3 eq, 115 mg, 0.810 mmol), and DIC (3 eq, 126 uL, 0.810 mmol) in DMF (15 mL) was added to the reaction vessel and agitated for 2 hours at ambient temperature and washed as previously stated. The Fmoc removal and coupling procedure was repeated as before using the same equivalencies with Fmoc-L-threonine(tBu)-OH, Fmoc-L-methionine-OH, Fmoc-L-proline-OH, and Fmoc-L-leucine-OH. The Fmoc group of L-leucine was deprotected and resin coupled with 5,6-carboxyfluorescein (2 eq, 203 mg, 0.810 mmol), HBTU (2 eq, 201 mg, 0.810 mmol), and DIEA (4 eq, 187 uL, 1.08 mmol) in DMF (15 mL) shaking over-night. The resin was washed as previously described. To remove the peptide from resin, a TFA cocktail solution (95 % TFA, 2.5% TIPS, and 2.5 % DCM) was added to the resin with agitation for 2 hours protected from light. The resin was filtered and resulting solution was concentrated *in vacuo*. The peptide was trituated with cold diethyl ether and purified using reverse phase HPLC using H_2O/MeOH to yield **Fl-LPMTG**. The sample was analyzed for purity using a Waters 1525 Binary HPLC Pump using a Phenomenex Luna 5u C8(2) 100A (250 x 4.60 mm) column; gradient elution with H_2O/CH_3CN.

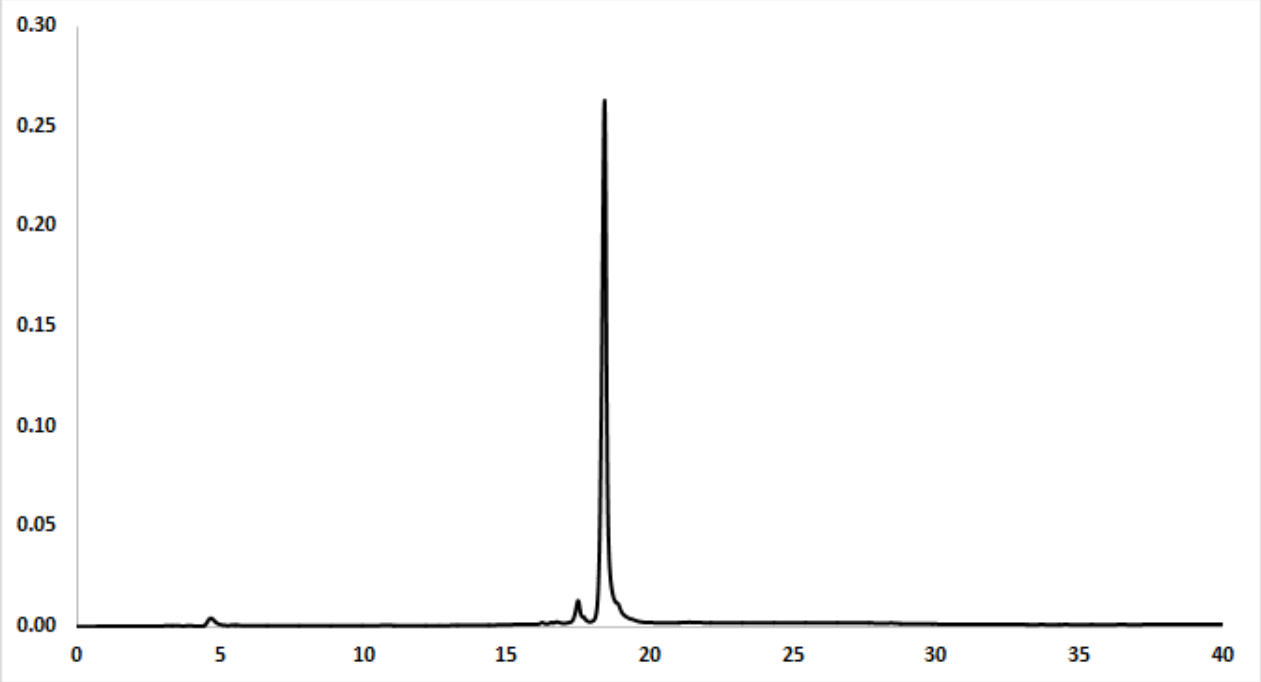

ESI-MS calculated $[M + H]^+$: 875.3280, found: 875.3529

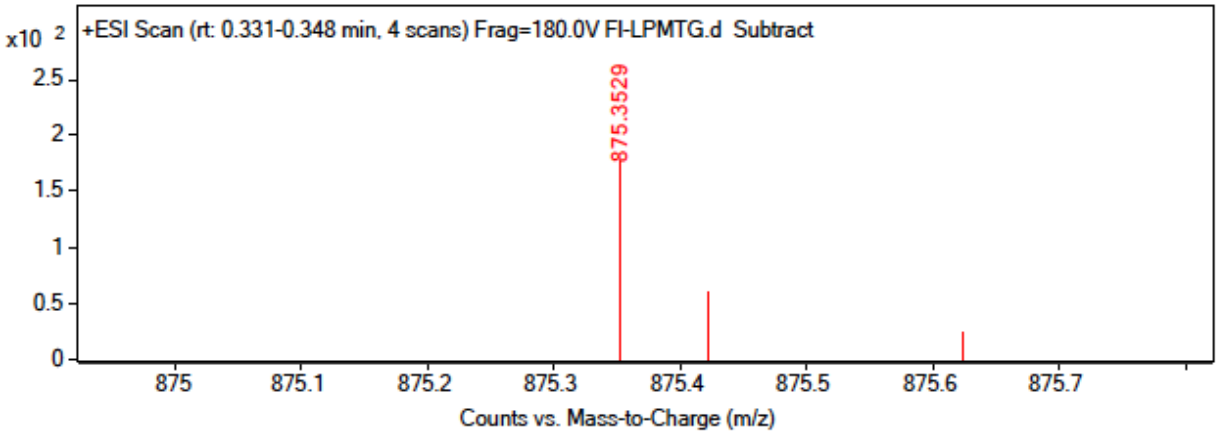

A.7 Synthesis and Characterization of Compounds in Chapter 7

Scheme S1. Synthesis of D- and L-Phe-Tetrazine.

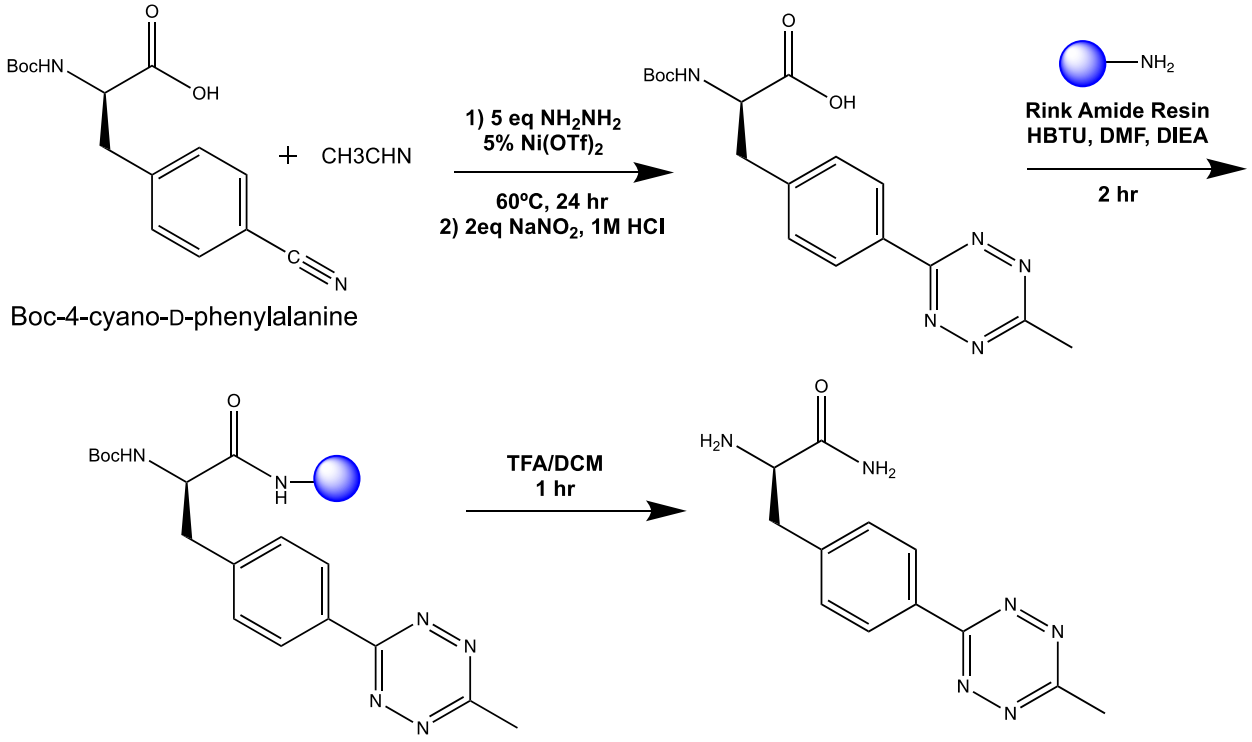

Boc-4-cyano-D-phenylalanine (1.00 g, 3.45 mmol) was added to a reaction vessel with a stir bar. Nickel (II) trifluoromethanesulfonate (61.6 mg, 0.17 mmol), acetonitrile (1.80 mL, 34.5 mmol), and anhydrous hydrazine (5.50 mL, 172 mmol) were added. The vessel was sealed, and the mixture stirred in an oil bath for 24 hr at 60ºC. The solution was cooled to room temperature, followed by the dropwise addition of sodium nitrite (4.76g, 69.0 mmol) in 8 mL of water. 1M HCl was added dropwise until gas evolution ceased and pH of the solution was 3. The mixture was extracted with EtOAc, organic phase dried with $MgSO_4$. The Boc-protected tetrazine was dissolved in DMF (20 mL), followed by the addition of HBTU (3 eq, 3.16g, 8.33 mmol) and DIEA (6 eq, 2.90 mL, 16.6 mmol). The mixture was added to a peptide vessel containing rink amide resin (5.00g, 2.05 mmol) and the vessel was incubated for 2 hr at ambient temperature with shaking. The resin was washed with DCM, MeOH, DCM, MeOH, DCM 2X (15 mL each). The resin was transferred to a round bottom flask and a solution of TFA/DCM (30:70, 30 mL) was added and stirred for 1 hr on ice. The residue was triturated with cold diethyl ether and the precipitate was purified by reversed phase HPLC (RP-HPLC) using a c18(2) column (Phenomenex) to yield **D-Tet-**

NH_2 or **L-Tet-NH_2** as a pink solid. For **D-Tet-OH**, there was no coupling to rink amide resin. The $MgSO_4$ dried solution was concentrated *in vacuo*, treated with TFA/DCM (30:70, 30 mL) to remove Boc, triturated with cold diethyl ether, and purified.

D-Tet-NH_2

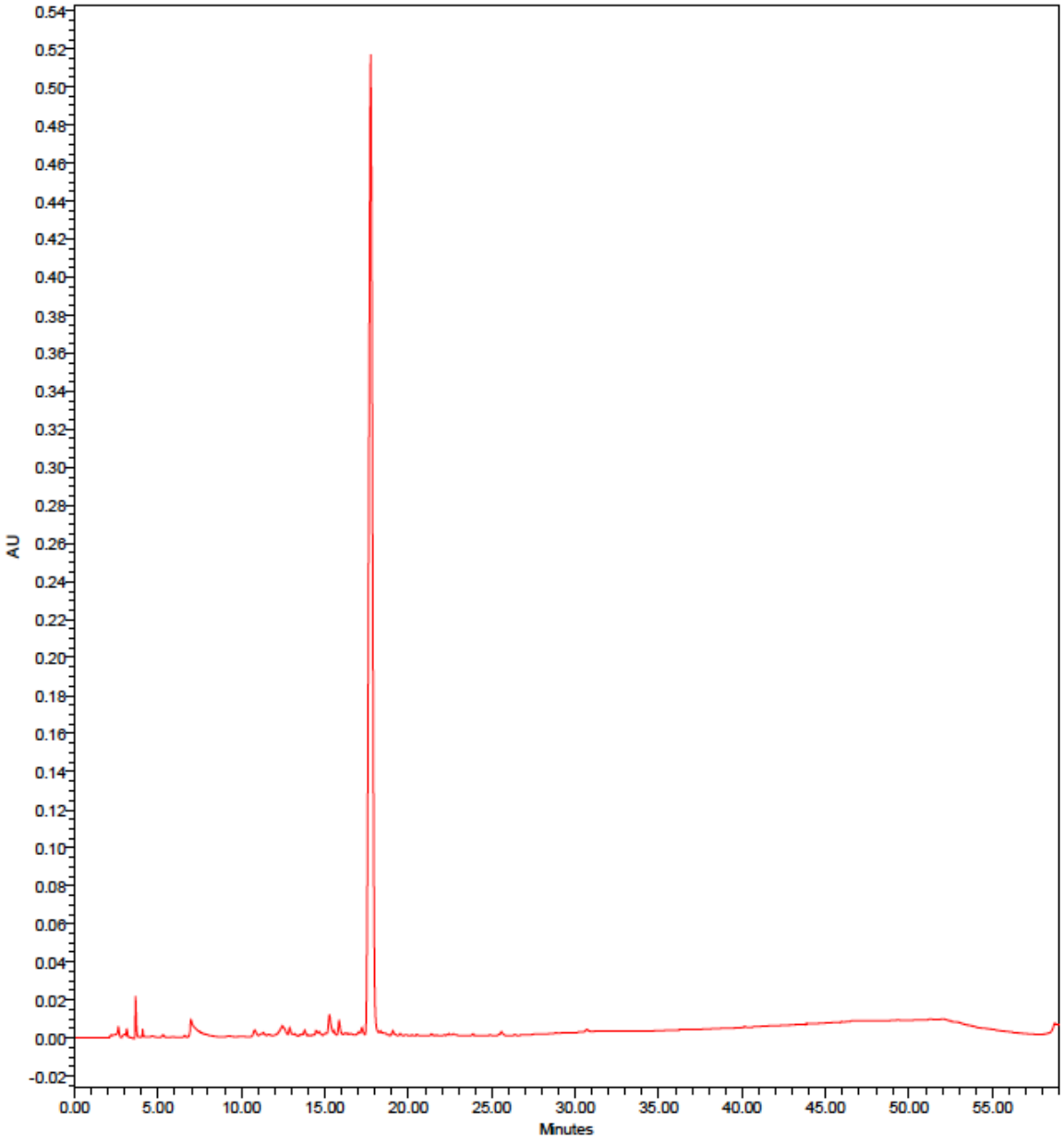
AU
0.54
0.52
0.50
0.48
0.46
0.44
0.42
0.40
0.38
0.36
0.34
0.32
0.30
0.28
0.26
0.24
0.22
0.20
0.18
0.16
0.14
0.12
0.10
0.08
0.06
0.04
0.02
0.00
-0.02
0.00
5.00
10.00
15.00
20.00
25.00
30.00
35.00
40.00
45.00
50.00
55.00
Minutes

$M+H^+$ calculated = 259.1302, observed = 259.1302

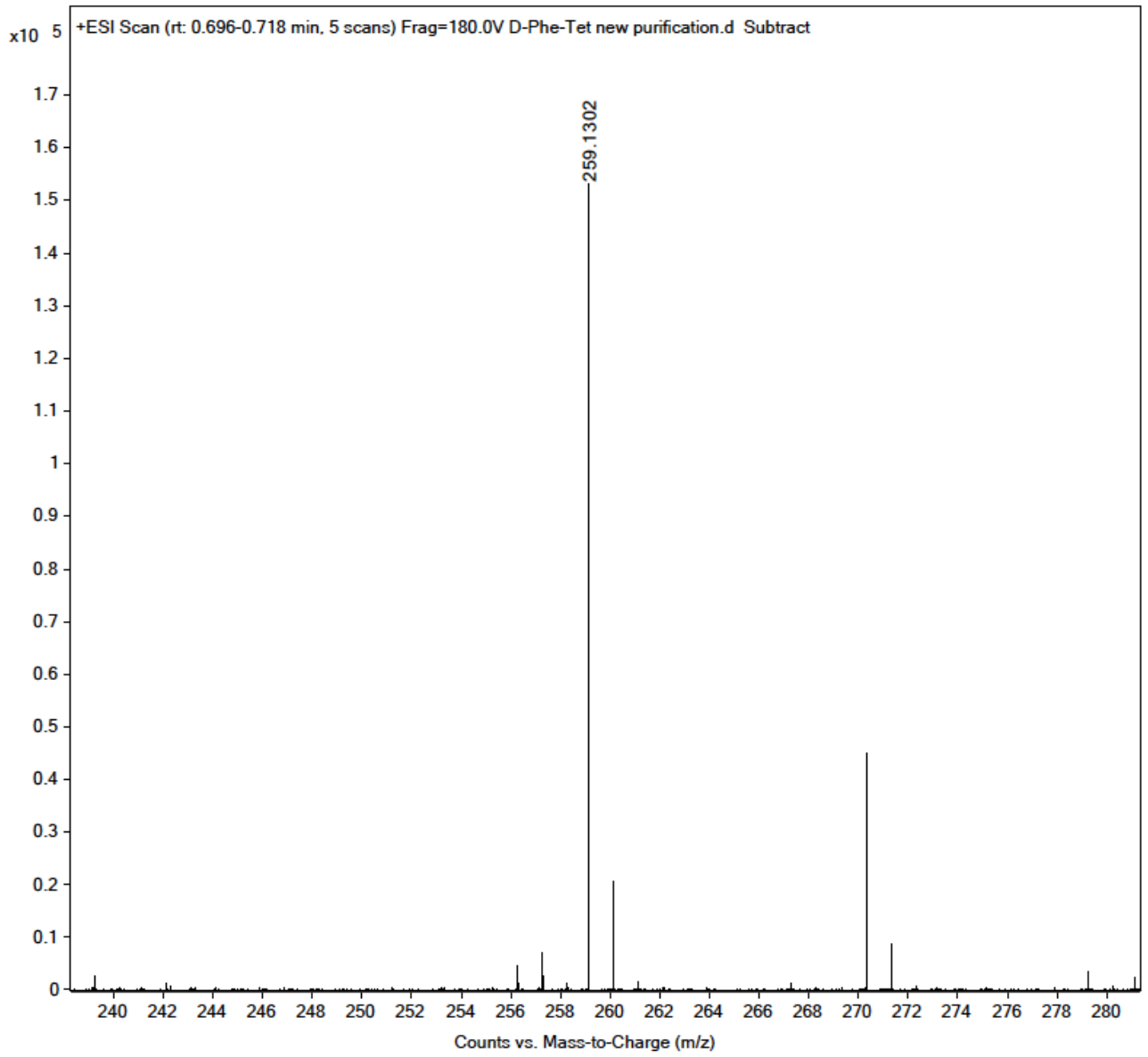

^{1}H NMR (600 MHz, CD_3OD) δ 8.56 (d, *J* = 6.0 Hz, 2H, 2'-ArH), 7.58 (d, *J* = 6.0 Hz, 2H, 3'-ArH), 4.19 (t, J=6.0 Hz, 1H, CH), 3.37 (dd, J=6.0, 18Hz, 1H, CH2), 3.19 (dd, J=6.0, 18Hz, 1H, CH2), 3.05 (s, 3H, CH3).

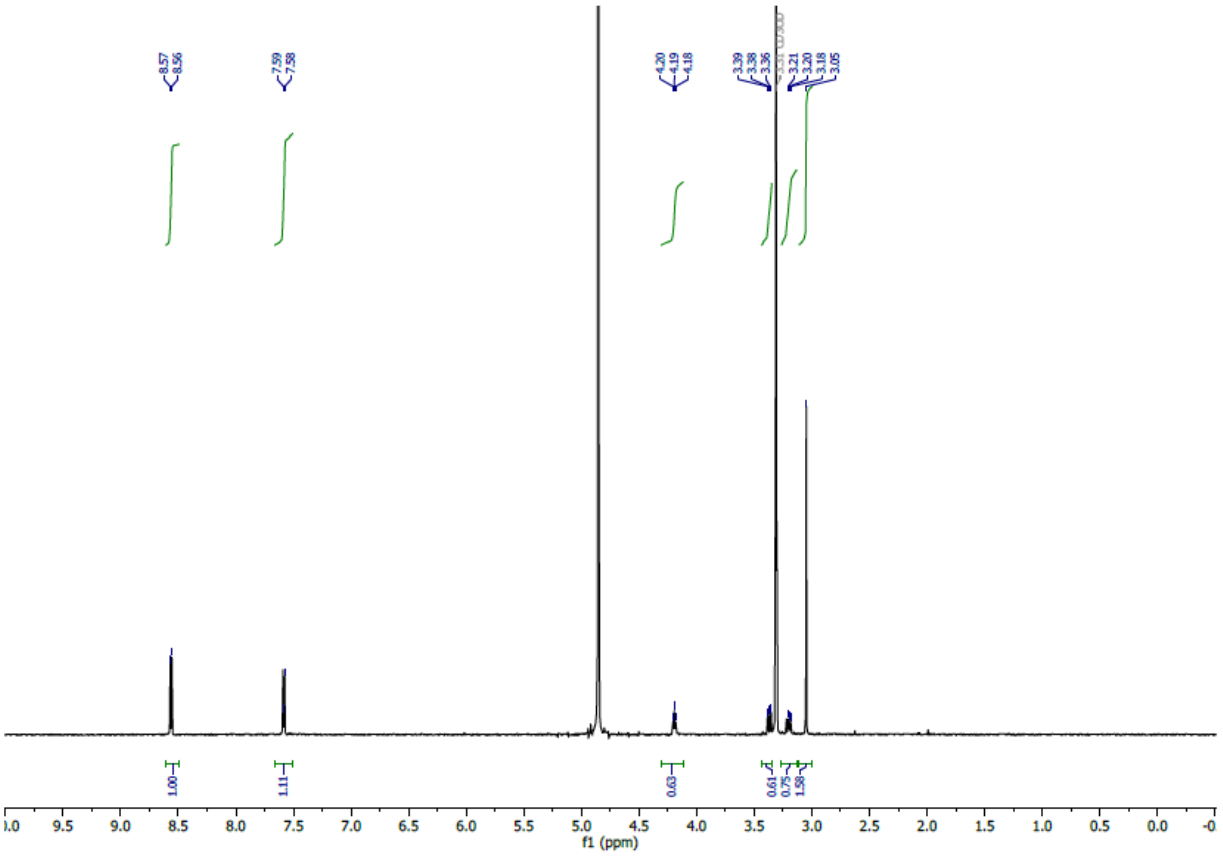

D-Tet-OH

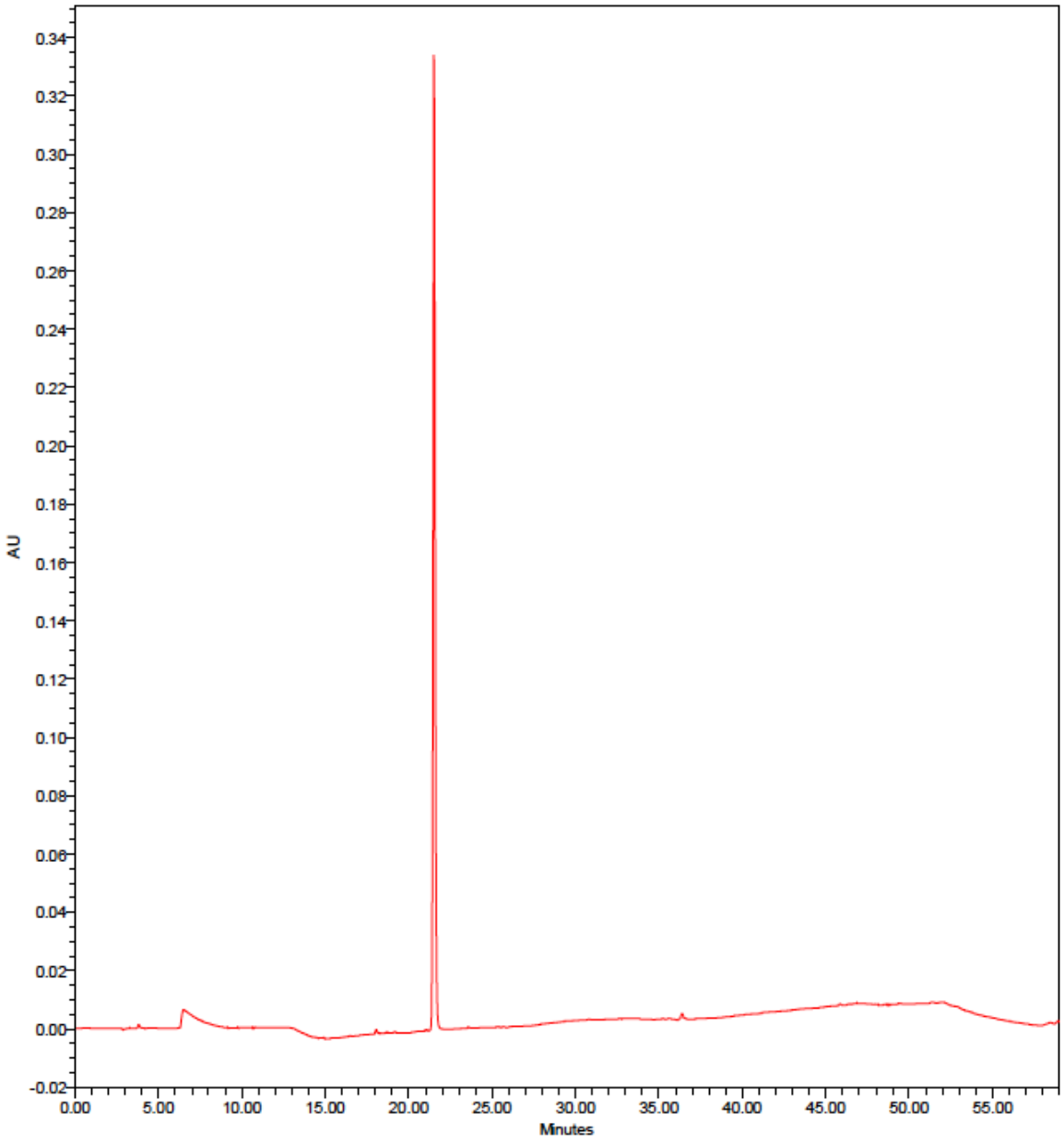
AU
0.34
0.32
0.30
0.28
0.26
0.24
0.22
0.20
0.18
0.16
0.14
0.12
0.10
0.08
0.06
0.04
0.02
0.00
-0.02
0.00
5.00
10.00
15.00
20.00
25.00
30.00
35.00
40.00
45.00
50.00
55.00
Minutes

$M+H^+$ calculated = 260.1142, observed 260.1143

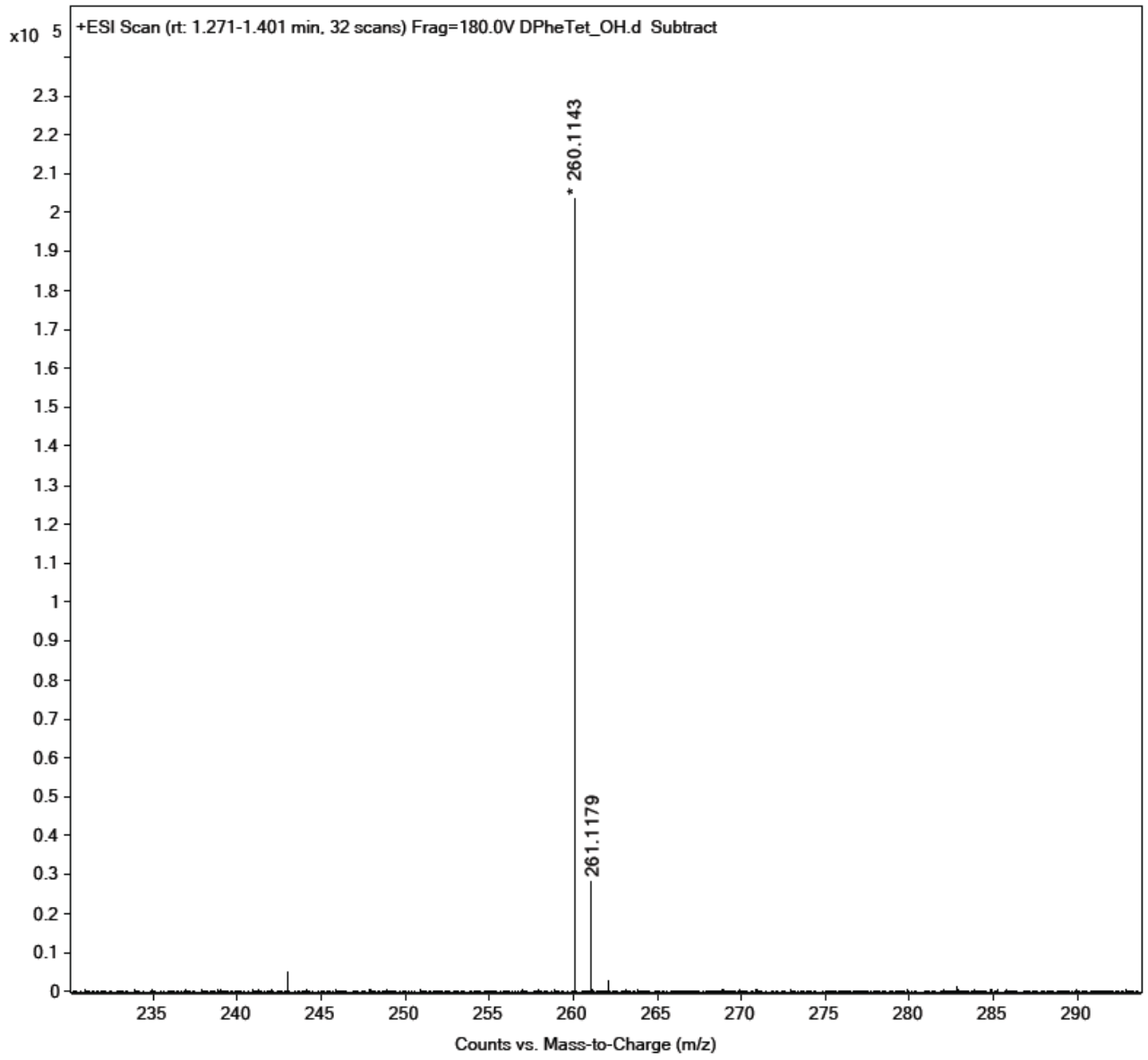

^{1}H NMR (600 MHz, CD_3OD) δ 8.56 (d, *J* = 6.0 Hz, 2H, 2'-ArH), 7.57 (d, *J* = 6.0 Hz, 2H, 3'-ArH), 4.32 (t, *J* = 6.0 Hz, 1H, CH), 3.32 (dd, *J* = 6.0, 18Hz, 1H, CH2), 3.31 (dd, *J* = 6.0, 18Hz, 1H, CH2), 3.05 (s, 3H, CH3).

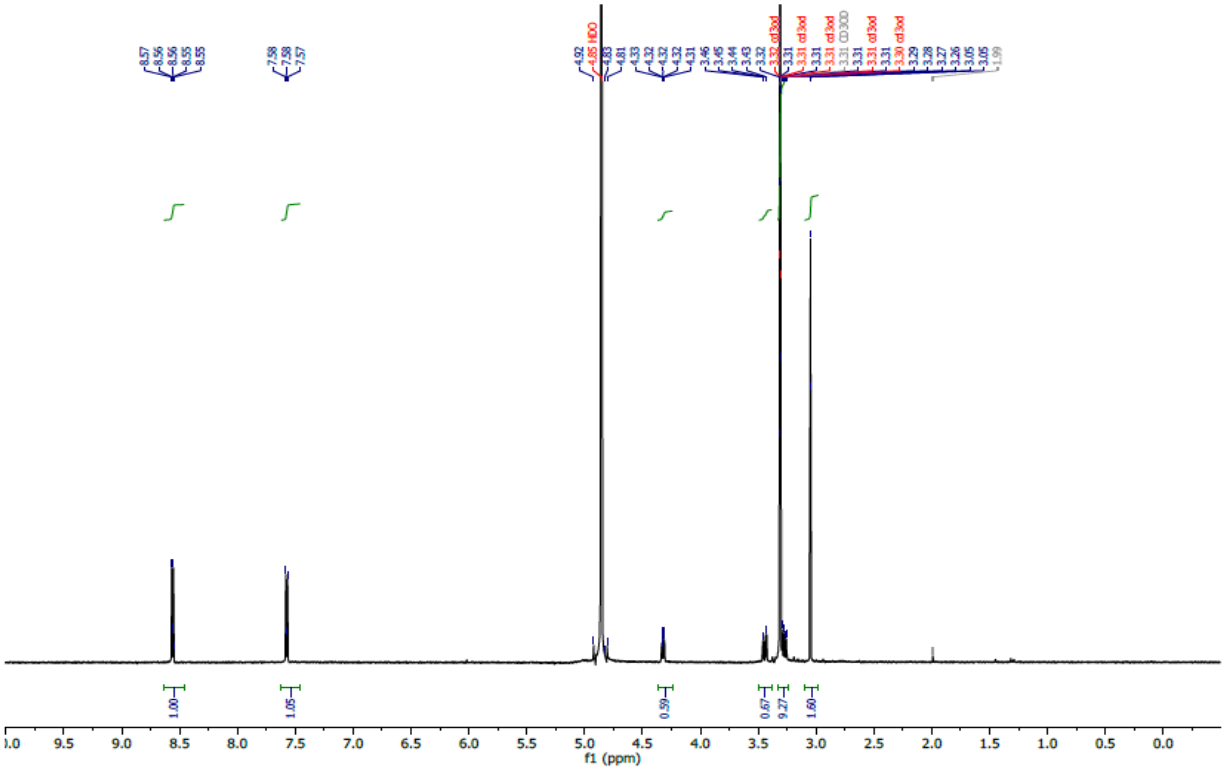

L-Tet-NH_2

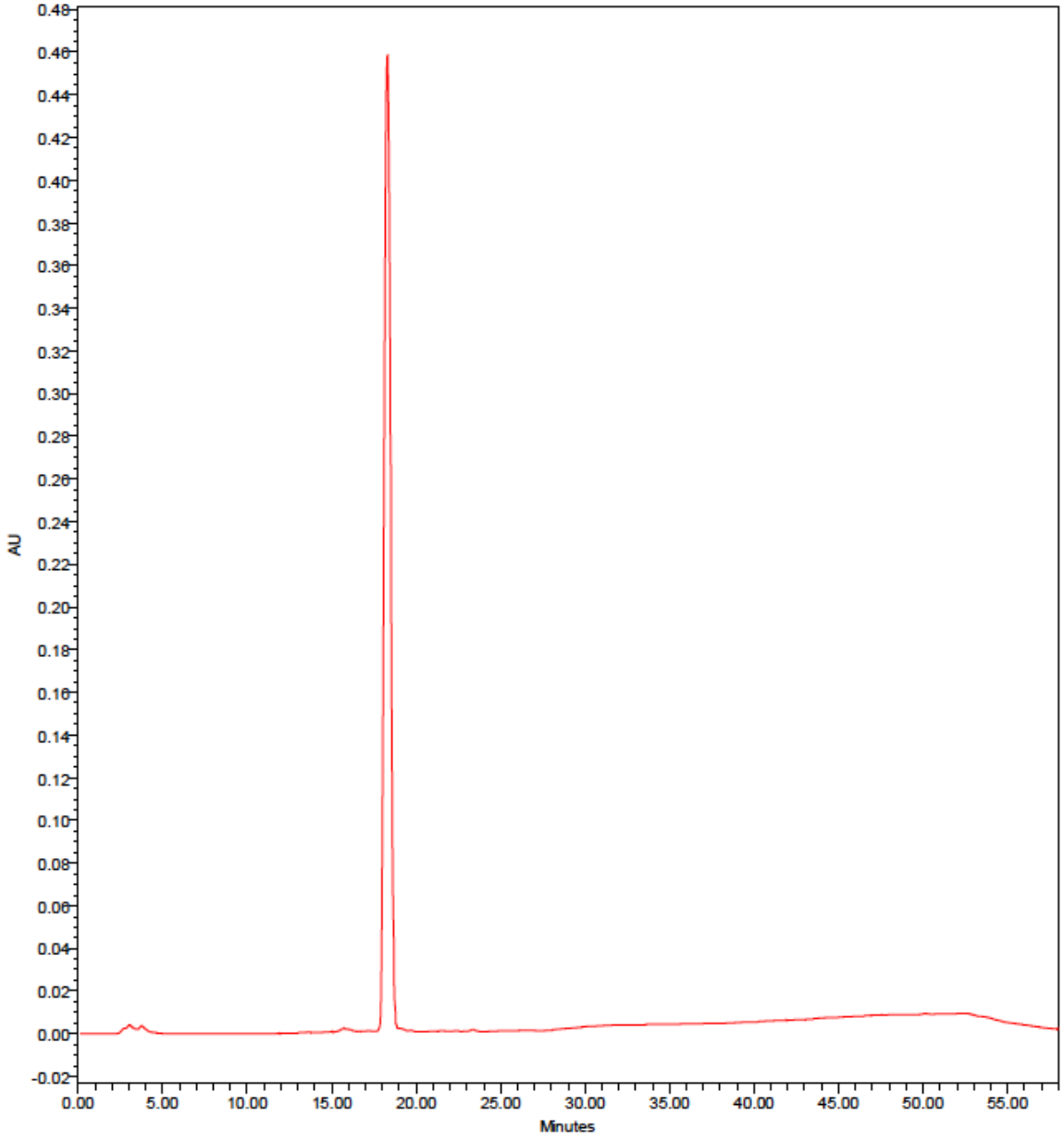
AU
0.48
0.46
0.44
0.42
0.40
0.38
0.36
0.34
0.32
0.30
0.28
0.26
0.24
0.22
0.20
0.18
0.16
0.14
0.12
0.10
0.08
0.06
0.04
0.02
0.00
-0.02
0.00
5.00
10.00
15.00
20.00
25.00
30.00
35.00
40.00
45.00
50.00
55.00
Minutes

$M+H^+$ calculated = 259.1302, observed = 259.1297

$M+Na^+$ calculated = 281.1121, observed = 281.1117

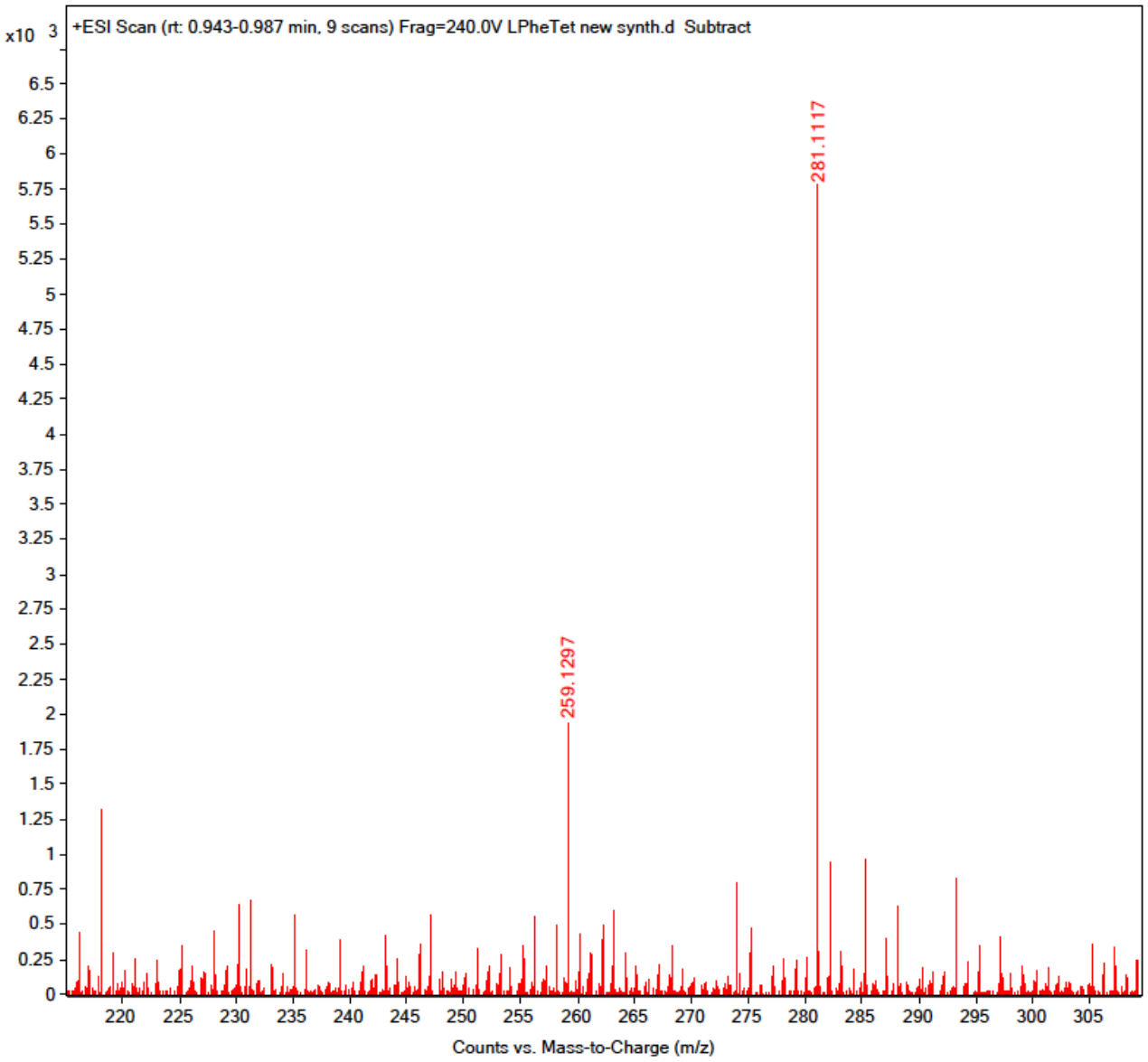

^{1}H NMR (600 MHz, CD_3OD) δ 8.56 (d, *J* = 6.0 Hz, 2H, 2'-ArH), 7.58 (d, *J* = 6.0 Hz, 2H, 3'-ArH), 4.18 (t, J=6.0 Hz, 1H, CH), 3.37 (dd, J=6.0, 18Hz, 1H, CH2), 3.20 (dd, J=6.0, 18Hz, 1H, CH2), 3.05 (s, 3H, CH3).

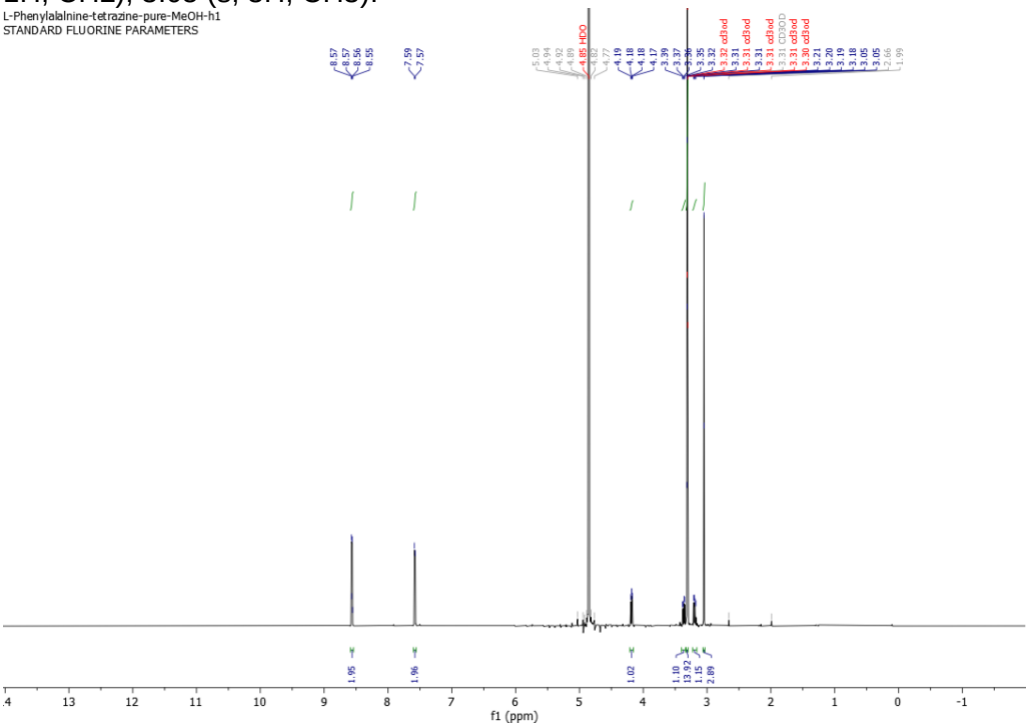

Scheme S2. Synthesis of SulfoCy7.5-TCO

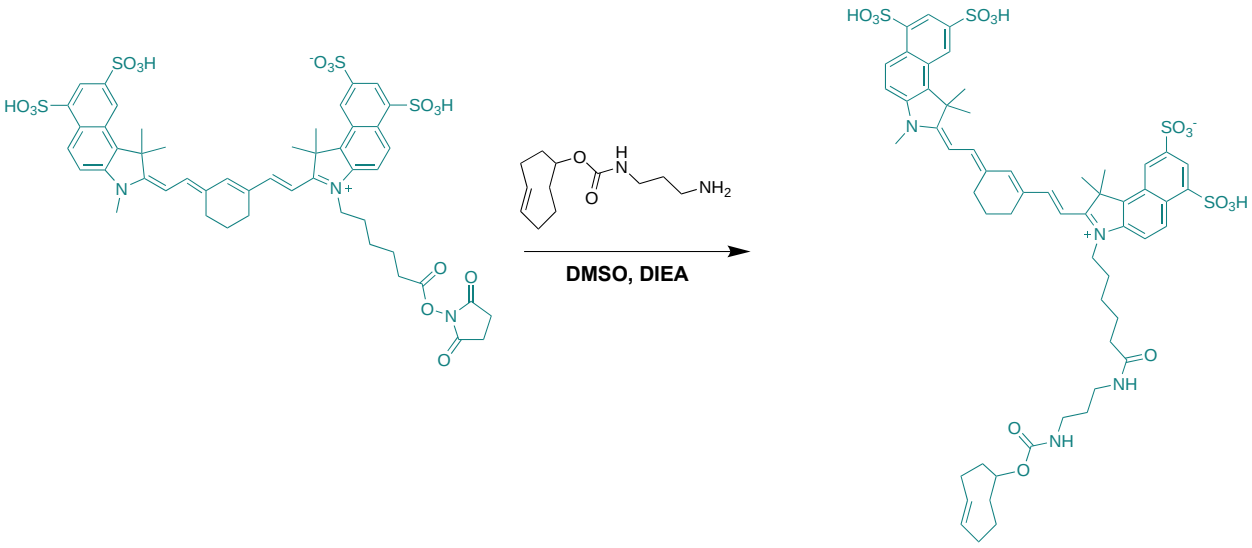

SulfoCy7.5 NHS Ester (Lumiprobe) was reacted with TCO-Amine HCl (Click Chemistry Tools) and DIEA was added to the solution (in DMSO, 1 Sulfo Cy7.5 NHS Ester : 1 TCO-Amine : 7 DIEA). The reaction was purified using RP-HPLC equipped with a C8(2) column.

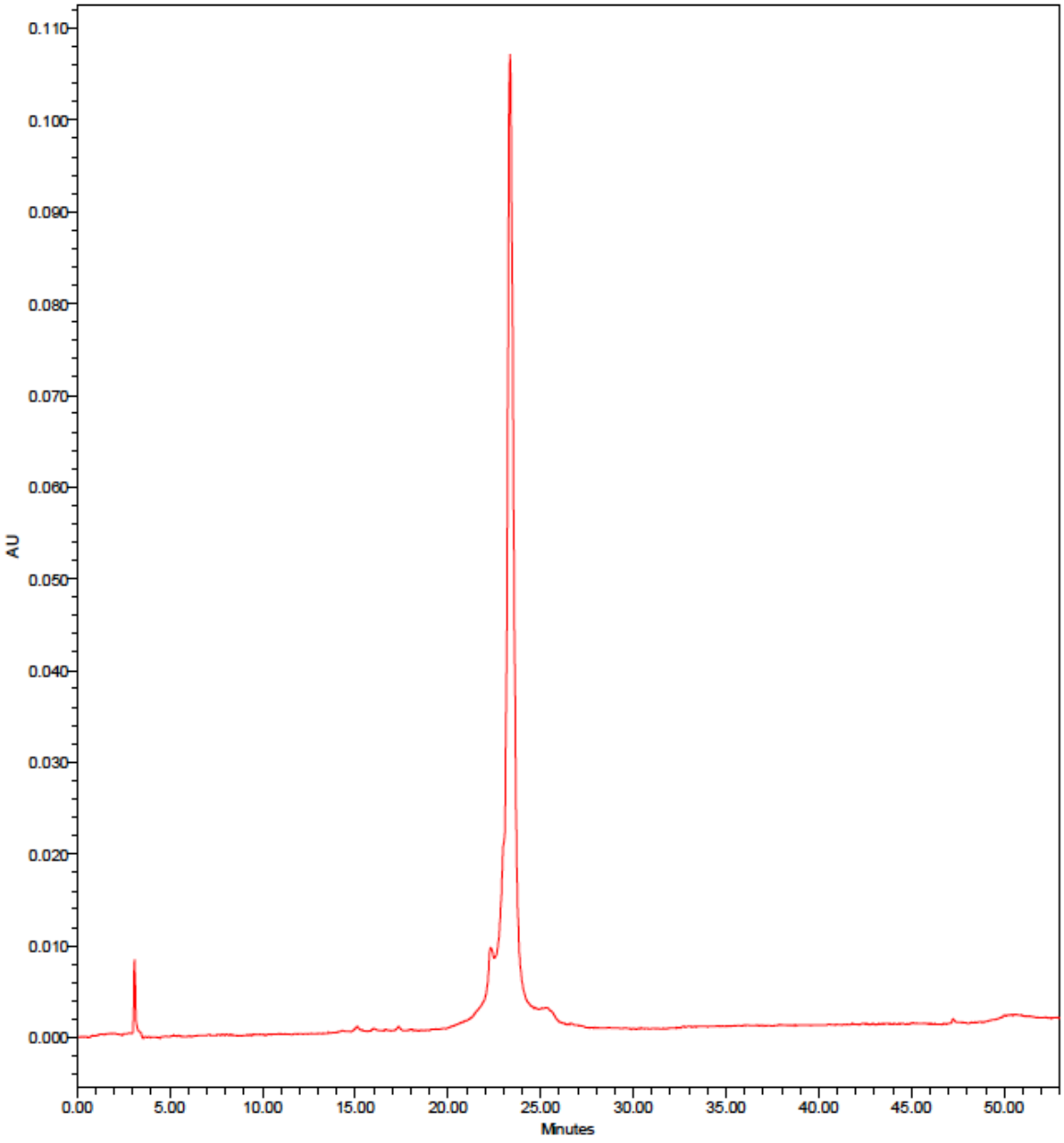
AU
0.110
0.100
0.090
0.080
0.070
0.060
0.050
0.040
0.030
0.020
0.010
0.000
0.00
5.00
10.00
15.00
20.00
25.00
30.00
35.00
40.00
45.00
50.00
Minutes

$M+H^+$ calculated = 1178.3710, observed = 1178.7711

$M+2H^+$ calculated = 589.6891, observed = 589. 4264

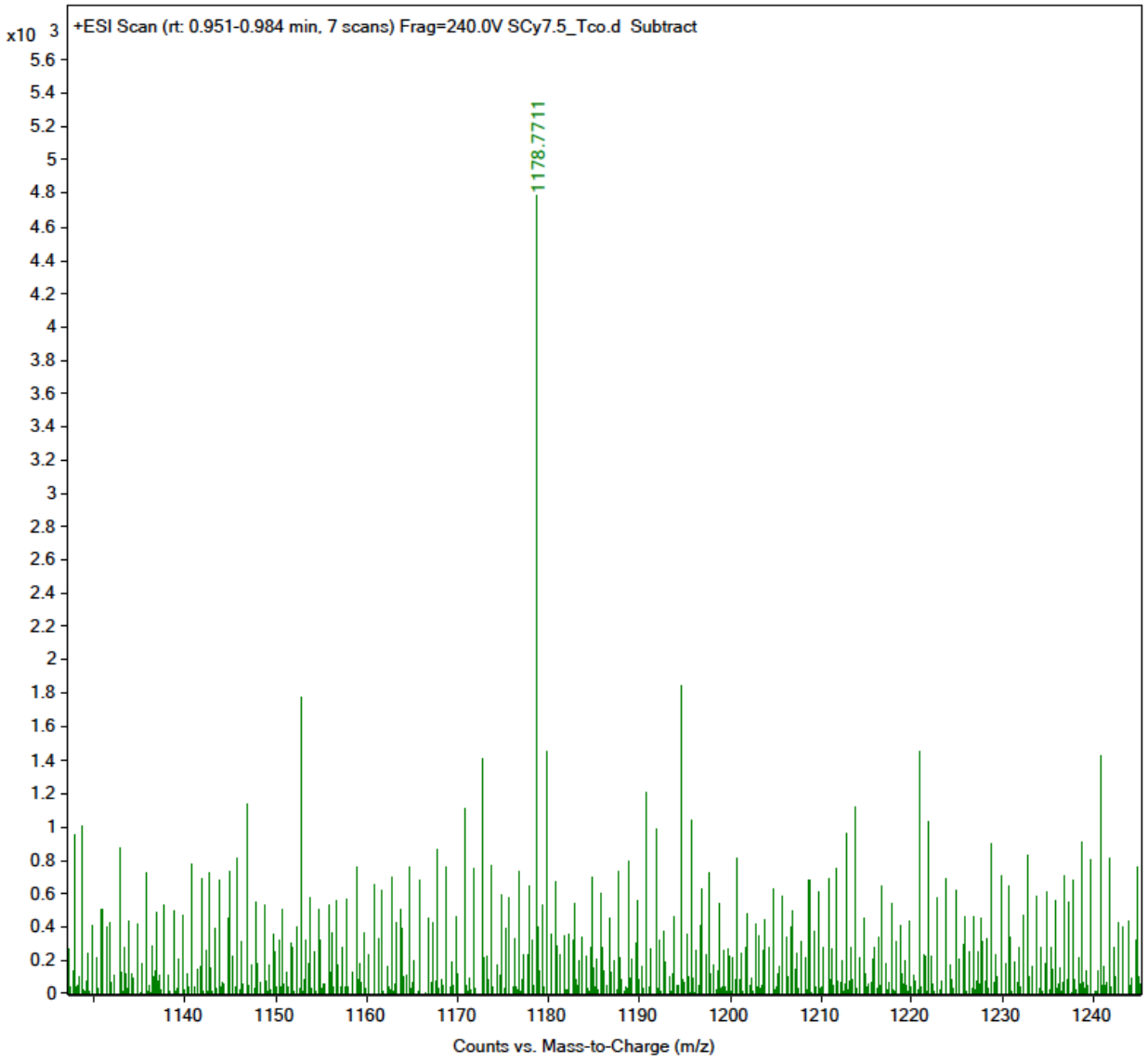

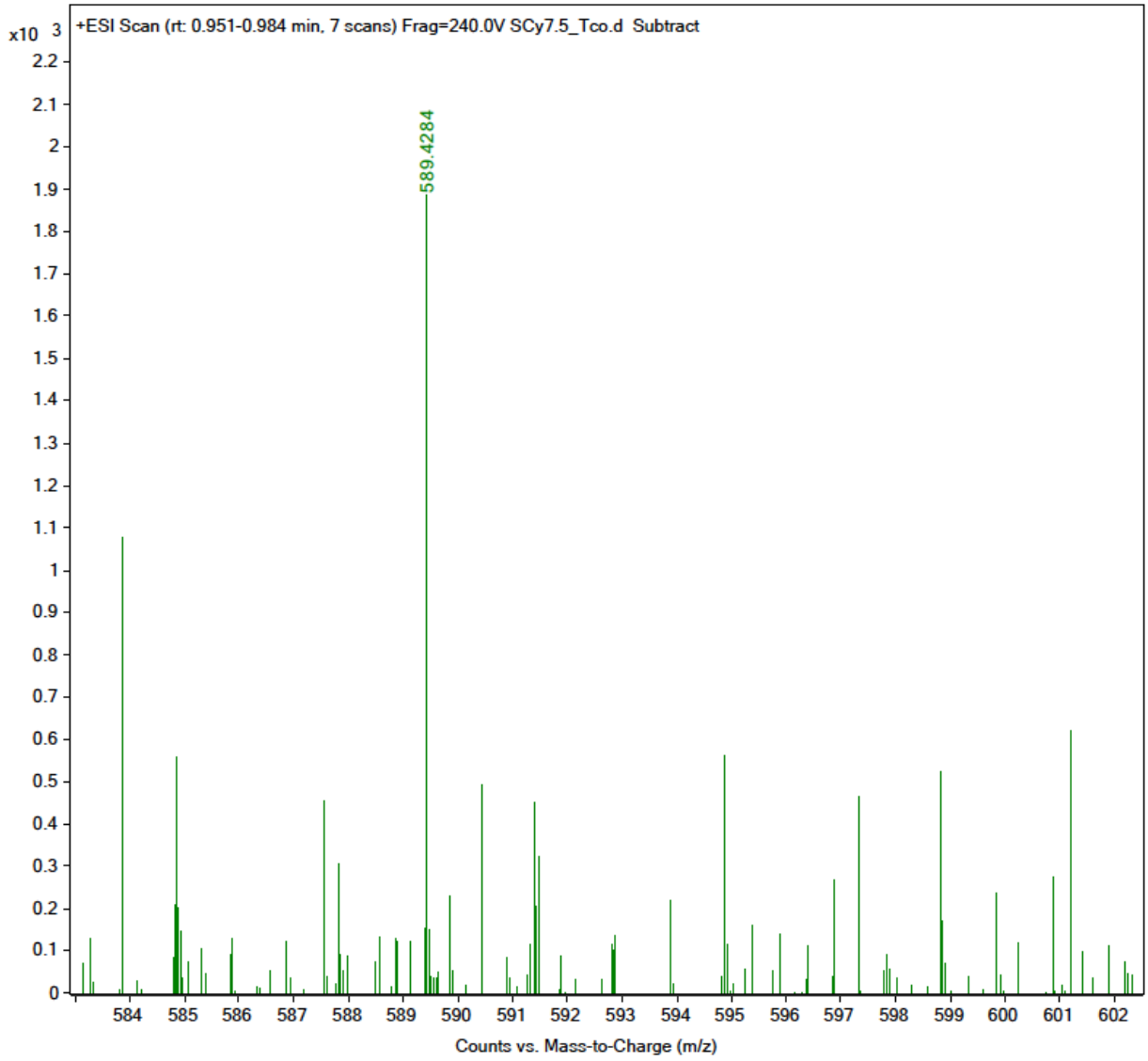
+ESI Scan (rt: 0.951-0.984 min, 7 scans) Frag=240.0V SCy7.5_Tco.d Subtract
x10 3
589.4284
Counts vs. Mass-to-Charge (m/z)

Scheme S3. Synthesis of SulfoCy7.5-Tetra$_Q$Lys(Ac)

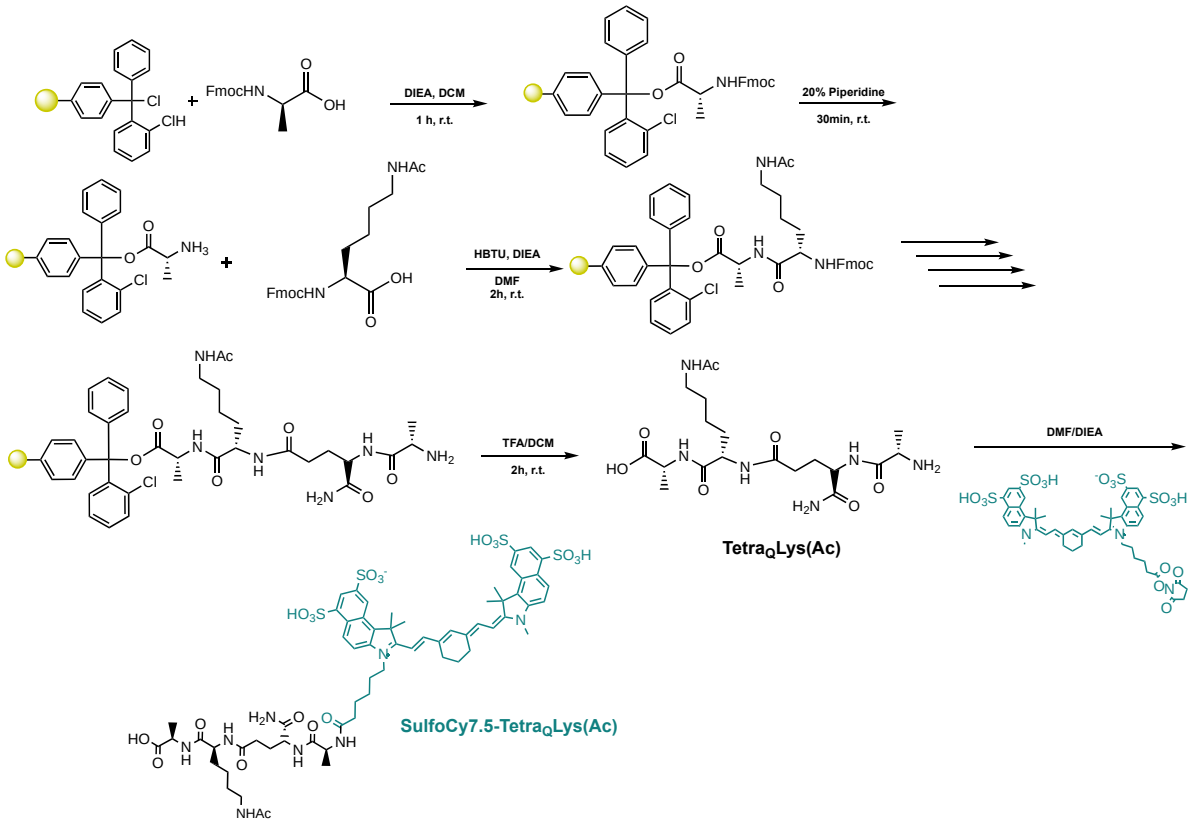

Fmoc-D-Ala-OH **or** Fmoc-L-Ala-OH (1.1 eq, 188 mg, 0.605 mmol) was added to a 25 mL peptide synthesis vessel charged with 2-chlorotrityl chloride resin (500 mg, 0.55 mmol) and DIEA (4 eq, 0.382 mL, 2.20 mmol) in dry DCM (5 mL). The resin was agitated for 1 h at ambient temperature and washed with MeOH and DCM (3 x 15 mL each). The Fmoc protecting group was removed with 20% piperidine in DMF (15 ml) for 30 min at ambient temperature, then washed as before. Fmoc-L-Lys(Ac)-OH (3 eq, 677 mg, 1.65 mmol), HBTU (3 eq, 625 mg, 1.65 mmol), and DIEA (6 eq, 0.574 mL, 3.30 mmol) in DMF (10 mL) were added to the reaction flask and agitated for 2 h at ambient temperature. The Fmoc deprotection and coupling procedure was repeated as before using the same equivalencies with Fmoc-D-glutamic acid α-amide (3 eq, 608 mg, 1.65 mmol) and then with Fmoc-L-Alanine-OH (3 eq, 514 mg, 1.65 mmol). The Fmoc group at the *N*-terminus was removed and the peptide was cleaved from resin with a solution of TFA/H_2O/TIPS (95%, 2.5%, 2.5%, 20 mL) with agitation for 2 h at ambient temperature. The resin was filtered and resulting solution concentrated *in vacuo*. The residue was triturated with cold diethyl ether and then reacted with Sulfo-Cy7.5 NHS ester (2 mg) in DMF (250 µL) and

DIEA (50 µL, 0.288 mmol) for 4 h at room temperature. The peptide was then crashed out in cold diethyl ether, concentrated *in vacuo*, and purified by RP-HPLC.

SulfoCy7.5-Tetra_Lala

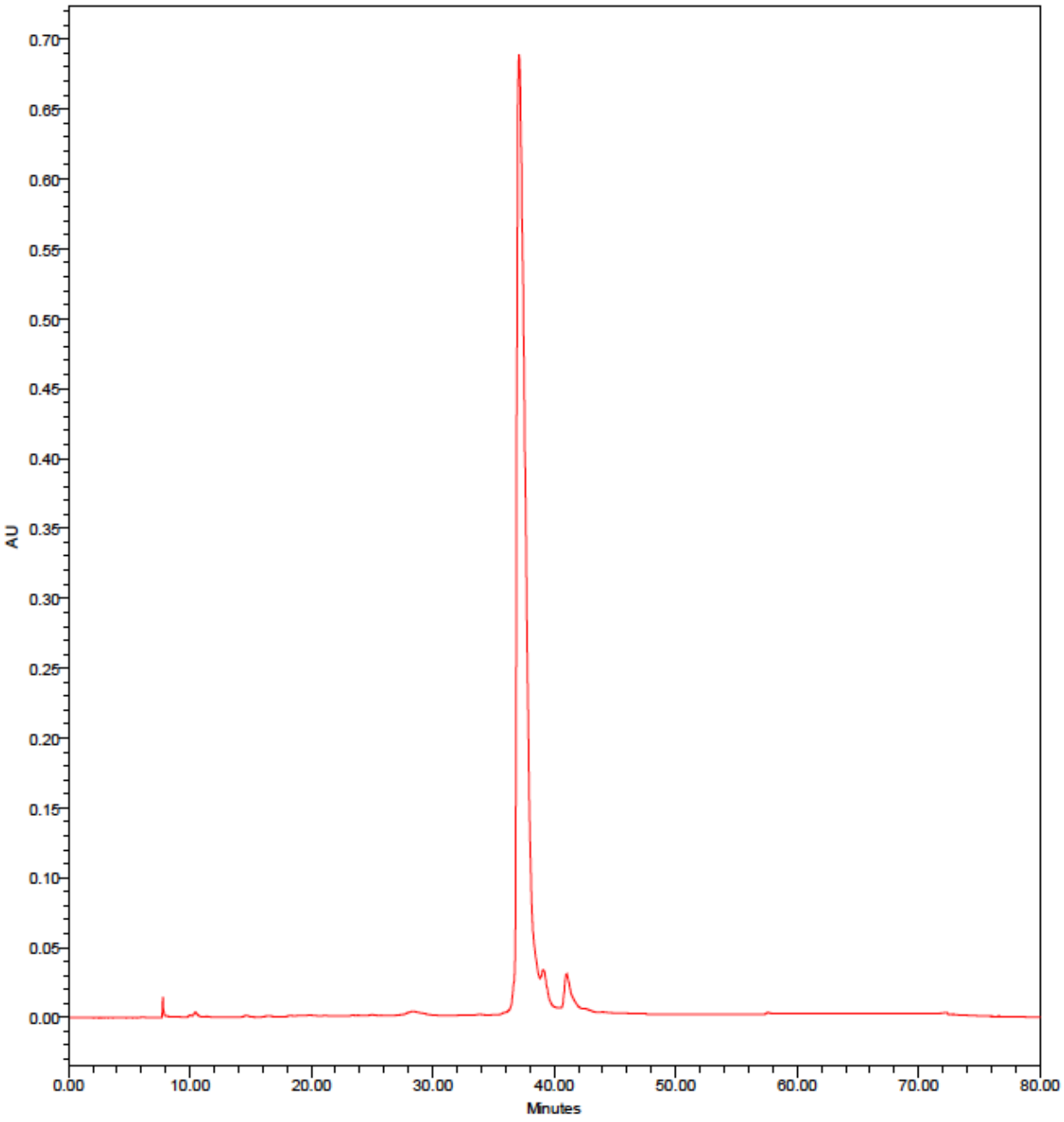

Expected $M+H^+$ = 1410.627, Observed = 1410.249

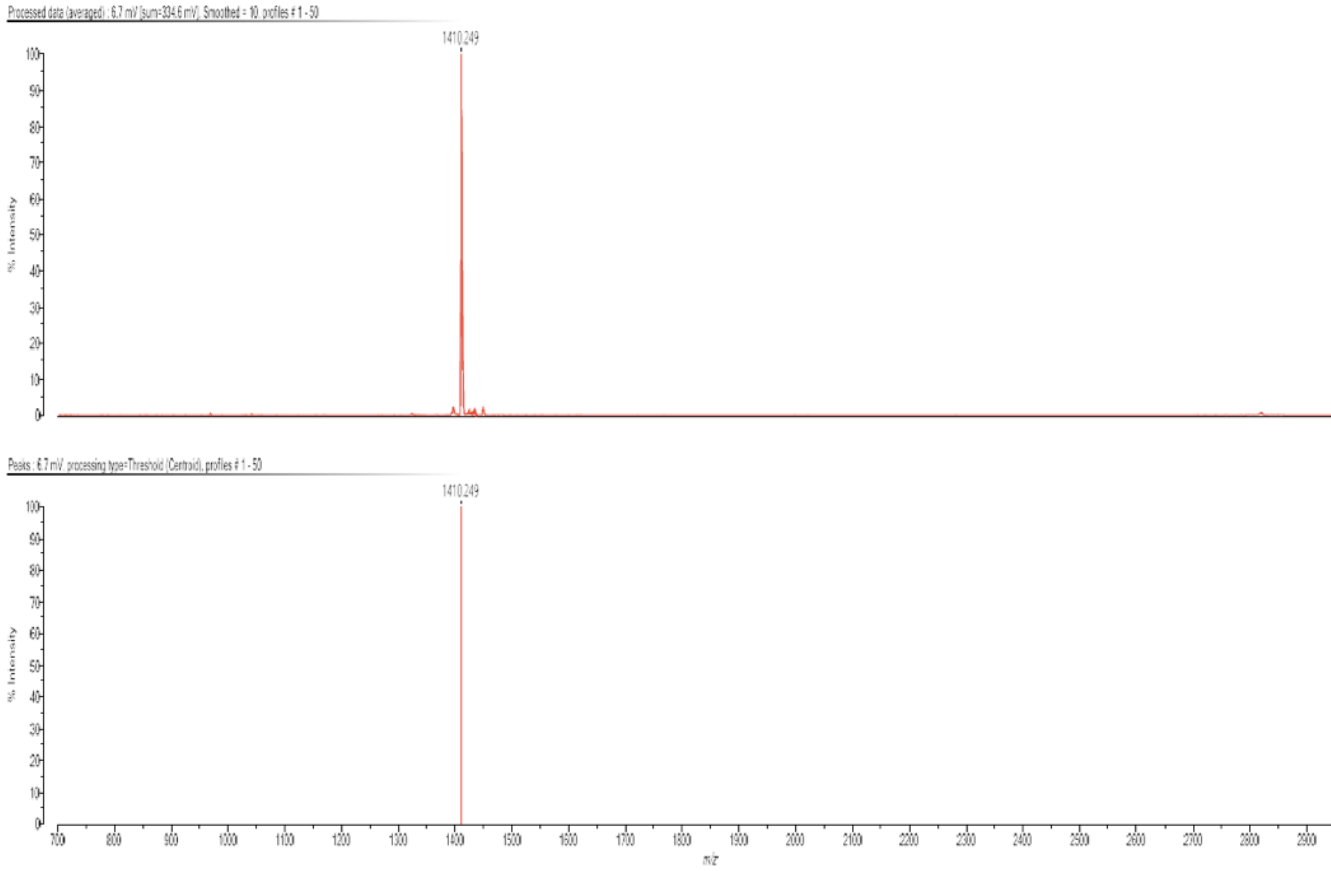

SulfoCy7.5-Tetra_Dala

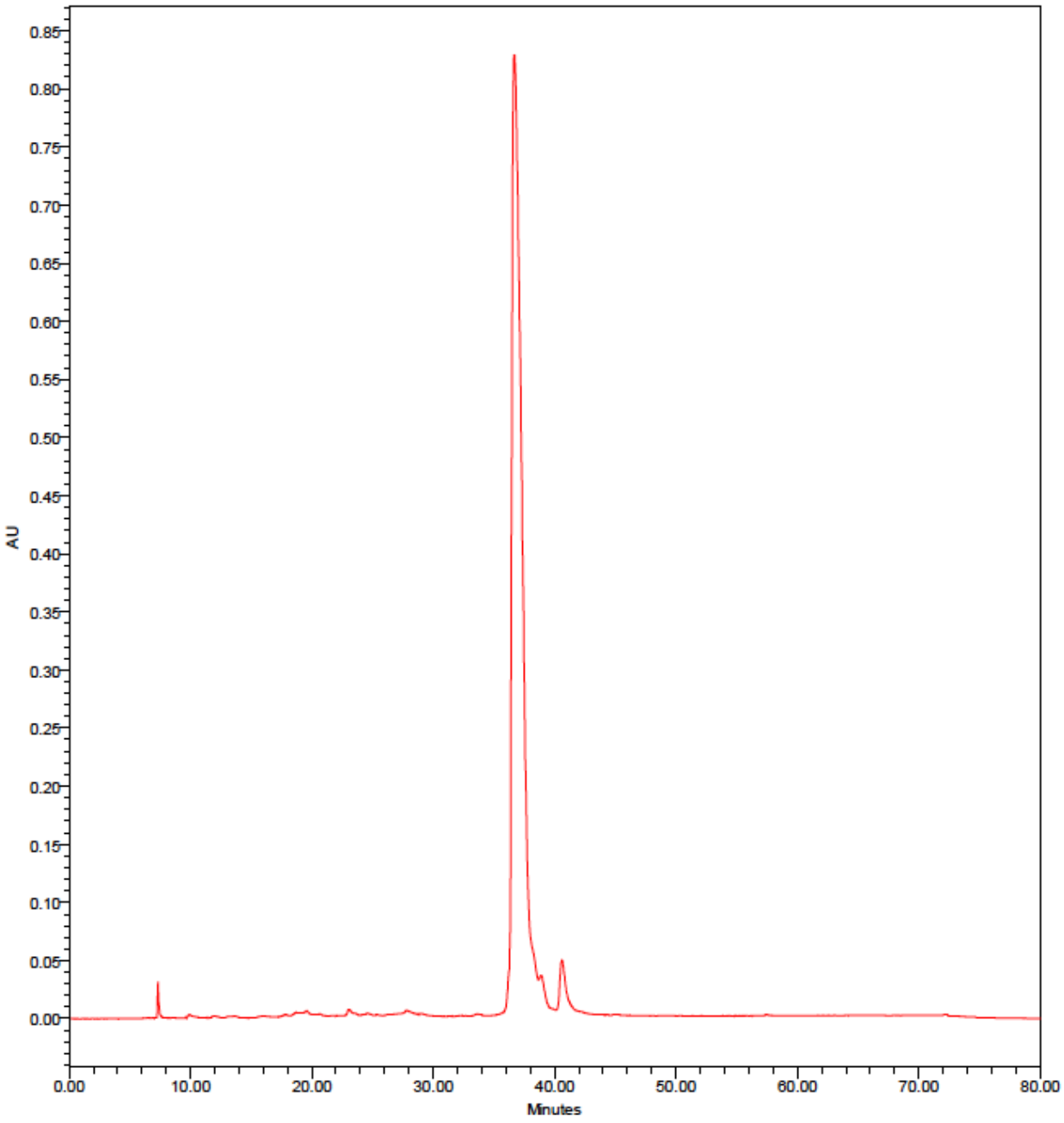

Expected $M+H^+$ = 1410.627, Observed = 1410.274